The University Of Sheffield.

Department Of Mechanical Engineering

PhD Thesis

The Low Adhesion Problem due to Leaf Contamination in the Wheel/Rail Contact: Bonding and Low Adhesion Mechanisms

KEI **ISHIZAKA**

September 2019

Professor Roger Lewis

Thesis submitted to the Department of Mechanical Engineering, University of Sheffield in fulfilment of the requirements for the degree of Doctor of Philosophy

SUMMARY

Fallen leaves on the railway track in the autumn cause many safety and business issues, such as signals passed at danger (SPADs) and delays in a timetable, leading to a decrease in ticket sales and poor customer satisfaction. Low adhesion conditions due to leaf contamination cause these problems, which form a black and slippery leaf film. When the leaf film is present, a train wheel is likely to slip and slide, resulting in severe damages to the wheel and rail. Hence, proper adhesion management is necessary to offer safe and cost-effective train transportation.

Railway industries currently conduct several countermeasures, and most of them attempt to remove leaf films. However, the removal is not straightforward as leaf films stick tightly to the rail. Accordingly, a different approach should be considered: prevention of the leaf film formation and mitigation of low adhesion. For the development of a new method of prevention and mitigation, it is important to understand the mechanisms of low adhesion and bonding of leaf contamination. Hence, the aims of this study were the clarification of the low adhesion mechanism and a better understanding of the bonding mechanism between leaf films and rails.

Tribological tests using a ball-on-flat method were carried out to figure out which material in leaves plays an important role to lower the adhesion in wet conditions. A black material synthesised with leaf extracts and rail steels was identified to decrease the adhesion. Chemical and material analyses were performed, and it was found that the black material was a mixture of graphitised carbon, iron carboxylate or iron oxide and various ions, including metal phosphates. Therefore, the graphite-like carbon was concluded to be the primary cause of low adhesion due to leaf contamination.

Chemical analyses of leaf extracts were conducted to elucidate the chemical reaction process. Organic acids in leaf extracts were likely to trigger the chemical reaction. Although the key organic acids are still unknown, a new direction of prevention and mitigation was proposed: heat application for the pyrolysis of the organic acids in leaf extracts. Following this idea, another tribological test using a twin disc machine was performed. It was found that the heat application was effective for mitigation of the adhesion and possibly prevention of the leaf film as well. Moreover, a scratch test found that the bonding energy of leaf films on the disc seemed to decrease as the creation temperature increased, suggesting that heat energy could help weaken the bond between leaf films and rails.

Based on the observation in the field test and findings in the experiments, a continuous tread braking was proposed as a potential measure. It can prevent the leaf film formation by removing leaf residue on the wheel surface, mitigating the low adhesion and weakening the bond by raising the surface temperature of the wheel.

NOMENCLATURE

μ	Friction/Traction/Adhesion coefficient
BBP	Black precipitation powder formed in brown leaf extract
BLE	Brown leaf extract
BLF	Brown leaf film
BLP	Brown leaf powder
BP	Black precipitation powder
DB	Deutsche Bahn
EDX	Energy Dispersive X-ray
ESCA	Electron Spectroscopy for Chemical Analysis
FT-IR	Fourier-Transform Infrared spectroscopy
GBP	Black precipitation powder formed in green leaf extract
GD-OES	Glow Discharge Optical Emission Spectroscopy
GLE	Green leaf extract
GLF	Green leaf film
GLP	Green leaf powder
LE	Leaf extract
LF	Leaf film
LP	Leaf powder
MTM	Mini Traction Machine
N.N	Normalised Number
RAIB	Rail Accident Investigation Branch
RHTT	Rail Head Treatment Train
rpm	rotations per minute
RSSB	Railway Safety and Standards Board
RTRI	Railway Technical Research Institute
SPADs	Signals Passed At Danger
wt%	Weight percent
XPS	X-ray Photoelectron Spectroscopy
XRD	X-Ray Diffraction
XRF	X-Ray Fluorescence

CONTENTS

ACKNOWLEDGEMENTS

First and foremost I would like to express my sincere gratitude to my supervisor, Professor Roger Lewis, for his continuous support, patience, motive and immense knowledge.

My sincere thanks also go to Dr. Stephen Robert Lewis, Dr. Tom Slatter and Dr. Deborah Hammond, who shared their wisdom with me during the course of this research.

I would also like to thank the East Japan Railway Company and the Rail Safety and Standards Board for their financial support, and Alan Lawton and Anup Chalisey of the Rail Safety and Standards Board for their help during the project.

For those who helped me in every aspect of this project; Dave Butcher, Luke R Callaghan, David Fletcher, Sandra van Muers, Robert J Hanson, Simon Thorpe, Heather Walker, Howard Davies, Benjamin White, Joseph Lanigan, Martin D Evans, Peter Krier, Boxiu Zhang, Reuben Kempka, Shinya Fukagai, Hiroyuki Suzuki, Zing S Lee, Ping Lu, William A Skipper, Thomas A Butcher, Matthew Harmon, Michael Watson, Nobuaki Shimada, Sho Yamanishi, Naoto Uchida, Osamu Sasaki, Ayano Kaneko, Naoko Kakinuma, Yasushi Sakamoto, Shunzo Miyake and Yoichi Kise. Apologies to those I missed.

My thanks also go to Dr. Makoto Ishida of the Nippon Koei and Dr. Hua Chen of the Railway Technical Research Institute for their help during this project.

Finally I wish to express my gratitude to my family, my wife Yoshiko Ishizaka, oldest son Ritsuto Ishizaka, middle son Naohisa Ishizaka, youngest son Eisho Ishizaka, my mother Takami Ishizaka and my grandmother Satie Fukada for their support and encouragement without which this project would not have been completed.

1 INTRODUCTION

1.1 Statement of the problem

A small piece of leaf has long been recognised as a problem for train operators and railway infrastructure companies in the autumn, as it causes many problems, e.g. platform overruns and signals passed at danger (SPADs) [1], [2]. In most cases, these problems are a result of low friction force between wheels and rails. Without sufficient friction level, a train vehicle could be out of control since traction and braking depend on this friction force in the case of an “adhesion” railway [3].

The slippery rail is produced by fallen leaves on the line in the autumn, leading to actual accidents in the UK. For example, there was a station overrun accident at Stonegate in 2010 [4], followed by a collision with the buffer stop at Chester station in 2013, as shown in Figure 1.1 [5]. There are many other incidents and near misses which are not found in the official reports of Rail Accident Investigation Branch (RAIB). Furthermore, similar issues due to the leaf contamination have been reported by Deutsche Bahn (DB) in Germany [6] and Railway Technical Research Institute (RTRI) in Japan [7]. Hence, leaf contamination could occur and be a problem anywhere trains are operated.

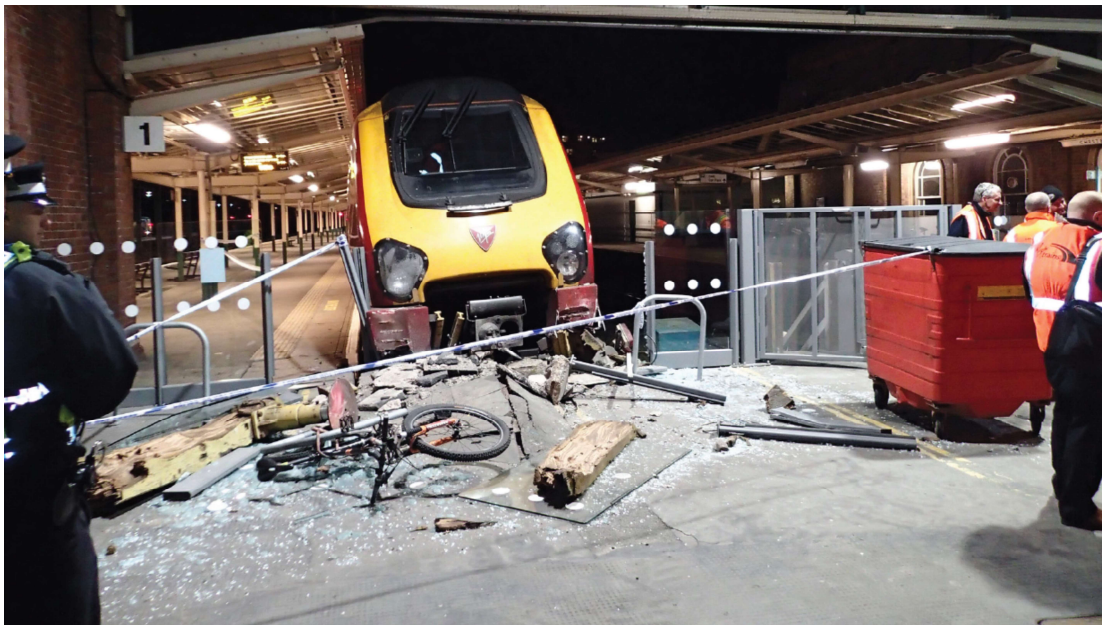

Figure 1.1 – A collision with the buffer stop at Chester station in 2013 [5]

The traction between wheels and rails, which is often expressed as “adhesion” in the railway industry, is one of the most important factors for train control, in particular, for acceleration and deceleration [3]. The adhesion coefficient is required to be at least 0.2 and 0.09 for traction and braking, respectively [1]. However, the rail surface is often contaminated by various sources due to its exposure to the environment, such as water, oil and dead leaves [8]. This contamination decreases the adhesion coefficient below that of dry levels, causing safety and operational issues. Therefore, the proper management of the adhesion level is significant for operational and infrastructure companies.

Among various contamination which causes low adhesion, leaves falling on the line in the autumn have a significant impact on train operation [1]. The leaves form a film on the rail, as shown in Figure 1.2 [2]. This leaf film reduces adhesion levels when a small amount of water, such as light rain, frost and morning dew, is present [9]. It has been reported that the adhesion coefficient decreases to approximately 0.1 or less when leaf contamination is mixed with water [1], [9], which is lower than the required level for traction and braking. Additionally, the leaf film tightly adheres to the rail surface so that the removal of leaf films is not straightforward [10].

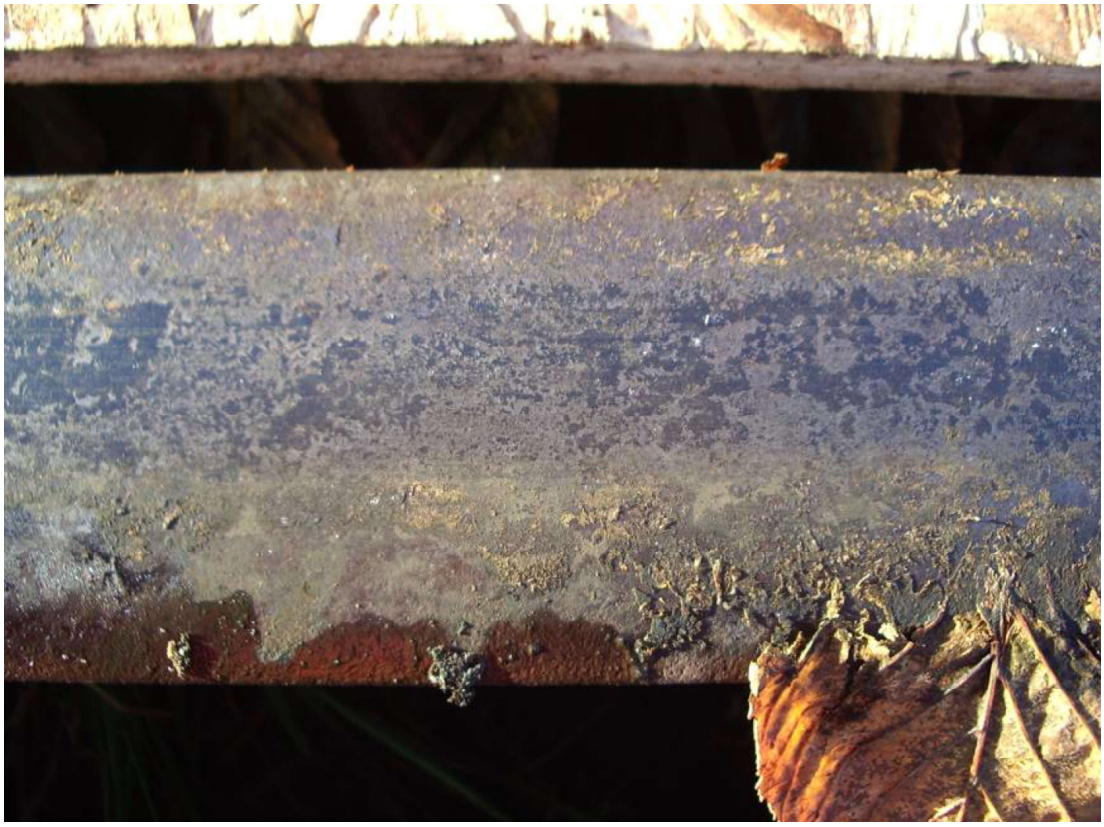

Figure 1.2 – Typical image of the leaf film on the railhead [2]

Various measures have been carried out, such as sanding and water-jet cleaning, to overcome this low adhesion condition due to leaves. These treatments are useful to some extent; however, the annual cost has been reported to be £50 million in the UK [11] and 100 million SEK in Sweden [12]. Additionally, a timetable is often subjected to changes to allow for longer braking and traction, and an operation of Rail Head Treatment Trains (RHTTs) with a water-jet cleaning and traction enhancer also needs modification of timetables since they are usually operated at a low speed in the early morning [2]. This amended timetable lowers customer satisfaction about the train transportation service. From the viewpoints of both cost and business, it is essential to develop cheaper and more effective methods to combat leaf contamination, making the train transportation more competitive than other transportation modes.

To sum up, the problems that the railway industries are facing is that the current measures are intrinsically imperfect. Further maintenance cost is inevitable due to damages on both wheels and rails in traction enhancer, and amended timetables cannot be avoided in RHTT operation. Therefore, a new approach to mitigating this leaf problem is necessary for pushing innovation in this field.

1.2 Aims

The aim of this research can be split into two topics: elucidating the manner in which the leaf film causes low adhesion and revealing the bonding mechanism between the leaf film and rail surface. Figure 1.3 shows a concept map of this aim. In this research, not only the fundamental tribology of leaves, but also the material of leaves was intensively studied to clarify the essential substances for the low adhesion and strong bonds. The final goal of this project is to suggest and develop better methods for prevention of leaf film formation or mitigation of low adhesion, using knowledge of the low adhesion and bonding mechanisms.

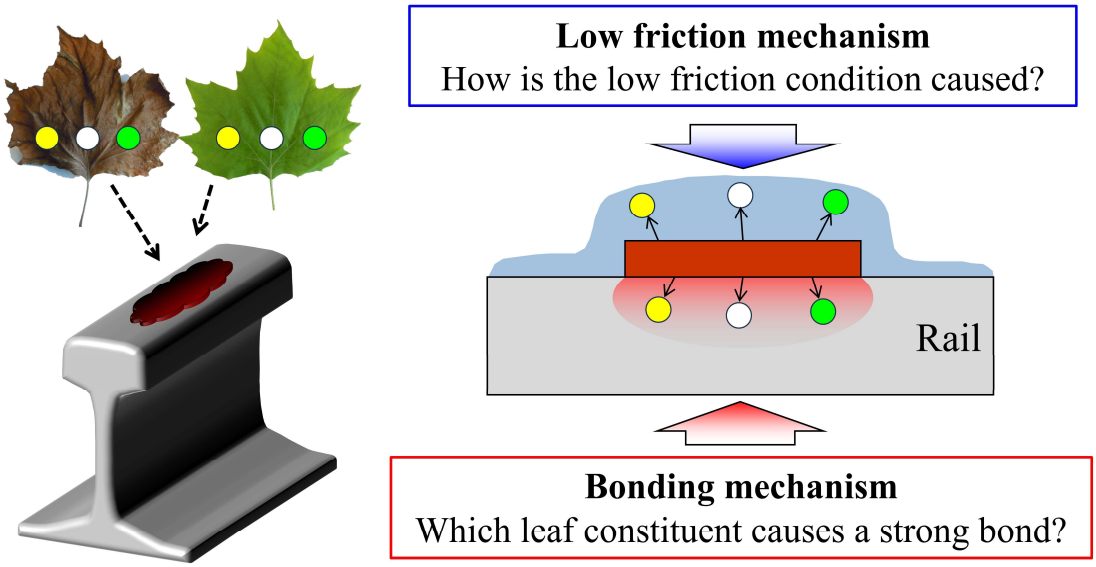

Figure 1.3 – Concept map of the aims

1.3 Novel aspects and impacts of this project

This research project involves various novel aspects and impacts which have not been considered before. They are shown in the following list:

- **Comprehensive analysis**

More than ten methods of chemical and material analysis were employed in this work to elucidate the chemical conditions of leaf and leaf-related material. The multiple analyses made it possible to overcome weak points in each method, leading to the correct understanding of the substance.

- **Identification of specific substance for low adhesion**

Through the chemical and material analysis, a key substance for low adhesion was identified by narrowing down the candidates.

- **Quantitative evaluation of bonding conditions**

Scratch tests of leaf films enabled evaluation of bonding strength in a quantitative way.

- **A new approach for the prevention and mitigation of low adhesion due to leaf films**

A new idea for the prevention and mitigation was attempted, i.e. heat application. Development of the prevention method is ideal for train operators and infrastructure companies if it does not involve any significant side effects, rather than just removal with mechanical methods. The method proposed in this study could prevent the leaf film formation as well as mitigate the low adhesion. If this method is proven to be

applicable to the actual railway operation, it should be an innovative technology for railway industries.

1.4 Thesis layout

Chapter 2 reviews general information related to leaf contamination problems, such as basic tribology, mitigation methods and leaf chemistry. Additionally, it also analyses the operational data and reviews the current models and theories of the low adhesion phenomenon. Finally, it identifies the research gap to be explored.

Chapter 3 presents the hypotheses of the low adhesion mechanism and bonding mechanism due to leaf contamination, drawn out from the information in Chapter 2.

Chapter 4 experimentally assesses the hypotheses of the low adhesion mechanism proposed in Chapter 3. A ball-on-flat method was used with four types of leaf samples: leaf powder, leaf film, leaf extract and black precipitation powder. The experiment also aims to identify the key materials of low adhesion.

Chapter 5 explores the chemistry of the black precipitation powder which was identified to cause low friction in Chapter 4, using five different methodologies: X-ray fluorescence, X-ray diffraction, Laser Raman spectroscopy, X-ray photoelectron spectroscopy and Fourier transformed infrared spectroscopy. This work aims to bring deeper understandings regarding the leaf chemistry as well as the low adhesion and bonding mechanisms.

Chapter 6 focuses on the leaf extract analysis to examine the suggestions of the chemical reaction between leaf extracts and rail steels developed in Chapter 5, using six techniques: viscosity measurement, pH value test, proton nuclear magnetic resonance, inductively coupled plasma-mass spectrometry, ion chromatography, high performance liquid chromatography and Benedict test.

Chapter 7 attempts to understand the low adhesion phenomenon due to leaves in rolling-sliding conditions, using a twin disc machine. The work also includes the examination to prevent the chemical reaction developed in Chapter 5 and Chapter 6.

Chapter 8 investigates the bonding mechanism between the leaf film and bulk rail, using a scratch test method. This chapter aims to examine the hypotheses of the bonding mechanism developed in Chapter 3.

Chapter 9 summarises the observation in the field test and suggests a practical method of the measure against leaf contamination for prevention and mitigation with a description of advantages and drawbacks.

Chapter 10 brings conclusions to this thesis, publications arisen from this work, and finally, further work recommended for the development of this research project.

2 REVIEW OF LEAF CONTAMINATION

2.1 Introduction

The leaf contamination problem has been studied by many researchers [1], [2], [19]–[21], [11]–[18]. These studies mostly focus on the mitigation measures: removal of the leaf films and recovery of the adhesion level. For example, sanding from a locomotive has been studied to increase adhesion and remove the leaf residue [18].

Recently, new research approaches for the leaf film issue have been attempted, by analysing the interface between the leaf film and the rail surface [2], [14], [22]–[24]. Several techniques for analysis, such as Fourier-Transform Infrared spectroscopy (FT-IR), Glow Discharge Optical Emission Spectroscopy (GD-OES) and Energy Dispersive X-ray (EDX), have been implemented for the leaf films obtained in both the laboratory and on the actual rail track. The results show that the leaf components react chemically with the active Fe ions originated from the rail steel. This chemical reaction seems to form a slippery organic layer strongly bonded to the rail surface.

Despite these efforts, the mechanisms by which a piece of leaf causes low adhesion and tightly sticks to the rail are still uncertain. If these mechanisms are clarified, further developments of the existing methods or innovative methods could be possible. Thus, more detailed research in this field is required, including identification of the key materials and parameters which cause low adhesion and strong bonds.

In this literature review, the current understanding of the low adhesion phenomenon due to leaves and the bonding mechanism between the leaf film and rail surface were studied. Then, research gaps were identified to make the research direction clear.

2.2 Definition of traction, friction and adhesion

The tribological conditions between the wheel and rail are commonly expressed using three words, namely, friction, traction and adhesion. Friction is the tangential force transmitted between two objects which slide against one another. On the other hand, traction is the force transmitted between a driven cylinder rolling along a flat plane [3]. The underlying friction level between two bodies of known materials will dictate the relationship between creep (the difference in relative surface speeds of the rolling/sliding body and the plane) and the traction force as shown in Figure 2.1 [13].

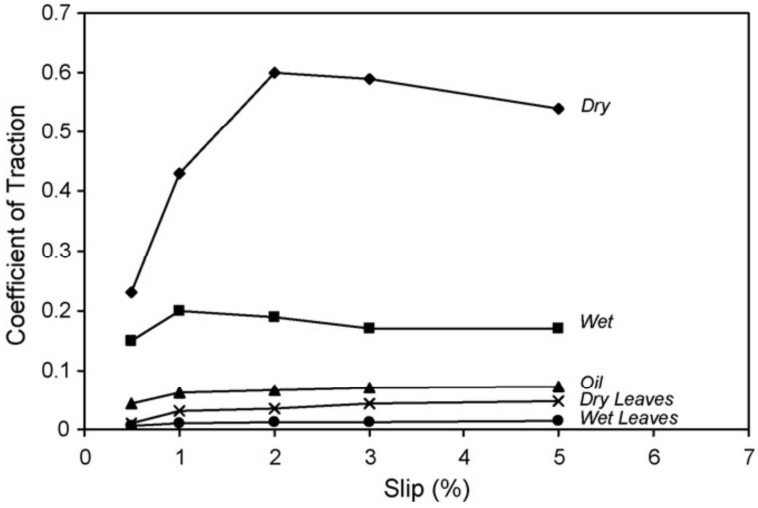

(a)

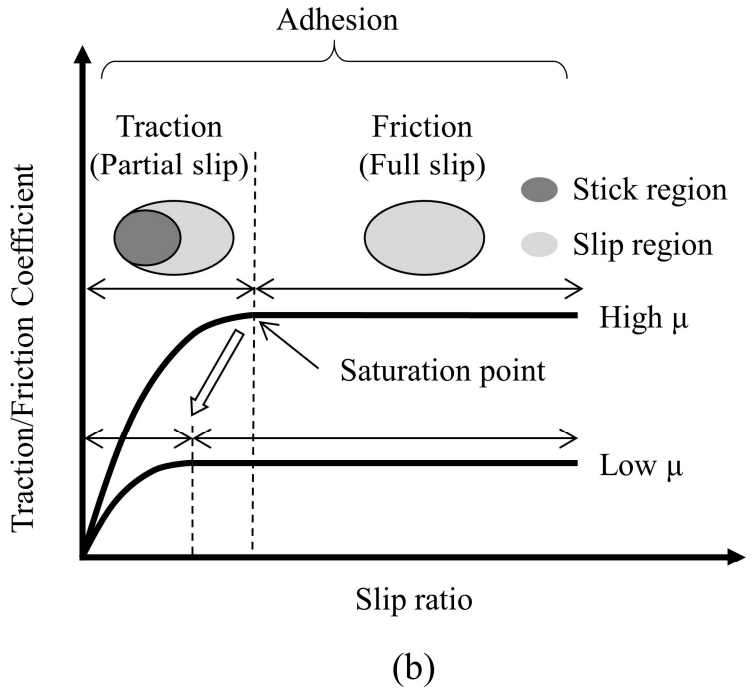

(b)

Figure 2.1 – Relationships between creep and friction/traction/adhesion:
(a) Creep curves in a twin-disc apparatus [13]
(b) Definitions of friction, traction and adhesion

Friction and traction are different properties of a contact. The term used depends on the measurement technique. For example, if a sliding device such as the pendulum is used [25], then any result will be a measurement of friction because the contact reaches a full slip condition. However, if a rolling/sliding device is used such as the hand pushed tribometer [26], then any result will be a measurement of traction since the contact probably contains a partial stick region. It should be noted that any friction or traction coefficient measured by such devices will be the coefficient between the rail and that device. Measuring the actual traction coefficient between

the wheel and rail is very difficult/impractical. Thus, devices such as the pendulum and tribometer can give reliable estimations of what the traction coefficient between the wheel and rail is likely to be.

Adhesion is a word which is commonly used in the railway community and can be used incorrectly when referring to the wheel/rail contact as discussed in [3]. However, adhesion seems to be a useful term which can be used to refer to the general state of friction on the rail head. For example, "low adhesion conditions" refers to a rail head which has low friction and thus will give low traction between the wheel/rail interface.

The traction force is determined by the traction coefficient μ between the wheel and rail and the normal force. It transmits both the accelerating force and the braking force from the wheel to the rail. Hence, the friction level in the contact patch is an important factor to determine the kinematic performance of trains.

In this study, the terminologies friction, traction and adhesion are used according to the definition above. Practically, "friction" is usually used in the ball-on-flat tribology tests, "traction" in the twin disc tests, and "adhesion" for the general terms.

2.3 Incident analysis

Analyses were carried out regarding data provided by Network Rail, which contains incident information for the autumn period, such as station overruns, track circuit failures and SPADs. These incidents are critical for train operators, and leaf contamination seems to be the main cause of these incidents.

Figure 2.2 shows a relationship between the time of the day and the total number of incidents (station overruns and SPADs), accumulated between 2010 and 2014. From this figure, a relatively high frequency of incidents is observed between the hours of 06:00 – 24:00, in which trains are frequently operated. In contrast, the incidents are dramatically decreased between 00:00 – 05:00 because of few train operations, and a medium number is observed between 05:00 – 06:00.

Figure 2.3 shows a relationship between the time and the number of incidents between the hours of 05:00 – 24:00, normalised by the number of stopping attempts on average. The data between 05:00 – 24:00 is chosen because of the relatively larger number of incidents. The normalised number (N.N) is calculated by Equation 2.1.

$$N.N = \frac{station\ overruns + SPADs}{average\ number\ of\ stopping\ attempts\ in\ the\ hour}$$

Equation 2.1

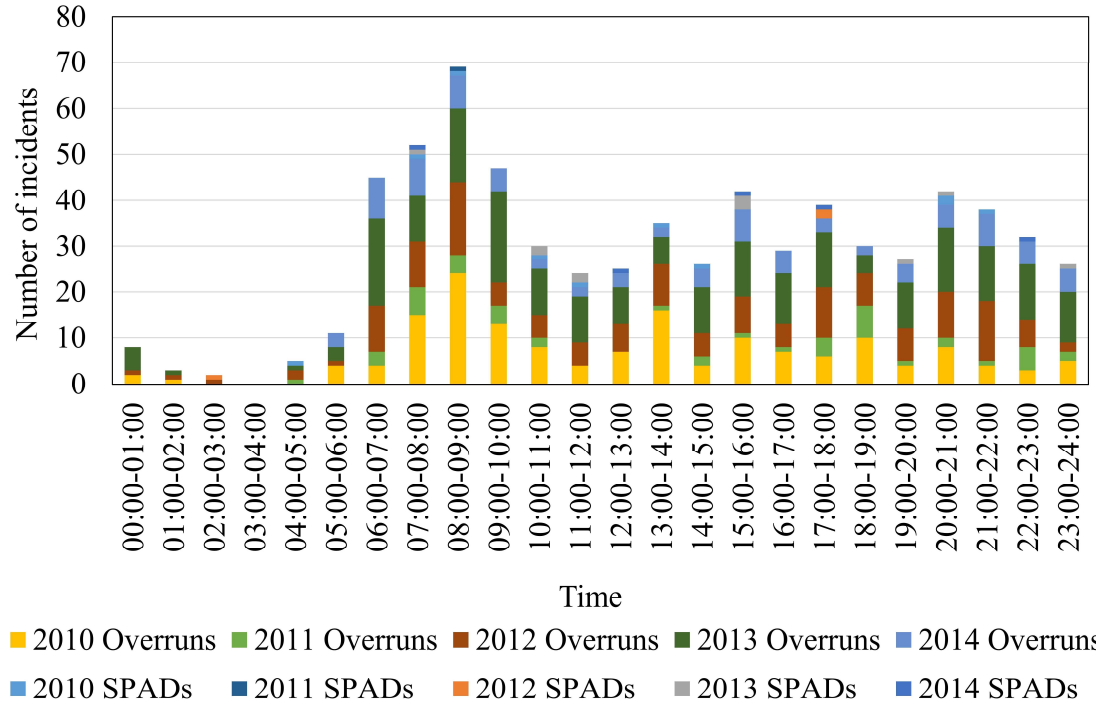

Figure 2.2 – Relationship between the time of day and total number of incidents (station overruns and SPADs) during autumns 2010-2014

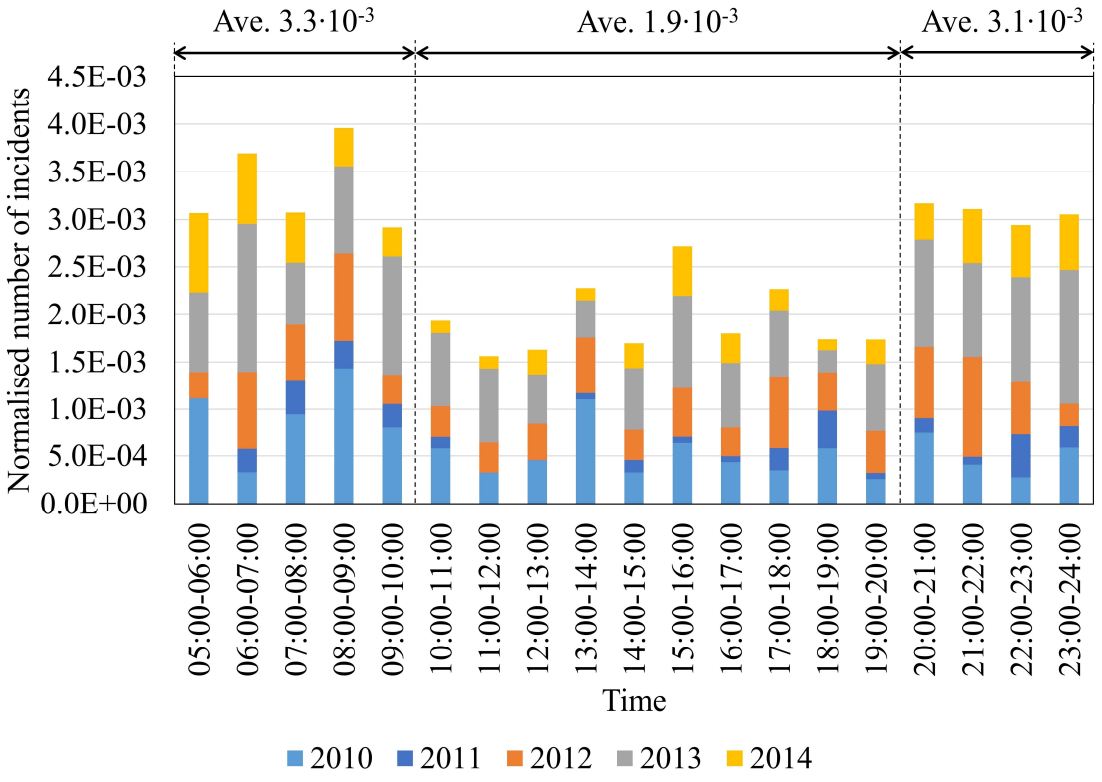

Figure 2.3 – Relationship between the time of day and the normalised number of incidents

As can be seen, the high probability is confirmed between the hours of 05:00 – 10:00 and between 20:00 – 24:00, and the average values are $3.3 \cdot 10^{-3}$ and $3.1 \cdot 10^{-3}$, respectively. Conversely, the relatively low possibility, $1.9 \cdot 10^{-3}$ on average, is confirmed between 10:00 – 20:00, although there are some fluctuations. This value is approximately 40 % lower than the values of 05:00 – 10:00 or 20:00 – 24:00. As a result, there is a distinctive relationship between the time and the incident probability.

Figure 2.4 shows a relationship between the time of day and the normalised number of leaf-related incidents in the hours between 06:00 and 24:00, analysed from data recorded between 2010 and 2012. The data in 2013 and 2014 are excluded because of fewer data categorised as "leaf contamination". As can be seen, a relatively high possibility is observed between the hours of 06:00 – 09:00; in contrast, a lower possibility is confirmed in the other hours. The average value between 06:00 – 09:00 is $1.3 \cdot 10^{-3}$, which is twice as high as the average value between 09:00 – 24:00, i.e. $5.9 \cdot 10^{-4}$. A slight increase can be seen between 20:00 – 24:00, however, the difference is not clear. From this analysis, it is shown that the probabilities of incidents related to leaf contamination depend on the time of a day, namely, early morning 06:00 – 09:00.

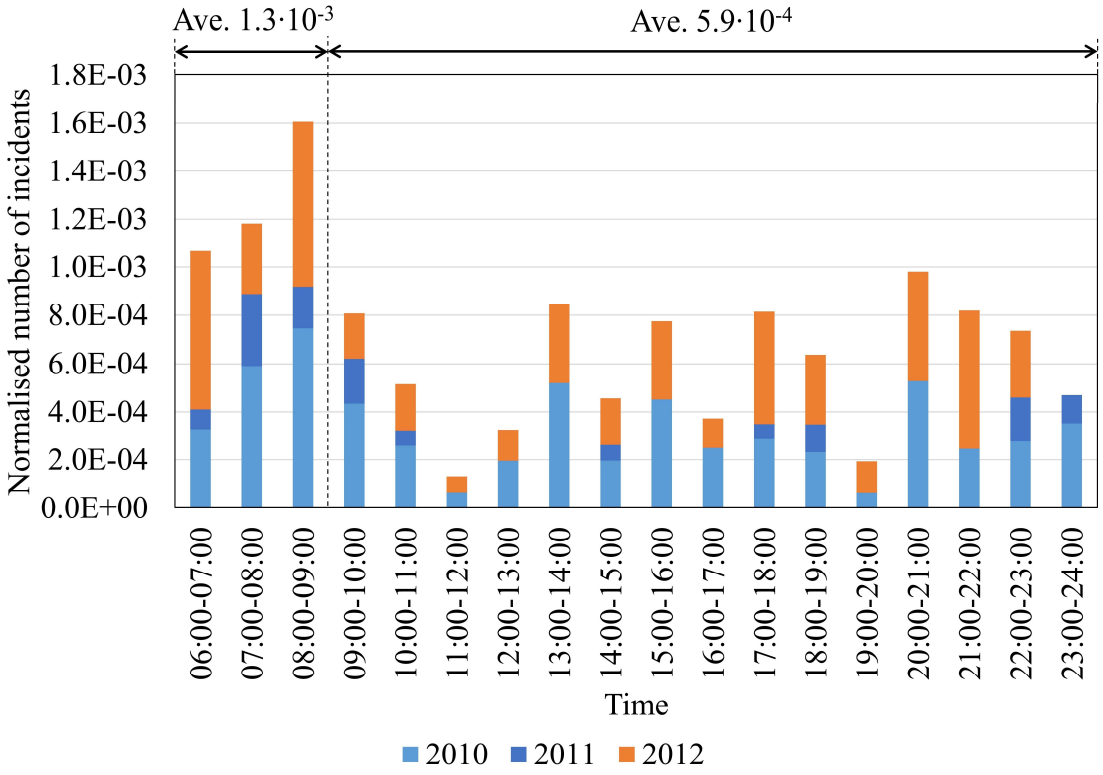

Figure 2.4 – Relationship between the time of day and the normalised number of incidents related to leaf contamination causes

The high probabilities between 05:00 – 10:00 and 20:00 – 24:00 in Figure 2.3 and Figure 2.4 could be attributed to the dew on the track [27]. Generally, dew is formed if relative humidity reaches 100 % or temperature drops the dew point, and it is often seen in autumn as air temperature becomes lower than that of summer. Indeed, relative humidity tends to increase from night to morning; relative humidity in south-east England between 22:00 and 10:00 is over 80 % [28]. Considering that the temperature close to the ground is lower than the air temperature, relative humidity around the rail is higher than 80 % due to low air temperature. Hence, dew is likely to be formed between 22:00 and 10:00, depending on other factors, including geographic features.

This feature corresponds to the tendency in Figure 2.3, i.e. the relatively high probabilities between the hours of 05:00 – 10:00 and 20:00 – 24:00. Furthermore, the high possibilities between the hours of 06:00 – 09:00 in Figure 2.4 suggest that dew is continuously absorbed into leaves around the rail from night to morning and creates the low adhesion condition due to the high moisture level in the leaf films, which seems to reach maximum value in early morning.

Overall, the incident data shows that dew formed during the night is likely to cause low adhesion conditions.

2.4 Low adhesion due to leaf contamination

The friction coefficient between wheels and rails strongly depends on the condition of the contact area. In reasonably dry conditions, friction coefficient in the contact area between wheel and rail is 0.3, and it needs to be 0.2 and 0.09 for traction and braking, respectively [1]. However, surface conditions of the rail are often changed due to environmental contaminations, and the friction coefficient decreases. Low adhesion levels are classified into three groups as shown below [15].

- Medium-low: $0.1 < \mu < 0.15$
- Low: $0.05 < \mu < 0.1$
- Exceptionally low: $0.02 < \mu$ 0.05

Fallen leaves in autumn reduce the friction coefficient to approximately 0.1 or less [1], [9], and leaves on the line are one of the main causes of the low adhesion problems [1], [2], [9]. According to this categorisation, a friction level when leaves are on the track presumably belongs to the low group.

Friction/traction coefficient values acquired during previous research are summarised in Table 2.1. As can be seen, the friction/traction coefficients with leaf contamination are often below 0.1. It is also found that the leaf type (such as sycamore and elm) does not affect friction/traction values.

Table 2.1 - Friction coefficient values acquired by the previous research

Literature	Test method	Leaf type	Test conditions	Friction coefficient
[11]	Twin disc	Cut sycamore	Dry 1 m/s with 0.5, 1, 2 % slip 1.2 GPa	< 0.05 *Typical value
[12]	Pin-on-Disc	Crushed elm	R.H = 40±5 and 95±5 % 0.1 m/s with 100 % slip 0.8 and 1.1 GPa	0.25 (average) R.H = 40 % 0.15 (average) R.H = 95 %
[13]	Twin disc	Mix Maple and Oak	Dry/Wet 1 m/s with 0.5, 1, 2, 3, 5 % slip 1.5 GPa	< 0.05 Dry, for all slip values < 0.02 Wet, for all slip values
[14]	Ball on disc MTM*	Chopped sycamore	Wet 0.02-1 m/s with 1, 50 % slip 1 GPa	0.01-0.07 Soaked brown leaf 0.04-0.14 Leaf extract
[15]	Twin disc	Unknown	Wet 1 m/s with 1 % slip 1.5 GPa	< 0.06 Leaf films
[16]	Twin disc	Cut sycamore	Dry 1 m/s with 0.5 % slip 1.2 GPa	0.02 *Minimum value
[17]	Twin disc	Mix + extract Soaked maple, beech, oak, birch	Wet 0.8-3 m/s with 1-10 % slip 1 GPa	< 0.1 Leaf mix ≈0.1 Leaf extract
[18]	Field Locomotive	Unknown	Dry/Wet Axle load 21.5 t	0.06 Dry, mean value in 1st run 0.04 Wet, mean value in 1st run
[22]	Twin disc	Sycamore paste	Wet 1 m/s with 3 % slip 1.5 GPa	0.05-0.15
[23]	Field Tribometer	Unknown	Wet (Light rain)	0.15 *Minimum value
[21]	Field Tribometer	Unknown	Dry 0.7 GPa	0.3
[29]	Field Test bogie	Pine needles	Dry/Wet 20 km/h at maximum	0.05 Dry, minimum value 0.05 Wet, minimum value

*MTM means Mini-Traction-Machine

From Table 2.1, the testing methodology is found to influence the measured friction coefficient values. For example, values measured by a twin disc apparatus tend to be lower than the value obtained by pin-on-disc equipment. A pin-on-disc test does not replicate the rolling-sliding conditions between wheels and rails but does offer greater controllability over parameters such as sliding velocity and contact pressure. Rolling-sliding conditions can be replicated by either twin-disc or ball-on-disc machine. The main difference between a twin disc machine and a ball-on-disc machine is that the former produces a line contact and the latter produces a point contact.

Figure 2.5 shows a typical traction result of a twin-disc test performed under varying contamination conditions [22]. A leaf layer was created on the rail disc and then run against wheel disc. In Figure 2.5, it is observed that wet leaves produce lower traction conditions than dry leaves and the lower traction tends to remain for a long time.

Figure 2.1 (a) shows a general relationship between the slip and the traction coefficient, obtained in a twin disc apparatus [13]. In [13], leaves were continuously fed into the disc contact, keeping the friction level low, in contrast to the method used in [22]. As can be seen, both dry and wet leaves yielded low traction levels at slip ratios between 0.5 and 5 %. These results suggest that leaf films are not easily removed by the wheel rolling with slip once they have formed on the rail surface, confirming what has been seen in previous studies [1], [15].

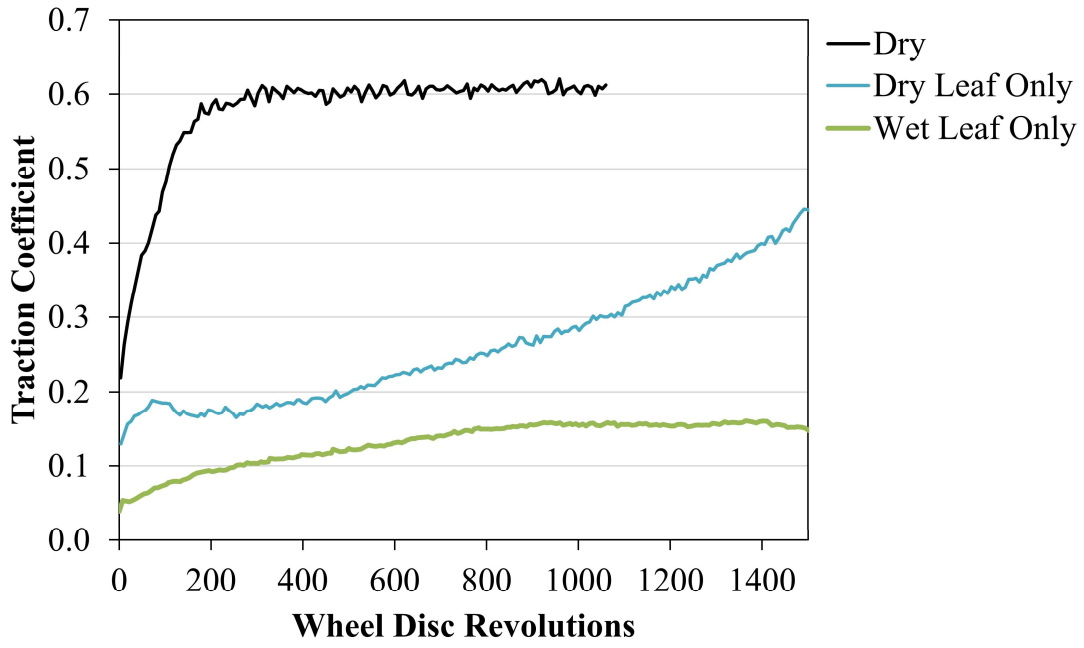

Figure 2.5 – An example of relationship between the rotational number and traction coefficient in a twin disc apparatus, showing the long effect of wet leaves

2.5 Mitigation methods

Several measures, which mitigate the low adhesion phenomenon due to autumn leaf films on the rail surface, have been carried out by train operating companies and infrastructure companies [1], [6], [9]. However, each mitigation method has a weakness in terms of practical applications, such as cost, time and labour. The specifications of representative methods are described below.

2.5.1 Sanding

Sanding is one of the traditional ways to increase adhesion, which has been used since the beginning of railways [18]. The sanding effect on leaf-contaminated rails has been investigated by laboratory-based tests with various parameters, such as sand grain size and slip ratio [13], [16], [17]. According to these studies, sanding recovers the adhesion to near dry contact levels with optimised parameters, and it also contributes to the removal of leaf films. Furthermore, these recovering and removing effects are confirmed in field investigations [18]. In this investigation, the adhesion improvement was achieved even at the non-sanding axles due to the leaf film removal. Accordingly, sanding seems to have a lot of positive effects on adhesion improvements.

However, there are some drawbacks to sanding, namely, the damage to the wheel and the rail surfaces [13], [16], [17], [30]–[32] and the electrical isolation of the wheel/rail contact area [33], [34]. Generally, train detection for a signal system is based on a track circuit system, which needs good conductivity between the wheel and the rail. The applied sand increases the electrical resistance of the contact area [33], [34], and causes the failure of track circuits. Track circuit failures cause unnecessary closure of the railway on safety grounds, leading to severe disruption and delays. Moreover, it is demonstrated that the applied sand damages the wheel and the rail, producing cracks and large deformation layers in the surface [13], [17], [31], [32]. The wear of these components in sanding conditions can be 10 ~ 100 times greater than in normal conditions [30], and this material damage decreases the life span of the components.

Therefore, sanding is effective for improvement in terms of adhesion and removal of the leaf residue. However, additional costs might be incurred, associated with operational issues and damage to track infrastructure.

2.5.2 Traction enhancer

Recently, a new type of product has been developed and tested, which is called traction enhancer (Adhesion enhancer) [11], [22], [35]. Traction enhancers aim to overcome low adhesion problems, in particular, leaf contamination. They mainly

consist of sand particles, steel particles, water or water-based gel, and they are usually applied to the top of the rail in liquid form. This liquid could improve the particle adherence in the contact patch, and boost friction/traction coefficients.

It is confirmed that traction enhancers can mitigate the low adhesion condition due to leaf contamination, recovering friction/traction levels close to dry conditions [11], [22]. For instance, the time to recover the friction/traction level can be shortened up to 70 % and 93 % in braking and traction, respectively [11]. Moreover, a wear rate of rail material is lower than that of dry conditions, indicating less damage compared to the sand application [22].

However, traction enhancers cannot remove leaf films completely [11]. Additionally, some type of traction enhancer still damages both the rail and wheel surface, such as indentation due to sand particles [11], [35]. This damage might lead to an increase in maintenance cost. Moreover, they are reported to show a high impedance in the contact area immediately after their application [22]. Although the impedance becomes stable after a few seconds, this high impedance could cause a signalling problem.

Therefore, a traction enhancer is one solution for the leaf contamination problem; however, they still have several drawbacks, such as surface damage and contact resistance.

2.5.3 High-pressure water

High-pressure water is often used to remove leaf films on the rail surface [1], [9], [15], and it is usually combined with sanding measures [1], [9]. A special train equipped with a sander and high-pressure washers (RHTT) is operated, focusing on the area where low adhesion conditions due to leaves are common. Although there is little work on the performance of high-pressure water when used for the removal of leaf films, it is confirmed to be effective to some extent, as reported in a previous study [6]. However, the leaf films on the rail cannot be removed completely by this method, showing that there is a 10 – 15 micron thick leaf film after cleaning [1]. This residual film could still produce low adhesion phenomena. In addition, the operational cost of cleaning trains is relatively high, estimated at £25 million per year [15].

2.5.4 Prevention of leaf film formation

Some methods used to prevent the formation of leaf films include patrolling around hot spots and vegetation management; however, a promising measure is the application of a controlled pH solution to the rail head [2], [20]. An alkaline environment (pH 9) has been reported to prevent the leaf film formation, resulting in

the improvements in leaf film properties, such as a reduced thickness, less coverage and increased skid resistance [20]. However, an acidic environment (pH 3) shows less effect on prevention than an alkali one [20]. These effects are closely related to the activation of ions, for example, $FeOH_2^+$ or FeO^- ions, which are from the Fe-oxides and believed to be key factors for the chemical reaction between leaf components and rail steel [2], [36]. The different results in varied pH values indicate that less H^+ ions deactivate the chemical reaction and prevent the formation of leaf films.

However, leaf film formations are not completely prevented by this method. For instance, there is only a 17% reduction in the film thickness when using a pH treatment compared to no treatment [20]. As well as the thickness evaluation, only 20 % reduction in coverage and 17 % increase in skid resistance under dry conditions are observed, indicating imperfections of the pH treatment. Moreover, pH solutions need to be continuously dispersed around the low adhesion area, incurring additional costs with regard to chemicals, equipment and labour.

Overall, the pH control method prevents leaf film formation and also has some effect on removal; however, the prevention effect is limited and as such may not provide the most cost-effective solution.

2.5.5 Findings

From the practical point of view, requirements for the measure are firstly effectiveness, followed by cost, and then other factors, i.e. environmental influence. To be critical, none of the reviewed methods is perfectly effective; there is still room to be developed, improved and amended. Thereby, it is worth trying to raise the quality of the existing method or develop a new method.

2.6 Chemical analysis of leaf contamination

As described in 2.1, a new attempt has been made to find out the chemistry of leaf films. In this section, recent achievements related to leaf chemistry were reviewed and summarised.

2.6.1 Fourier-Transform Infrared spectroscopy (FT-IR)

An FT-IR analysis is a method to detect molecular bonds in samples, mainly organic bonds such as C-O. This method was applied to laboratory-developed samples [14]. The black samples were made during friction measurements by MTM, with both actual leaves and leaf extract (water-soluble contents of leaves). Several organic bonds were detected in the black samples, e.g. O-H, C=O, C-O-C, C-C. These organic bonds were thought to be derived from pectin and cellulose in leaves. In

particular, pectin was expected to play an important role to form black colour as it was detected in the black material made with the leaf extract.

One problem of this analysis is that it had a bit biased interpretation of acquired spectra. For example, the absorption around 1420 and 1630 cm^{-1} was assigned to asymmetric and symmetric vibration of carboxylate, RCOO, where R stands for organic groups. This assignment itself seems reasonable; however, it does not need to belong to pectin salts, and other forms of salts or esters are also possible. To determine that this absorption derived from pectin salts, additional evidence is required, e.g. detection of pectin molecules in the leaf extract.

This work made significant progress and brought new knowledge with respect to leaf chemistry. However, the interpretation should be considered more carefully to grasp the chemical conditions of leaf contamination.

2.6.2 X-ray Photoelectron Spectroscopy (XPS)

A leaf-contaminated sample taken from an actual rail in Sweden was examined by XPS (Or ESCA: Electron Spectroscopy for Chemical Analysis) [23]. Many elements were detected: C, O, Fe, N, Si, F, S, Ca, Al and Mn, where C, O and Fe made up for 48, 29.3 and 13.2 weight %. These contents, except for Fe and Mn, did not originally derive from the rail bulk material; hence, there should be a chemical reaction between leaves and rails at the surface.

XPS has an advantage that chemical shifts could show the status of each element. However, the sample was charged up due to the release of photoelectrons, and therefore the chemical shifts were not correctly analysed. If this charge-up problem is resolved, XPS could give much information.

2.6.3 Glow Discharge Optical Emission Spectroscopy (GD-OES)

A depth profile was measured by GD-OES for the field sample [23]. It was revealed that the leaf-contaminated sample had a thick layer which contains organic elements, such as Ca and P, indicating that a layer reacted with leaf organics covers the sample surface approximately up to 500 nm in depth.

Figure 2.6 shows the profile of O and Fe of the field sample. As can be seen, the sample with leaf contamination is covered with a thick oxide layer where the crossing point is around 300 nm, which is not a natural oxidised layer. This result suggests that the thick oxide layer could lower the adhesion due to its mixed structure: leaf organics, rail steel and oxide.

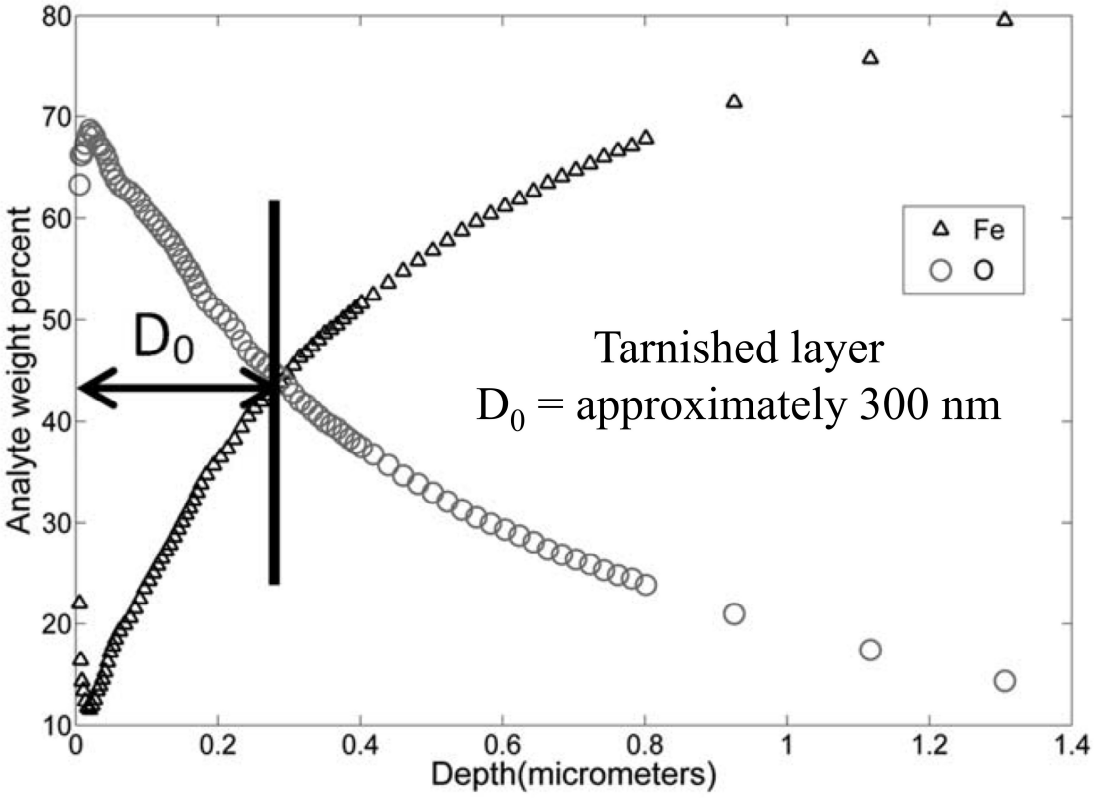

Figure 2.6 – Iron and oxygen depth profile from the leaf-contaminated sample [23]

2.6.4 EDX (Energy Dispersive X-ray spectroscopy)

Several organic elements were detected with EDX in the laboratory-developed sample: C, O, Ca and Fe. They showed a good agreement with other analyses, such as XPS and GD-OES. However, this method is unable to identify the chemical conditions of each element. Hence, further information cannot be expected.

2.7 Models of low adhesion and bonding mechanisms

Several models of leaf contamination were proposed based on the chemical analyses and biochemistry of leaves, explaining the principle of low friction and chemical bonds of leaf films.

2.7.1 A laboratory-based model

Figure 2.7 shows a schematic view of the laboratory-based model presented in [24]. This model consists of the three layers, which are a coated slippery layer at the top, an easily sheared chemically-reacted layer in the middle and a rail bulk at the bottom. In the case of the leaf contamination, the coated slippery layer is a leaf film, and the easily sheared chemically reacted layer corresponds to a bonding layer between leaf films and rails. GD-OES analysis shows relatively high levels of calcium and phosphorus in rail samples which had been prepared in the laboratory by rolling with

a leaf. These samples did not have a visible leaf layer, and these substances (Ca, P) are likely to have been deposited on the rail by the leaf, suggesting the existence of a chemically-reacted layer.

However, it has not yet been clarified which leaf constituents makes up the coated slippery layer and easily sheared chemically-reacted layer. Furthermore, a detailed chemical reaction process for the formation of these layers is still unclear. This lack of understanding limits the further development of measures based on this model. It is, therefore, necessary to analyse the interface between the leaf film and bulk rail chemically, leading to a better understanding of the low adhesion mechanism as well as the strong bond mechanism.

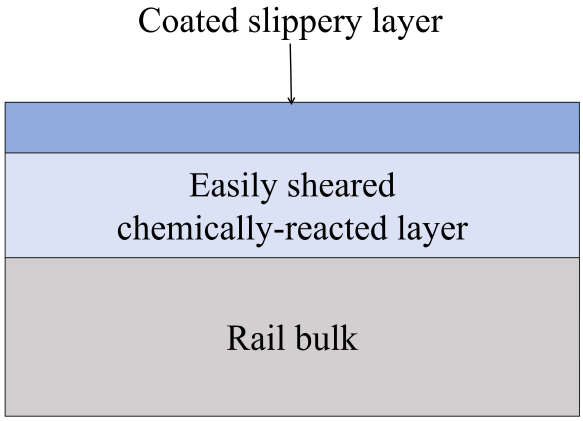

Figure 2.7 - A laboratory-based model with a three-layer structure [24]

2.7.2 A field-based model

Figure 2.8 shows a schematic view of the field-based model, explained in [23]. This model has been developed through analyses of XPS and GD-OES, and it has a three layer structure as well, i.e. a tarnished layer at the top, a friction-reducing layer in the middle, and a rail bulk material at the bottom. In this model, the bonding mechanism can be explained in two steps: firstly, a leaf is deposited on the rail surface, providing carbon, nitrogen, calcium and other elements. Secondly, these elements and iron oxides chemically react and form the chemically reacted layer with strong bonds to the rail bulk.

The tarnished layer mainly consists of organic components from leaves, and the friction-reducing layer contains a high amount of iron oxides. The thickness of a friction-reducing layer is approximately 300 nm, which corresponds to D_0 in Figure 2.6 and is four times thicker than the other samples. This thick oxide layer seems to decrease the friction/traction coefficient [37]–[39] and to be a result of more complete chemical reactions between leaf debris and rails. Therefore, the chemical reaction probably produces strong bonds between leaf film and rail.

However, chemical conditions in the tarnished layer have not yet been clarified, because of the charge-up problems in XPS analysis. Furthermore, the accelerator of a chemical reaction has not yet been revealed, which is the most important parameter to prevent leaf film formation. Therefore, this model explains the low adhesion and strong bond mechanisms to some extent, and more detailed analyses toward the clarifications of chemical and bonding conditions seem to be necessary to make this theory stronger.

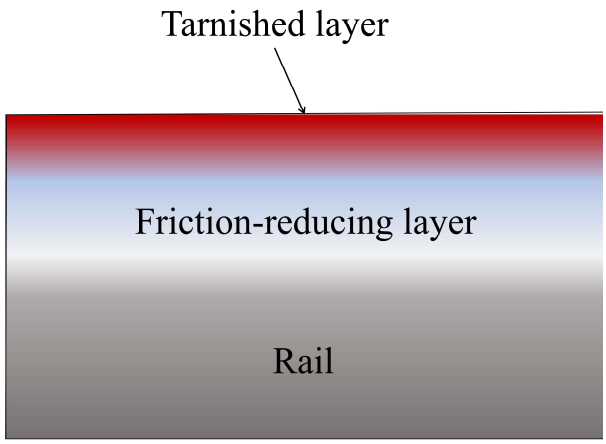

Figure 2.8 - A field-based model with a three-layer structure [23]

2.7.3 Other hypotheses

There are some other hypotheses for the leaf layer chemistry and the bonding mechanism. For example, pyrite (FeS_2) is expected to be one of the bonding materials, which is produced by active Fe ions (Fe^{2+} and Fe^{3+}) and sulphur included in the leaf [36]. Other components possibly react chemically and form the strong bond, namely, fatty acids from cutin and carbohydrates from pectin, cellulose and lignin [36]. All these hypotheses are based on the chemical reaction with radical Fe ions emitted from the steel surface iron oxides, and the high contact pressure seems to enhance or trigger the reaction. However, the proposed reaction processes have not yet been examined experimentally. The chemical analyses carried out in previous studies support these ideas [14], [23], [24]; thus, more detailed research is required to demonstrate them.

2.8 Expected key parameters

Chemical analyses and models in 2.6 suggest that there is a chemically reacted layer between the leaf film and rail, providing low adhesion and strong bonds. In general, the chemical reaction needs two things: reaction energy and materials, which are referred to as “parameter” in this thesis. Possible parameters for the chemical reaction between leaves and rails were reviewed and summarised in this section.

2.8.1 Pressure

The contact pressure between wheels and rails ranges from 0.6 to 2.7 GPa [40], and this high pressure seems to crush leaves and accelerate the chemical reaction. The black leaf films have been formed both in laboratory-based tests and field tests, where high pressure is applied in the contact area [2], [11], [13], [15], [16], [18]–[20], [22]. Although there are many parameters other than pressure, this fact suggests the significance of high pressure for leaf film formation on the rail surface.

Another effect of high pressure is the refinement of material microstructure [41]. This phenomenon is confirmed in a third body layer, where the structure of a third body is very fine or sometimes nano-crystalline with long sliding distance [42]. Although such a refinement seems to depend on the material combinations, a rolling-sliding contact between the wheel and rail might induce similar phenomenon, leading to a reduction in grain size at the surface, 20 nm on average [43]. Accordingly, these investigations show that high contact pressures affect the formation of leaf layers with severe deformation of the rail surface [41], [42]. Furthermore, they might assist in the strong bond formation between leaf films and rails, providing the mechanically mixed layer.

2.8.2 Temperature

A high slip ratio between the wheel and the rail causes a rise in temperature in the contact patch due to frictional work in the contact [44]–[46]. Examples of contact temperature are shown in Table 2.2. As can be seen, the maximum temperature is estimated to be over 727 °C in real tracks, forming a white etching layer with martensite transformation [46]. Temperature is an essential parameter in chemical reactions, which activates ions and accelerates the reaction process. From this viewpoint, the thermal energy must be considered for the chemical reaction between the leaf residue and the rail.

Table 2.2 – Achievable contact temperature

Literature	Temperature	Features
[44]	100 °C	Twin disc with 5 % slip
[45]	200 °C	Pin-on-disc with 100 % slip
[46]	Over 727 °C	Field, Martensite transformation observed

2.8.3 Iron oxide

Generally, iron oxides are easily formed by oxygen in the air, and the types of oxides strongly depend on environmental parameters, such as temperature, pH and oxygen level [36]. Fe_2O_3 (red oxide) is the most common oxide in nature [36], [47]; Fe_2O_3 exists in the form of iron oxyhydroxides as a result of hydration, such as α-FeOOH, β-FeOOH and γ-FeOOH [36], [48]. Another iron oxide, Fe_3O_4 (black oxide) can generally act as a passivation film to protect from further corrosion [49].

The existence of Fe-based oxide on the rail surface has been recognised, particularly, in areas near to the sea, where the rail can be easily covered with rust [39], [48]. Haematite (Fe_2O_3) and magnetite (Fe_3O_4) are well-known to be formed on the rail surface [38], [39], [48]. These oxides are deemed to form a mechanically mixing layer, presumably leading to the formation of third body layers [50]. As a result, iron oxides are thought to be an important material to determine the tribological behaviour of the contact area [37]–[39], [51], [52].

The decrease of friction/traction coefficient due to iron oxides on the rail surface has been reported by many researchers [38], [39], [51], [52]. Iron oxide films are considered to be the mixture of Fe_2O_3 and Fe_3O_4, and the relatively soft Fe_3O_4 reduces the friction although hard Fe_2O_3 increases or maintains the friction level [38]. However, Fe_2O_3 is also reported to have a tendency to decrease the friction coefficient compared to clean samples, depending on relative humidity [52]. Consequently, iron oxides produce low adhesion conditions, although the magnitude depends on the oxide types and other factors.

Both Fe_3O_4 and Fe_2O_3 (transformed into Fe_3O_4 during the reaction [53]) are discovered to act as a catalyst in the decomposition of biomass materials, which contain a high amount of cellulose [53], [54]. Although relatively high temperatures and pressures are required (e.g. 300 to 400 °C and 3.5 MPa) [54], these iron oxides enhance the chemical reaction, and also the production of gasification or dissolution into an organic solvent [53], [54]. Furthermore, Fe_3O_4 seems to act as a catalyst more than Fe_2O_3, because the transformation from Fe_2O_3 to Fe_3O_4 is observed after the reaction [53]. However, the detailed process of the chemical reaction related to the catalyst has not been clarified.

Overall, both Fe_2O_3 and Fe_3O_4 can be produced on the rail surface, and they seem to have a significant effect on tribological characteristics in the contact area as well as the chemical reaction between leaves and rail steels.

2.8.4 Cellulose

Cellulose is a glucose polymer and a predominant material in plant cells [36], [55], and it is one of the main components in biomass, which is recently re-evaluated as a green energy source [54], [56]. Cellulose is also contained in both leaves and leaf films, and it is expected to be one of the key materials which form a strong bond to the rail [2], [36]. Usually, cellulose is dissolved into water; however, it maintains a crystal structure and is not decomposed under normal circumstances [55], [56]. This suggests that special circumstances, such as high temperature and high pressure, are required to form a cellulose complex with other materials.

The usages of cellulose are varied, with cellulose being found in the manufacture of paper, foods, chemicals [56]. One interesting way to use cellulose is a source of adhesives [57]. This usage suggests that cellulose can be transformed into adhesive between the leaf residue and rail under certain conditions.

2.8.5 Lignin

Lignin is a polymer that forms plant cell walls [36], [58], and it accounts for 15-25 wt% of plant biomass material [59]. FT-IR analysis reveals that lignin is contained in leaf residue produced by laboratory experiments and thought to be the main component of leaf film [11], [16]. However, lignin is regarded as a structural material rather than a water-soluble material, and it seems to have nothing to do with the black coloured material formed with leaf extracts and steels [14]. Thus, lignin has not been the main focus of previous low adhesion research.

Recent studies in chemistry show that the long chain polymer structure of lignin can be broken down under high temperature and high pressure, which is sometimes a sub- or supercritical environment [58]–[63]. According to these studies, lignin is transformed into gas and dissoluble fragments in a relatively short time [58], depending on the experimental conditions. This result suggests that decomposition of leaf lignin might be possible under the wheel/rail contact, due to the high pressure and the high temperature.

Another aspect of lignin is that it can act as an adhesive, forming a polymer through crosslinking with other components, such as furfural and phenol [64], [65]. The properties as an adhesive of lignin are extremely strong, meeting 90% tensile strength of phenol-formaldehyde resin, which is commercially used in the wood industry [64]. In contrast to the advantages as an adhesive, this crosslinking reaction is a problem in the decomposition process [58]–[63]. The sub- or supercritical conditions degrade lignin into small fragments; however, they are concurrently re-polymerised through crosslinking effects [60]–[63]. As a result of re-polymerisation, these fragments sometimes produce solid residues, in particular, when the solvent is

only water [61]. These results indicate the possibility that the lignin-based adhesive could be formed with wet leaves on the rail, due to the high temperature and high pressure produced by the wheel/rail contact.

A hypothesis has been proposed, in which lignin has an important role in forming a strong bond between leaves and rails [36]. In this hypothesis, an iron carbohydrate complex is formed as an interfacial layer, and this carbohydrate is from lignin of the cell wall. Although there is no reported experimental research, lignin might be one of the key bonding materials.

2.8.6 Pectin

Pectin is a soluble chemical compound, which can exist in one of three forms, namely, protopectin, pectin and pectic acid [66]. One of the main features of pectin is that it is easily transformed into a gel. Divalent metal cations, such as Ca^{2+} and Cu^{2+}, change the pectin into gel with crosslinking effects [67], [68]. Studies of the leaf residue show that it is likely to contain pectate esterified to some extent and a relatively small amount of cellulose [14]. Due to the high solubility of pectin in water, pectin gel, which is probably crosslinked by Fe ions, is thought to produce low adhesion conditions [14]. The black colour of leaf films may be attributed to the chemical reaction between pectin and iron, and clusters agglomerated with cellulose fibres might form a bond [14]. This suggests that pectin is one of the key materials in the black layer for the strong bonds.

However, the effect of pectin has not yet been clarified. In particular, the mechanism by which pectin chemically reacts with other components is still unclear. For example, the detailed reaction process is not determined for the black colour formation, and the bonding strength of pectin gel has not yet been evaluated. Thus, further experimental work is required.

2.9 Research gaps

Research gaps were identified by a knowledge map generated by grading the cited academic papers.

2.9.1 Drawbacks of current studies and the derived models

Despite the significant progress in chemical conditions of leaf films, essential parameters, which control conditions of the chemical reaction in the leaf film growth, have not yet been determined. For example, few experiments have been carried out focusing on parameters, such as temperature, pressure and material. More studies need to be implemented with various parameters to specify the key factors, which produce low adhesion and strongly bonded leaf layers.

The models based on the previous studies have some drawbacks; the detailed process of the chemical reactions has not been demonstrated. For instance, the elements of the friction-reducing layer are clarified in the field-based model; however, it is not confirmed to what extent the detected elements contribute to the low adhesion and bonding mechanism. Moreover, few experimental works have been implemented to verify the other hypotheses of bonding mechanism. As a result, the bonding mechanism cannot be fully explained by these models or hypotheses. Hence, there is a need to perform more detailed chemical analyses, clarifying the low adhesion and strong bonds.

2.9.2 Paper grading

The citations used for this review have been graded to visualise the research area and determine what research has been carried out and where published research is lacking, using the same evaluation method as used in [69].

The citations are divided into four categories, namely, “General adhesion”, “Prevention”, “Fundamental research” and “Mitigation”. Each category has several groups, for example, the “General adhesion” category has groups such as academic research, laboratory testing and field testing. Some citations have several aspects, and as such belong to several groups. This is shown in combination forms with numbers and letters, such as 1A and 1B, which means paper 1 and aspect A or B.

After grouping, the paper is evaluated in seven areas as described below.

- Is the citation peer reviewed?
- Does the paper contain theory supported by testing?
- Is the test small scale?
- Is the test full scale?
- Does the citation contain real world measurements?
- Are the conclusions in the citation evidenced within the data?
- Are the conclusions validated by operational experience?

All the questions are “yes or no” interrogatory sentences, and “yes” obtains one point. Then, the citations are ranked into 3 categories by the accumulated points, namely, C (0-2), B (3-4) and A (5-7). For example, the citation obtains 3 yes scores, then the citation will get 3 points. In this case, the paper is ranked as “B”. The summary of this evaluation is shown in Appendix A. The score is not a reflection of

research quality, but more up score is associated with the full-scale tests than laboratory scale tests alone. Finally, the ranking results are shown as a knowledge map, which visualises the research area and scores. In this map, research gaps are shown as the areas marked with less density of circles, which means that there is no work or little work in this area.

2.9.3 Research gaps

Figure 2.9 shows the generated knowledge map with the score calculated in 2.9.2. As can be seen, “General adhesion” and “Mitigation” have many previous studies on their sub-categories. In contrast, there has not been much-published work in “Prevention” or “Principle research”. Furthermore, “Chemical” in the Mitigation has no previous work. Possibly, a lack of understanding of principles about leaf chemistry prevents developments of prevention methods or mitigations by chemicals, and these three areas or groups are still vacant. Consequently, exploring these fields should be worth trying to develop an innovative measure against leaf contamination.

Research gaps and details are summarised in the following lists:

- Parameter specifications (Principle)

Parameters which affect low adhesion conditions and strong bonds between the leaf film and rail should be identified by experiments and analyses. Namely, each material is separately tested, and then it is evaluated by mechanical and chemical analysis. This process could involve friction measurement, evaluation of bonding energy and chemical analysis with different materials and various conditions.

- Reaction process presumptions (Principle)

Based on the results of parameter specifications, the chemical reaction should be assumed and hypothesised. Further analysis or test might be needed to examine the ideas.

- Development of prevention or mitigation methods

Several methods for prevention and mitigation should be considered and tested. Field tests are ideal for the examination; however, a small-scale rig can be alternatively used to examine the idea.

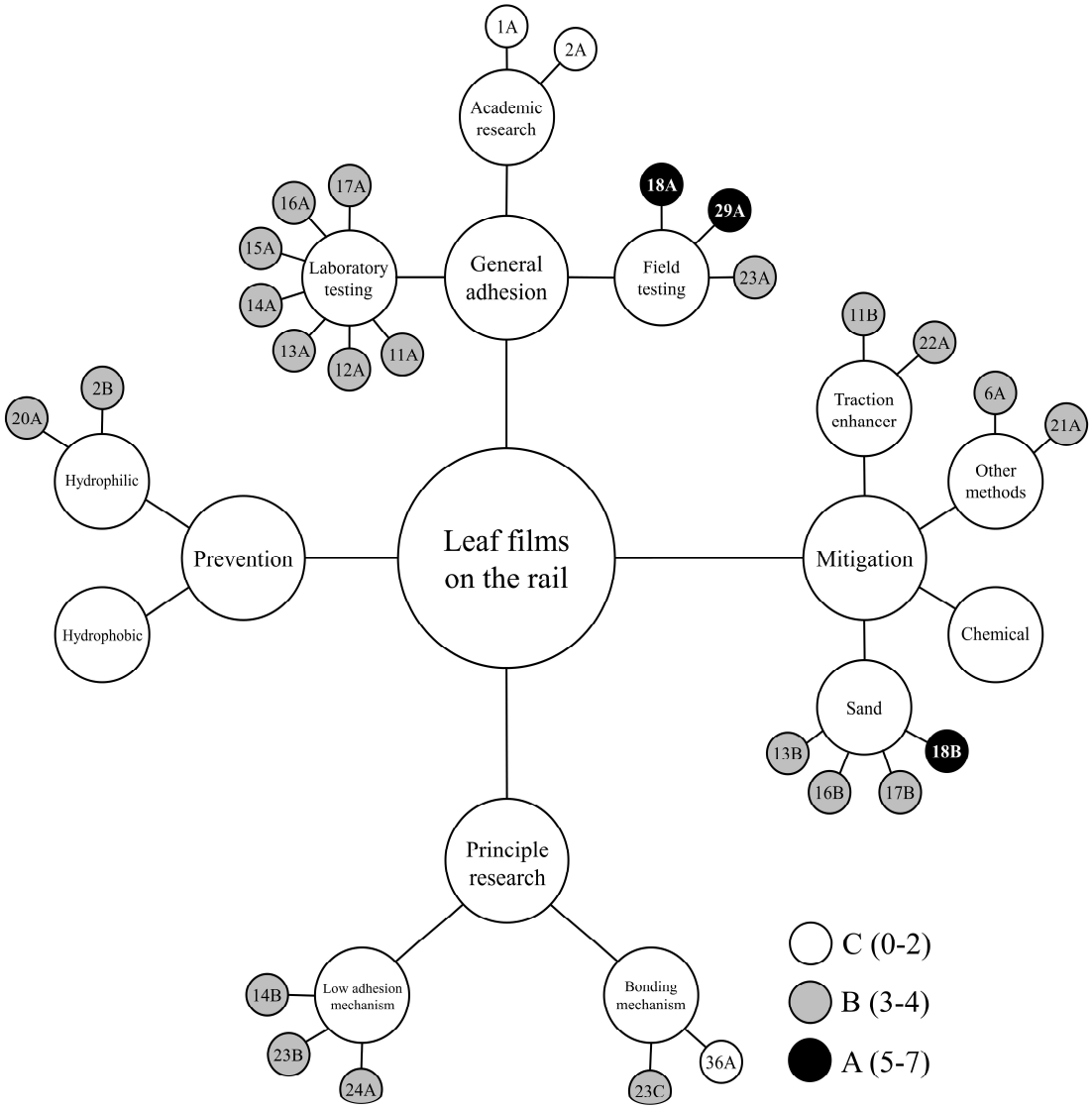

Figure 2.9 – A knowledge map of previous studies regarding leaf films on the rail

2.10 Conclusions

The main objective of this literature was to understand the phenomenon of low adhesion due to the leaf contamination on the railway track. In this literature review, firstly the operational data was analysed, and then the information related to the low adhesion due to leaf contamination was summarised. After that, the current mitigation method was reviewed, followed by a summary of the chemical analysis of leaf contamination. Furthermore, the suggested models of low adhesion and bonding mechanisms were studied, and then the expected parameters were considered focusing on pressure, temperature and materials. Finally, the research gaps were identified using the knowledge map. The main findings were listed below:

- Incident analysis with the operational data found the relatively high possibility of station overruns and SPADs between the hours of 05:00 to 10:00 and 20:00 to 24:00, which could be attributed to wet leaf films moistened by dew due to the high relative humidity in the morning and night.
- The friction/traction coefficient where leaf films are on the rail was identified as below 0.1 in both laboratory and field studies, which is categorised as a low adhesion level. Wet leaves tend to produce low friction/traction coefficients of around 0.05.
- Mitigation methods, such as sanding, traction enhancer and high-pressure water, were found to be effective to some extent; however, there are still some issues in terms of performance and cost.
- Chemical analysis of leaf contamination recently showed significant progress in the understanding of the interface between the leaf film and bulk rail; the mixed layer is likely to be formed, containing the leaf-derived organics and iron oxides.
- Several hypotheses were proposed based on the findings of the chemical analysis; however, they have not yet been experimentally examined and more detailed investigation is necessary for the better understanding.
- Key parameters for the chemical reaction were identified as follows: high pressure, high temperature, iron oxides, cellulose, lignin and pectin, which should be considered to be an important factor for the experiments performed in this study.
- The research gaps were identified as specifications of parameters for the low adhesion and bonding mechanisms, elucidation of the chemical reaction process and development of prevention or mitigation methods.

3 HYPOTHESES

Several hypotheses were developed from the literature review, to explain the mechanisms of low adhesion and strong bonds between leaf films and rails.

3.1 Introduction

As discussed in 2.7, the existing two models cannot fully explain the reasons why leaf films cause low adhesion and tightly adhere to the rail. To be exact, the detailed process of chemical reaction is not proposed, and thereby these mechanisms are unclear. Moreover, other hypotheses lack experimental evidences. Hence, more consideration should be taken: important factors for chemical reaction, key materials and theories of low friction and strong bonds.

In this chapter, factors to trigger the chemical reaction are firstly discussed, followed by proposal of a leaf contamination model, and finally developments of hypotheses.

3.2 Proposed factors for the chemical reaction

Figure 3.1 depicts a process of heat generation and following chemical reaction. As reviewed in 2.8, high pressure and high temperature can occur in the wheel/rail contact. In the case that wheels pass fallen leaves on the track, wheels are likely to slip on them. This slip could involve a large slip distance under high contact pressure, followed by friction heat generation. The high temperature due to the friction heat could enhance the chemical reaction between leaves and rail steels, discharging organic components from leaves as well as iron ions from the rail. After the fleet passes by, the rail is gradually cooled down, and the bonding layer between the top leaf layer and the bulk rail could be formed.

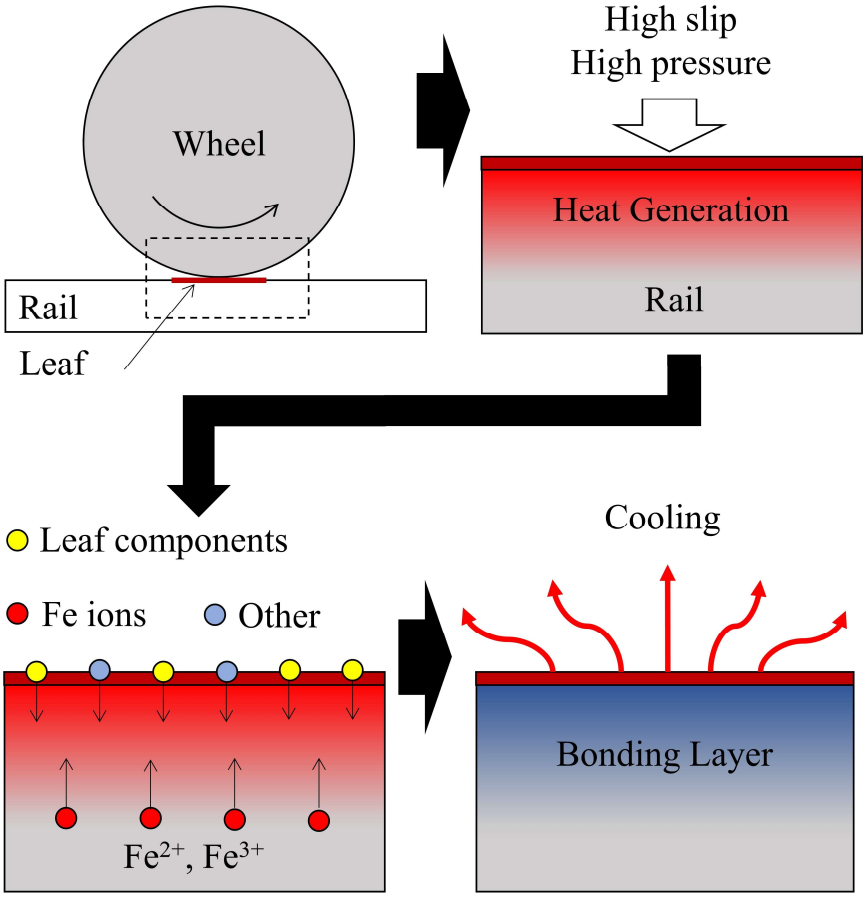

Figure 3.1 – Generation and reaction process with high pressure and temperature

Figure 3.2 illustrates a schematic figure of model proposed in this study. After the heat and pressure application by wheels, three-layer structure is supposed to be formed: a leaf layer on the top, a bonding layer in the middle and a bulk rail steel at the bottom. In another way, the leaf layer is bonded to the rail via the bonding layer. The bonding layer could have an intermediate property between leaf organics and rail steels, acting as a buffer layer which is a common technique to relax a lattice mismatch between films and substrates and to improve the film quality. The bonding layer could work analogously to the buffer layer, forming a strong bond.

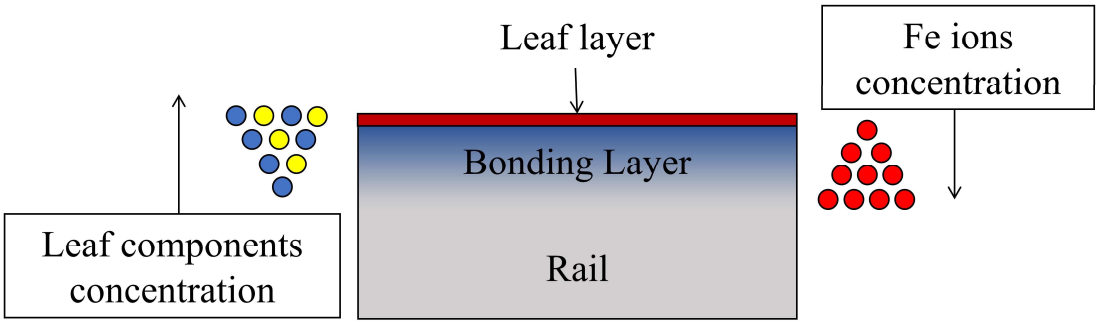

Figure 3.2 – Schematic figure of proposed model

3.3 Hypotheses for low adhesion

There are several arguments regarding the reason why the leaf residue causes low adhesion. However, the main cause has not yet been determined because of the many parameters, such as relative humidity, third bodies and temperature. Therefore, some hypotheses were proposed to consider the main cause of low adhesion, focusing on how leaves work as a lubricant.

3.3.1 Bulk leaf

This hypothesis assumes that there are many fallen leaves on the line because of strong winds, as shown in Figure 3.3. If wheels pass over the leaves, they are compacted and adhered to the rail. During the wheel passages, leaves might act as a solid lubricant because the thickness will be large enough to prevent metal-to-metal contact. Consequently, the friction coefficient on the contact area is lowered. After the wheel passages, natural third body layers, namely, leaf films, are presumably formed, and the low adhesion problem continues for a long time.

Both laboratory experiments and experiences in train operation support this hypothesis. It is demonstrated that continuous applications of leaves into the contact area of a twin disc machine produce a low friction/traction coefficient (<0.05) in both dry and wet conditions [13]. Furthermore, train operation is often suspended or delayed because of sudden and heavy leaf falls, which is caused by strong winds.

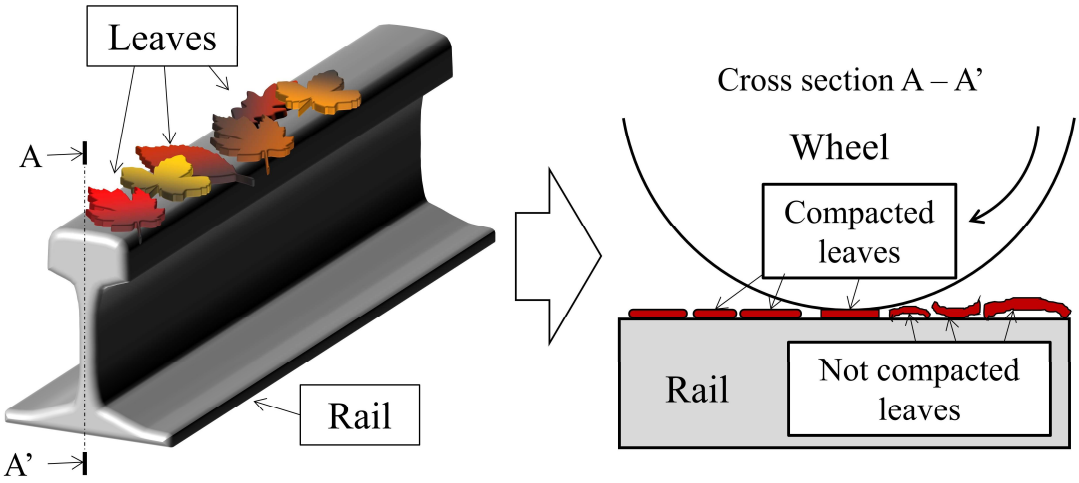

Figure 3.3 – Low adhesion due to bulk leaves fallen on the line

3.3.2 Adhered leaf film in dry and wet conditions

In this hypothesis, the leaf film is assumed to work as a lubricant in both dry and wet conditions. The terminology “leaf film” is different from a bulk leaf; it means an adhered and black leaf residue in the running band, which is composed of both the leaf layer and bonding layer in Figure 3.2. As the leaf film should contain a lot of iron oxides and leaf-related organics, it can possibly cause low friction conditions.

Figure 3.4 shows a schematic view of the low adhesion mechanism of leaf films in dry conditions. In dry conditions, a friction reducing layer works as a third body layer and lowers friction levels, because of its rich amount of iron oxides and leaf-related organics. Iron oxides can decrease the friction coefficient, and the residual leaf organics might cause low adhesion. As a result, lower adhesion can be expected when they are mixed as a leaf film.

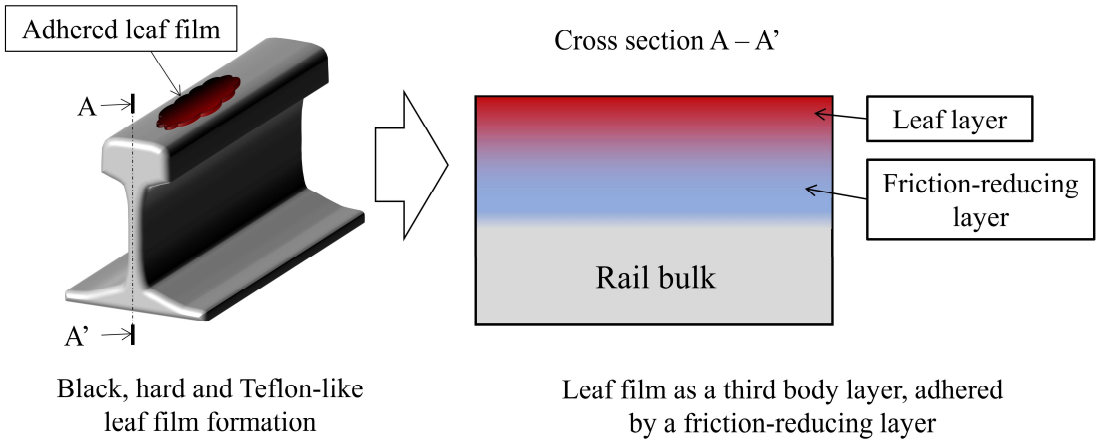

Figure 3.4 – Low adhesion due to adhered leaf films in dry conditions

Figure 3.5 shows the low adhesion mechanism in wet conditions. In this hypothesis, leaf films are supposed to absorb water, such as dew formed on the rail surface, and then they are deteriorated or softened, making a gel-like substance of leaf film. This soft material made of iron oxides and leaf-related organics could cause poor friction level.

Leaf films created on test specimens were confirmed to lower friction coefficients [11], [15], [16], [22]. Furthermore, the statistical data of train operation in 2.3 suggests that morning dew affects adhesion condition and increases the number of accidents. All the information above supports this hypothesis.

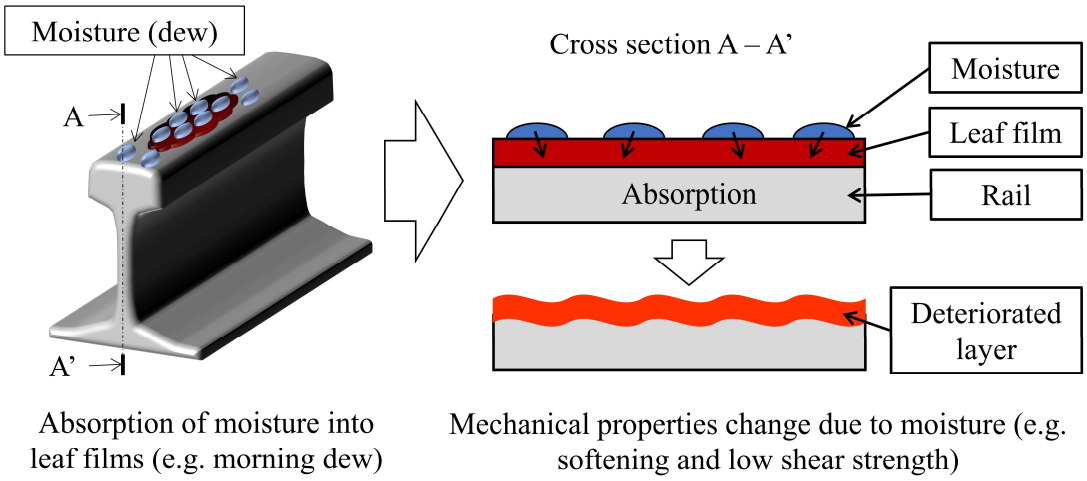

Figure 3.5 – Low adhesion due to adhered leaf films in wet conditions

3.3.3 Pectin gel

This hypothesis is based on the suggestion that the pectin gel forms a slippery film on the surface, which is discharged from the leaf residue [14]. Figure 3.6 shows the low adhesion mechanism when pectin gel is formed with water and leaf film. FT-IR analysis demonstrated that pectin and cellulose are likely to be a water-soluble component, and pectin transforms into the pectin gel by reacting with Fe ions [14]. Therefore, this pectin gel on the leaf film is thought to form lubrication films, leading to low friction conditions. Furthermore, it is suggested that EHL films (elastohydrodynamic lubrication) might be formed due to the gel's high viscosity, although it depends on the speed range [14].

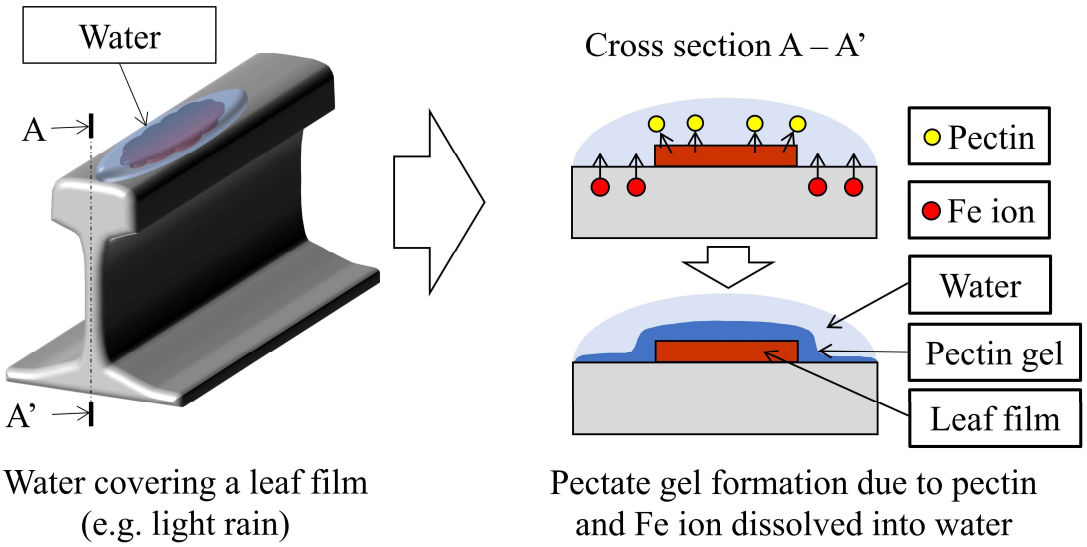

Figure 3.6 – Low adhesion due to pectin gel formed with water and leaf film

To sum up, four hypotheses were proposed in this study: bulk leaf, adhered leaf film in dry and wet condition, and pectin gel. These theories will be examined by experiments in this study.

3.4 Hypotheses for strong bonds

Based on the model, three hypotheses for the bonding mechanism have been developed.

3.4.1 Sub- or supercritical water

Generally, leaf components, including lignin, are stable material, and they are not easily decomposed into fragments. However, they can be decomposed under sub- or supercritical conditions where temperature is greater than 374.2 °C and pressure greater than 22.1 MPa (Critical point). The schematic figure of this idea is shown in Figure 3.7. As described in section 2.8.1 and 2.8.2, high temperature (ex. over 727 ˚C [49]) and high pressure (ex. 0.6 – 2.7 GPa [50]) are achievable in the contact area.

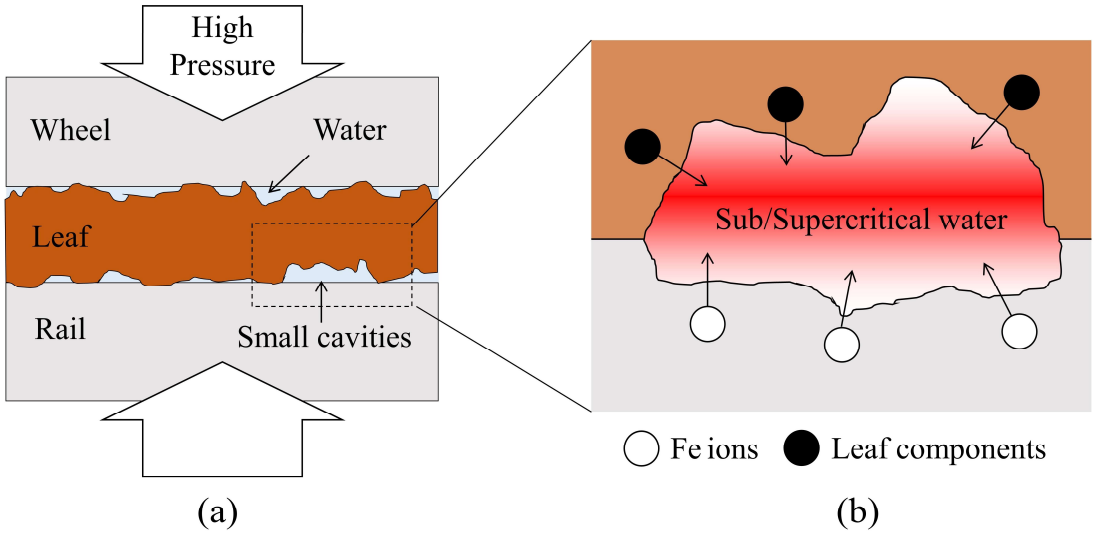

Figure 3.7 – A dissolution process of leaf components and Fe ions
(a): Small cavities filled with water between the leaf and rail under high pressure
(b): Zoomed in, leaf components and Fe ions dissolved into water under sub or supercritical conditions (Pressure>22.1 MPa and temperature >374 °C)

The reaction process is divided into four steps. As a first step, the high pressure is applied to wet leaf films on the rail surface as shown in Figure 3.7 (a). Then, the contact temperature increases due to thermal energy induced by sliding in the contact, and the water in the leaf film becomes sub- or super critical. During the sliding, leaf components and Fe ions are discharged from leaves and rail surface, and they are dissolved into the sub/super critical water as shown in Figure 3.7 (b).

Subsequently, the dissolved leaf components react with Fe ions, and a mixture of this material is formed. Finally, a bonding layer is formed after cooling.

3.4.2 Catalyst function of iron oxides

Figure 3.8 shows a decomposition process of leaf components due to iron oxide catalyst. Iron oxides have a catalyst function, which enhances the decomposition of cellulose or lignin with high temperature and high pressure. Although the magnitude of the catalyst function is not significant [53], [54], the active surface of iron oxides accelerates decomposition of leaf components more than under normal conditions.

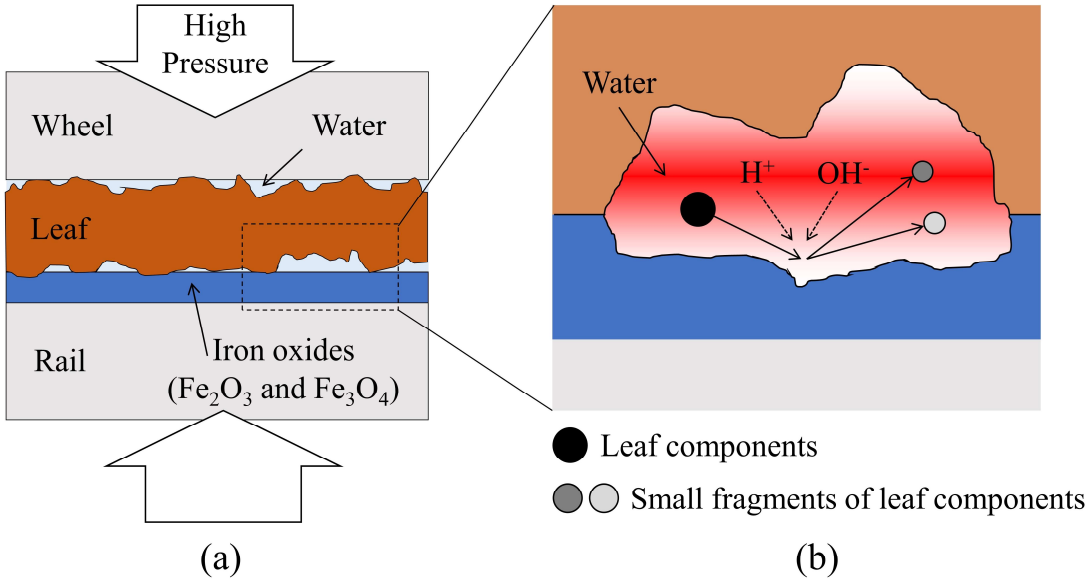

Figure 3.8 – A decomposition process of leaf components with the iron oxide catalyst
(a): A contact condition with the surface iron oxides such as Fe_2O_3 and Fe_3O_4
(b): Zoomed in, degradation process of leaf components into small fragments with the assistance of iron oxide catalysts

There are three steps in the degradation process due to an iron oxide catalyst. First of all, high temperature and high pressure are applied to wet leaf films on the iron oxide film formed on the rail surface. After that, leaf components, such as cellulose and lignin, are dissolved into the water, subjecting any water in the contact to sub/supercritical conditions. Immediately, dissolved components are decomposed into small fragments on the surface of iron oxides, such as Fe_2O_3 and Fe_3O_4. In this step, iron oxides work as a catalyst. Finally, these fragments react together, or react with Fe ions discharged from the surface, and a bonding layer (mixing layer) is formed.

It is noteworthy that this hypothesis has a close relationship to the sub/supercritical hypothesis; both of them need high temperature and high pressure for chemical

reaction. Therefore, chemical reactions based on these two hypotheses could occur concurrently.

3.4.3 Cellulose or lignin adhesives

Figure 3.9 depicts a schematic figure of mechanical interlocking principle of leaf adhesives. In this hypothesis, dissolved leaf components and Fe ions are assumed to form an adhesive layer after chemical reaction because cellulose and lignin have properties as an adhesive, as described in 2.8.4 and 2.8.5. Although there are many mechanisms regarding adhesives, one of the main theories is mechanical interlock theory, which explains that adhesive material fills surface asperities and anchor the two materials [70].

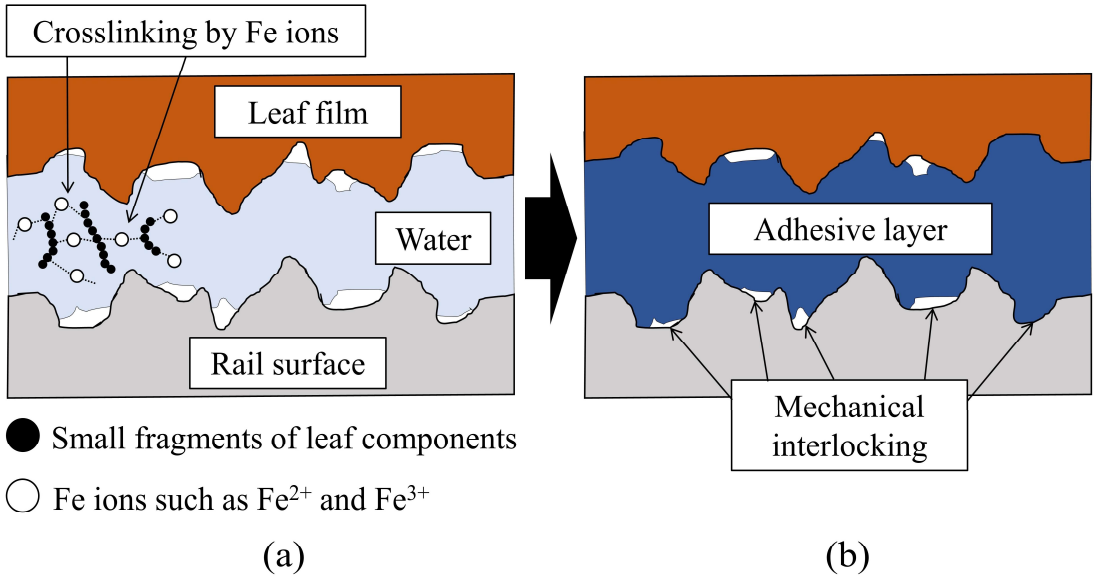

Figure 3.9 – A schematic figure of adhesive layer formation
(a) Re-polymerisation process through crosslinking by Fe ions
(b) Mechanical interlocking by adhesive layers produced by re-polymerisation

The process of adhesive formation can be divided into three steps. First, leaf components and Fe ions are dissolved into water, and leaf components are decomposed into small fragments. Following the decomposition, the small fragments are cross-linked by other elements, such as Fe ions. Through this crosslinking, decomposed fragments are re-polymerised in the water. As a result, an adhesive layer is formed by the re-polymerisation process, filling the asperities on the rail surface. Since the water easily penetrates the surface roughness, the adhesive effect might be strong due to mechanical interlocking.

3.5 Conclusions

Several hypotheses were proposed to explain the low adhesion mechanism as well as the bonding mechanism, based on the information attained in the literature review. Four hypotheses were proposed for the explanation of the low adhesion mechanism: bulk leaf, adhered leaf film in dry conditions, adhered leaf film in wet conditions and pectin gel. Three hypotheses of the bonding mechanism were also proposed as follows: sub- or supercritical water, catalyst function of iron oxides and adhesives of cellulose or lignin. These hypotheses need to be demonstrated by experiments.

4 BASIC TRIBOLOGY OF LEAVES: A BALL-ON-FLAT TEST

4.1 Introduction

This chapter investigates basic tribological properties of leaves, which were measured with leaf and leaf-related samples. The aim of these tests is to identify the key leaf materials for the low adhesion and examine the hypotheses in 3.3.

4.2 Samples

Figure 4.1 illustrates typical images of green and brown leaf samples. Sycamore leaves were chosen as they are recognised as one of the problematic leaves [1], [2], [71], and they have been found to cause low adhesion conditions in previous work [11], [14], [22], [35]. Both green and brown leaves were collected in the garden of St. George's lecture theatre in Sheffield, S1 4DP. The green leaves were taken from the branches between October and November 2016 and kept in a freezer to minimise decay. The brown leaves were picked up at the same location between November and December 2015 and kept at room temperature.

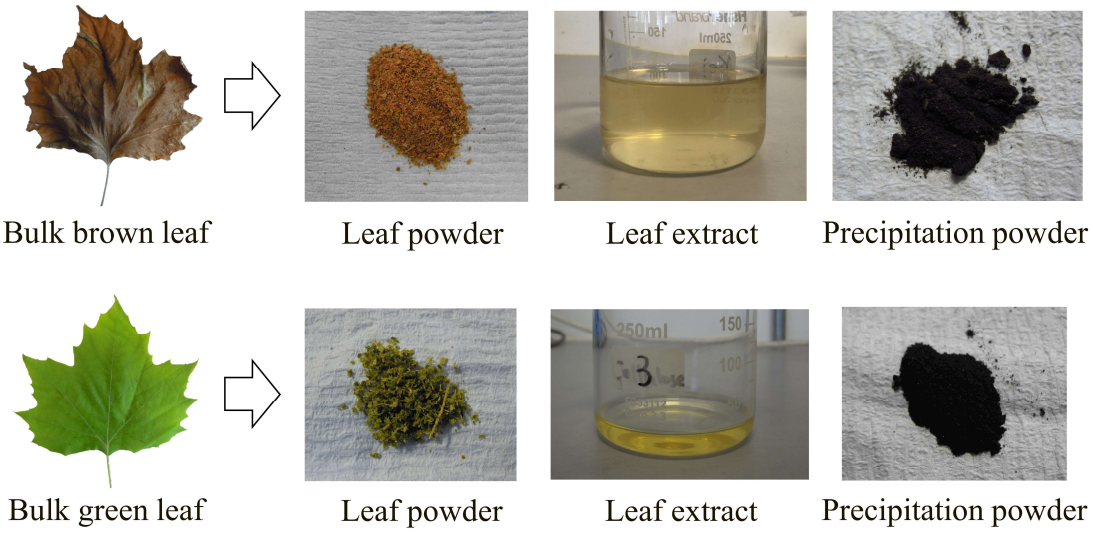

Figure 4.1 Typical images of leaf samples

4.2.1 Leaf powder

Figure 4.2 illustrates the preparation process of the leaf powder (LP). Firstly, the bulk leaves were put in the general food processor and chopped into small pieces. After that, the leaf pieces were filtered using a general tea strainer, removing the big pieces (leaf mulch). The typical size of the brown powder is between 15µm and 300µm; the green powder is between 100µm and 800µm, measured with an optical

microscope. This difference in the size could be attributed to the brittleness of leaf, which means that green leaves are more ductile than brown leaves. After the filtering process, the brown leaf powder (BLP) was stored at room temperature, and the green leaf powder (GLP) was tested immediately after the screening process.

It should be noted that leaf mulch was not used for the ball-on-flat test due to less fluidity of leaf mulch and water mixture. As described later in 4.3.1, the ball-on-flat method measures a friction force between the ball and rail plate, and it needs the constant presence of sample in the contact area. As a result of trial tests, it was confirmed that the wet leaf mulch (five wt%) was likely to be removed from the contact area after a few cycles of reciprocating. From the viewpoint of repeatability, this behaviour was undesirable; therefore, leaf mulch was excluded as a testing sample.

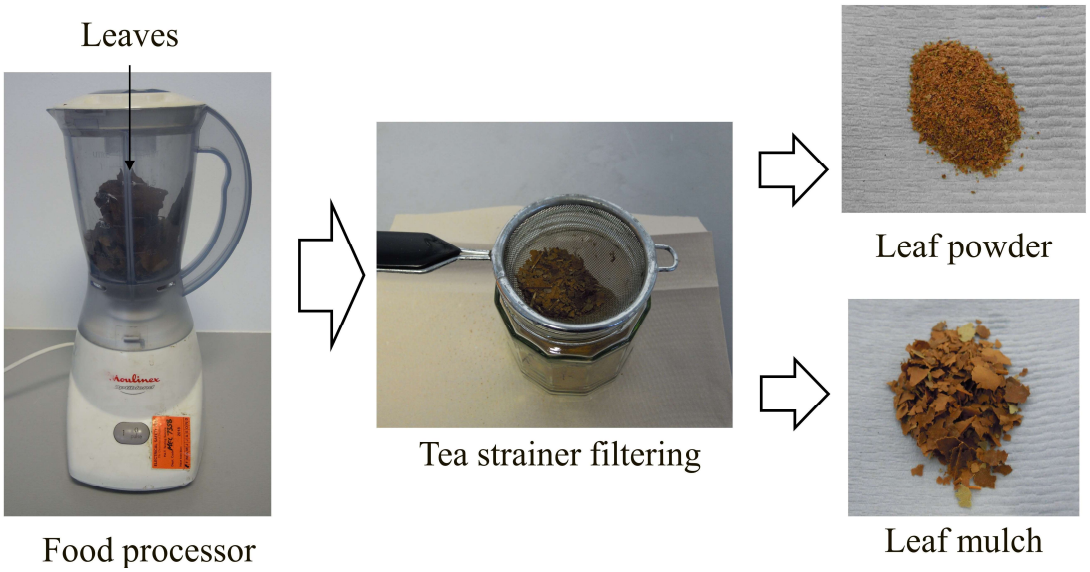

Figure 4.2 Preparation process of leaf powder

4.2.2 Leaf extract

Figure 4.3 shows the preparation process of the leaf extract (LE). The leaf mulch was used for leaf extract preparation. The ratio was typically 1g (leaf mulch):50 ml (distilled water), according to the previous study [14]. After the immersion of leaf mulch, the mixture was typically left for one day to eight days, depending on the purpose of the experiment. Before the friction test, the leaf extract was filtered with filter-paper, removing small particles.

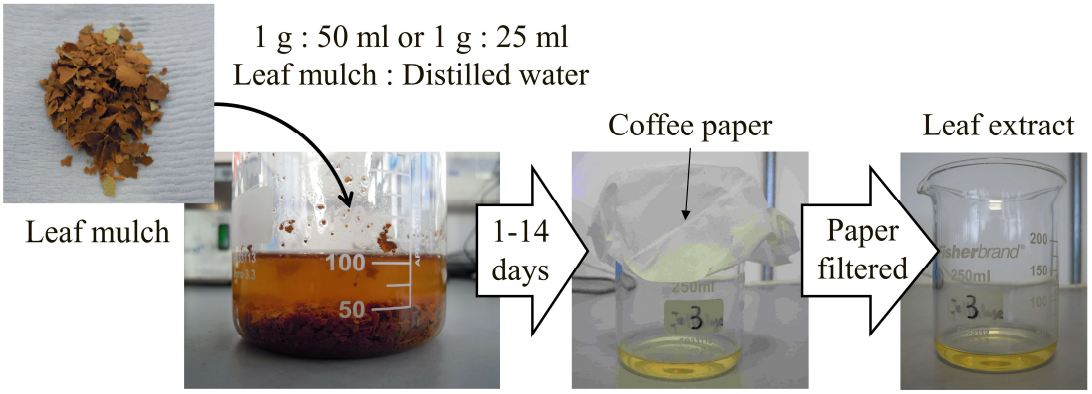

Figure 4.3 Preparation process of leaf extract

4.2.3 Leaf film

Figure 4.4 depicts set-up of the PLINT TE77 which was used to form leaf films (LFs) on the rail steel plates. The PLINT TE77 can apply a compressive force up to 250 N, to a moving head which is placed on a plate. The plate is fixed in the oil bath, and there is a heater and force sensor under the oil bath. The heater can raise temperature up to 600 ºC. The head is reciprocated with a stroke of 15 mm, by a rotating motion converter and motor. Figure 4.5 shows the head with two track rollers, which was originally developed for this study. The lower roller presses leaf materials in pure rolling conditions, forming a leaf film on the rail plate.

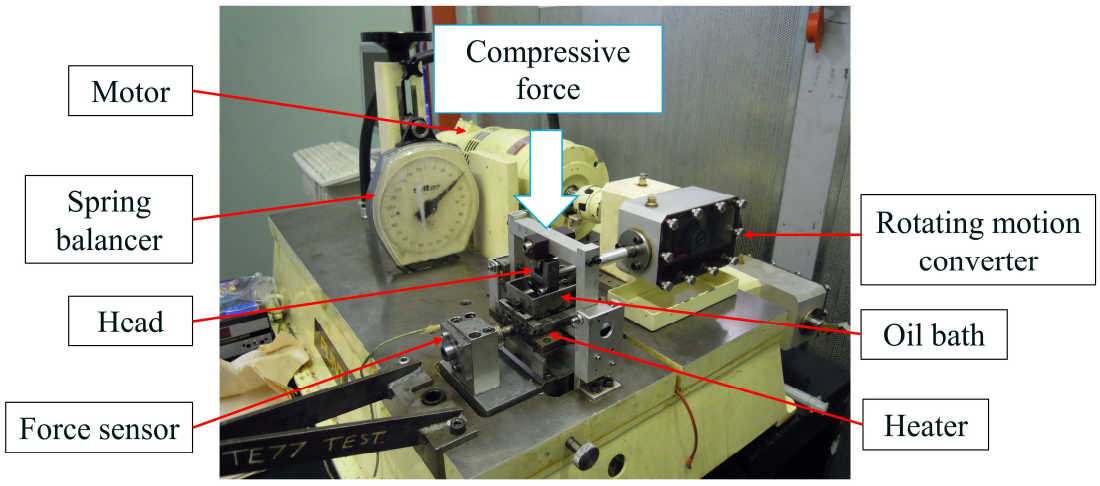

Figure 4.4 PLINT TE77 for leaf film creation

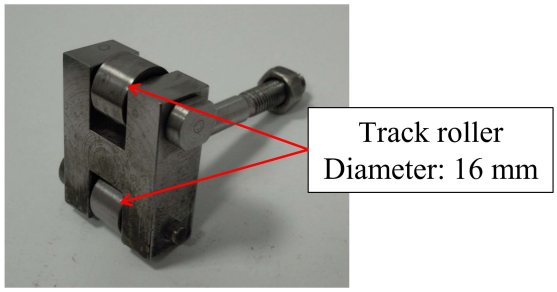

(a)

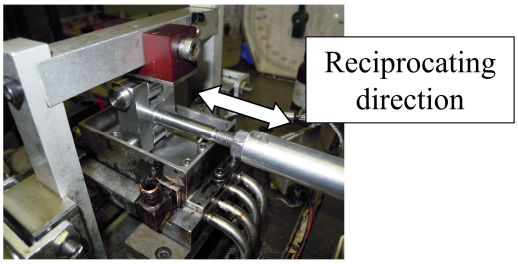

(b)

Figure 4.5 Original head with two track rollers
(a) Head, (b) Head movement

Table 4.1 shows a summary of parameters in the leaf film formation. The whole creation process is described below. Step 4 to 6 are illustrated in Figure 4.6.

1. The temperature is increased to 200 ºC.
2. The head is operated at 200 N for 120 seconds as a pre-treatment.
3. The head operation is stopped.
4. The leaf powder suspension (5 wt%) is applied to the contact area by a spatula.
5. The head is operated at 60 rpm (1 Hz) for 15 s.
6. The head operation is stopped.
7. Repeat steps 4 to 6 several times, consuming 6 – 7 ml/film on average.
8. The experiment is ended after 150 seconds, approximately 90 – 120 rolling times on average.

Table 4.1 Summary of parameters in leaf film formation

Parameter	Value
Applied force (N)	200
Hertzian pressure (MPa)	285
Temperature (°C)	200
Frequency (Hz)	1
Rolling (cycles)	Typically 90 – 120
Material	5 wt% green/brown leaf powder suspension Typically 6 – 7 ml/film

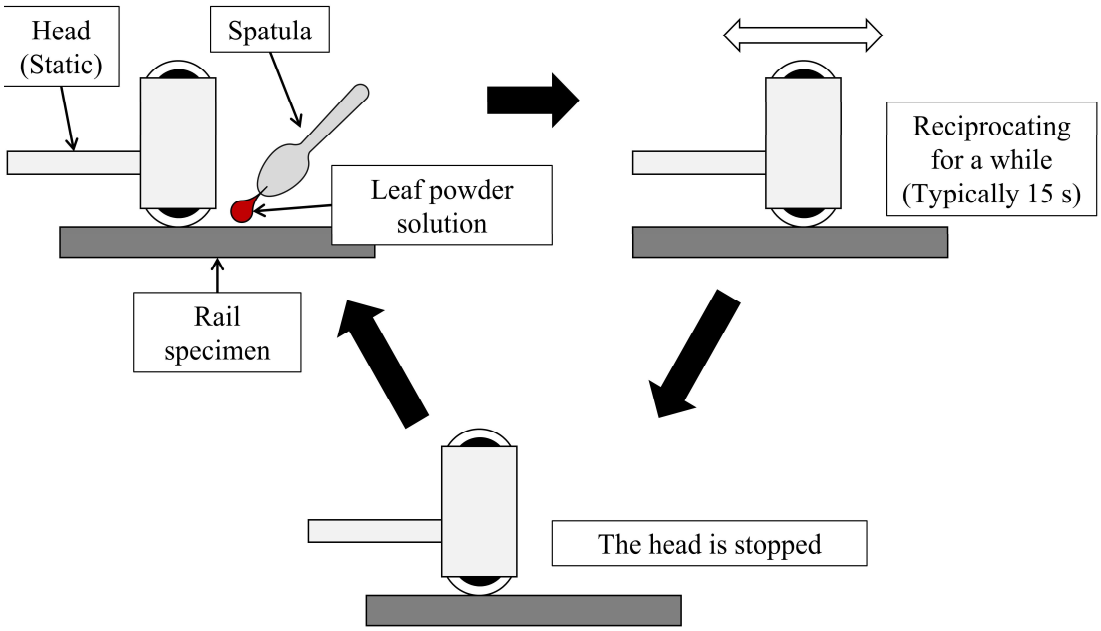

Figure 4.6 Standard process of leaf film creation

The temperature was fixed at 200 ºC since the created LF seemed to adhere to the rail plate most strongly in comparison with the LFs at room temperature, 50, 100, 150 and 250 ºC. This temperature is achievable in the wheel/rail contact when the wheel slips on the rail. The compressive force 200 N was applied, producing 285 MPa on average. The actual pressure between the wheel and rail is from 600MPa upwards [40]; however, 285 MPa is the maximum value due to the strength of axle which supports the track roller. The amount of suspension was typically 6 – 7 ml per film, although the amount was not precisely controlled.

4.2.4 Black precipitation powder

The black colour has been reported as one of the characteristics of leaf films [1], [2], and leaf extract has been known to form a black material after the friction test [14]. Pectin in leaf extracts seemed to cause the chemical reaction with the rail steels, and this black material could be one of the candidates of low adhesion material. Therefore, the friction features of the black material were individually tested to find out the cause of low adhesion. The black precipitation was successfully synthesised with leaf extracts and rail steels after several trials.

Figure 4.7 illustrates the preparation process of black precipitation powder (BP). Firstly, 200 to 250 ml leaf extract was prepared in the way described in 4.2.2. After that, the flat specimen made of rail steel (R260) was immersed in the LE from one day to three days. Usually, the colour of the green leaf extract started changing to black after the immersion in minutes, suggesting that the chemical reaction had occurred. In contrast, the brown leaf extract needed more time than green leaf extract for the colour change to occur, which usually happened in an hour. After the black precipitation had been formed, the leaf extract was boiled on a hot plate until the water was completely evaporated. Finally, the dried precipitation at the bottom of the beaker was collected and ground in a stone mortar. Typically, the size of the black precipitation powder was between 10 μm and 100 μm, measured with an optical microscope. The amount of black precipitation was always larger in green leaf extracts and smaller in brown leaf extracts.

It is noteworthy that the artificial pectin solution (0.1 wt%) did not form the black material at all, suggesting that the other material is necessary for the formation of BP.

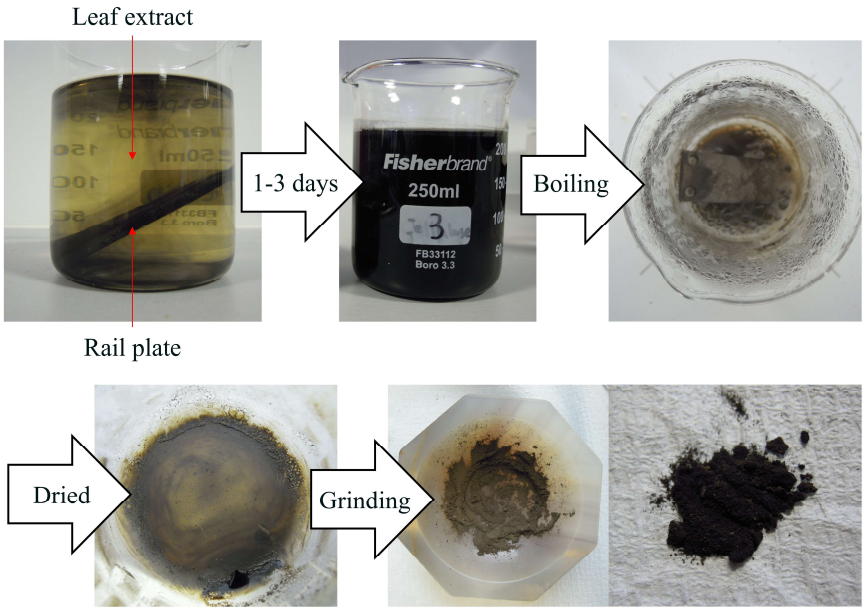

Figure 4.7 Preparation process of black precipitation powder

4.3 Methodology

4.3.1 Machine set-up

Figure 4.8 shows a schematic view of the test set-up. A Bruker UMT was used for the ball-on-flat tests. A 5 mm stainless steel ball was pressed on a rail plate at 10 N which corresponds to the maximum Hertzian contact pressure of 1.6 GPa. After the force had reached 10 N, the ball holder reciprocated for 6 minutes with a 10 mm stroke at 10 mm/s as a set value.

The calculated contact area was $9.3 \cdot 10^3$ μm^2, and the size of leaf powder distributed between $0.7 \cdot 10^3$ and $2.0 \cdot 10^6$ μm^2.This distribution is one of the scale effects of this method; the actual leaf contamination always happens where the leaf is larger than the wheel/rail contact patch.

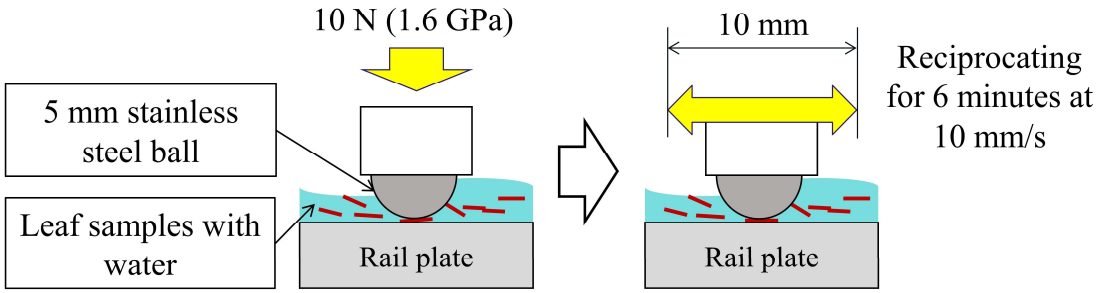

Figure 4.8 Schematic view of the test set-up

Table 4.2 summarises the experimental parameters used in the friction tests. The tests were conducted with 0.2 ml solution or suspension, and the LF with 0.2 ml of distilled water. The liquid sample was directly applied on the plate by a syringe. In the case of leaf films, 0.2 ml of distilled water was applied to the surface. Additionally, pure distilled water, engine oil (Servol 15W-40, Morris lubricant) and pectin 0.1 wt% solution (Pectin from citrus peel, P9135, Sigma-Aldrich, CAS number: 9000-69-5) were measured as a baseline to compare the results.

Table 4.2 Experimental conditions

Parameter	Value
Applied force [N]	10
Maximum Hertzian pressure [GPa]	1.6
Time [seconds]	360
Stroke [mm]	10
Frequency [Hz]	0.4
Sampling frequency [Hz]	100
Top stainless-steel ball diameter [mm]	5
Sample amount [ml]	0.2
Concentration (LP and BP) [wt%]	5

4.3.2 Analysis of the data

Figure 4.9 shows an example of raw data, both overview and zoomed-in. As the head moved forward and backwards, the friction force was recorded both positively and negatively. The ball was reciprocated at 0.4 Hz, and the actual interval was around 2.57 seconds.

Friction coefficient μ was obtained by dividing the friction force by the normal force, 10 N. Then, the average value of friction coefficient was calculated for every 20 seconds. The friction tests were repeated at least three times. Finally, the average friction coefficient was calculated; each mean value at every 20 seconds was totalled, and the sum was divided by repeating times. The standard deviation was calculated as an error at this stage.

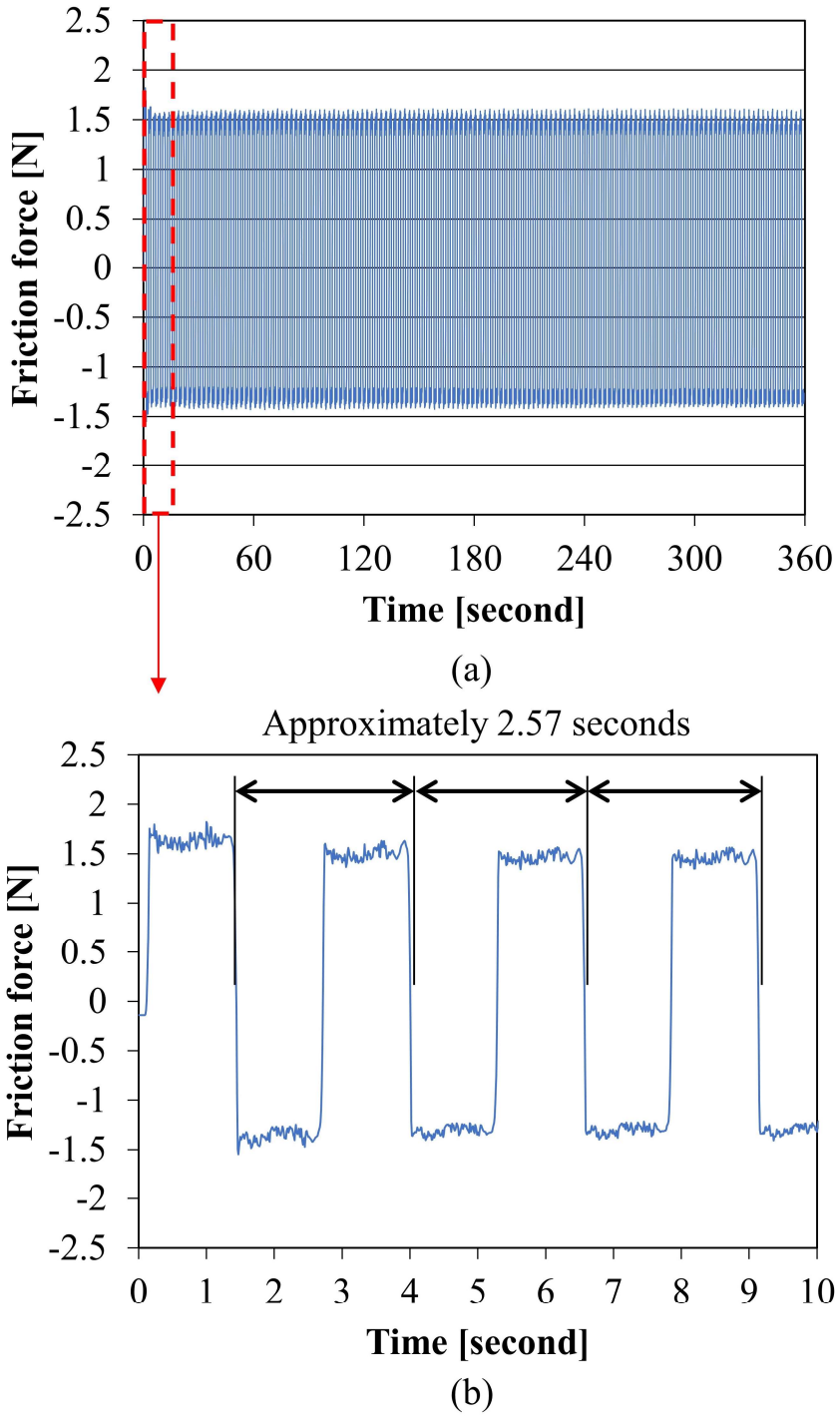

Figure 4.9 Example of raw data (Engine oil 0.2 ml)
(a) Overview of raw data, (b) Zoomed-in between 0 and 10 seconds

4.4 Results

Friction properties of both green and brown leaves are presented below along with discussion of the possibility of each hypothesis for low adhesion.

4.4.1 Leaf powder

Figure 4.10 and Figure 4.11 illustrate the change in the friction coefficient of green leaf powder (GLP) and brown leaf powder (BLP), respectively. The error bar (standard deviation) was shown only for the baselines to simplify the graphs. As can be seen, both GLP and BLP suspensions showed lower friction levels than the distilled water and pectin solution. In particular, they demonstrated lower friction than the engine oil until 60 seconds, and then they reached the same level at 80 seconds. After 80 seconds, GLP and BLP suspensions exhibited an increase in friction coefficient, resulting in the friction coefficient around 0.2. The initial low friction should be brought by the LP in the contact between the ball and rail plate; it seemed to prevent the metal-to-metal contact, lowering the friction coefficient than the engine oil. It should be noted that the leaf powder in suspension was gradually removed from the contact area as the experiment proceeded, and this removal could be the reason of the gradual increase in friction coefficients after 80 seconds.

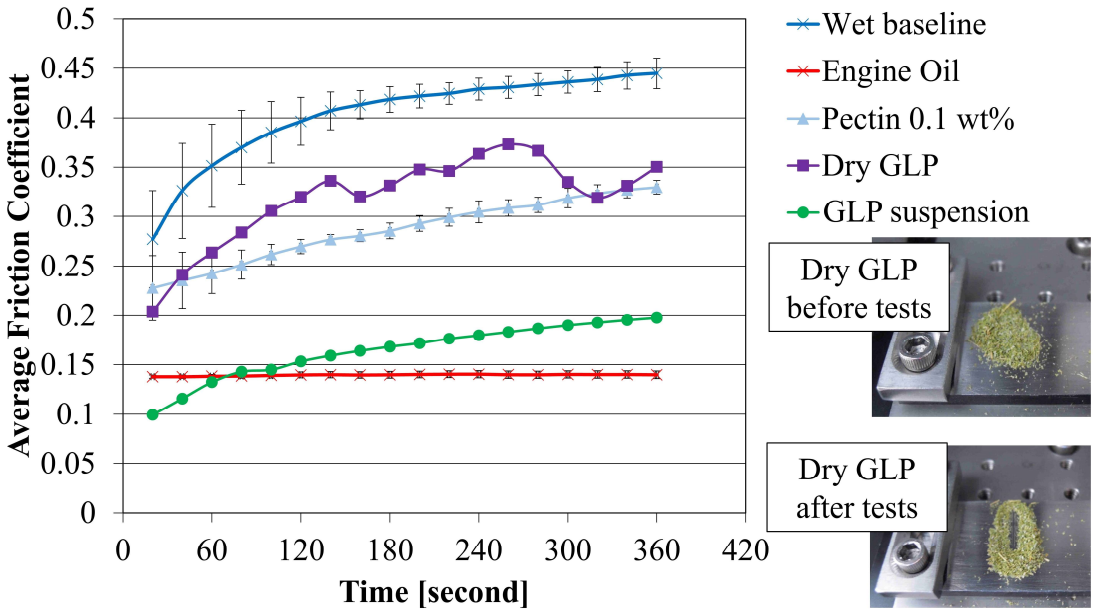

Figure 4.10 Friction properties of green leaf powder

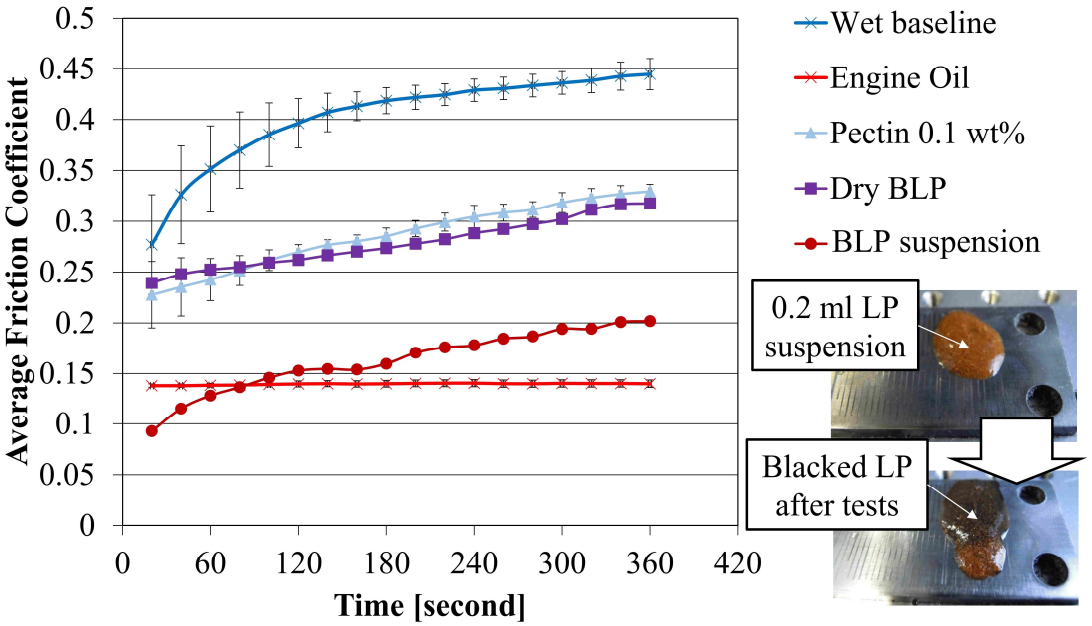

Figure 4.11 Friction properties of brown leaf powder

In contrast to the suspension, both dry GLP and BLP showed relatively high friction coefficient. The dry GLP showed around 0.2 for the first 20 seconds and increased the friction coefficient with some fluctuation, ending around 0.35 after 6 minutes. The dry BLP exhibited a relatively mild increase, starting from the friction coefficient around 0.25 and reaching slightly over 0.3 after the continuous increment for 6 minutes. These friction levels are lower than the wet baseline, however, it is not significantly low compared to the engine oil. It should be noted that the dry samples were removed from the contact area, quicker than the suspension samples.

As a result, it was found that the leaf powder suspension caused low adhesion, but the dry leaf powder did not. This difference indicates two possibilities; some materials dissolved into the water lowered the friction level; the water helped the leaf powder being caught in the contact area. Since the dry powder showed the medium level of friction from the beginning, it is expected that leaf powder is not a significant cause of low friction. The combination effect of the dissolved material and solid leaf should cause the low friction.

One of the interesting findings in the test was that the colour of BLP suspension was turned to black. This change could be the same phenomenon which is often seen in the field.

4.4.2 Leaf extract

Figure 4.12 illustrates friction characteristics of green leaf extracts (GLE). All the GLEs, except for GLE for one day, showed a medium level of friction between 0.2 and 0.3 for 360 seconds. This friction level was lower than distilled water and pectin

solution, taking into account the error bars which were typically 0.01 – 0.02 or lower. Furthermore, the immersion time of GLEs did not affect the friction level. For example, GLE three days exhibited lower friction coefficient than GLE five days.

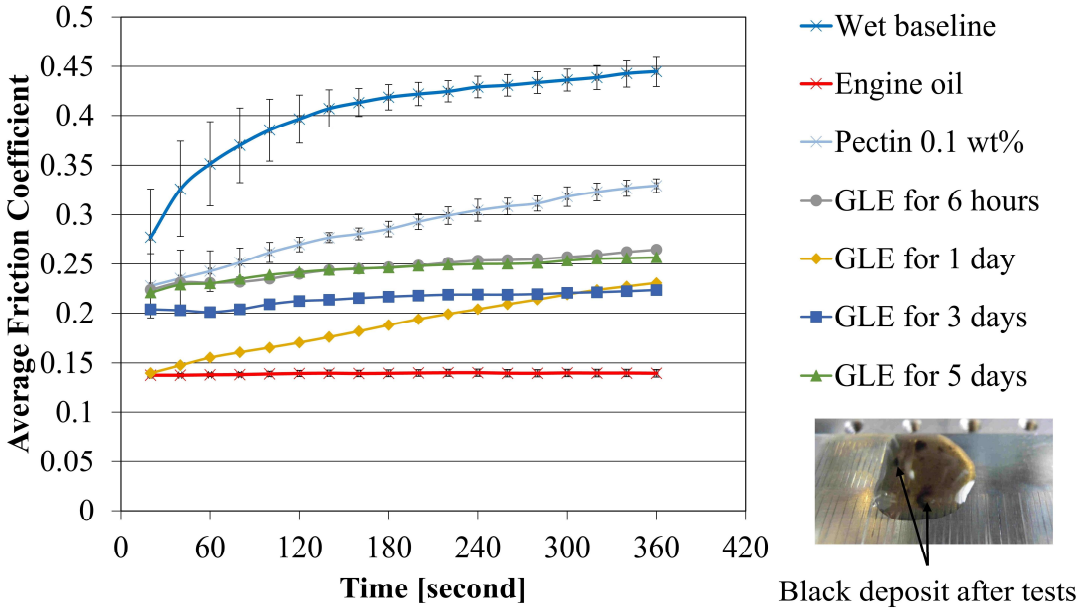

Figure 4.12 Friction properties of green leaf extracts

Figure 4.13 depicts friction characteristics of brown leaf extracts (BLEs). All the BLEs exhibited medium-low friction levels; it is lower than the distilled water and pectin solution but higher than the engine oil. Like GLEs, there was no clear relationship between the friction coefficient and immersion time; all GLEs showed around 0.15 for the first 60 seconds and increased the friction level around 0.25.

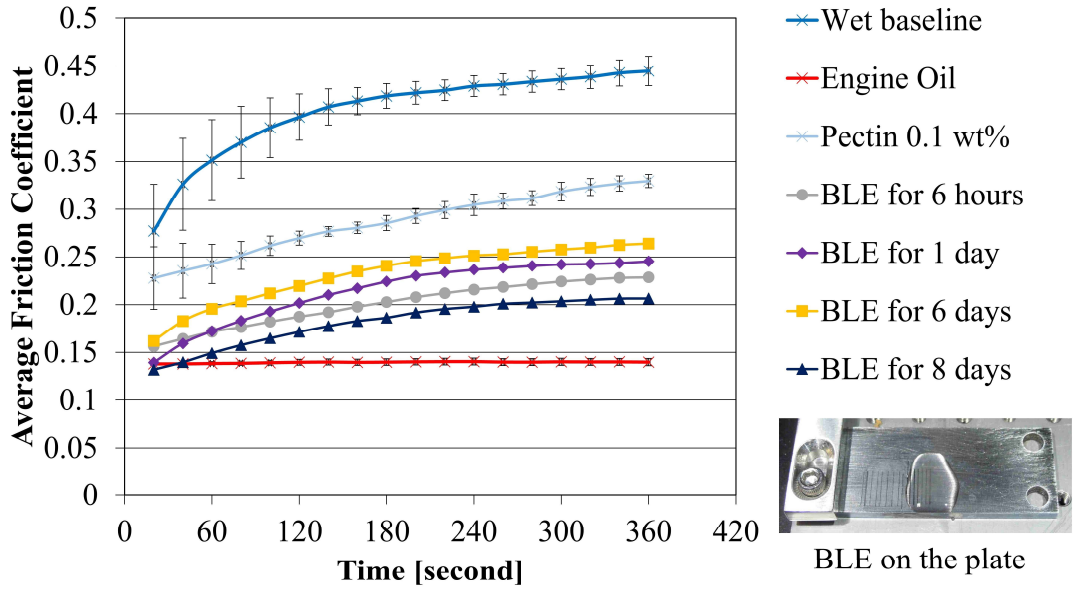

Figure 4.13 Friction properties of brown leaf extracts

These two results indicate that the both green and brown leaf extract had some unique material dissolved into the leaf extracts. It could cause the medium-low friction conditions and maintain the friction level, as seen in Figure 4.12 and Figure 4.13. Considering the results described in 4.4.1, LE might combine with LP and cause lower friction than the single leaf extract. Furthermore, that material can be extracted with relatively short immersion time, because the sample extracted for six hours showed the same level of friction as the samples for 5 or 8 days.

It should be noted that the black deposits were observed after some friction tests of GLEs, like the previous study [14]. These black deposits are likely to be the same material as the black precipitation in 4.2.4. However, no black deposits were seen after the experiment using the pectin solution, reflecting the notes in 4.2.4. Moreover, the friction level of the pectin solution was not dramatically low, showing that the pectin does not seem to be the main material for the low adhesion mechanism in this test conditions.

4.4.3 Leaf film

Figure 4.14 and Figure 4.15 depict the friction characteristics of green leaf film (GLF) and brown leaf film (BLF), respectively. Both dry and wet GLFs showed a relatively high friction coefficient, 0.3-0.35 for the first 20 seconds and 0.35-0.4 for the last 20 seconds. In contrast, wet BLF exhibited low friction for the first 20 seconds, roughly the same level as the engine oil. However, the friction coefficient continuously increased and reached around 0.35 after 6 minutes. The dry BLF exhibited a medium level of friction, between 0.25 and 0.35. Overall, both GLF and BLF showed a medium level of friction, and BLF tends to exhibit lower friction than GLF. This low friction could have happened with the same mechanism as the LP suspension; the BLF prevented the metal-to-metal contact with the help of water, but the long-term low friction was not seen.

This medium friction level could be attributed to the quick removal of leaf films from the contact area; the contact between the ball and plate became a similar condition of wet baseline immediately after the ball started sliding. The quick removal reflects that the leaf film did not adhere to the plate as tightly as expected. This weak bonding might be because of lower pressure (285 MPa) than the actual wheel/rail contact (at least 600 MPa) in the creation process, considering the poorer bonding energy of the LFs created at different temperatures.

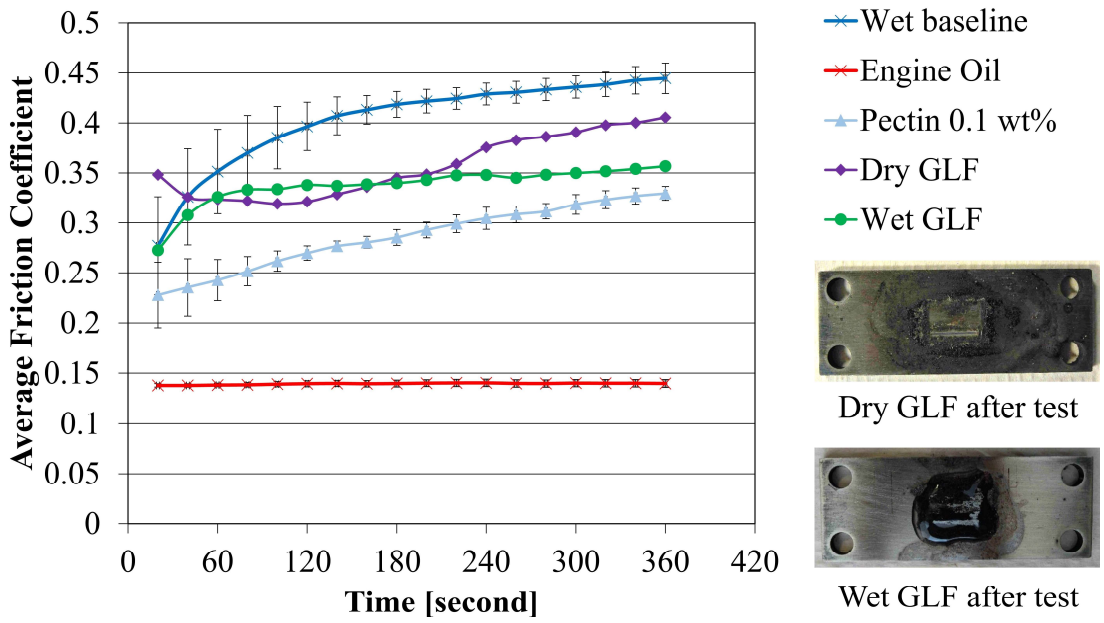

Figure 4.14 Friction properties of green leaf films

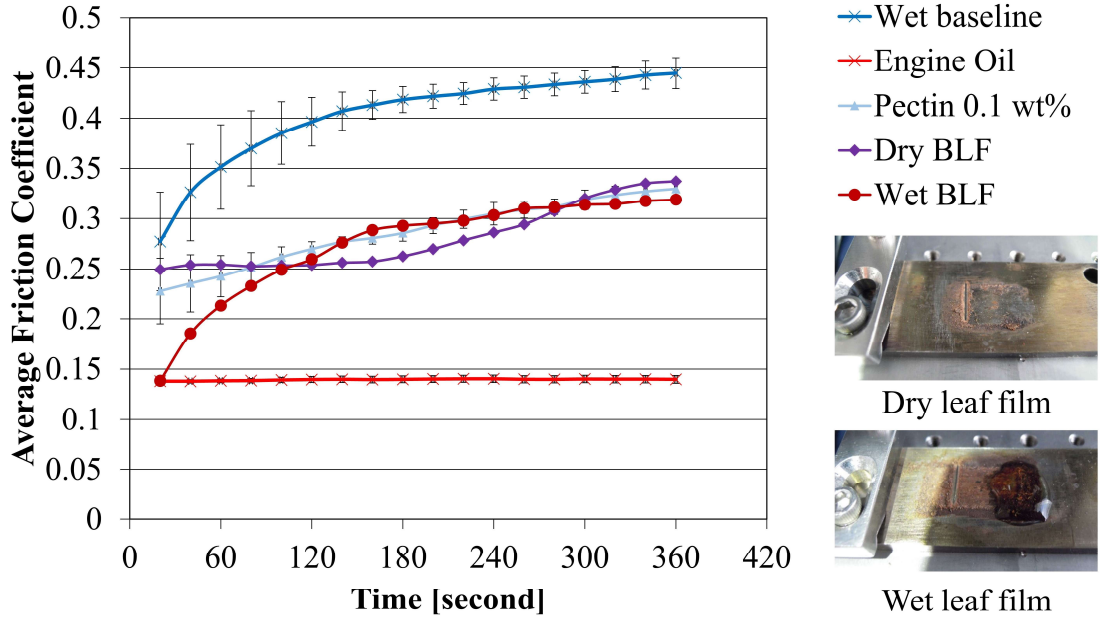

Figure 4.15 Friction properties of brown leaf films

4.4.4 Black precipitation powder

Figure 4.16 illustrates the friction characteristics of black precipitation powder made from green leaf extracts (GBP) and brown leaf extracts (BBP), which was applied as a five wt% suspension. BBP suspension significantly lowered the friction level below the level of the engine oil for approximately 120 seconds and maintained the same level for 360 seconds. In contrast, GBP suspension showed the medium-low

level of friction around 0.2, although it exhibited a lower value than the engine oil at the first 20 seconds. This result demonstrates that the BP should be the responsible material for the low adhesion mechanism; especially, BBP should contain a specific or unique substance which can causes low adhesion.

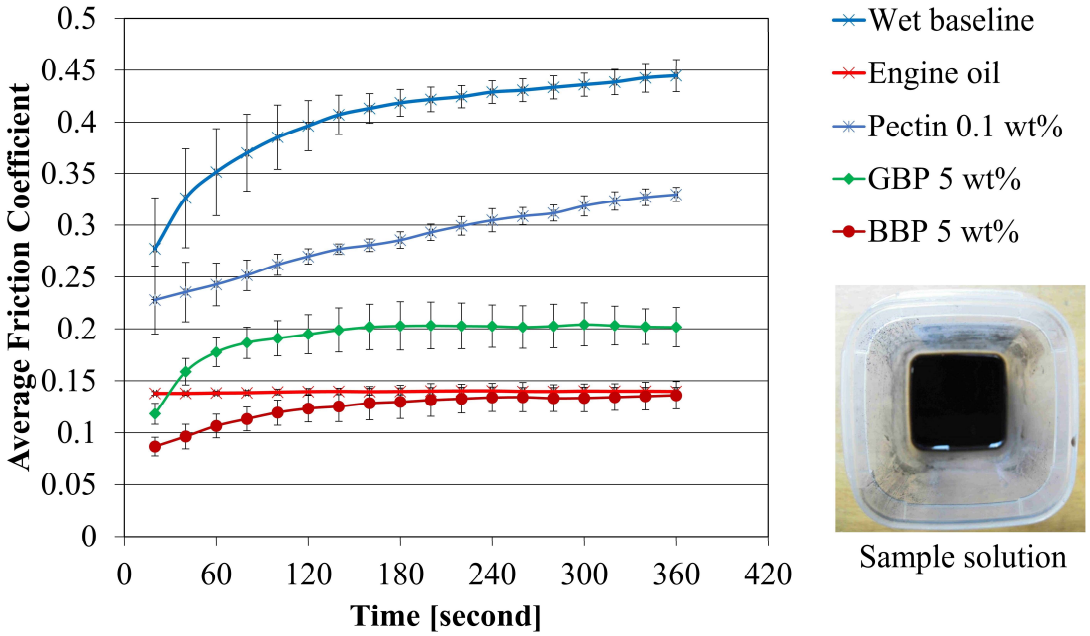

Figure 4.16 Friction properties of GBP and BBP

To sum up, the results of friction tests demonstrated the following five points:

- Leaf powder suspension can cause low friction conditions, corresponding to the indication of operational data.
- Dry leaf powder and leaf extract did not show extremely low friction when they were separately applied; however, they could lower the friction level if combined.
- Wet brown leaf film exhibited low friction for the first 20 seconds; however, the friction level increased afterwards due to the quick removal of leaf film.
- Black precipitation powder formed in brown leaf extracts was identified to cause low friction conditions, which was lower than the engine oil or the same level as the engine oil.
- The black precipitation could contain some materials which cause low adhesion.

4.5 Discussion

4.5.1 Hypothesis examination

The first hypothesis in 3.3, “Bulk leaf”, assumes that the bulk leaf prevents the metal-metal contact between the wheel and rail, leading to the low adhesion condition. This hypothesis is partially true in wet conditions since the lower friction coefficient than the engine oil was seen in the experiments using the GLP and BLP suspension. Taking into account the gradual removal of the LP at the later stage of the experiment, the low friction should happen as long as the LP exists in the contact. However, the water was necessary to trigger the low friction, as the dry LP was shown to have fewer effects on the friction level than the LP suspension. This result corresponds to the finding in the incident analysis; the dew is likely to cause low adhesion in the morning and night. Therefore, “Bulk leaf” should be able to lower the friction with the combination of a small amount of water.

The second hypothesis “Adhered leaf film in dry conditions” should be untrue, as presented in 4.4.3. The third hypothesis “Adhered leaf film in wet conditions” could be partially true, since the wet BLF exhibited the low friction, which was roughly at the same level as the engine oil. The mechanical property of the LFs seemed to change due to the absorbance of water; however, the water also helped remove the LFs, resulting in the short-term low friction. Furthermore, the results shown in 4.4.2 also suggest that the coated-slippery layer and friction-reducing layer in the models described in 2.7 are unlikely to have significant effects on the friction level. If they are present, the lower friction coefficient should have been observed in wet conditions. Although there could be better methods to develop the LF as well as these layers, potentially deteriorated and softened bulk leaf films seem to have a more significant impact on the friction conditions.

The fourth hypothesis "Pectin gel" could be unlikely to cause low friction in the ball-on-flat test conditions, according to the following facts:

- Artificial pectin solution, 0.1 wt%, showed the medium level of friction between 0.2 and 0.3.
- No black material was formed after the experiment of the artificial pectin solution.
- No black substance precipitated with the artificial pectin solution and rail plate, unlike the leaf extracts.

On the other hand, there could be another material which triggers the chemical reaction and forms the black precipitation, using pectin in leaf extracts. Hence, a more detailed analysis is necessary to examine this hypothesis, although the possibility seems to be very low.

Overall, the hypothesis “Bulk leaf” is likely to be true, but only in wet conditions, and the other hypotheses are seemingly untrue. Other than these initially-developed hypotheses, the black precipitation synthesised with leaf extracts and rail steels is deemed to be a promising material to explain the low adhesion mechanism.

4.5.2 Low adhesion material

As shown in 4.4.4, the five wt% suspension of black precipitation powder formed in brown leaf extract was found to cause extremely low friction, which was lower or as the same level as the engine oil. This finding clarifies that BBP should be the primary cause of low friction due to leaf contamination. Another finding was that the black precipitation powder formed in green leaf extract had a stable but slightly higher friction coefficient than the engine oil, around 0.2. This result shows that there could be a difference in terms of material, although both BBP and GBP seem to be a compound of leaf organics and rail steels. Therefore, chemical and material analysis of BP is necessary to understand the low adhesion mechanism properly.

Another material which contributes to the low adhesion was identified as both green and brown leaf powder in wet conditions, possibly preventing the metal-to-metal contact between the steel ball and rail plate. Considering that the colour of the LP suspension turned into black after the experiment, the similar chemical reaction to the black material synthesis should have taken place on the surface of the LP with the help of water. Hence, the low friction in the case of the LP suspension could be the mixed effects of the black material as well as the mechanical separation by LP.

The friction tests with the BP are not the perfect replication of the leaf film seen in the field; no leaf film on the line seems to have such a pure black material. However, it is still likely to represent the surface of leaf films as they usually exhibit the black colour [2]. Moreover, the concentration of the BP suspension was relatively low (five wt%), and this fact suggests that a tiny amount of BP could induce low adhesion when mixed with water. Considering that the surface can be lubricated by the film with the thickness of a few molecules [72], the superficial formation of the black material on leaf films could be enough to cause low adhesion.

Figure 4.17 illustrates the formation of a blackened layer on the leaf surface. Assuming that this change in colour is a result of chemical reaction, the water which covers the surface of leaf or leaf residue should have a high concentration of dissoluble constituents. Hence, only surface and subsurface are changed into the

black layer, which might contain the same substances as the black precipitation. To determine which material is the key to the low adhesion phenomenon, chemical and material analyses are needed.

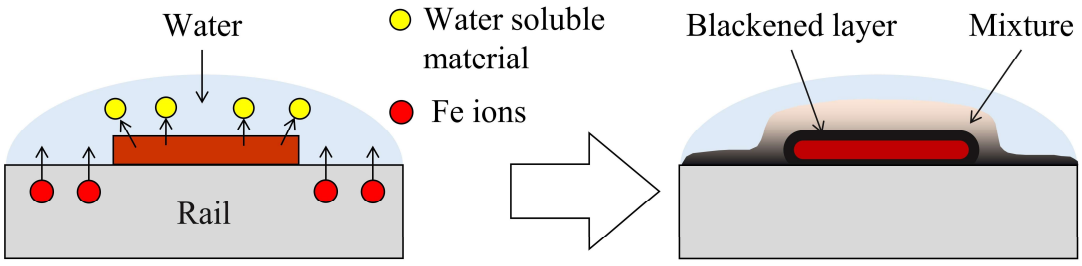

Figure 4.17 Formation of blackened layer

4.6 Conclusions

A ball-on-flat test showed that the black precipitation powder synthesised with leaf extracts and rail steels caused low friction with a combination of water. Furthermore, the leaf powder between 15μm and 300 μm was found to lower the friction level in wet conditions. Based on the results, four hypotheses, “Bulk leaf”, “Leaf film in dry conditions”, “Leaf film in wet conditions” and “Pectin gel” were examined. “Bulk leaf” was concluded to be likely since the black material was formed on the leaf powder during the experiment, and the other three hypotheses seemed to be unlikely. To understand what kind of material in the black precipitation causes low friction conditions, chemical and material analyses should be performed.

5 MATERIAL ANALYSIS

As discussed in 4.5, the black precipitation synthesised with leaf extracts and rail steel was chemically analysed for the clarification of the low adhesion and bonding mechanisms.

5.1 Introduction

The bonding and low adhesion mechanisms of the leaf film have not yet been clarified. To reveal these mechanisms, chemical analyses of leaves and leaf films may be effective as a first step. Especially, the black precipitation which was created and tested in Chapter 4 needs to be investigated since it was confirmed to cause low friction and believed to be the same substance as the black material seen on the actual railway track.

The aim of this material analysis is to identify the key materials for the bonding and low adhesion mechanisms, using many techniques of chemical analysis. In this chapter, the results and findings are shown, excluding the detailed information, e.g. fundamentals and principles.

5.2 Analysis methodology

Generally, each method of chemical analysis has a limitation; there is always some undetectable substance in principle. Accordingly, it is important to combine several methods to understand the key materials in the sample correctly. In this study, the black precipitation powder was intensively investigated, using five analysis methods.

5.2.1 Sample preparation

Black precipitation powder (BP) was intensively analysed. A BP thin film was also prepared on a small piece of rail steel, approximately 10×10×4 mm, for some chemical analysis. Figure 5.1 shows the preparation method of the BP thin films. They were formed following the procedure of BP formation; however, no heat was applied to the steel piece unlike in the BP formation. This method allows replication of the black material on railway tracks as naturally as possible. BP thick films were formed on the small steel piece, fully following the procedure of BP formation described in 4.2.4

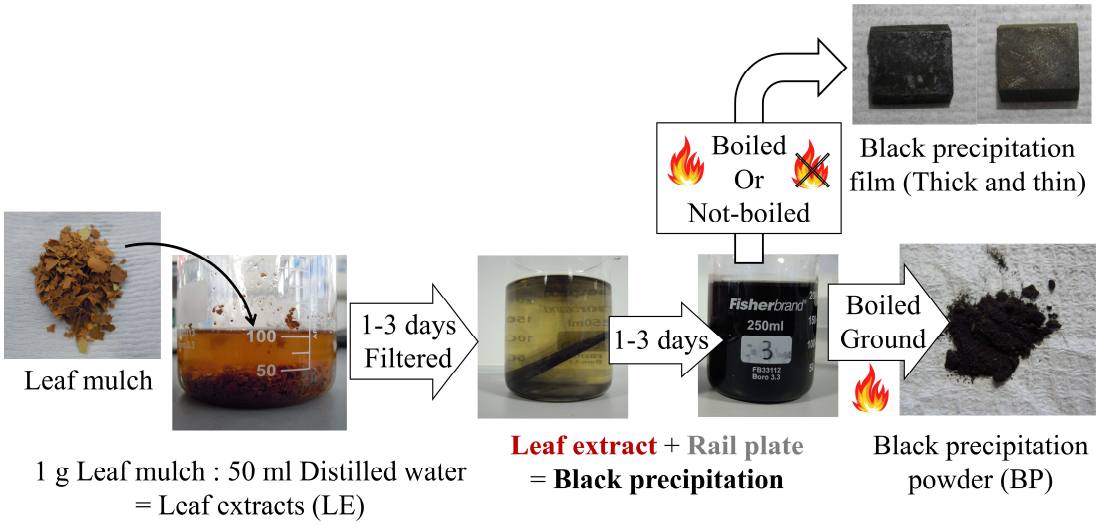

Figure 5.1 Preparation of BP thin films

5.2.2 X-Ray Fluorescence (XRF)

A Fisherscope XAN 250 was used for XRF analysis of BP and LP. The main limitation of this method was incompleteness in detection. In this machine set-up, the elements between aluminium (Al, 13) and uranium (U, 92) are measurable; the light elements between hydrogen (H, 1) and magnesium (Mg, 12) cannot be detected.

5.2.3 X-Ray Diffraction (XRD)

A PANalytical X'Pert^3 Powder was used to obtain XRD data. The data was taken at an angle between 10° and 80°, with a scanning step of 0.01313° and Cu-Kα x-ray source. It should be noted that XRD can only detect material which has a crystal structure. Therefore, no peaks in the acquired data could mean an amorphous structure.

5.2.4 Laser Raman Spectroscopy (RS)

A Renishaw inVia Raman Microscope was used for RS analysis, with BP and BP thin films. The wavelength of the laser was 514.5 nm (green), and the original laser power was set as 20 mW. In all experiments, the objective lens x50 was used, and the spot size was approximately five μm in diameter. Typically, the spectrum was acquired between 50 and 4000 cm^{-1} with the exposure time of 10 or 20 seconds and five-time accumulation, reducing the laser power to 5 or 10 % (approximately one or two mW). A baseline of the acquired spectrum was subtracted, and the noise on the spectrum was removed with WiRE software, making the spectrum flat and smooth. For some spectra, peak fittings were also conducted. As a reference, activated charcoal was also analysed, which was purchased from Sigma-Aldrich (product number: C9157, CAS number: 7440-44-0).

5.2.5 X-Ray Photoelectron Spectroscopy (XPS)

XPS analysis was performed for BP thin and thick films with a Kratos Analytical Axis Supra. The sample piece with BP films was fixed to the stage by a double-sided sticky tape to achieve the electrical isolation. A piece of paper was used to guarantee the insulation between the sample and stage: stage-double sided tape-paper-double sided tape-sample. Due to this structure, the whole sample surface would be uniformly charged-up, and the neutraliser could keep the electrical level constant with low energy electrons. Before a measurement, Ar ion sputtering was conducted to remove thin contamination layer on the top, i.e., a natural oxide layer, with Ar 2000+ clusters at 5 kV for 20 seconds, targeting an area 5×5 mm. Then, X-rays were irradiated at 1486.6 eV with an Al source, spotting the area of 300×700 μm.

Spectra between 0 and 1200 eV were measured at 160 eV pass energy, 1 eV intervals, and with five minutes of acquisition time. After that, the high-resolution spectrum of each element was collected at 20 eV pass energy and 0.1 eV intervals for 5 to 15 minutes. These acquired spectra were analysed with CasaXPS processing software (Version 2.3.19). Firstly, they were calibrated with carbon 1s peak at 285 eV to cancel a shift due to charging-up. Then, each peak was fitted with appropriate Gaussian-Lorentzian (GL) ratio and full width at half maximum (FWHM) to acquire an accurate value of chemical shift in each peak. Finally, the chemical shift values were compared to data in the references. The measurement was repeated three times or more at different spots.

It should be noted that this series of tests was kindly conducted by Dr. Deborah Hammond at Sheffield Surface Analysis Centre, the University of Sheffield, and the obtained result was analysed by the author.

5.2.6 Fourier Transform Infrared Spectroscopy (FT-IR)

A Bruker ALPHA Platinum-ATR was used, and FT-IR spectra were taken for BP and LP, between 400 and 4000 cm^{-1}, scanning 16 times with the resolution of 4 cm^{-1}. The region between 4000 and 1500 cm^{-1} was mainly analysed, as the fingerprint region between 1500 and 600 cm^{-1} usually shows complex absorption patterns and they are relatively difficult to analyse. Additionally, the spectra had a noise between 1900 and 2200 cm^{-1}, which is attributed to the diamond stage of the machine. Hence, assignments to specific molecular bonds in these regions could be inaccurate. Similarly, there is no special equipment to remove water in the sample, and OH bond might appear around 3200 cm^{-1}.

In general, a FT-IR spectrum can be divided into three regions: 4000-2000 cm^{-1}, 2000-1500 cm^{-1} and 1500-600 cm^{-1} (fingerprint region) [73]. The former two regions contain important data for interpretation of chemical bonds. However, the latter

fingerprint region usually shows a complex spectrum, and it cannot be used for precise determination. Therefore, the peak assignments in the fingerprint region should be taken for a reference.

5.3 Results

5.3.1 XRF

Figure 5.2 depicts the XRF results of GLP, GBP, BLP and BBP. Both GLP and BLP contained a relatively large amount of Calcium (Ca) and Potassium (K), as well as a small amount of Chlorine (Cl), Manganese (Mn) and Iron (Fe). In contrast, GBP and BBP were found to contain mainly Fe, followed by K, Ca, Cl and Mn. This result shows that Fe ion dissolves into LEs from rail plates, and it causes the chemical reaction with leaf organics in LEs. The dissolved Fe ion presumably reacts with various ions and molecules in LEs, including K, Ca and Cl ions. It should be noted that the number of counts cannot be directly compared to each other, because the amount of sample powder was not accurately controlled. Thereby, the counts ought to be taken as reference only.

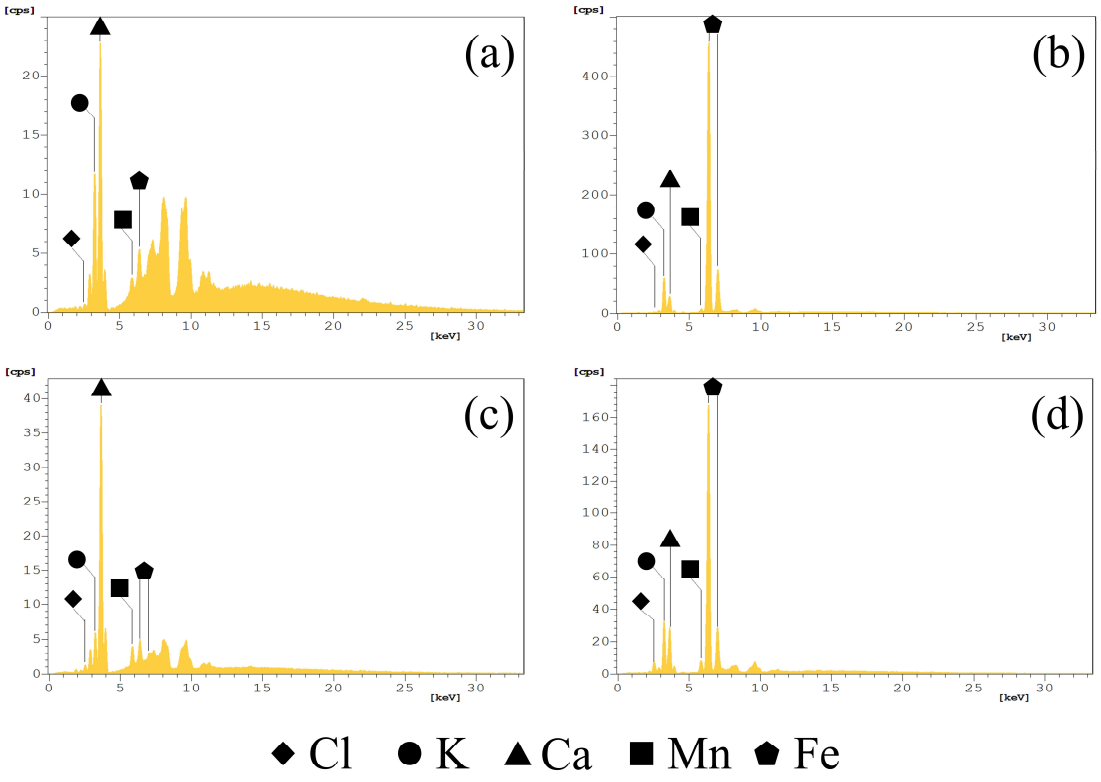

Figure 5.2 XRF results: (a) GLP, (b) GBP, (c) BLP, (d) BBP

5.3.2 XRD

Figure 5.3 illustrates the XRD data of GBP and BBP. BBP exhibited several sharp peaks, indicating that some crystal materials were present. In contrast, GBP did not show any peaks, suggesting no crystal structure was in the sample. Table 5.1 shows the assignments of the peaks in BBP. The assignments were conducted by searching in the database (Powder Diffraction File provided by the International Centre for Diffraction Data: PDF-4). It was found that these XRD patterns of BBP derived from potassium chloride (KCl: strong peaks) and calcium sulphate ($CaSO_4$: relatively weak peaks), although the small two peaks at 20.7 and 31.05 were not identified. Unexpectedly, iron oxides were not detected, suggesting that the iron detected in XRF analysis has an amorphous structure. It should be noted that amorphous KCl and $CaSO_4$ could be present in GBP, as Cl, K and Ca were detected in GBP by XRF analysis.

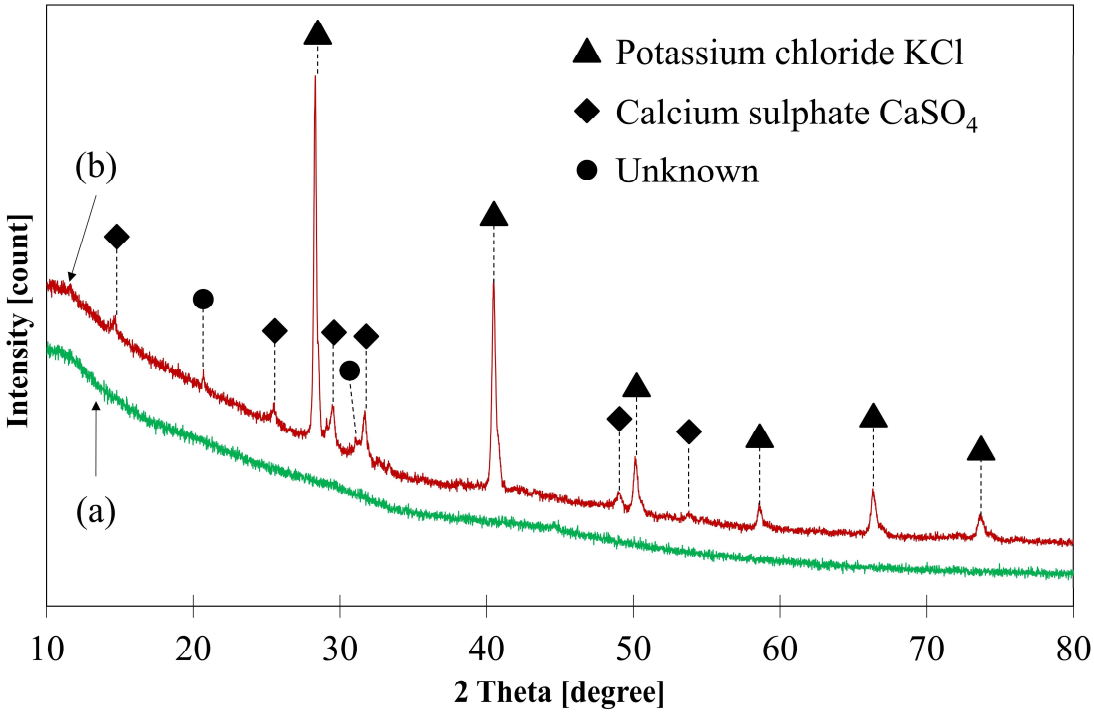

Figure 5.3 XRD results: (a) GBP, (b) BBP

Table 5.1 Assignments of XRD peaks measured in BBP

Measured 2θ	2θ in reference	Assignment
14.7	14.6208	$CaSO_4$
20.7	-	-
25.51	25.4645	$CaSO_4$
28.31	28.3453	KCl
29.09	29.1521	$CaSO_4$
29.51	29.4867	$CaSO_4$
31.05	-	-
31.69	31.8395	$CaSO_4$
40.48	40.5074	KCl
49.02	49.0628	$CaSO_4$
50.15	50.1688	KCl
53.8	53.8096	$CaSO_4$
58.58	58.6402	KCl
66.35	66.3809	KCl
73.67	73.7331	KCl

KCl: PDF number 00-041-1476

$CaSO_4$: PDF number 04-016-3271

5.3.3 RS

Figure 5.4 exhibits the acquired Raman spectra of GBP, BBP and activated charcoal, and their peak fittings are shown in Figure 5.5. Both GBP and BBP showed similar peaks, which are around 1350 cm^{-1} (shoulder, small) and 1570 cm^{-1} (strong), respectively. They are typical features of amorphous carbon [74], called disordered band (D) and graphitic band (G), respectively [75], [76]. The broad peak around 2850 cm^{-1} was assigned to amorphous carbon as well [75], although these peaks in GBP and BBP were not as clear as the activated charcoal. The small and broad peak around 600 cm^{-1} in BBP could be a mixture of magnetite (Fe_3O_4) and hematite (α-Fe_2O_3), which has a shift of 533.6 cm^{-1} and 611.9 cm^{-1}, respectively [77]. The overlapping band around 1430 cm^{-1} was difficult to be assigned; it could be carboxylate ions (COO^-) in carboxylic acid salts [78], taking into account the result of FT-IR analysis described later in 5.3.5.

In general, an intensity ratio of D and G band (I_D/I_G) can be used to evaluate the degree of graphitisation [75], [76], [79], [80]; the ratios were around 0.77, 0.83 and

1.09 for the GBP, BBP and activated charcoal, respectively. These relatively low ratios in GBP and BBP suggest that their carbon materials have a less disordered structure, possibly forming a mixed structure of sp^2 and sp^3 carbon according to the definition in [81]. Hence, both GBP and BBP are likely to have partially graphitised carbon in them. It should be noted that similar spectra were obtained with a real leaf film acquired in the field test, which is described in Chapter 9.

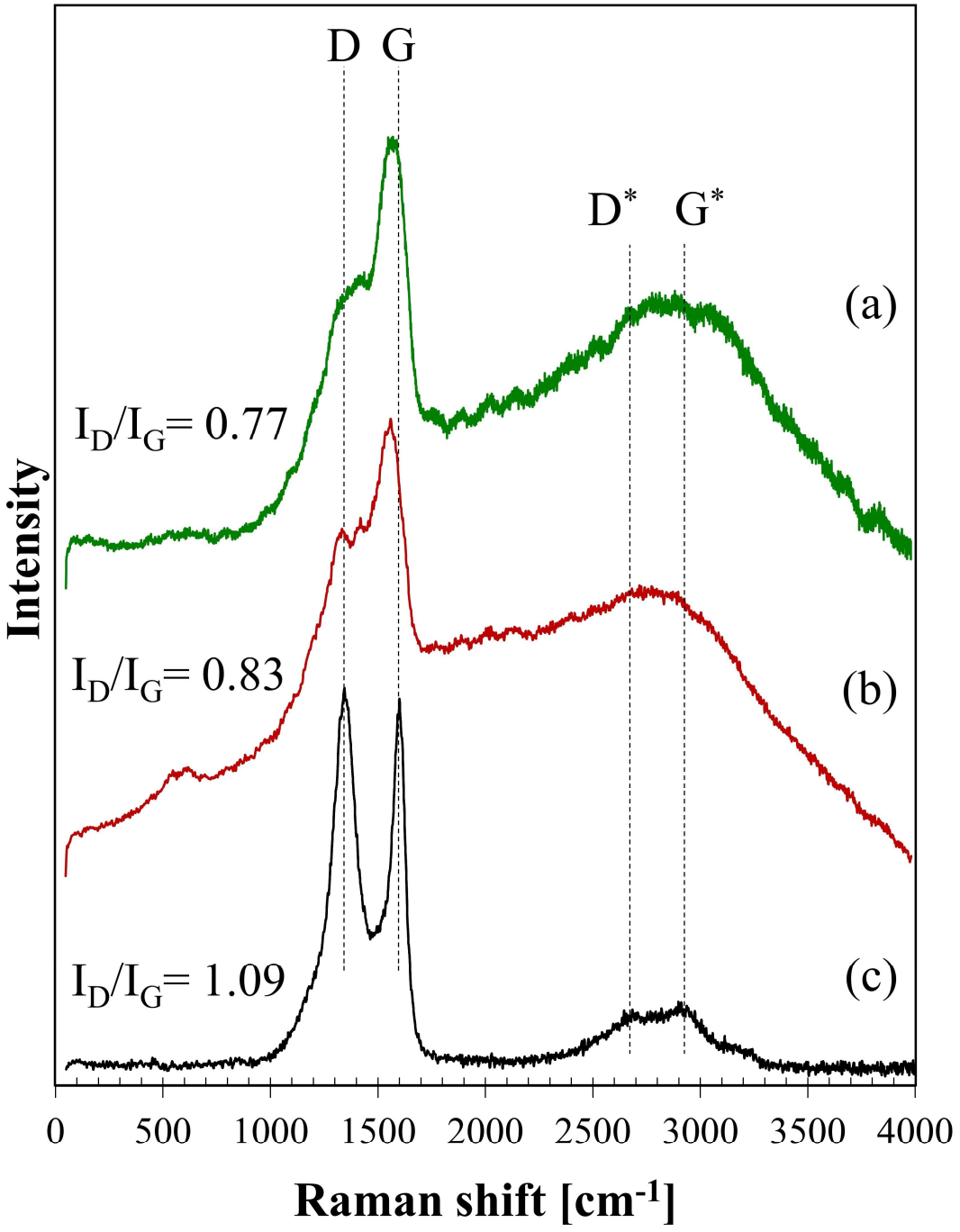

Figure 5.4 Raman spectra: (a) GBP, (b) BBP, (c) Activated charcoal

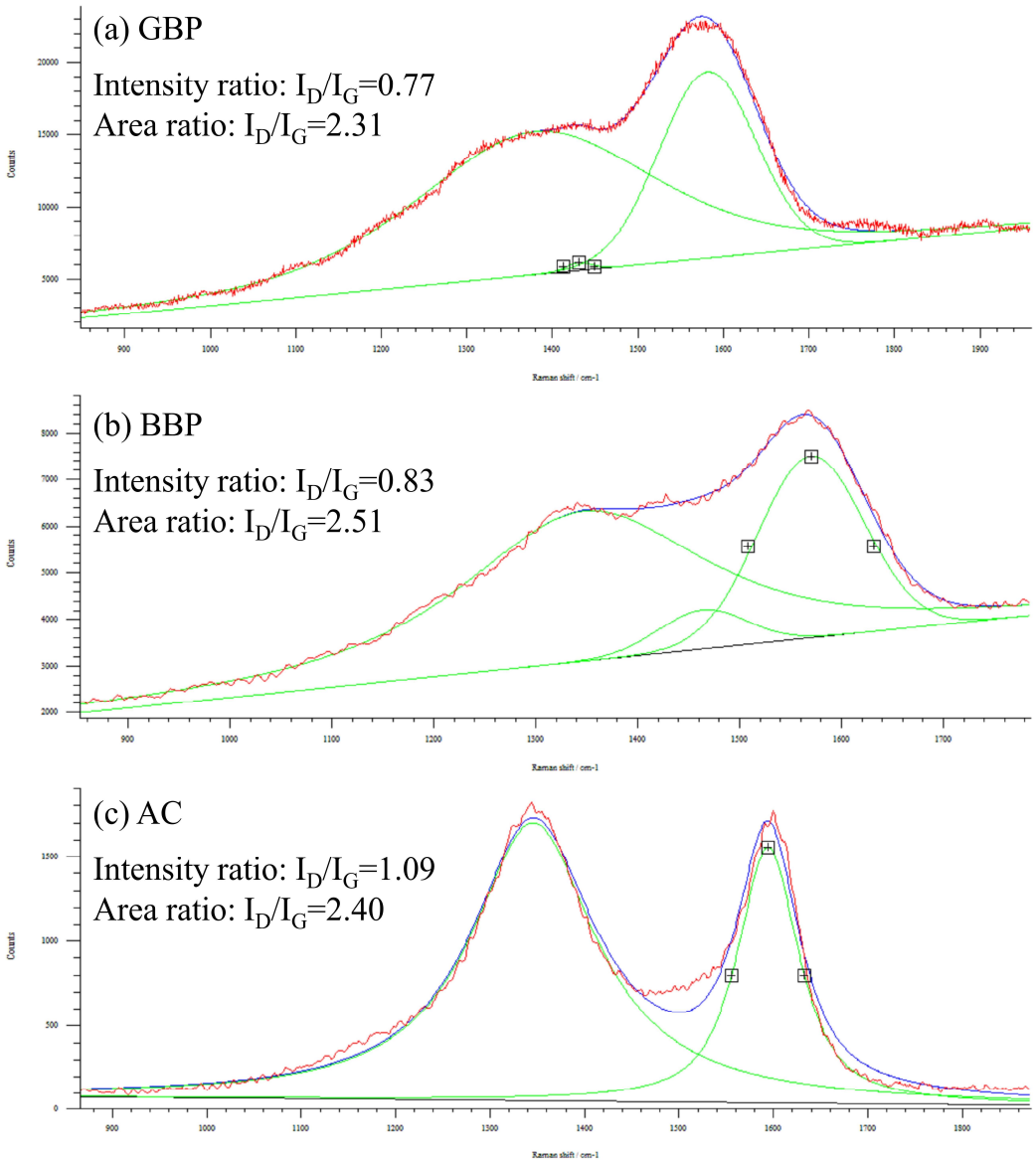

Figure 5.5 Peak fittings of the acquired Raman spectra
(a) GBP, (b) BBP, (c) Activated charcoal

This graphite-like carbon could be one of the reasons why low friction happened during the friction test. Furthermore, a sugar-derived carbon, which is often studied as a material of electrodes, has been reported to have a more graphitic structure than amorphous carbon, e.g. carbon black [76], [79]. Hence, the Raman spectra also indicate that GBP and BBP might derive from dissolved sugars in LEs, which are highly likely in water-extract of plants, such as green tea [82].

Figure 5.6 depicts the Raman spectra of GBP and BBP thin films formed on a small piece of rail steel without boiling. For these samples, two different levels of laser power were tested: 1 and 2 mW. Both GBP and BBP samples showed sharp peaks with the 2 mW laser. In contrast, these clear peaks were not seen in the spectra measured with the 1 mW laser power except D and G bands of carbon. Table 5.2

summarises the observed Raman shifts and their assignments. The relatively sharp peaks around 220, 290, 400, 600 and 1310 cm^{-1} were assigned to α-Fe_2O_3. The broad and small peak around 650 cm^{-1} could belong to a mixture of Fe_3O_4 and FeO (Wüstite), and the broad but the high peak around 1560 cm^{-1} was assigned to amorphous carbon. The difference between the measured and reference values could be attributed to the different laser power since the Raman shifts of peaks move to lower wavenumbers when higher laser power is used in the case of iron oxides [77].

The broad peak at 650 cm^{-1} in the spectra measured with 1 mW laser indicates that Fe_3O_4 initially exists in the samples; FeO is often seen in the transformation process from Fe_3O_4 to other types of iron oxides, which could be α-Fe_2O_3 in this case [77]. This transition happens if the laser power is intense enough to cause decomposition of Fe_3O_4. Therefore, these peaks seem to originate from Fe_3O_4.

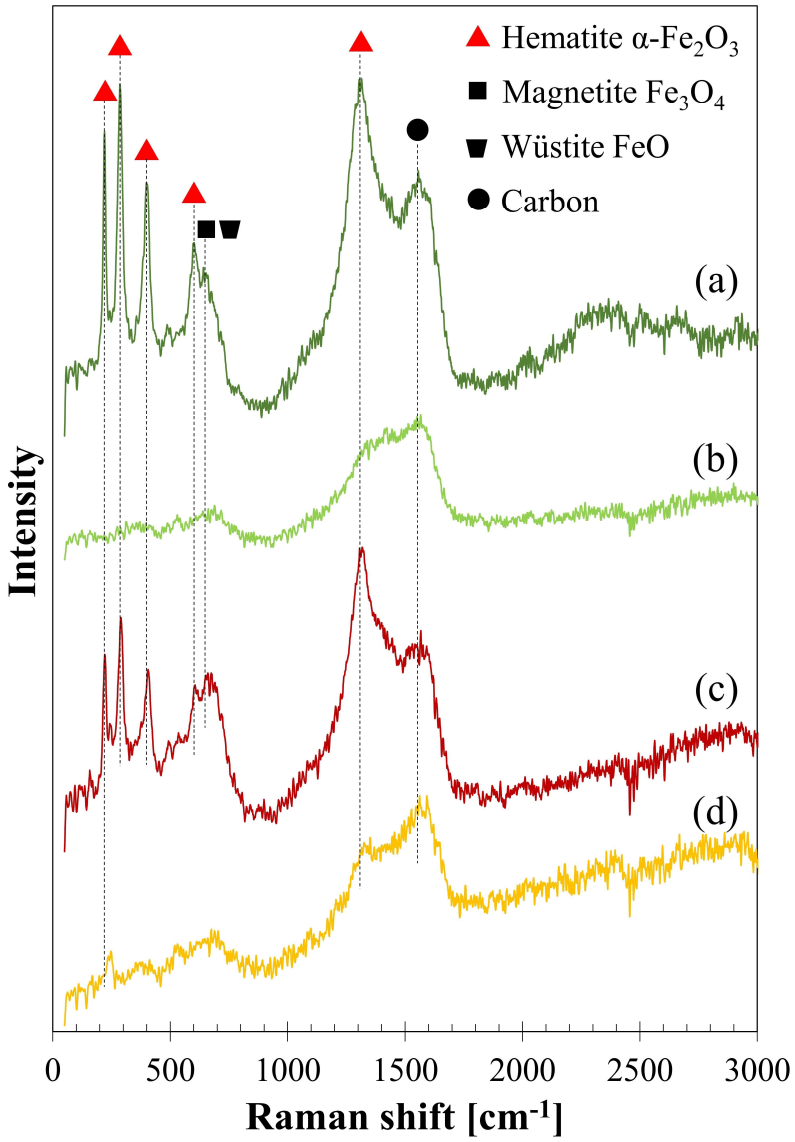

Figure 5.6 Raman spectra of GBP and BBP thin films with different laser power: (a) GBP 2 mW, (b) GBP 1 mW, (c) BBP 2 mW, (d) BBP 1 mW

Table 5.2 Raman shifts and assignments of GBP and BBP thin films

GBP 2 mW Raman shift cm^{-1}	BBP 2 mW Raman shift cm^{-1}	Assignment	Reference	
220	222	α-Fe_2O_3	226.7	[77]
286	290	α-Fe_2O_3	292.5 299.3	[77]
398	406	α-Fe_2O_3	410.9	[38], [77]
602	606	α-Fe_2O_3	611.9	[77]
642	651 662	FeO Fe_3O_4	652 662.7	[77] [38]
1305	1317	α-Fe_2O_3	1320	[38], [77]
1556	1567	Amorphous carbon Sugar-derived carbon	1575 1580	[74] [83]

In RS, the sample surface may be degraded if the laser power is too high [84], and heat induced by the laser affects measurements [85]. In fact, the laser with high power, such as 10 mW, burned the surface of BP during trials. In Figure 5.6, it seems that the 1 mW laser gives no damage, but the 2 mW laser does, and it possibly burns the surface carbon layer and exposes the iron oxides underneath the surface layer. The detected peaks of iron oxides do not derive from the rail plate since the depth penetration of graphite is approximately 50 nm [74]. Thus, the Raman spectra in Figure 5.4 and Figure 5.6 predict a structure of GBP and BBP; Fe_3O_4 or a mixture of α-Fe_2O_3, Fe_3O_4 and FeO becomes a core, and a thin amorphous carbon layer grows on the surface of the iron oxide, which is partially graphitised carbon.

5.3.4 XPS

Figure 5.7 shows the XPS spectra of GBP thick film and GBP thin film, which were formed with and without heat treatment, respectively. In the same manner, Figure 5.8 depicts the XPS spectra of BBP thick film and BBP thin film. Both GBP and BBP films were found to contain various elements, such as carbon, oxygen and iron, showing a good agreement with the previous study [23] and the results of XRF and XRD. Some elements, e.g. calcium and potassium, were only seen in thick film samples, indicating that the heat treatment affects the chemical reaction for the formation of compounds which contain calcium, sulphur, potassium, magnesium, chlorine and silicon.

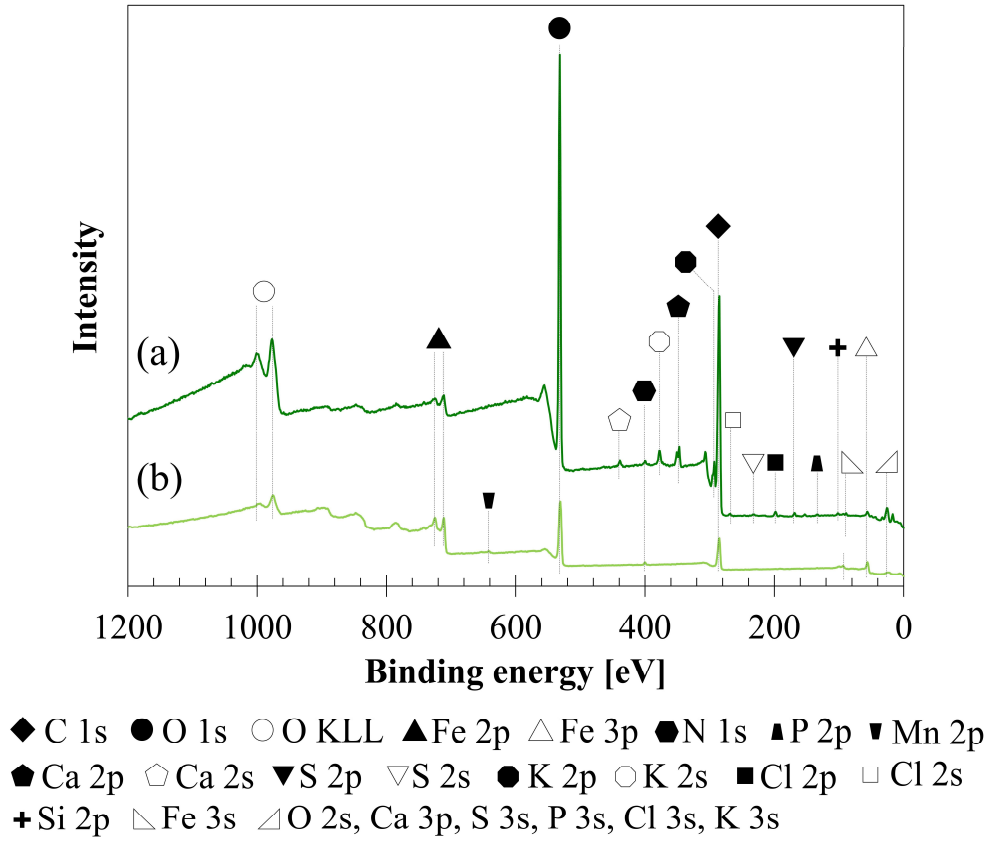

Figure 5.7 XPS results of GBP: (a) Thick GBP film, (b) Thin GBP film

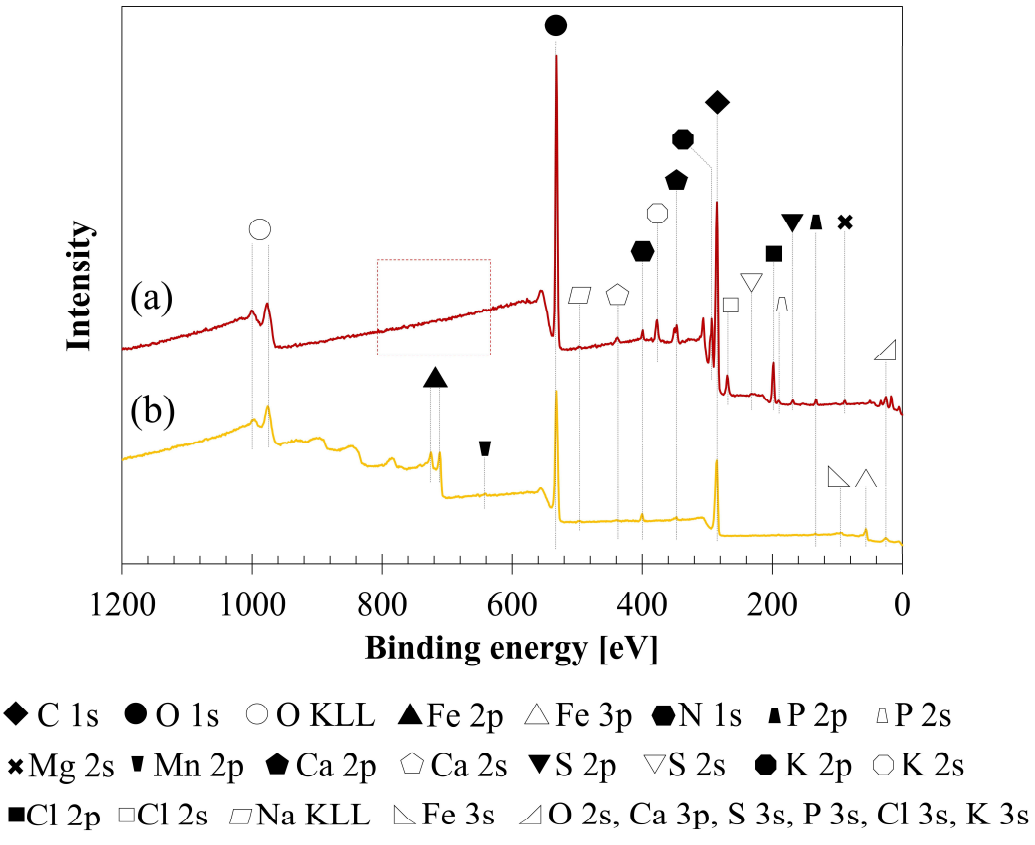

Figure 5.8 XPS results of BBP: (a) Thick BBP film, (b) Thin BBP film

Table 5.3 summarises the chemical composition of each element shown in average atomic percent (at%) with the standard deviation. It was revealed that carbon and oxygen accounted for approximately 90 at% in both thick and thin films, possibly forming an organic layer on the surface. Iron was also present in GBP and BBP thin films, accounting for 3-7 at%. However, less or no iron was observed in GBP and BBP thick films, showing that the heat treatment enhanced the chemical reaction which formed the organic layer. This change in the iron composition supports the prediction of a structure: organic layer (carbon layer) on an iron oxide core described in 5.3.3. It should be noted that the concentration of sodium was not taken into account due to the lack of the detection in the primary region: Na 1s at 1071.8 eV.

Table 5.3 The average chemical compositions of GBP and BBP films in atomic percent

Atomic %	C	O	Fe	N	Mg	P	Mn	Ca	S	K	Cl	Si
Thick GBP	59.3 ±1.3	35.3 ±0.9	0.8 ±0.1	0.7 ±0.1	-	0.2 ±0.1	-	1.4 ±0.1	0.6 ±0.1	1.0 ±0.3	0.4 ±0.1	0.4 ±0.1
Thin GBP	55.1 ±2.0	35.0 ±0.8	7.2 ±0.8	1.8 ±0.3	-	0.5 ±0.2	0.5 ±0.2	-	-	-	-	-
Thick BBP	55.2 ±1.1	31.7 ±2.2	-	1.4 ±0.1	1.5 ±0.2	1.2 ±0.1	-	1.8 ±0.1	1.0 ±0.3	2.2 ±1.2	4.0 ±1.4	-
Thin BBP	63.3 ±0.3	28.8 ±0.7	3.4 ±0.4	2.8 ±0.3	-	0.8 ±0.3	0.2 ±0.1	0.7 ±0.1	-	-	-	-

Figure 5.9 illustrates C 1s high-resolution spectra and curve fittings of thin and thick films of GBP and BBP. In the same manner, O 1s and Fe 2p high-resolution spectra and curve fitting are shown in Figure 5.10 and Figure 5.11, respectively. Chemical shifts of each element were obtained with these zoomed-in spectra. Table 5.4 summarises the chemical shifts in binding energies (B.E) and the assignments of GBP samples, and Table 5.5 does the same for BBP samples. It should be noted that high-resolution spectra of potassium (K 2p) were not acquired since K 2p has a narrow range of chemical shifts, and they are difficult to interpret accurately [86], [87]. Besides, chlorine (Cl 2p) was measured only one time because XRD analysis revealed that KCl was present in BBP.

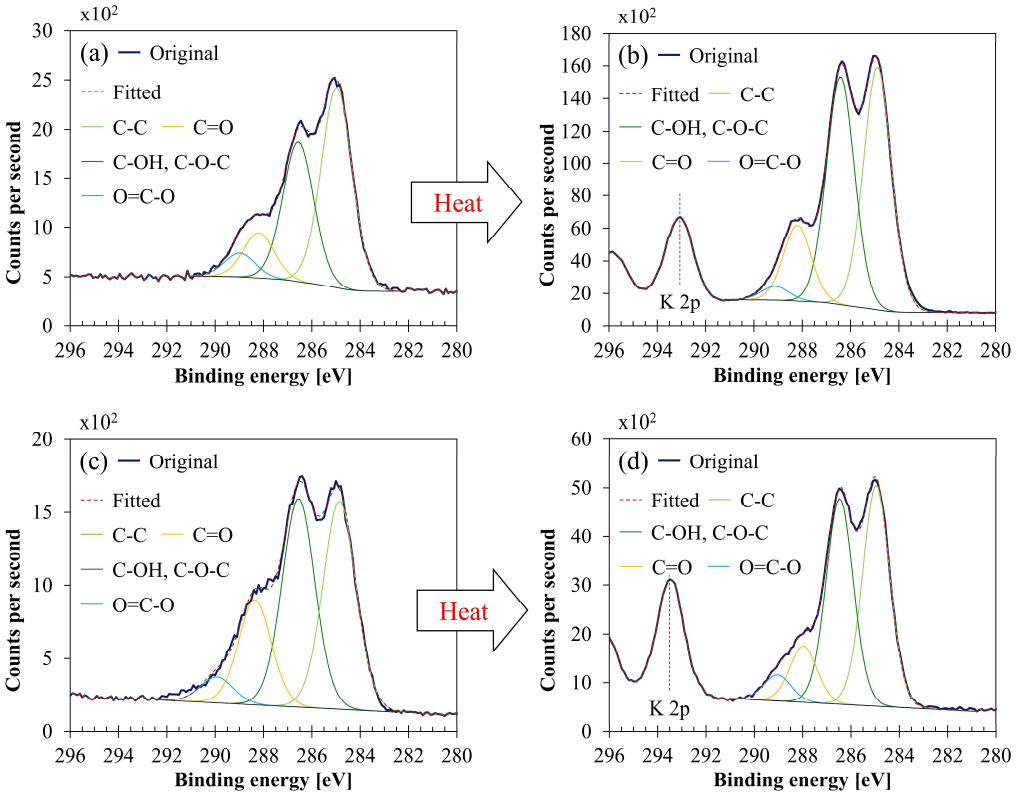

Figure 5.9 C 1s curve fittings

(a) GBP thin film, (b) GBP thick film, (c) BBP thin film, (d) BBP thick film

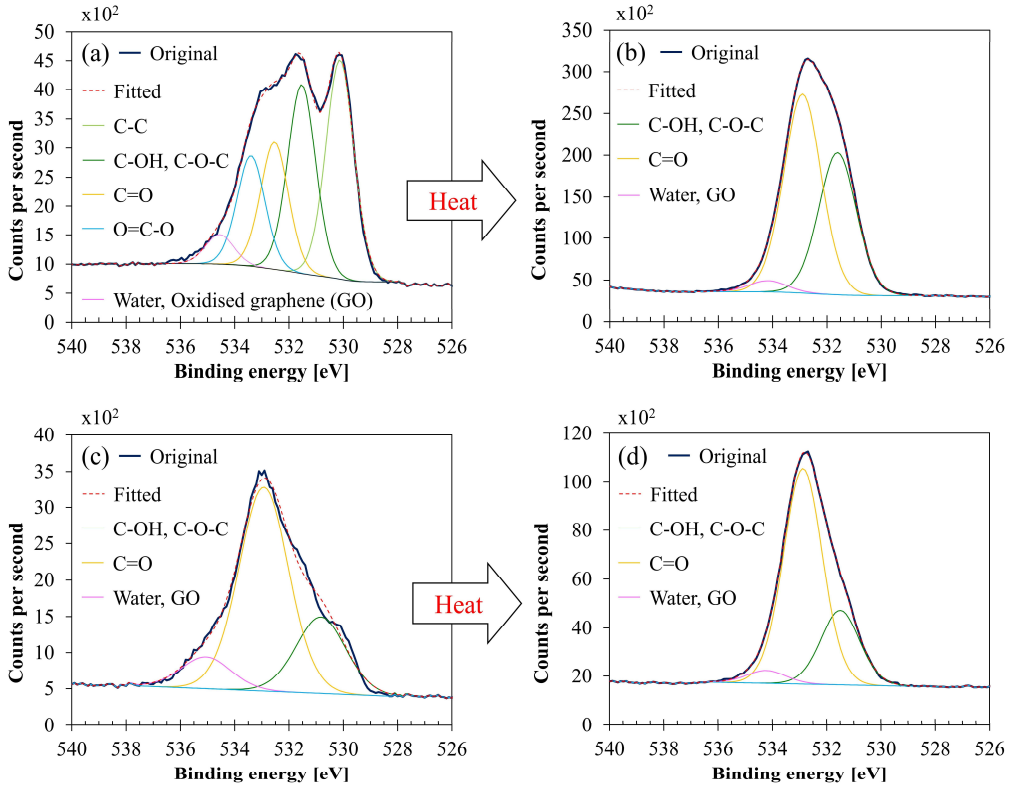

Figure 5.10 O 1 s curve fittings

(a) GBP thin film, (b) GBP thick film, (c) BBP thin film, (d) BBP thick film

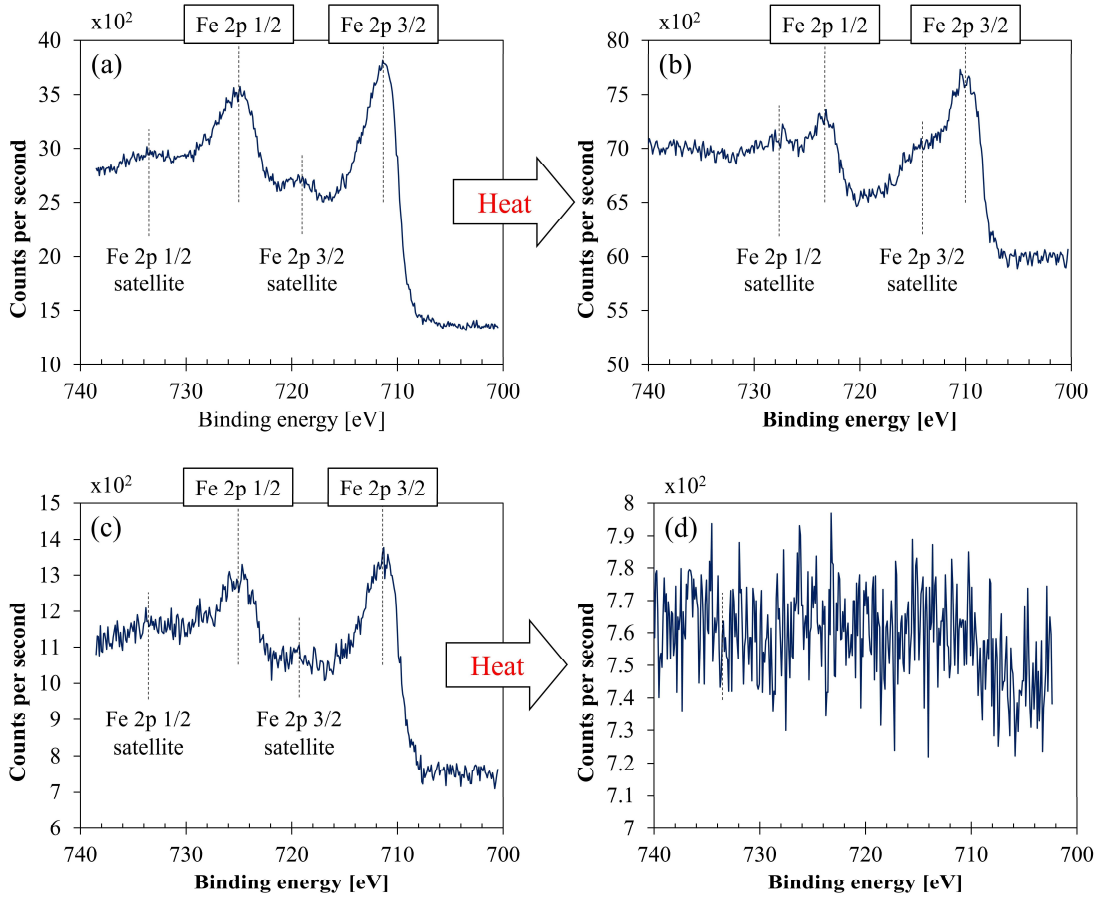

Figure 5.11 Fe 2p curve fittings
(a) GBP thin film, (b) GBP thick film, (c) BBP thin film, (d) BBP thick film

Table 5.4 Binding energy (B.E) and assignments of GBP films

Element	Thick GBP B.E	Chemical bonds Expected material	Thin GBP B.E	Chemical bonds Expected material	Reference
P $2p_{3/2}$	-	-	134.1 ±0.1	Metal phosphate	[87], [88]
S $2p_{3/2}$	168.7 ±0.1	Metal sulphate $CaSO_4$	-	-	[86], [87]
(Cl $2p_{3/2}$)	198.2 ±0.0	Metal chloride KCl	-	-	[86]
C 1s	285.0 ±0.1	C-C	285.0 ±0.1	C-C	[86], [87], [89]
	286.5 ±0.1	C-OH C-O-C	286.6 ±0.1	C-OH C-O-C	[87], [89], [90]
	288.3 ±0.0	C=O	288.2 ±0.2	C=O	[87], [89]
	289.1 ±0.1	O=C-O	289.3 ±0.4	O=C-O	[86], [87], [89]
Ca $2p_{3/2}$	347.6 ±0.1	$CaSO_4$	-	-	[87]
N 1s	400.1 ±0.0	Organic matrix C-NH_2	400.4 ±0.0	Organic matrix C-NH_2	[86], [87]
O 1s	-	-	530.1 ±0.1	Metal oxides Fe_2O_3	[86], [87]
	531.5 ±0.1	Organic C-O	531.5 ±0.1	Organic C-O	[86]
	532.9 ±0.1	Organic C=O	532.5 ±0.0	Organic C=O O=C-O	[86], [90]
	-	-	533.4 ±0.0	O=C-O	[90]
	534.4 ±0.2	Water Oxidised graphene	534.5 ±0.0	Water Oxidised graphene	[91]–[93]
Mn $2p_{3/2}$	-	-	641.8 ±0.2	Mn with O	[87]
Fe $2p_{3/2}$	710.2 ±0.3	Iron oxides Fe^{2+} and Fe^{3+}	711.2 ±0.1	Iron oxides Fe^{3+}	[86], [87], [94], [95]
(Fe $2p_{1/2}$)	723.6 ±0.2		724.8 ±0.2		

* Bracket means a reference value: measured only one time or not useful for the determination

Table 5.5 Binding energy (B.E) and assignments of BBP films

Element	Thick BBP B.E	Chemical bonds Expected material	Thin BBP B.E	Chemical bonds Expected material	Reference
Mg 2s	89.3 ±0.1	$MgSO_4 \cdot MgO$	-	-	[96]
P $2p_{3/2}$	133.2 ±0.1	Metal phosphate ex. $CaHPO_4$	133.7 ±0.2	Metal phosphate ex. $FePO_4$	[86], [88], [97]
S $2p_{3/2}$	169.0 ±0.2	Metal sulphate $CaSO_4 \cdot MgSO_4$	-	-	[86], [87]
(Cl $2p_{3/2}$)	198.4	Metal chloride KCl	-	-	[86]
C 1s	284.9 ±0.0	C-C	284.9 ±0.1	C-C	[86], [87], [89]
	286.5 ±0.0	C-OH C-O-C	286.5 ±0.1	C-OH C-O-C	[87], [89], [90]
	288.0 ±0.0	C=O	288.3 ±0.3	C=O	[87], [89]
	289.1 ±0.1	O=C-O	289.8 ±0.5	O=C-O	[86], [87], [89]
Ca $2p_{3/2}$	347.6 ±0.1	$CaSO_4$	347.7 ±0.1	$CaSO_4$	[87]
N 1s	400.1 ±0.0	Organic matrix $C\text{-}NH_2$	400.3 ±0.1	Organic matrix $C\text{-}NH_2$	[86], [87]
O 1s	-	-	530.6 ±0.3	Metal oxides Fe_2O_3	[86], [87]
	531.5 ±0.1	Organic C-O	(531.7)	Organic C-O	[86]
	532.8 ±0.0	Organic C=O	532.9 ±0.1	Organic C=O	[86]
	534.4 ±0.3	Water Oxidised graphene	(534.1)	Water Oxidised graphene	[91]–[93]
	-	-	535.1 ±0.2	Water Na KLL	[86], [96]
Mn $2p_{3/2}$	-	-	641.8 ±0.1	Mn with O	[87]
Fe $2p_{3/2}$	-	-	711.2 ±0.1	Iron oxides Fe^{3+}	[86], [87], [94], [95]
(Fe $2p_{1/2}$)	-	-	724.8 ±0.2		

* Bracket means a reference value: measured only one time or not useful for the determination

C 1s was found to contain four components, and their chemical shifts were not dramatically changed after the heat treatment for both GBP and BBP as shown in Table 5.4 and Table 5.5. Carbon in GBP and BBP seems to be pure carbon (approximately 50 at%), and oxygen-bonded carbon (C-O, C=O and COO). This complex structure is often seen in graphene oxide; it is generally obtained by oxidising graphite particles [92], [98], although observed C 1s did not contain clear sp^2 at 284 eV [86].

O 1s showed a complex structure as well; GBP thin film contained five components, and BBP thin film had three components. It should be noted that the five components in O 1s were also seen in BBP thin film; however, they were observed only one time and thus classified as a reference value. As shown in Figure 5.10, the heating process affected the chemical conditions in O 1s; the component at 530.1-530.6 eV vanished in GBP and BBP thick films. This disappearance means that metal oxides, which are highly likely to be iron oxides, are buried in the organic layer due to the accelerated chemical reaction by the heat treatment. This result also supports the idea of the structure described above.

Another suggestion from the chemical shifts around 534.5 eV is that there could be oxidised graphene (GO). This large chemical shift (+3.5 eV) is unusual for O 1s, and thereby, the assignment is difficult [86], [87], [90]. However, GO has been reported to exhibit a large chemical shift around 534-534.5 eV, and this chemical shift is attributed to water contamination [91], [92] or oligomer of vinylene carbonate on a graphene surface [93]. Considering that the surface carbon seems to be partially graphitic, the small component peaked around 534.5 eV might come from the oxidised or water-contaminated graphene.

As shown in Figure 5.11, both GBP and BBP thin films contained subtle satellite peaks of Fe $2p_{3/2}$ and Fe $2p_{1/2}$, and thus Fe^{3+} (α-Fe_2O_3) is likely to be present [94]. In contrast, the satellite peak in GBP thick film was relatively intense and overlapped with Fe $2p_{3/2}$ and $2p_{1/2}$. The chemical shifts were around 710.2 eV (Fe $2p_{3/2}$) and 714 eV (Fe $2p_{3/2}$ satellite), and this satellite peak should come from Fe^{2+} high spin compound [86], [94], [95]. In terms of the chemical shifts in Fe $2p_{3/2}$, Fe^{3+} is highly likely, possibly forming magnetite [94]. On the other hand, the intense satellite peak is often seen in FeO [86], [94] and iron-ligands [95]. As RS suggests the presence of FeO, there could be a mixture of Fe_3O_4 and FeO on the surface of the thick GBP film. Thick BBP film exhibited no iron on its surface, suggesting that the iron is covered with organic layers. This is a clear difference between the GBP and BBP thick films.

The chemical shift of N 1s shows that organic matrix (C-NH_2) is likely in both GBP and BBP rather than nitrites or nitrates [86], [87]. Phosphorus is likely to exist as a

metal phosphate, possibly bonding to calcium or iron. The concentration of phosphorus is relatively higher in thick BBP film than the other film, and it could be the reason why only BBP showed lower friction than GBP. Calcium, sulfur, potassium and chloride were mainly assigned to $CaSO_4$ and KCl respectively, as they were detected in the XRD analysis of BBP. Magnesium, silicon and manganese do not seem to play an important role in the chemical reaction since they were occasionally detected, and their concentrations were small.

5.3.5 FT-IR

Figure 5.12 shows the FT-IR spectra of GBP and BBP with the original GLP and BLP spectra for comparison. Both GBP and BBP exhibited a similar absorbance: around 3250, 2930, 1600, 1400, and 1100 cm^{-1}. In contrast, the GLP and BLP showed more complex absorption with peaks around 3260, 2920, 2850, 1610, and 1030 cm^{-1}. These absorption bands were assigned as follows: OH stretching at 3260 cm^{-1}, CH stretching at 2920 and 2850 cm^{-1}, C=O double bonds around 1610 cm^{-1}, and C-O stretching around 1030 cm^{-1}, although some small peaks were unable to be assigned. The comparison between BP and LP shows that the BP is different from raw leaves, e.g. less clear CH stretching or another peak of C=O.

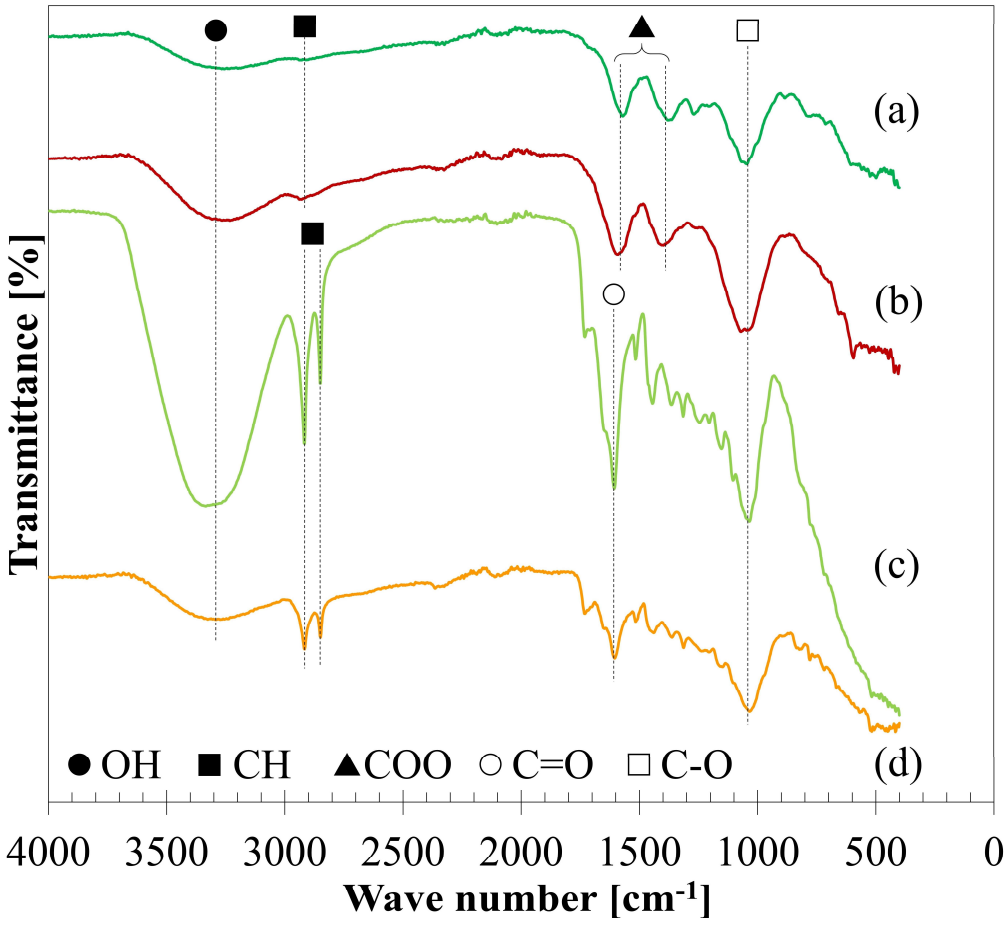

Figure 5.12 FT-IR spectra: (a) GBP, (b) BBP, (c) GLP, (d) BLP

The assignment of each absorbance in GBP and BBP is shown in Table 5.6, referring to the literature [14], [78], [99]–[101]. The absorption around 3250 cm^{-1} is attributed to OH, which could form both types of hydrogen bonds: inter- or intra-molecular hydrogen bonds. The weak peak at 2930 cm^{-1} presumably comes from saturated CH bonds because unsaturated and aromatic CH frequencies usually are slightly over 3000 cm^{-1} and two sharp peaks should be observed in the case of methyl or methylene groups. In the same manner, NH stretching mode is unlikely because it shows relatively sharp peaks around 3500-3300 cm^{-1}.

Table 5.6 Assignment of each infrared band in GBP and BBP

Assignment	Possible conditions	GBP absorption cm^{-1}	BBP absorption cm^{-1}	Reference
OH stretch	Inter- or Intra-molecular H bonds	3280	3232	[99]
CH stretch	Saturated CH	2934	2938	[99]
COO^- ion Asymmetric	Chelate structure with metal ions	1570	1593	[14], [78], [99]–[101]
Symmetric		1379	1398	
C=O stretch				
CO stretch	Any organics	1046	1071	[14], [99]

Due to the unlikely presence of aromatic CH bonds, two absorbances around 1600 and 1400 cm^{-1} were assigned to carboxylate ions (COO^-), which usually show a doublet at 1610-1550 (asymmetric) and 1420-1300 cm^{-1} (symmetric) [14], [78], [99]. C=O double bonds in esters or ketones could be possible in this region, which should appear around 1740 and 1710 cm^{-1}, respectively [99]. However, the significant shifts of the observed absorptions to lower wavenumbers show that they derived from carboxylate ions rather than esters and ketones. N=O double bonds are possible in this region; however, they are unlikely due to the small atomic concentration of nitrogen and the chemical shift found in the XPS analysis.

The band around 1030 cm^{-1} should be CO stretching mode which comes from various organics in GBP and BBP. Further analysis and assignment were not conducted for this CO bond since the region below 1500 cm^{-1} is not diagnostically useful [99].

As XPS analysis confirmed the presence of iron, iron-carboxylic salts might be formed in GBP and BBP. Fe ions can form a chelate (ligand) structure with some carboxylates, such as oxalate (ferric oxalate) and acetate (ferric acetate) [102], [103]. Synthesised metal carboxylates exhibit COO^- absorption around 1510-1590 cm^{-1} for asymmetric mode and 1400-1430 cm^{-1} for symmetric mode [101], which roughly corresponds to the observed values in GBP and BBP. Hence, the observed COO^- in the FT-IR analysis possibly derive from iron carboxylates in BP.

RS and XPS analyses suggest that iron oxides are likely rather than iron carboxylate. However, the thermal energy by laser irradiation in RS could induce the transition of iron carboxylate to iron oxides in this study. Moreover, XPS reflects only properties of the surface up to 10 nm, and the chemical shifts of ferric oxalates in XPS show approximately the same values as iron oxides [104]. In addition, the intense Fe^{2+} satellite might derive from ligand structures, and XRD analysis did not detect crystal iron oxides. Considering all the information from RS, XPS and FT-IR analyses, it can be concluded that the GBP and BBP contain both iron carboxylates and iron oxides; iron carboxylates are predominant in the bulk black material and iron oxides are on the surface. The iron carboxylates are likely to be formed with dissolved Fe ions and carboxylic acids in LEs, then some of them transform to iron oxides due to further oxidisation, especially on the surface.

5.4 Discussion

Material analyses of the black precipitation was carried out, and it was revealed that it consisted of iron-ligand structure covered with graphite-like carbon as well as other ions, including phosphates. Considering all the results, the low adhesion mechanism should be discussed in this section, as well as the chemical reaction process for the formation of black precipitation.

5.4.1 Low adhesion mechanism

As described in 4.4, BP was identified as the main leaf-lubricant for low friction, followed by solid leaf powder, although solid leaves seem to have a limited effect. Table 5.7 summarises the main findings in the material analyses. In terms of tribology, three of them are very important: graphitic carbon, iron oxides and phosphate compounds.

Table 5.7 Main findings in the material analyses

Analysis	Main findings
XRF	• Fe ions are dissolved into LEs and cause the chemical reaction
RS	• Graphitic carbon covers the surface of BP • This structure is often seen in RS spectra of a sugar-derived carbon • Iron oxides are underneath the carbon surface
XPS	• BP mainly consists of carbon, oxygen, iron and nitrogen • Oxidised graphite might exist according to the chemical shifts of C 1s and O 1s • The thick organic layer is formed on the surface of BBP, covering iron oxides • The relatively high concentration of phosphate is detected only in heated BBP
FT-IR	• Chelate structure of iron-carboxylate seems to be formed

Figure 5.13 shows a schematic diagram of the low adhesion mechanism due to leaves on the line. Low adhesion conditions seem to be caused by four factors: graphitic carbon, solid leaf, iron oxide and possibly phosphate compound. Graphite has been recognised as a solid lubricant and widely used [72]. Although the BP does not have a perfect graphite structure, it is partially graphitised, contributing to low adhesion conditions. Solid leaves can reduce the friction level when they are present in the contact area, preventing contact between wheels and rails. Iron oxides are also well-known for their lubricity in the wheel/rail contact [10], [38], although the mixture of iron oxides and iron carboxylates could be present in the BP.

Phosphate compounds are one of the typical anti-wear additives for lubricating oils, such as Zinc dialkyl-dithiophosphate (ZDDP) [72], [105]. Iron phosphate films formed on steels have been reported to protect the iron surface and reduce wear [106], and phospholipid can decreases the friction levels in wet conditions [107]. The formation of iron-phosphate containing film usually requires worn steel surface under certain pressure and relatively high temperature [72], [105], so that metal phosphates are unlikely to be the main reason for low friction. On the other hand, metal phosphate is one of the differences between GBP and BBP, and it might have a small effect on friction conditions. Overall, the graphite-like carbon should be the primary cause, followed by bulk leaves and iron oxides, and the phosphate compounds might have a very limited effect on low friction.

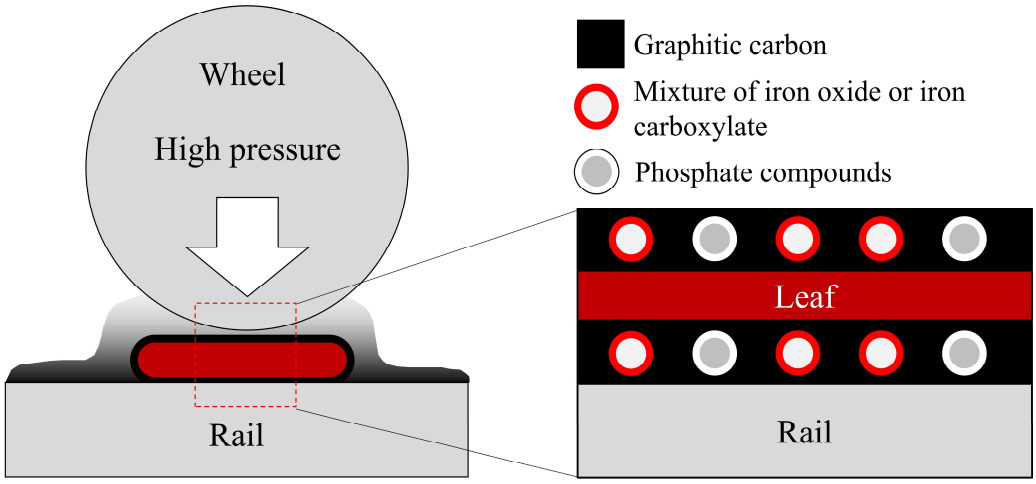

Figure 5.13 Schematic figure of low adhesion mechanism due to leaves

The synthesised black material was found to contain potassium chloride (KCl) and calcium sulphate ($CaSO_4$), and they might be lubricants as well. However, the reported COF of KCl thin films is not significantly low, around 0.27 [108]. Additionally, $CaSO_4$ has a low COF between 0.15 and 0.2 at high temperature (500 or 600 °C), but it is generally brittle at room temperature and does not work as a lubricant [109], [110]. Thereby, KCl and $CaSO_4$ in the synthesised black powder are unlikely to be a lubricant. They might have been formed in BBP for a number of reasons, e.g. a higher concentration of K^+, Cl^-, Ca^{2+} and SO_4^{2-} ions in BLEs than GLEs. Chemical analysis should be carried out for leaf extracts, i.e. ion chromatography and inductivity coupled plasma mass spectrometry.

As discussed in 4.5, the hypothesis "Bulk leaf" is the most likely theory for the low adhesion mechanism among the hypotheses developed in this study. The results of the chemical and material analysis support this theory. Leaves on the railway track could form the black material, and the graphite-like carbon in that black material seems to be responsible for the low adhesion.

5.4.2 Literature review of a chemical reaction

In this study, organics in leaf extracts were found to involve the chemical reaction with dissolved iron ions, and they might be sugars or acids which can form a chelate structure with Fe ions as summarised in Table 5.7. Hence, literature was reviewed to find a possible theory of a chemical reaction process between organics and iron.

RS revealed that sugar in LEs is one of the factors which induce the chemical reaction. Based on this information, the Maillard reaction could be the most realistic candidate for the black material formation. The Maillard reaction is caused by reducing sugars and amino acids, and odorous brown pigments, called melanoidin,

are generally produced after the reaction [111], [112]. Both GBP and BBP have a strong and honey-like smell, especially after the boiling process. Furthermore, nitrogen was detected in XPS analysis with the chemical shift of organic matrix containing nitrogen, which might come from amino acids dissolved into LEs.

Reducing sugars, such as glucose and fructose, have been detected in tea, as well as amino acids, such as glutamine and threonine [82], [113], [114]. LEs used in this study are practically a cup of sycamore tea; therefore, the Maillard reaction could happen in terms of materials. Furthermore, iron and iron oxide have been reported to promote the Maillard reaction [115], [116]. Additionally, melanoidin is known to have antioxidant activity [111]; melanoidin can catch metal ions, possibly forming a chelate structure with them [117]–[119]. It is also noteworthy that charred meats made by barbecue, which are typical melanoidin, have been reported to contain graphene oxide and nanocarbon particles [120]. These facts seem to have a close linkage to the findings in this study: sugar-derived carbon in RS, a chelate structure of iron carboxylate in FT-IR and a graphene oxide in XPS. In fact, the FT-IR spectrum of Maillard reaction products presented in [111] has a very similar absorption band: 3411, 1635, 1404 and 1076 cm^{-1}.

Another possibility to produce a black pigment with organics and irons is iron-based ink, such as iron-gall ink [121]–[124]. Although the chemical reaction process has not yet been elucidated, black pigments can be made with irons and tannin-derived polyphenolic materials, such as gallic acids, ellagic acids and catechin derivatives. They have been detected in tea as a water-soluble material [82], [114], [125], and also they can form a chelate structure with iron oxides [126]–[128], which shows a good agreement with the results in this study. Moreover, the FT-IR spectrum of the laboratory-made iron gall ink shows similar absorption patterns (1640, 1424 and 1083 cm^{-1}) [122]. Furthermore, the RS spectra of iron gall ink and historical ink sample also exhibit similar Raman shifts: 1475, 1310 and broad 640-490 cm^{-1} in [124] and 1590, 1315 and 1006 cm^{-1} ($CaSO_4$, detected in XRD and XPS analysis) in [121].

It could be possible to suppose that organic acids simply form a chelate structure with dissolved iron ions, and then a further chemical reaction occurs on its surface. For example, oxalate or malate can be found in plant leaf extracts [113], [129], and ferric oxalate or iron malate could be formed in LEs. Alternatively, iron ions might be able to react with gluconic acids [100] or form an iron-sugar complex [130], [131].

To sum up, three candidates that can explain the chemical reaction process are proposed through the literature review: Maillard reaction, iron-based ink and other organic acid.

5.4.3 Possible chemical reaction process

Figure 5.14 shows the supposed chemical reaction process. As revealed in XRF analysis, Fe ions are dissolved into LEs, possibly with the help of organic acids. Then, the dissolved Fe ions form a chelate structure with the acids, e.g. carboxylic acids, tannic acids and other organic acids in LEs, as suggested in FT-IR analysis. Subsequently, Fe ions are wrapped with organic molecules such as reducing sugars and amino acids. At step four, a chemical reaction occurs with organics on the surface of Fe ions, forming a carbon layer on the surface; it could be the Maillard reaction or formation of iron-gall ink. The process stages one to five can be applied to other dissolved Fe ions, and finally, black precipitation is formed with a three-layer structure: carbon layer on the surface, chelate layer in the middle and Fe ion as a core.

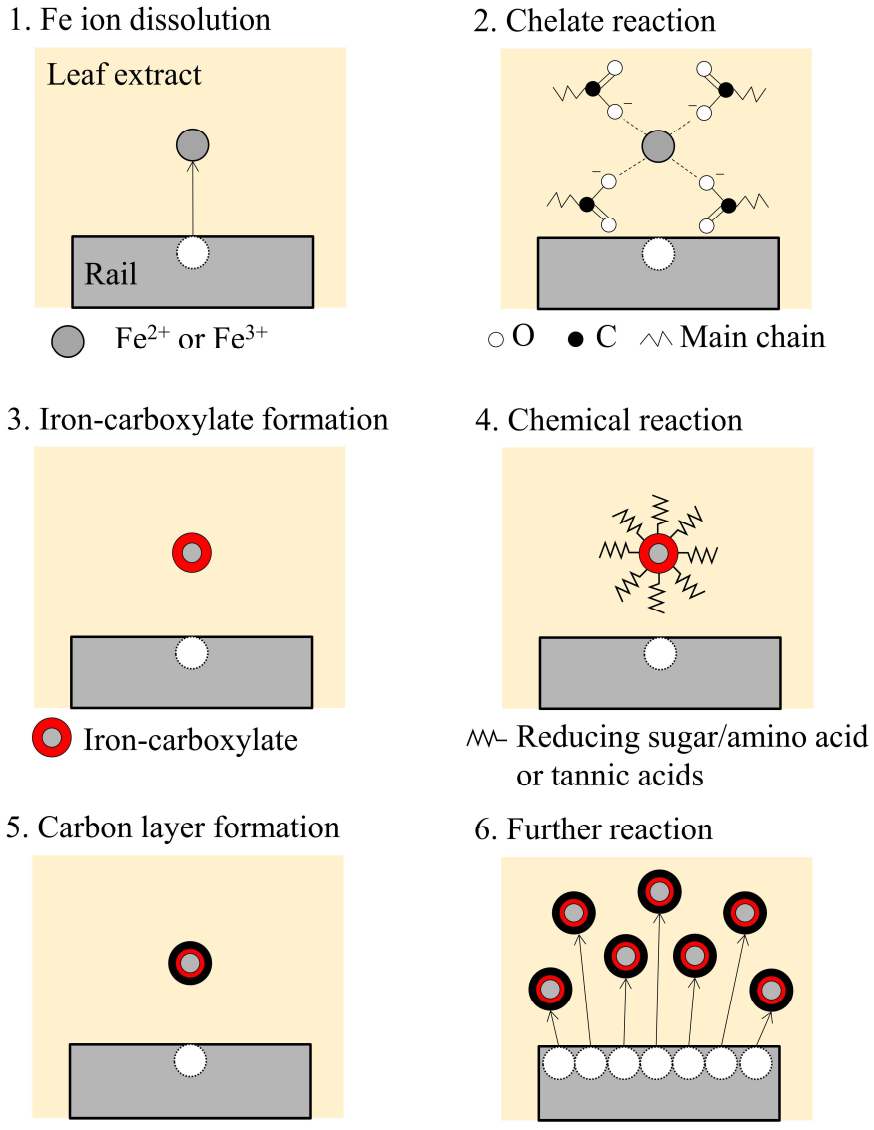

Figure 5.14 Supposed chemical reaction process

It should be noted that this process is a suggestion based on the information from the material analysis of the black materials synthesised in this study. In the actual wheel/rail contact, high pressure applied to leaves could affect the chemical reaction process, as well as high temperature induced by sliding in the wheel/rail contact [10]. To examine the proposed chemical reaction process, further experiments and analyses are necessary: identification of key organics in leaf extracts and comparison between a laboratory-developed black material and a blackened leaf film seen on the actual railway tracks.

5.5 Conclusions

In this chapter, the black material synthesised with sycamore leaf extracts and rail steels was chemically and materially analysed, using five techniques: X-Ray Fluorescence, X-Ray Diffraction, Laser Raman Spectroscopy, X-Ray Photoelectron Spectroscopy and Fourier Transform Infrared Spectroscopy. These analyses revealed that dissolved iron ions in leaf extracts react with organics, such as reducing sugars, amino acids and tannic acids, possibly forming a chelate structure. Then, the graphitic carbon layer is formed on the formed iron carboxylates or iron oxides with a small amount of KCl, $CaSO_4$ and phosphate compounds. This carbon material is seemingly a result of the Maillard reaction or iron-gall ink formation. Taking into account the results of the analyses, low adhesion was highly likely to have been brought by four factors: firstly graphitic carbon, secondly bulk leaves, thirdly iron oxides, and finally phosphate compounds in the black material. The chemical reaction process of the black material synthesis was proposed; however, further experiments and analyses are necessary to examine this proposal by analysing sycamore leaf extracts.

6 LEAF EXTRACT ANALYSIS

As discussed in 5.4, leaf extract analyses were performed to examine the potential theories of the chemical reaction process.

6.1 Introduction

The chemical reaction process has been suggested in 5.4.3; organic acids and iron ions dissolve in leaf extracts, and then they seem to precipitate the black material after the formation of an iron-ligand structure. Following this theory, the chemical reaction could be stopped if the organic acids are decomposed by some measures, such as pH value control, chemical substance and heat application. If this prevention of the chemical reaction is achievable, no black material should be formed when leaves are crushed by wheels, and low adhesion ideally never happens.

Hence, the aim of this leaf extract analysis is to identify the key organic acids which trigger the chemical reaction, using several methods of chemical analysis. This identification was attempted by comparing the results before and after the black leaf precipitate formation, as shown in Figure 6.1. Three hypotheses of the black substance formation developed in 5.4.2 were examined: Maillard reaction, iron-based pigment and organic acid.

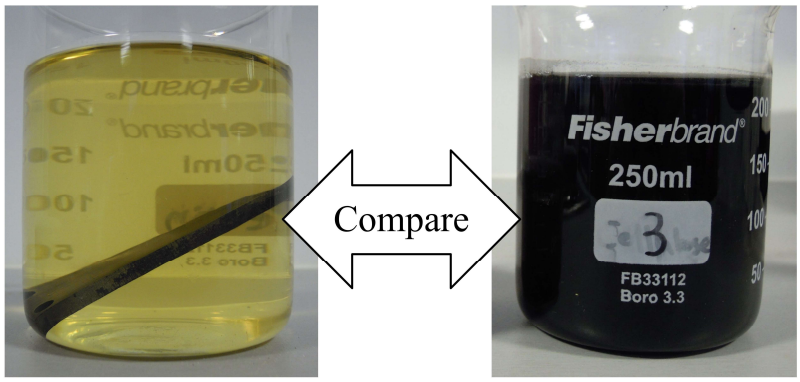

Figure 6.1 Concept figure of the leaf extract analysis

6.2 Methodology

Seven techniques of chemical analysis were used to investigate the key substance of the chemical reaction between leaf extracts and rail steel. It is noteworthy that only brown leaf extract (BLE) was examined in this series of analysis since very low friction was confirmed only in the black material formed in BLEs. Moreover, brown leaves were a more realistic material in the autumn, and thus, BLEs had to be given a priority in terms of research.

6.2.1 Viscosity measurement

Viscosity measurements were performed with a Brookfield DV1 Viscometer. A viscosity value was measured at 100 rpm and 30 °C, with a SC4-18 spindle. The purpose of this measurement is to gain an idea whether a leaf component with a high molecular weight dissolves into BLEs as suggested in [14].

6.2.2 pH value measurement

pH value was measured with a pHep pocket-sized pH meter. The meter was calibrated with a standard solution which has pH 4.0 and 7.0 before the measurement.

6.2.3 Inductively Coupled Plasma-Mass Spectrometry (ICP-MS)

A Perkin Elmer ICP-MS equipment (model: Elan DRC II) was used to analyse BLEs, which estimates a concentration of each ion by comparing with the standard solution. The main purpose of this analysis is to confirm the dissolution of iron from rail steels as well as other minor ions are present in BLEs, such as aluminium and manganese. This analysis was kindly conducted by Mr. Andrew Fairburn, the laboratory manager of Groundwater Protection and Restoration Group at the University of Sheffield.

6.2.4 Ion Chromatography for general ions (IC)

Leaf extracts were investigated by an IC equipment, detecting nine typical elements in natural water. Although the name of the equipment is unknown, this analysis was kindly carried out by Mr. Andrew Fairburn, the laboratory manager of Groundwater Protection and Restoration Group at the University of Sheffield.

6.2.5 Benedict reaction test

Benedict's reagent was purchased from Scientific Laboratory Supplies (Product number CHE1280, CAS number 63126-89-6). The test procedure is described as follows:

1. Leaf extract is made for the extraction time one day.
2. The leaf extract is then filtered in the same way described in 4.2.2.
3. 2 ml of leaf extract is mixed with 2 ml of Benedict's reagent.
4. The mixture is then warmed up to 80 °C and kept for ten minutes.
5. The colour change is observed.

The main aim of the Benedict test is a detection of any reducing sugars in leaf extracts, which are necessary to make the Maillard reaction happen.

6.2.6 High Performance Liquid Chromatography (HPLC)

The machine information is not available as this analysis was performed by a private company. The main aim of this analysis is to examine the possibility of the Maillard reaction theory by detecting the specific types of sugars which are typical in foods and plants: fructose, glucose, lactose, maltose and sucrose. It should be noted that all sugars mentioned here are a reducing sugar except for sucrose. Moreover, Hydroxymethylfurfural (HMF) analysis was also attempted for some samples prepared after the chemical reaction. This HMF analysis aims to find a trace of the Maillard reaction; an increase in HMF concentration can indicate that the Maillard reaction is likely to have occurred [111].

This work was kindly carried out by Mr. Howard Davies, Senior analyst at Campden BRI Group in the UK.

6.2.7 Proton Nuclear Magnetic Resonance (H-NMR)

Bruker AVIIIHD 500MHz was used in this H-NMR analysis. The aim of this analysis is to examine the possibility of the iron-based pigment theory suggested in 5.4.2 by detecting phenolic compounds, such as gallic acids, catechin and tannic acids.

This analysis work was kindly performed by Dr. Sandra van Meurs at the Department of Chemistry, the University of Sheffield.

6.2.8 Ion Chromatography for oxalate ion (IC)

IC analysis was performed with Dionex IC S5000 Dual Channel Ion Chromatography using the standard oxalate solution for IC purchased from Fisher Scientific (Alfa Aesar Oxalate, MDL number MFCD00012465). The iron-carboxylate theory was examined by detecting oxalate ions in BLEs before and after the chemical reaction. This analysis was kindly conducted by Mr. Alastair D. Bewsher, Senior analytical technician at the School of Earth and Environmental Sciences, the University of Manchester.

6.3 Results

6.3.1 Viscosity measurement

Table 6.1 summarises viscosity values of brown leaf extract (BLE), distilled water and pectin 0.1 wt% solution. The viscosity values of GLE and BLE were found to be at the same level as distilled water. In contrast, the artificial pectin 0.1 wt% solution exhibited a higher value than the LEs. This result indicates that leaf components with high molecular weight are unlikely to dissolve into LEs in terms of viscosity values. If pectin dissolves in LEs as suggested in [14], a concentration of pectin in LEs could be very low, under 0.1 wt% at least. Or pectin is decomposed from polysaccharide to monomer (a structural unit), such as a galacturonic acid [132], and it does not affect viscosity values.

Table 6.1 Viscosity measurements

Extraction time	Viscosity [mPa·s]		
	BLE	Reference	
1 day	1.08	Distilled water	1.08
2 days	1.05	Pectin 0.1 wt%	1.62

6.3.2 pH value measurement

The pH value of the BLE sample before and after the chemical reaction was 4.6 to 4.7 and 5.9 to 6.1, respectively. The BLE sample after the chemical reaction was found to be neutralised compared to the weak acidity of the BLE sample before the chemical reaction. This result shows that some acidic substances, possibly organic acids in BLEs, were consumed during the chemical reaction, supporting the proposed chemical reaction process in 5.4.3.

6.3.3 ICP-MS

Table 6.2 shows the detected metals in the ICP-MS analysis with the data of distilled water used in the extraction process. Note that the only top four metals were shown here, and the whole list can be found in Appendix B. The concentration of iron dramatically increased to around 31000 μg/L from 308 μg/L, and this result clarifies that iron dissolved into the leaf extract, inducing the chemical reaction.

Table 6.2 ICP-MS result of BLE samples

Element	BLE before [µg/L]	BLE after [µg/L]	Distilled water [µg/L]
Fe	308	31040	1.9
Mn	1703	2262	0.0
Al	27	1254	0.7
B	552.6	588.6	34.9

6.3.4 IC for general ions

Table 6.3 shows the result of IC analysis for the general ions. No significant difference in the concentration of each ion was observed; this result suggests that these ions are unlikely to trigger or cause the chemical reaction. Thereby, there could be other ions which show a dramatical change in the concentration before and after the chemical reaction.

Table 6.3 IC result for the general ions

Element	BLE before [mg/L]	BLE after [mg/L]	Distilled water [mg/L]
SO_4^{3-}	66.98	79.10	0.40
PO_4^{3-}	47.09	50.71	< 0.30
NO_3^-	0.25	0.68	0.12
NH_4^+	2.46	3.57	< 0.20
Na^+	11.29	7.91	1.61
Mg^{2+}	34.03	33.51	< 0.10
K^+	103.38	101.59	0.44
Cl^-	45.95	44.26	0.17
Ca^{2+}	112.54	107.28	< 0.30

6.3.5 Benedict reaction test

Figure 6.2 illustrates the result of the Benedict reaction test. Both BLE samples, before and after the chemical reaction, obtained orange precipitates after heating at 80 ℃, showing that both samples contained reducing sugars in them. However, the amount of precipitation seemed to be smaller in the BLE after the chemical reaction. This observation suggests that the reducing sugars have been consumed in the chemical reaction, although the precise weight or amount of the precipitate was not measured.

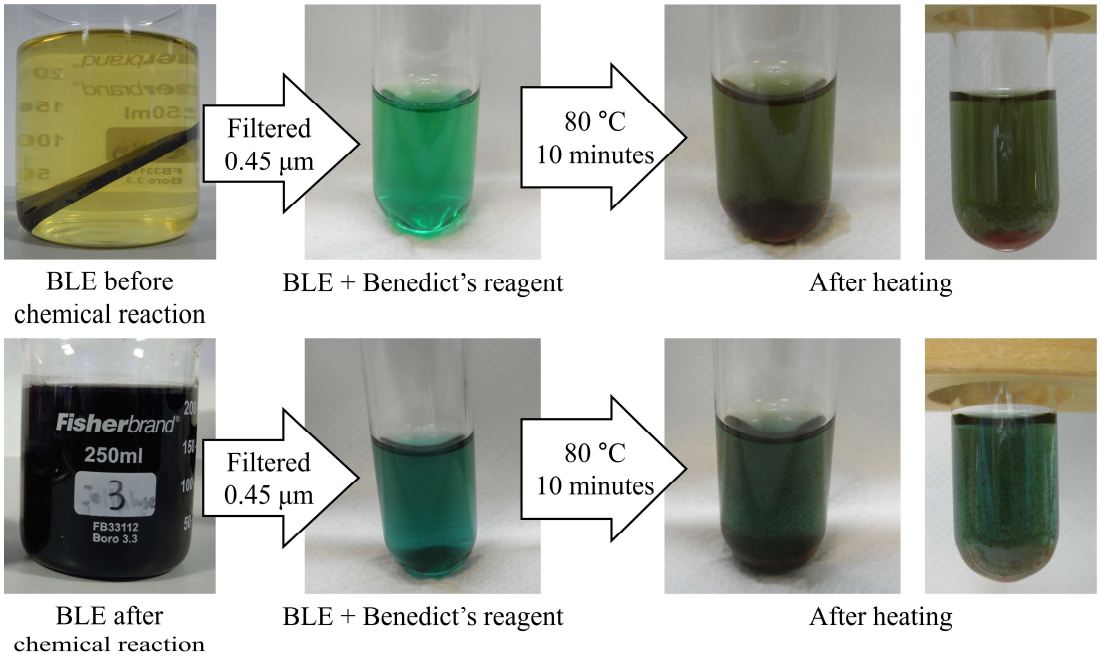

Figure 6.2 Results of the Benedict reaction test

6.3.6 HPLC

Table 6.4 shows the change in the amount of several types of sugars, detected by HPLC. In contrast to the result of the Benedict reaction test, the amount of typical reducing sugars, such as fructose and glucose, were found to be very small in both BLEs. The values lowered the detection limit of the equipment (0.01 g/100 g); therefore, it was not possible to evaluate the change in the amount.

Table 6.4 HPLC results (Sugars)

Type of sugars	BLE before [g/100 g]	BLE after (1) [g/100 g]	BLE after (2) [g/100 g]
Fructose	0.02	0.02	0.02
Glucose	< 0.01	< 0.01	< 0.01
Lactose	< 0.01	< 0.01	< 0.01
Maltose	< 0.01	< 0.01	< 0.01
Sucrose	< 0.01	< 0.01	< 0.01

Table 6.5 presents the amount of HMF detected in the BLEs prepared after the chemical reaction. The amount of HMF was very little, reaching the lower detection limit. This result shows that the Maillard reaction is unlikely to happen in terms of the HMF indicator and reducing sugars. On the other hand, the Benedict reaction test showed the difference between the BLEs before and after the chemical reaction. Therefore, these results indicate that the chemical reaction process could be very complex and not straightforward to clarify. More detailed work is necessary to understand the phenomenon correctly.

Table 6.5 HPLC results (HMF)

Component	BLE after (1) [mg/ kg]	BLE after (2) [mg/ kg]
HMF	< 25	< 25

6.3.7 H-NMR

Figure 6.3 illustrates the overview of the acquired H-NMR spectra of the BLEs before and after the chemical reaction. Both spectra were found to contain a lot of organics, particularly, in the region of the chemical shifts between 0.5 and 4.0. These peaks can derive from various organics, including methyl, methylene and methine protons in various conditions [99]. The assignment to each peak has not been considered here, since leaf extracts were expected to contain a lot of organics, and it is unrealistic to determine the organic material without other supporting information, e.g. expected molecular structure.

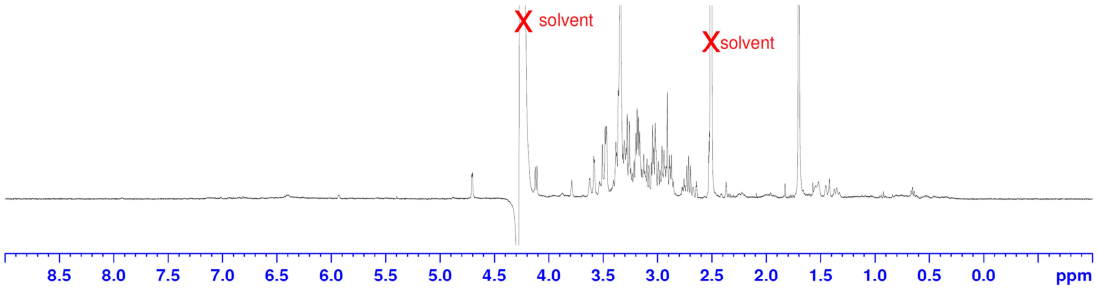

(a) BLE before the chemical reaction

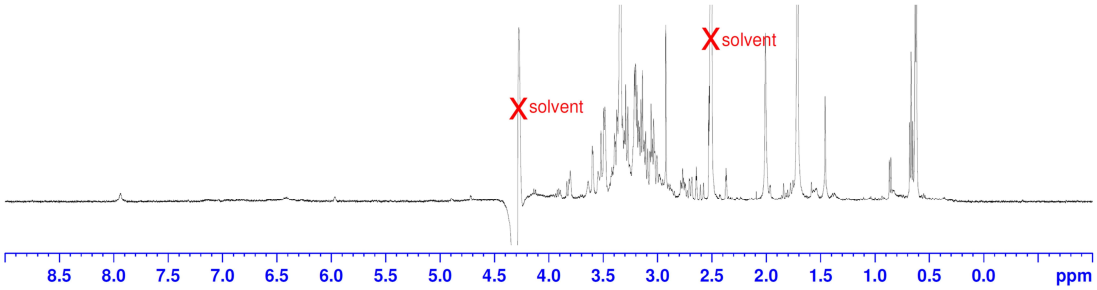

(b) BLE after the chemical reaction

Figure 6.3 Overview H-NMR spectra: (a) BLE before, (b) BLE after

Figure 6.4 depicts the zoomed-in view of the spectra in the high field. Some changes in the spectra can be seen, e.g. a sharper peak around 0.6 ppm. Despite these changes, no dramatic change was seen in the spectra. Thus, the components generating these peaks seem to be still in the BLEs, although the concentration could be different.

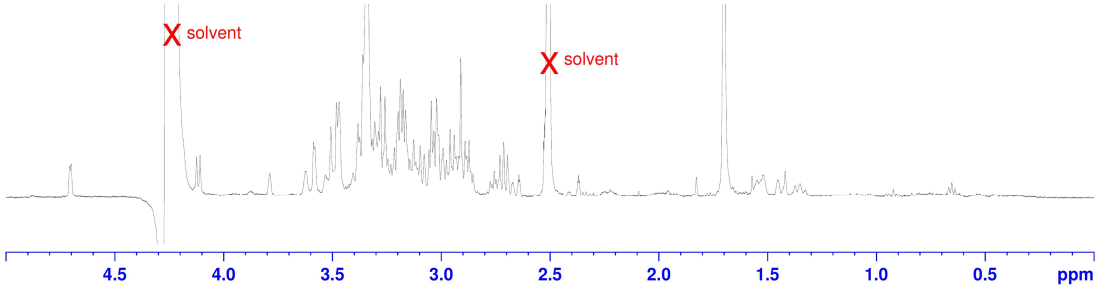

(a) BLE before the chemical reaction

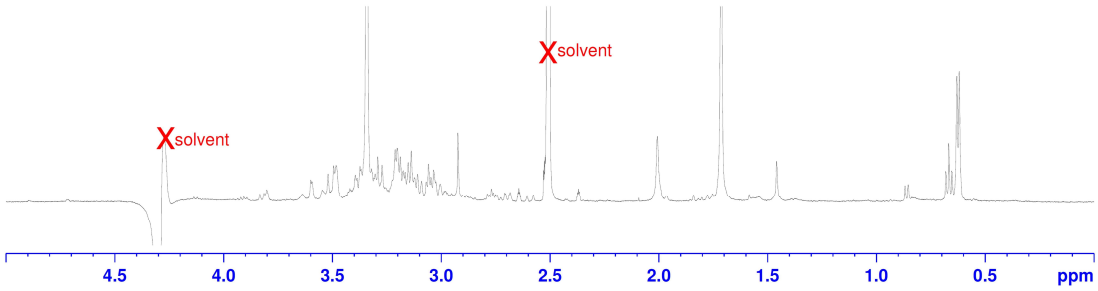

(b) BLE after the chemical reaction

Figure 6.4 Zoomed-in H-NMR spectra between 0 and 5 ppm:
(a) BLE before, (b) BLE after

Figure 6.5 illustrates the zoomed-in view of the spectra between 5 and 8.5 ppm. In general, protons bonded to aromatic groups have the chemical shifts in the low field, e.g. 6.5 to 8.5 ppm [99]. However, only weak and small peaks were seen in this region, suggesting that a lot of organic substances with aromatic rings are unlikely to be present in both BLEs. Therefore, the "iron-based pigment" theory is unlikely, since the tannin-derived polyphenolic material must have protons which show the chemical shift in the lower region.

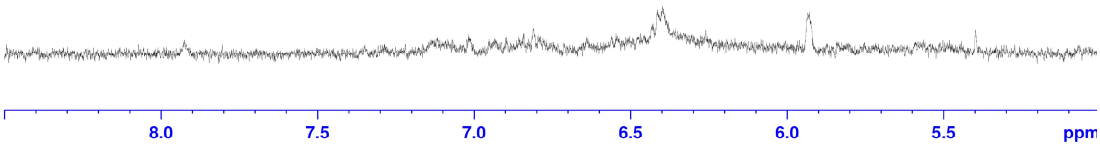

(a) BLE before the chemical reaction

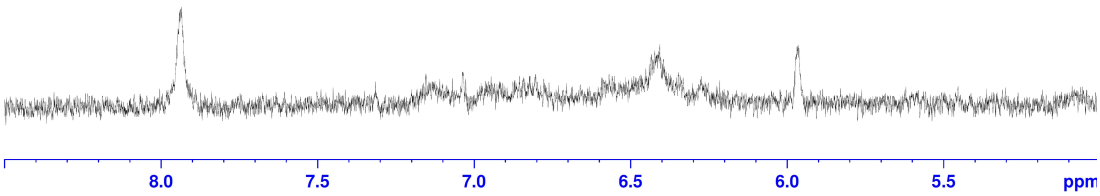

(b) BLE after the chemical reaction

Figure 6.5 Zoomed-in H-NMR spectra between 5 and 8.5 ppm: (a) BLE before, (b) BLE after

6.3.8 IC for oxalate ion

Figure 6.6 shows the IC result, which specifically detects oxalate ions in the BLEs. Oxalate ions were present in both BLE samples (five times diluted), and the concentration was estimated to be 5.33 mg/L and 6.21 mg/L for the sample before and after the chemical reaction, respectively. This result shows that the oxalate ions in BLEs are unlikely to contribute to either the chemical reaction or formation of iron-ligand structure. Hence, other carboxylate ions or different organic acids should be responsible for the chemical reaction.

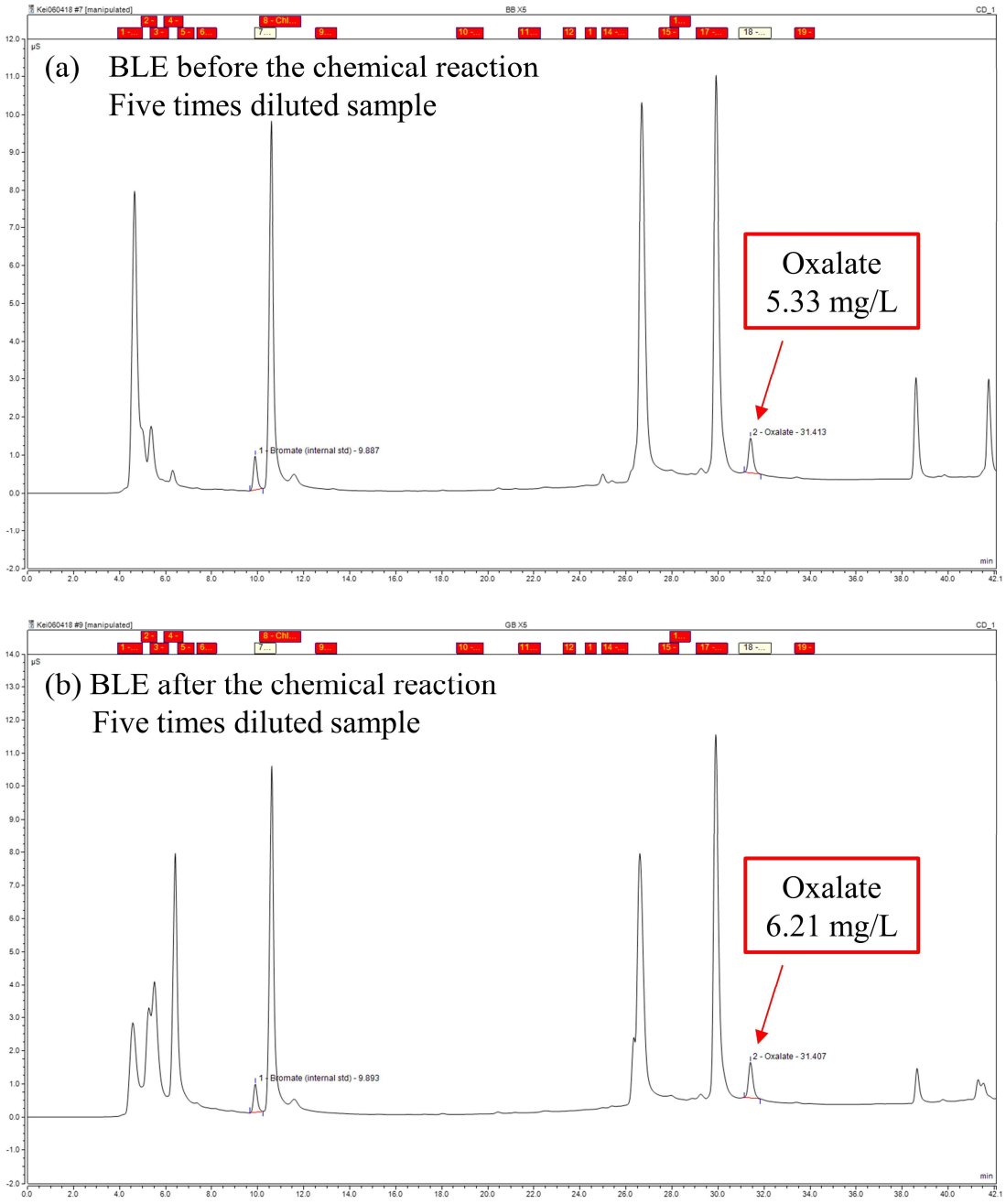

Figure 6.6 IC results for oxalate ion:
(a) Before chemical reaction, (b) After chemical reaction

6.4 Discussion

6.4.1 Examination of the chemical reaction process and hypotheses

The result of the viscosity measurement supports the idea that pectin is not likely to be dissolved in BLEs, suggested in 4.5.1. Moreover, the change in the pH values of the BLEs before and after the chemical reaction strongly supports the chemical reaction process proposed in 5.4.3, in which organic acids from leaves play an important role to trigger the reaction. The ICP-MS analysis showed the dramatical increase in the iron concentration after the chemical reaction; hence, the main idea in the proposed chemical reaction process seems reasonable.

The proposed three hypotheses for the chemical reaction between leaf extracts and rail steels were examined in this chapter: Maillard reaction, iron-based pigment and organic acid.

The "Maillard reaction" hypothesis could be incorrect because the HMF level in the BLE sample after the chemical reaction was under the lower limit of the detection, which is a by-product of the Maillard reaction and also an indicator of that reaction [111]. Moreover, reducing sugars, including fructose and glucose, were not successfully detected in the BLEs, indicating that the Maillard reaction is also unlikely.

However, Benedict's test clarified that reducing sugars were present in the BLEs, and the amount of the orange precipitate seemed to be smaller in the BLE sample after the chemical reaction to the naked eye. This result could suggest that other molecules with a free aldehyde group might make the precipitate instead of reducing sugars. Therefore, the molecular which causes the precipitate should be determined as the first step. For example, the change in concentration could be investigated using a colourimetric method of the Benedict reagent, and then the molecular weight determination could be carried out using a Liquid Chromatography-Mass Spectrometry (LC-MS) with the possible candidate having a free aldehyde in its structure.

The "Iron-based pigment" hypothesis is unlikely in the case of sycamore leaves, since the H-NMR analysis showed small peaks in the lower region, indicating less presence of tannin-based acids, such as gallic acids and catechin derivatives. There could be tannin-based acids in LEs of other type of leaves which might be responsible for the chemical reaction, further analysis should be necessary to investigate this theory.

The "Organic acid" hypothesis should be incorrect in the case of oxalate ions, as the IC analysis showed. There are several candidates which could form an iron-ligand structure or complex, including malic acids and acetic acids. Hence, these candidates

should be investigated with an appropriate method; possibly, IC analysis could be the first choice for the detection of each ion or component.

6.4.2 A potential prevention method of the leaf film formation

One of the aims of this research is to develop better methods for the prevention of leaf films on the railway track, as well as mitigation of low adhesion. These prevention and mitigation can be achieved if the key organic acids in leaf extracts are removed in some way, although the specific organic acids have not yet been determined. The removal method could be either evaporation or thermal decomposition of that organic acids. For example, acetic acids are reported to boil at 118 °C [133], and malic acids can decompose over 225 °C [134]. Hence, the heat application at stage 2 in Figure 5.14 could prevent the production of black material, decomposing the organic acids in leaf extracts.

Figure 6.7 illustrates the potential prevention method due to heat application. The heat can be applied to the leaf extract, and it helps prevent the chemical reaction by degrading the organic acids which form a ligand structure with the iron ion. The heat possibly enhances the water evaporation as well, removing the leaf extract itself from the rail surface. As a result, the black material should not be formed, and thus, low adhesion is unlikely to happen, leading to both the prevention and mitigation.

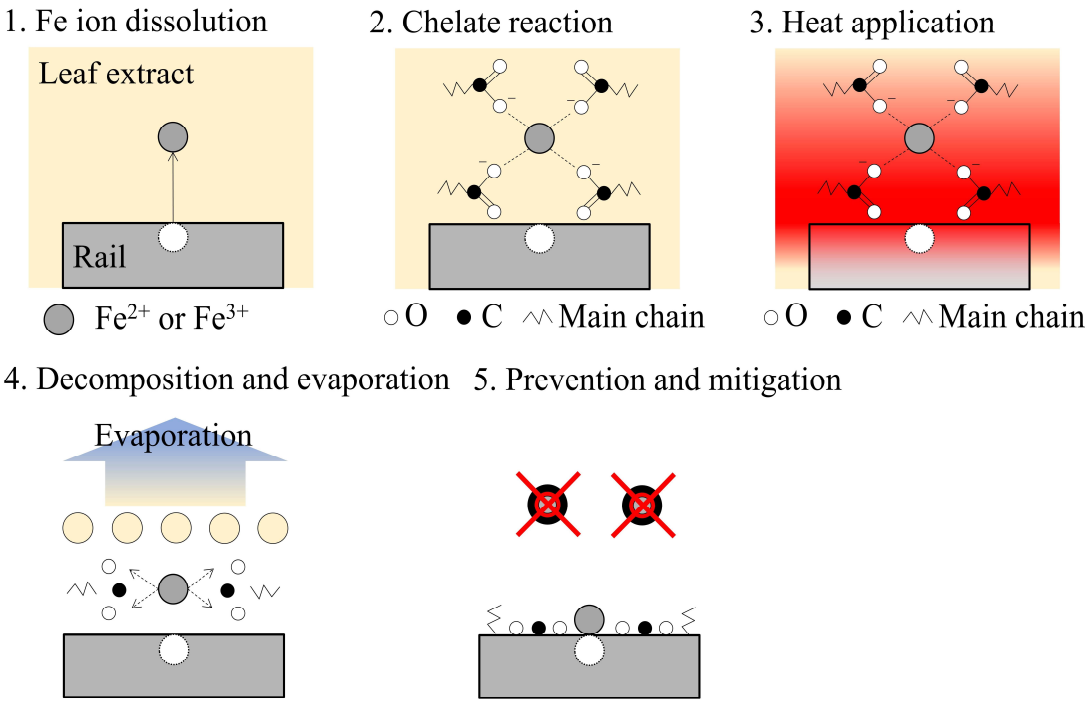

Figure 6.7 Potential prevention method due to heat application

One of the drawbacks of this prevention method is that the appropriate temperature to degrade the key organic acids has not yet been studied. In other words, some work is necessary to determine the target temperature to prevent the leaf film formation. Another disadvantage is that leaf films might stick to the rail surface tightly, as hypothesised in 3.4. If this tight bonding happens, the heat application might make the situation worse. Therefore, the work regarding these research topics must be carried out.

6.5 Conclusions

The proposed chemical reaction process in 5.4.3 was found to be reasonable; iron dissolves into the leaf extract and reacts with organic acids, as the pH value and ICP-MS analysis showed. However, the suggested three hypotheses in 5.4.2 were found to be unlikely or have a room for further discussion, showing that this series of leaf extract analysis could not find the key organic acid which triggers the chemical reaction. Further investigation is necessary to identify this acid; it could be begun from Benedict's test with a colourimetric method, and then some analysis, such as IC and LC-MS, can be carried out to narrow down the candidates.

Based on the results of the leaf extract analysis, the heat application to the leaf extract has been suggested as a potential prevention and mitigation method. The heat might be able to decompose the key organic acids, leading to the prevention of the leaf film formation. It is also able to cause boiling, removing the leaf extract itself from the wheel/rail contact. These research ideas will be examined in Chapter 7 and 8.

7 INFLUENCE OF TEMPERATURE: A TWIN DISC STUDY

7.1 Introduction

As discussed in 6.4, the heat application is a potential method to prevent the leaf film formation as well as mitigate the low adhesion due to leaves. However, no research has been conducted, which investigates to what extent the temperature is effective on the prevention and mitigation, to the best of the author's knowledge. If the most appropriate temperature is found, it will be possible to judge whether the heat application can be a realistic measure or not.

In general, temperature has a significant effect on a lubricant viscosity, and thus, the lubrication regime can be affected by the temperature [105]. In the case of wheel/rail contact, high temperature in the contact is recognised to lower a friction coefficient [135]. As the temperature increases, this negative impact must appear in the adhesion behaviour. Thereby, the effects of temperature on the adhesion behaviour should be investigated.

The basic characteristics of sycamore leaves were investigated, showing that they have lower friction coefficient (Chapter 4). However, the test method used (a ball-on-flat test) does not reflect the rolling-sliding contact between the wheel and rail. This rolling-sliding condition can be replicated by a twin disc machine, and the leaf contamination has been tested by the twin disc machine developed at the University of Sheffield, called SUROS [22].

Hence, the aim of this twin disc study is to investigate the temperature influence on the adhesion level of sycamore leaves in a rolling-sliding conditions, examining the possibility of the heat application method as a countermeasure against leaf contamination.

7.2 Methodology

7.2.1 Sample preparation

Figure 7.1 shows the fine leaf powder used in this study. Brown sycamore leaves were collected in Sheffield between October and December in 2017. They were chopped in a food blender, followed by grinding procedure with a manual coffee grinder, making fine leaf powder. The leaf powder was then filtered using a 160 μm sieve (purchased from Fisher Scientific) to obtain the finest leaf powder. In addition to this fine leaf powder, the black precipitation powder formed in brown leaf extracts was also tested, which was prepared by following the method described in 4.2. It should be noted that green sycamore leaves and their derivatives were excluded in

this study, as they were found to show a relatively high friction coefficient (COF) compared to brown sycamore leaf derivatives.

In addition to the leaf-related samples, some standard materials were also examined: distilled water, engine oil (Servol 15W-40, Morris lubricant) and activated charcoal (AC), which was purchased from Sigma-Aldrich (product number: C9157, CAS number: 7440-44-0).

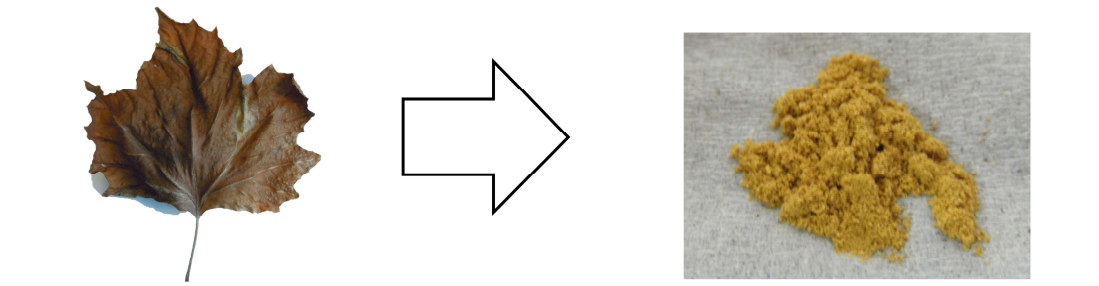

Figure 7.1 Preparation of the fine leaf powder

7.2.2 Test equipment and specimens

The Sheffield University ROlling Sliding (SUROS) machine was used to replicate a rolling-sliding contact between train wheels and rails and investigate tribological properties of the samples under such conditions. Figure 7.2 illustrates the schematic diagrams of the SUROS machine and 47 mm diameter disc specimens cut from rail steel (R260) and wheel steel (R8). These two discs were loaded against each other by a hydraulic pump, and they were individually driven by a Colchester Mascot lathe and an AC motor. The wheel disc was driven faster than the rail disc, replicating traction conditions between wheels and rails. The tangential contact force between the two discs was measured by a torque transducer on the shaft of the rail disc side, and traction coefficient was calculated with the tangential contact force and disc diameter. More detailed information about the test set-up of the SUROS can be found in previous studies [11], [16], [22], [35].

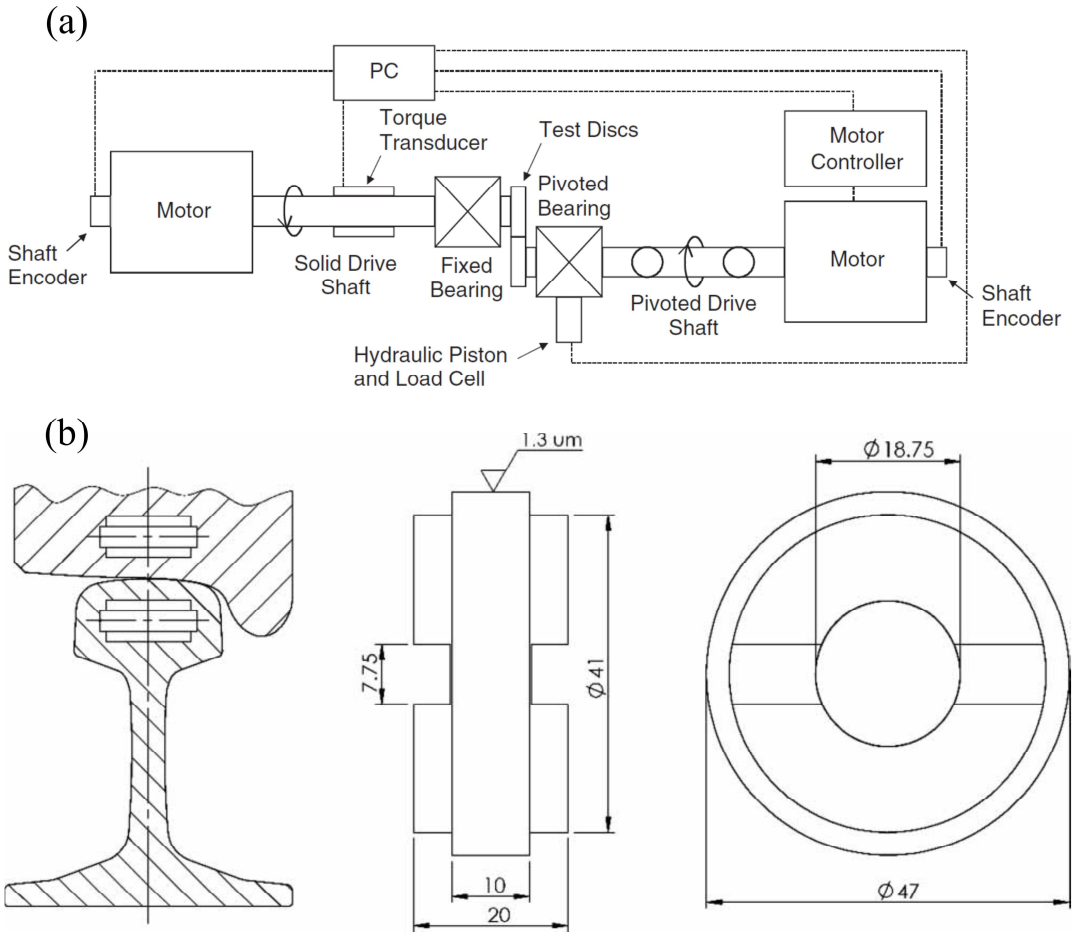

Figure 7.2 Schematic figures of test equipment [16]
(a) SUROS machine, (b) Disc specimens

7.2.3 Friction test procedure without pre-heating

Figure 7.3 shows a schematic figure of the traction curves in the SUROS tests at different slip ratio. The traction coefficient data can be divided into three phases: running-in, sample application and recovery. The traction coefficient usually showed a stabilised value during the running-in period, and then it plunged when the sample suspension was applied. The traction maintained low level during the sample application (approximately 20 seconds), and then it showed the recovery, back to the dry level.

Figure 7.4 illustrates the application process of the sample suspension to the rail disc. Friction tests were carried out as follows.

1. Two discs were cleaned with acetone in an ultrasonic bath and then mounted in the machine.

2. The discs were allowed to run under dry conditions for four to five minutes until the traction coefficient stabilised.

3. The sample suspension was then applied to the upper rail disc while measuring the traction coefficient.

4. The test was then stopped after the traction coefficient had roughly recovered to the dry condition level.

5. The test was repeated three times at each slip value.

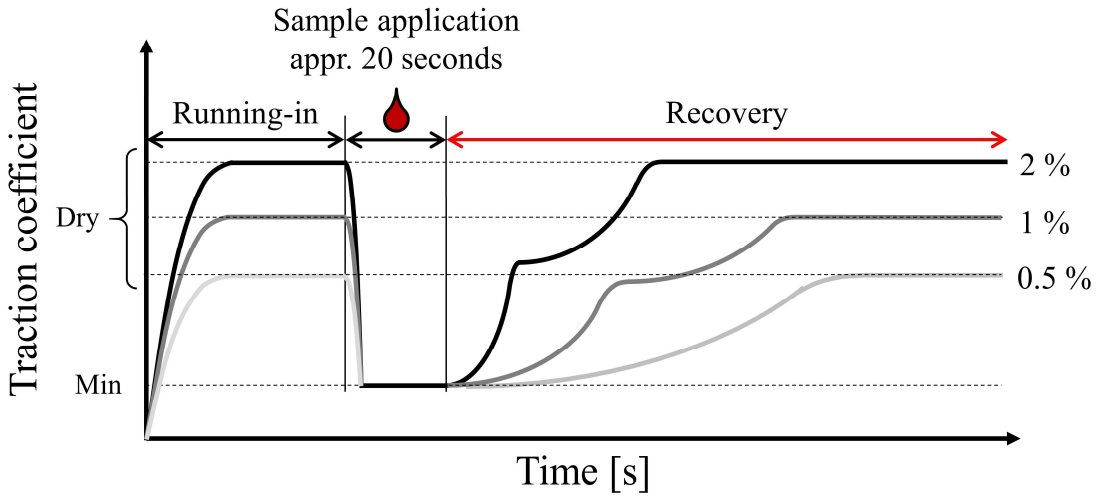

Figure 7.3 Schematic figure of traction curves at different slips

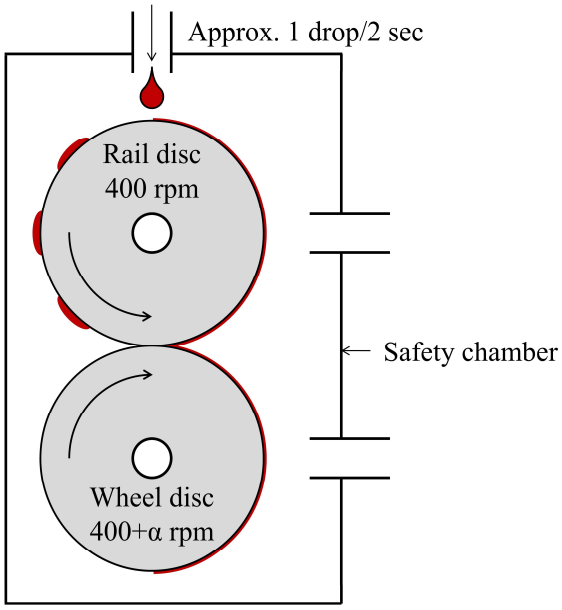

Figure 7.4 Schematic diagram of friction test procedure with liquid samples

Table 7.1 summarises the experimental conditions. The rail disc was driven at 400 rpm, which is approximately 1 m/s, but the wheel disc was driven at more than 400 rpm, depending on the slip values. Slip values were calculated following the definition shown in Equation 7.1[11], and 0.5, 1 and 2 % were chosen since the contact at small slip values, which has both stick and slip region, is important in terms of vehicle dynamics [135].

$$\frac{w_{wheel} \cdot r_{wheel} - w_{rail} \cdot r_{rail}}{w_{wheel} \cdot r_{wheel} + w_{rail} \cdot r_{rail}} \cdot 200\%$$

Equation 7.1

Where w stands for the disc speed, and r does for the radius of the disc, respectively. In the wheel/rail contact, the traction coefficient is likely to saturate at around 1-2 % slip and the whole contact patch becomes pure-sliding in dry conditions [3], [40]. Hence, the friction behaviour at these small values was explored in this study.

The concentration of sample suspension (LP, BBP and AC) was fixed at five weight percent (wt%), and 0.4 to 0.6 ml of sample suspension was applied to the rail disc at approximately 1 drop/2 seconds (around 20 seconds for 10 drops). It should be noted that only 1 drop of the engine oil was applied as it showed such low friction with three drops that the comparison between the other samples was difficult.

Table 7.1 Experimental conditions of SUROS friction tests

Parameter	Value
Disc diameter [mm]	47
Average Hertzian pressure [GPa]	1.2
Speed (Rail disc) [rpm]	400
Slip value [%]	0.5, 1, 2
Sampling frequency [Hz]	1
Concentration of sample suspension [wt%]	5
Application rate [drop(s)/second]	0.5
Sample amount in total [ml]	0.4-0.6 (10 drops) *1 drop for engine oil
Repetition [times]	3 *Only for the test without pre-heating

7.2.4 Friction test procedure with pre-heating

Figure 7.5 exhibits the pre-heating procedure, conducted only with 5 wt% LP suspension. In this test, both rail and wheel discs were heated up before the actual friction tests. The procedure of friction tests with pre-heating is described below.

1. Two discs were cleaned with acetone in an ultrasonic bath and then mounted in the machine.

2. The discs were tested for five to seven minutes at one of these slip values: 4, 7, 10, 15 or 20 %, depending on the target temperature.

3. The test was stopped, and the surface temperature of the rail disc was measured with a k-type thermocouple.

4. The machine was restarted and operated for one to two minutes at 0.5 or 1 % slip to stabilise the traction coefficient.

5. LP suspension was then applied to the upper rail disc.

6. The test was then stopped after the traction coefficient had roughly recovered to the dry condition level.

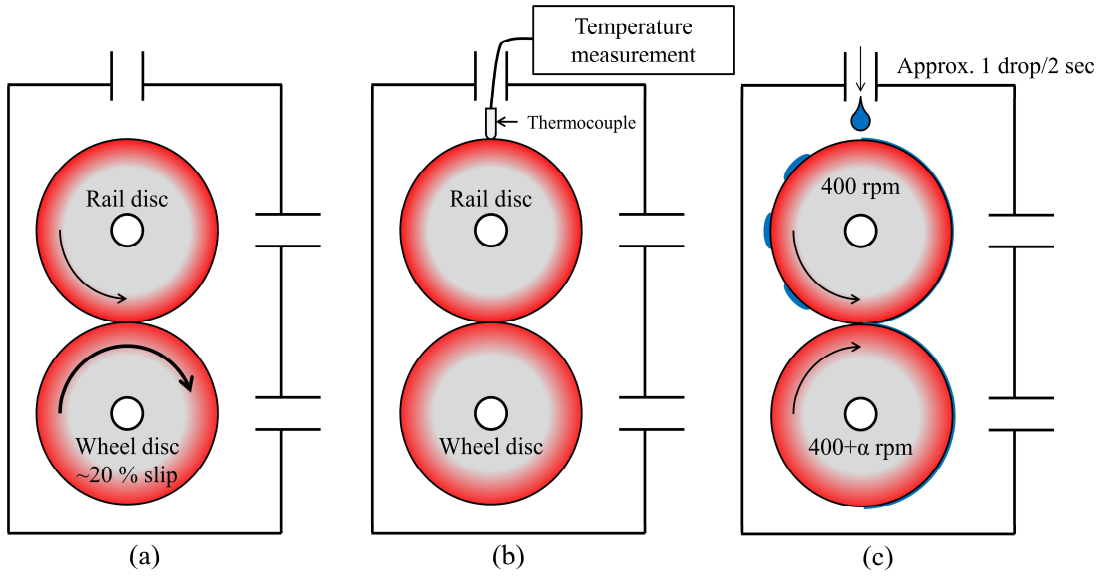

Figure 7.5 Friction test procedure with pre-heating process
(a) Running-in dry conditions at higher slips, (b) Surface temperature measurement, (c) friction test

The measured temperature was defined as the surface temperature, although the actual temperature during the test seems to be slightly lower than that because of the time lag between the measured point and experiment. A few trial tests showed that this pre-heating process uniformly heated up the whole disc: not only the surface.

Hence, the temperature drop in the stabilisation process was believed to be small, e.g. up to 10 °C, and the surface temperature mentioned in this chapter is an estimation based on the measurement before the stabilisation process.

The slip value in the pre-heating process was determined considering the proportional relationship between surface temperature and slip values in [44]. The pre-heating test at 4, 7, 10, 15 and 20 % increased the surface temperature approximately to 80, 100, 140, 180 and 200 °C, respectively. A trial experiment estimated these temperature values. It should be noted that the test was conducted only once, not three times like the friction test without pre-heating.

7.2.5 Evaluation of the data

Figure 7.6 shows the evaluation method of the acquired traction data. Three figures were calculated from the curve: average traction coefficient of the running-in (μ_D), sample suspension (μ_L) and average recovery time (T_R). μ_D is the average value for 30 sec before the sample application commences, and μ_L is the average traction coefficient for 15 sec after the sample suspension is applied. T_R is the time when the traction coefficient reaches 0.2 after the sample suspension is applied, which is the minimum requirement for traction [1]. Based on this T_R, the sliding distance SD_R was calculated following Equation 7.2.

$$\boldsymbol{SD_R = \alpha V T_R}$$

Equation 7.2

Where α stands for the slip ratio, and V does for velocity (m/s). In this test, V is approximately 1 m/s, and α is either 0.5, 1 or 2.

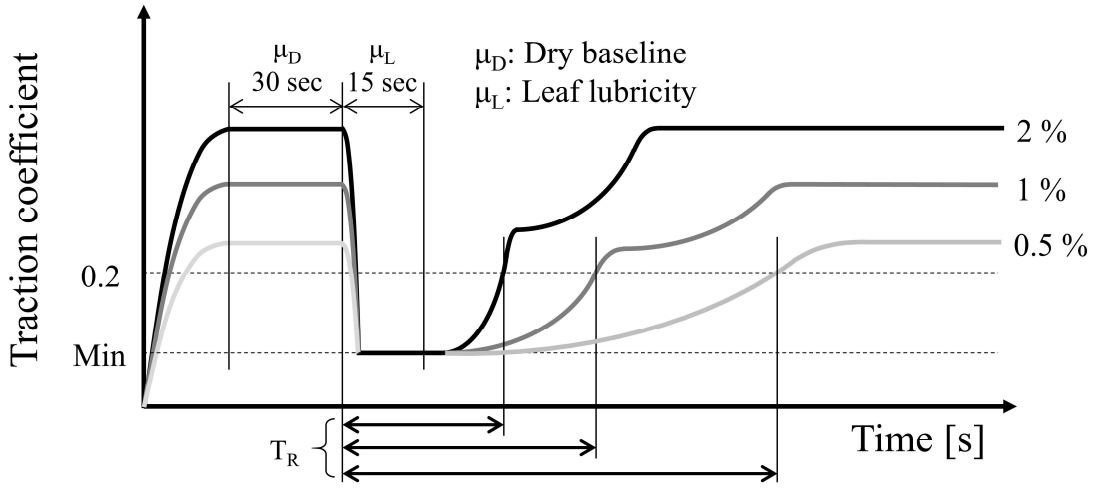

Figure 7.6 Definition of terms for evaluation

7.3 Results

7.3.1 Friction test without pre-heating

Figure 7.7 exhibits an example of the friction test result, which was taken with the LP suspension at 2 % slip without the pre-heating process. The friction behaviour showed the pattern described in 7.2; constant traction coefficient in dry conditions, followed by the sudden decrease due to the sample application, and then the recovery. As can be seen, μ_D represents the baseline traction coefficient in dry conditions, and μ_L shows the traction coefficient due to the sample suspension.

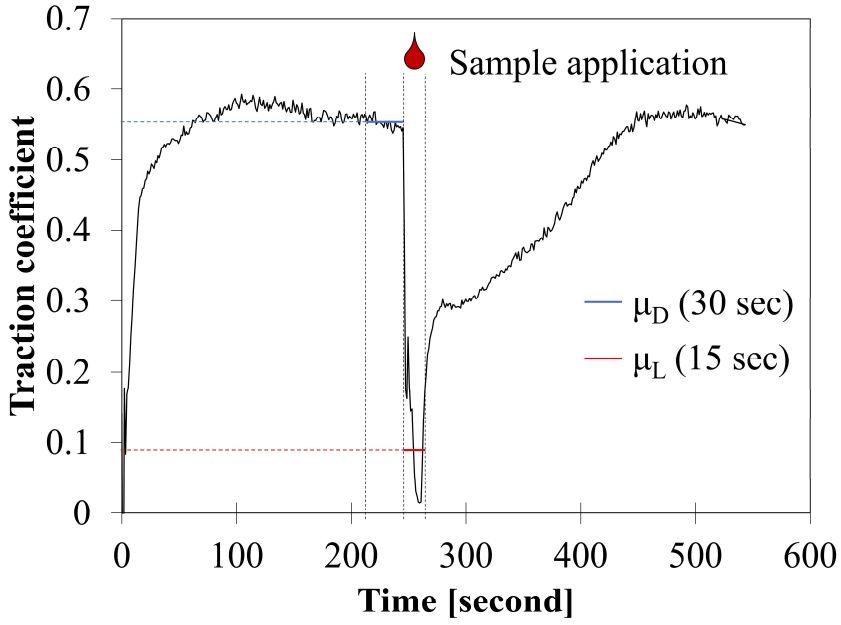

Figure 7.7 Example of the friction test: 5 wt% LP suspension at 2 % slip without pre-heating

Figure 7.8 (a) shows an example of raw traction data at 0.5, 1 and 2 % taken with the distilled water. At all the slips values, the traction coefficient dropped after the water application, and then the recovery was seen. The recovery behaviour depends on the slip value; the gradual recovery was seen at 0.5 %, but there was a relatively quick recovery at 2 %. Figure 7.8 (b) shows the creep curves of the average traction coefficient: μ_D and μ_L. μ_L was around 0.2 at all slip values, showing a good agreement with the previous study apart from 0.5 % slip [13].

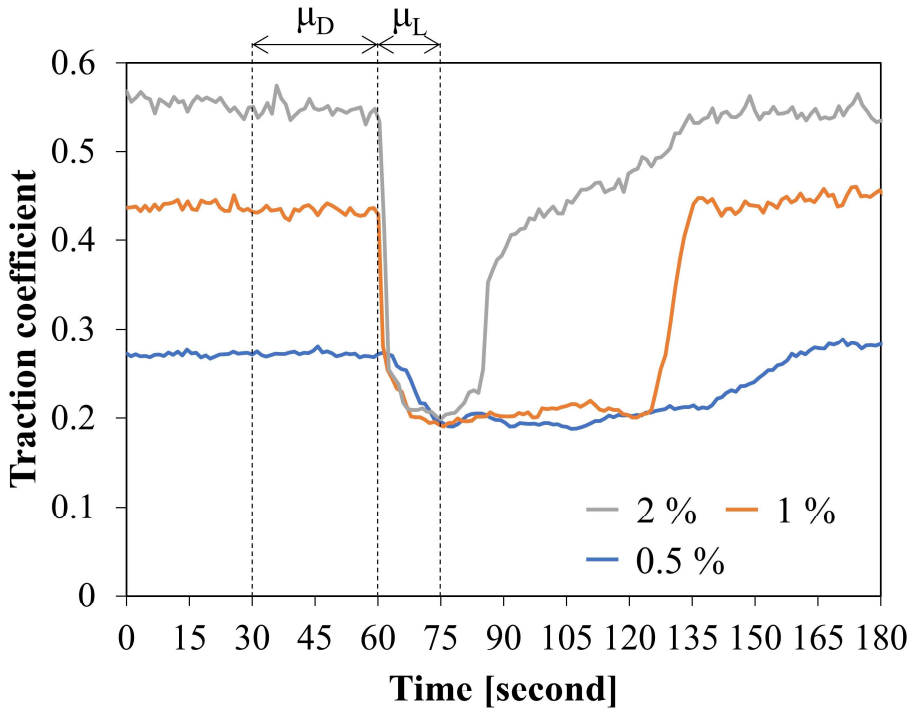

(a)

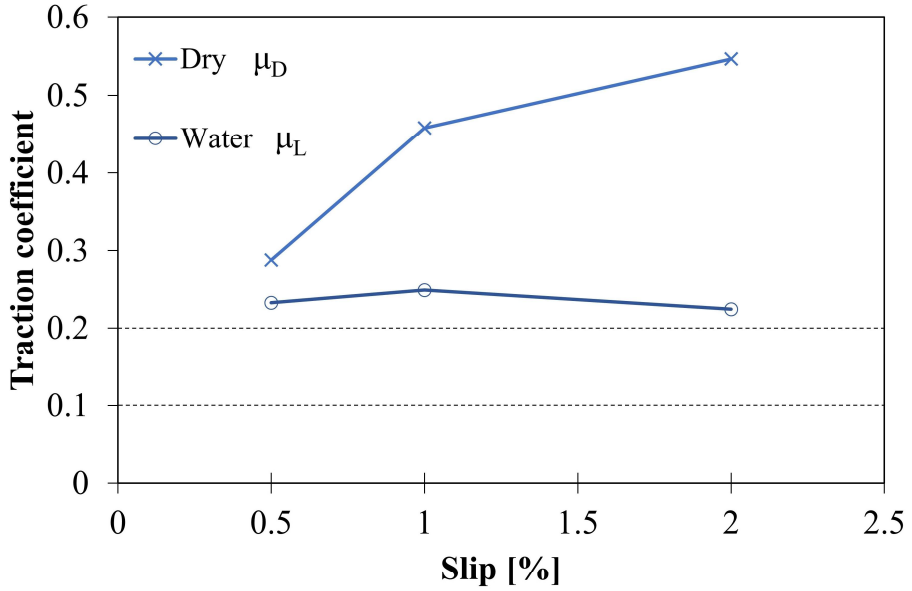

(b)

Figure 7.8 Traction behaviour of distilled water
(a) Comparison of typical traction data at 0.5, 1 and 2 % slip, (b) Creep curves

Figure 7.9 (a) shows an example of the frictional behaviour of the engine oil, and Figure 7.9 (b) exhibits the creep curves of μ_D and μ_L. There was no clear recovery region, and μ_L was around 0.1 at all the slip values. As expected, the engine oil exhibited a very stable and low traction coefficient, and the higher slip did not seem to affect its performance.

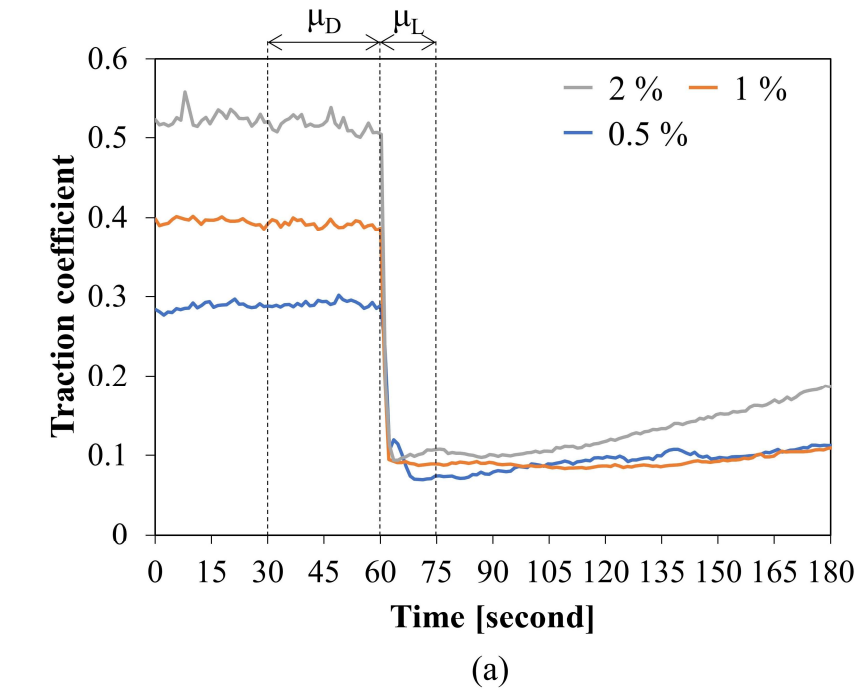

(a)

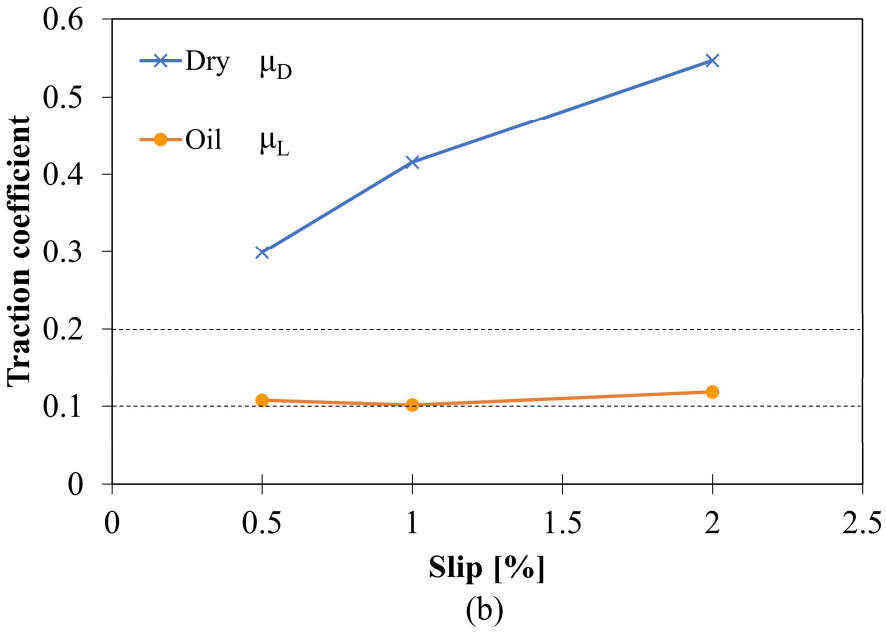

(b)

Figure 7.9 Traction behaviour of engine oil
(a) Comparison of typical traction data at 0.5, 1 and 2 % slip, (b) Creep curves

Figure 7.10 illustrates the frictional behaviour and creep curves of the LP suspension. LP suspension was found to show the low traction coefficient at all slip values. In particular, μ_L reached almost the detection limit at 0.5 %, and it still kept the low level at 1 and 2 % slip. As shown in Figure 7.10 (b), μ_L at 0.5 and 1 % slip met neither the traction requirement 0.2 nor braking requirement 0.1 [1], and μ_L at 2 % slip did not reach 0.2. Moreover, μ_L at all slip values was lower or at the same level as the engine oil, showing a good agreement with the result in [136]. On the other

hand, the recovery after the sample application became more distinct as the slip increased. It should be noted that the LP suspension became black immediately after it was applied to the disc surface, indicating that the chemical reaction between leaf organics and iron had happened.

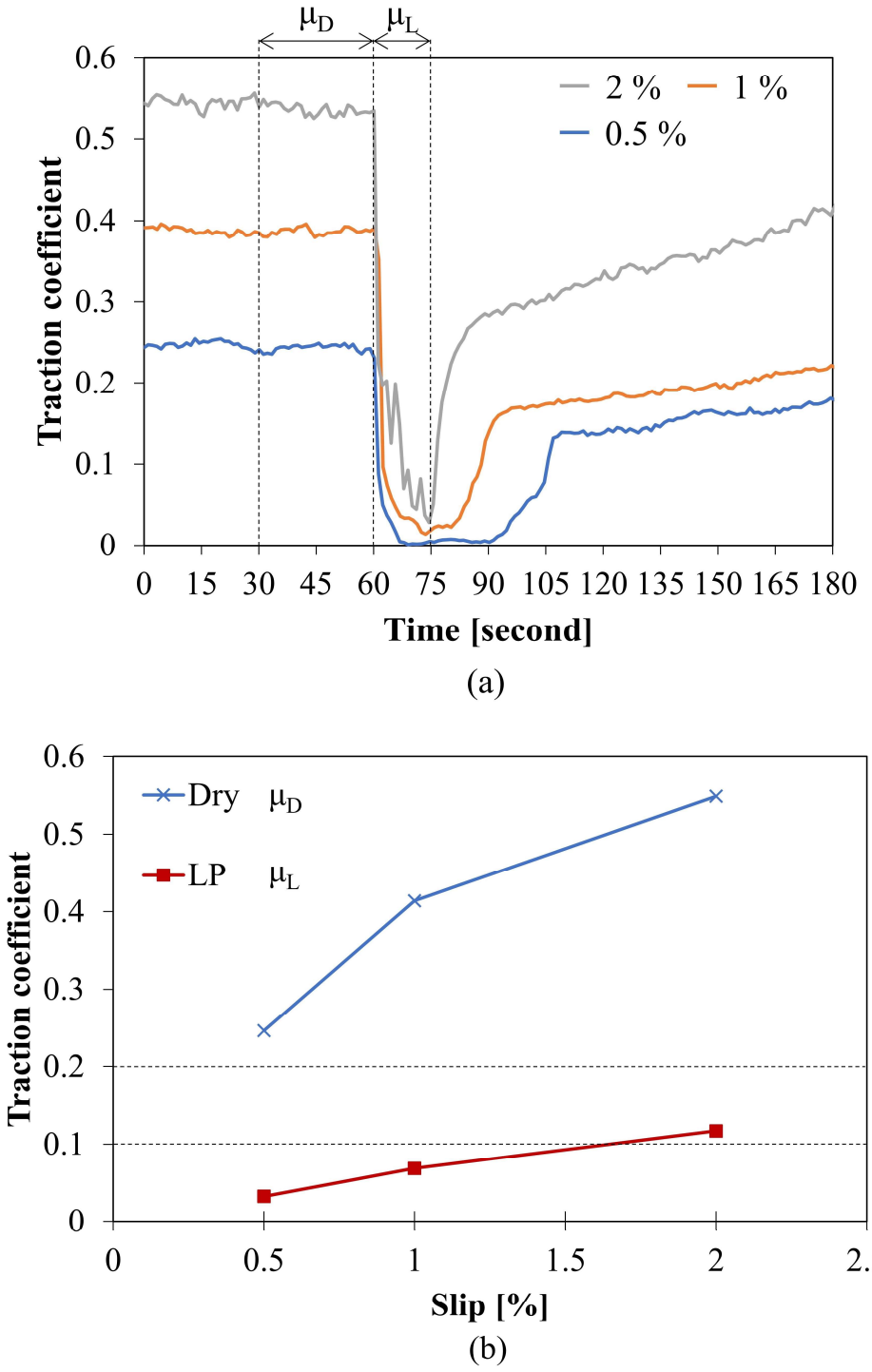

Figure 7.10 Traction behaviour of LP suspension
(a) Comparison of typical traction data at 0.5, 1 and 2 % slip, (b) Creep curves

Figure 7.11 depicts the frictional behaviour and creep curves of BBP suspension. The frictional behaviour was analogous to the LP suspension; low traction coefficient and more noticeable recovery as the slip value increased. μ_L was lower than 0.1 at 0.5 and 1 % slip, and it met the braking requirement but failed to reach 0.2 at 2 % slip, as shown in Figure 7.11 (b).

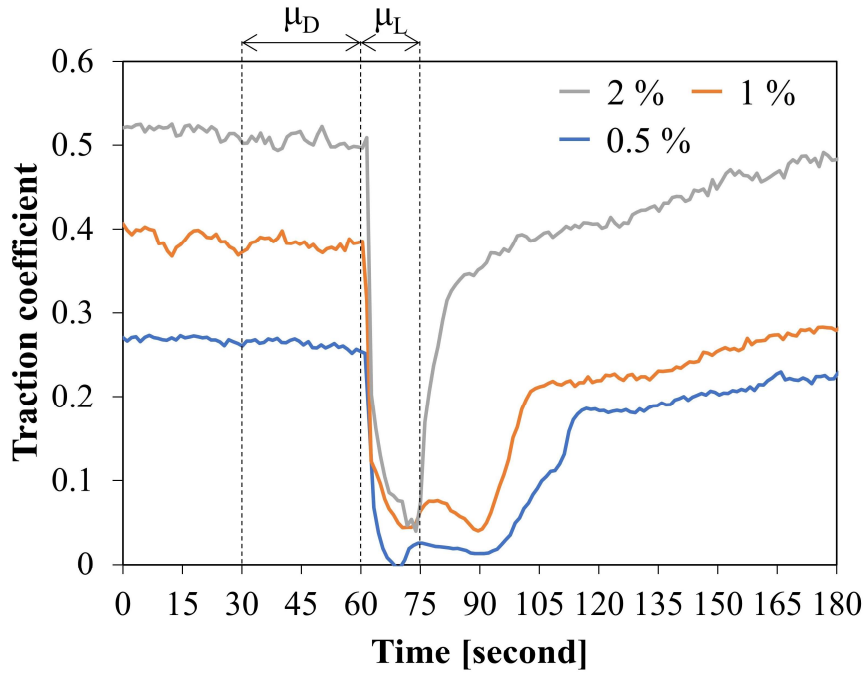

(a)

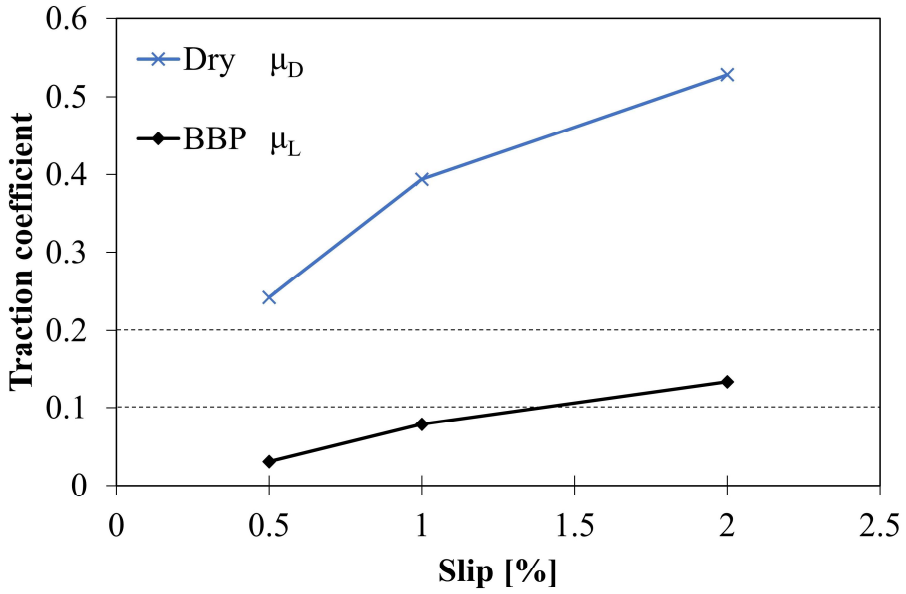

(b)

Figure 7.11 Traction behaviour of BBP suspension
(a) Comparison of typical traction data at 0.5, 1 and 2 % slip, (b) Creep curves

Figure 7.12 illustrates the comparison of traction data and creep curves of AC suspension. Unlike the LP and BBP suspension, the AC suspension showed a low and constant traction coefficient between 0.1 and 0.2, and there was no distinct initial recovery region. This consistently low traction shows that the black material formed in the LP and BBP tests had different tribological property from the AC.

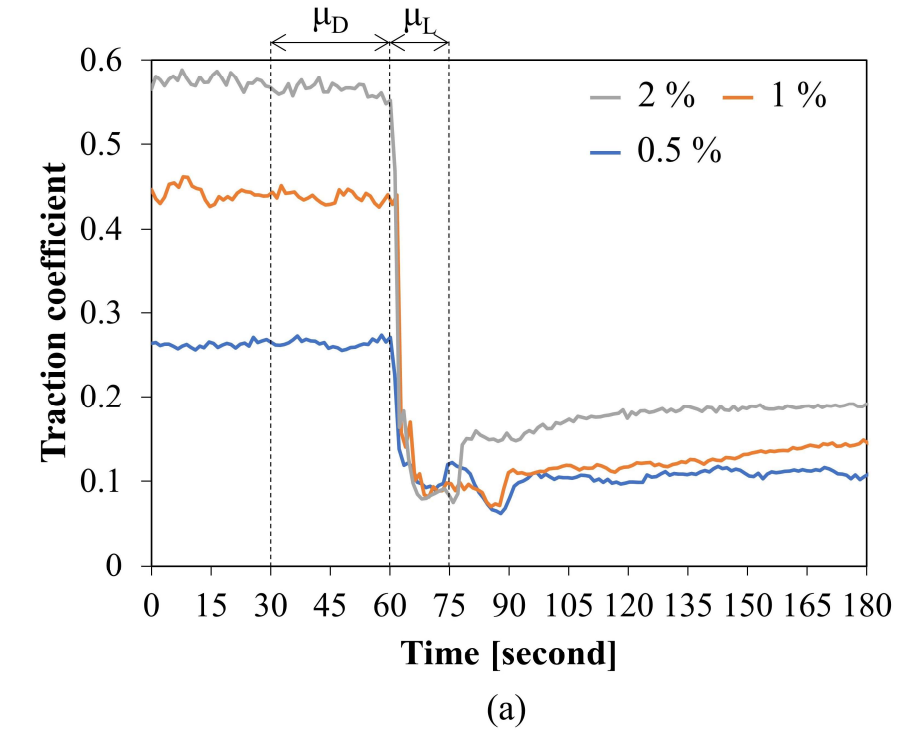

(a)

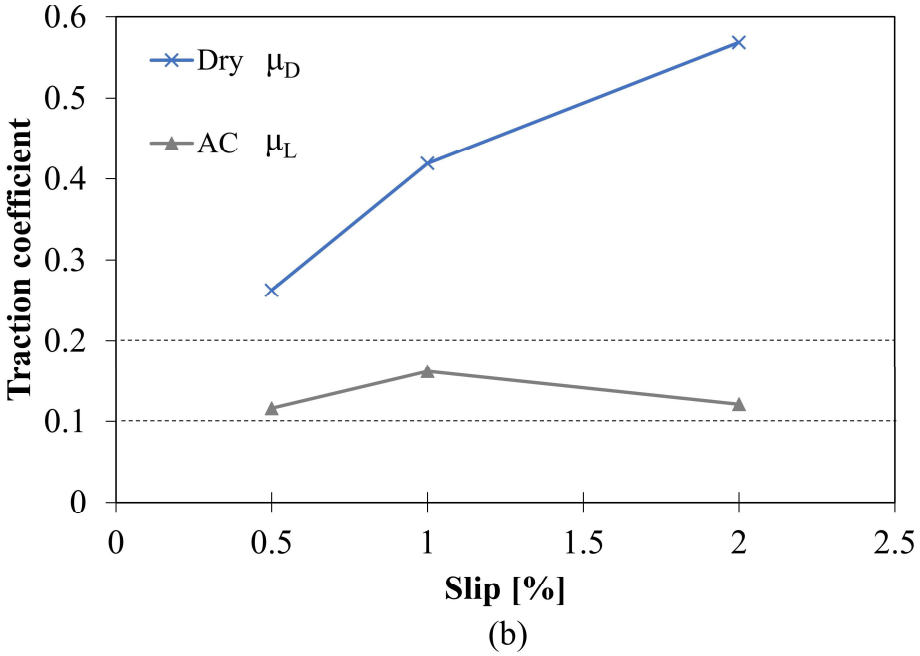

(b)

Figure 7.12 traction behaviour of AC suspension
(a) Comparison of traction data at 0.5, 1 and 2 % slip, (b) Creep curves

Figure 7.13 shows the SD_R of AC, engine oil, BBP and LP. In comparison with the AC and engine oil, BBP and LP were found to have less SD_R. BBP had the same SD_R at all slips around 0.4 m like the engine oil; however, LP had less SD_R at 2 % slip, around 0.4 m, than the SD_R at 0.5 and 1 % slips. This different trend in the SD_R means that other factors might be able to contribute to the recovery in the case of LP suspension, not simply depending on the sliding distance.

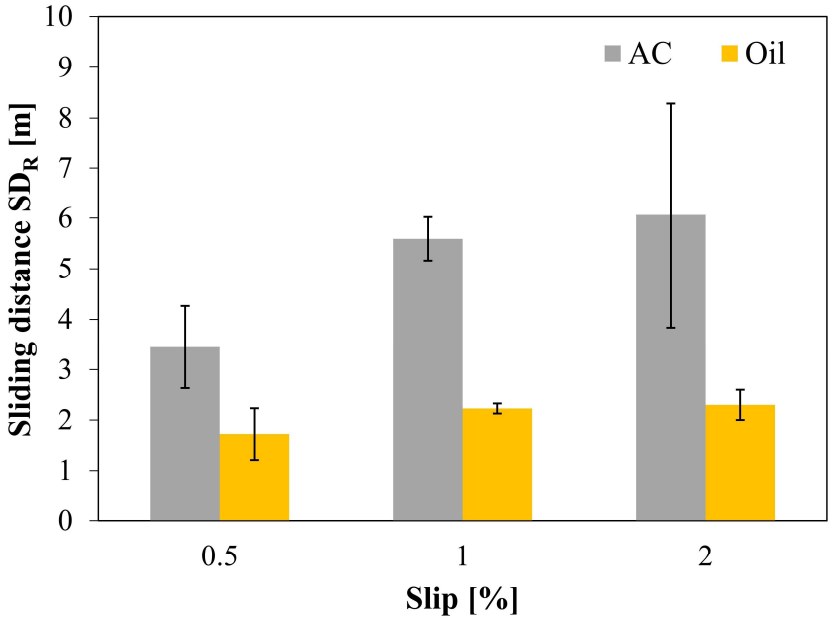

(a)

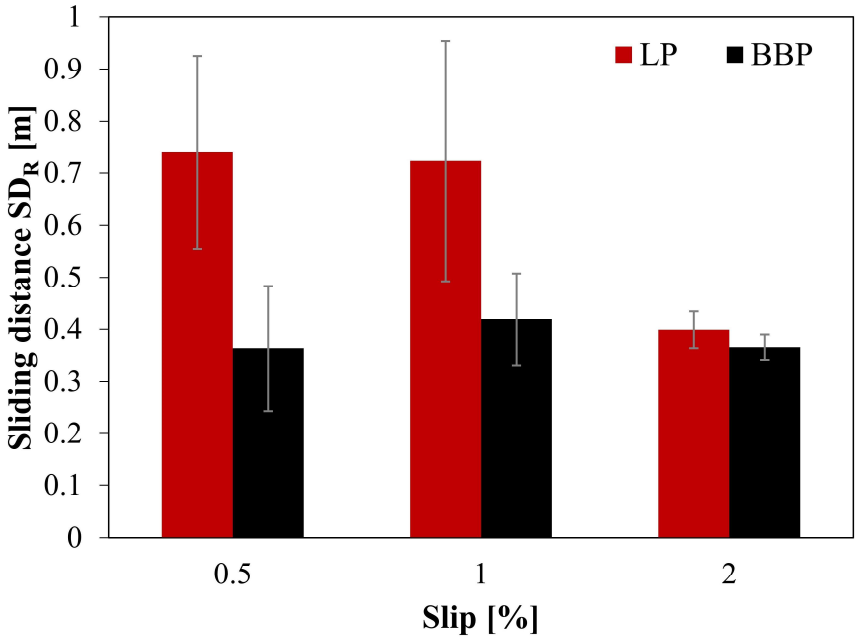

(b)

Figure 7.13 Comparison of the SD_R for each sample
(a) AC and engine oil, (b) LP and BBP

Potential differences related to a higher slip value could be an increase in surface temperature during the running-in period. The surface temperature was measured by the method presented in 7.2.4 after five minutes operation at 0.5, 1 and 2 % slip in dry conditions. The result was summarised in Table 7.2. The surface temperature was confirmed to increase as the slip value increased, and the difference between 0.5 and 2 % slip was around 20 °C. Since the change in the surface temperature was found, the effect of surface temperature on traction coefficient was investigated.

Table 7.2 Surface temperature after the operation at 0.5, 1 and 2 % slip

Slip value [%]	Surface temperature [°C]
0.5	44.3 ±2.8
1	51.8 ±1.5
2	63.7 ±0.6

7.3.2 Friction test with pre-heating

Figure 7.14 depicts the traction behaviour of LP suspension at 0.5% slip, which was taken at various temperatures with pre-heating process. Figure 7.14 (a) is the comparison of the acquired traction data at 42, 106, 180 and 211 °C (zoomed-in view). As the temperature increased, the traction coefficient μ_L in the sample application region increased, and only a subtle drop was observed at 211 °C. Moreover, the recovery region started much earlier at 106 °C than 42 °C, and no significant drop was observed at 180 and 211 °C

Figure 7.14 (b) shows the relationship between the surface temperature and traction coefficient μ_L, with μ_D as a reference value. The proportional relationship was observed, and the traction requirement 0.2 would be achievable at around 240 °C if this linear trend continues. In contrast, μ_D showed a slight increase as the temperature increased, meaning that the temperature had fewer effects on traction in dry conditions.

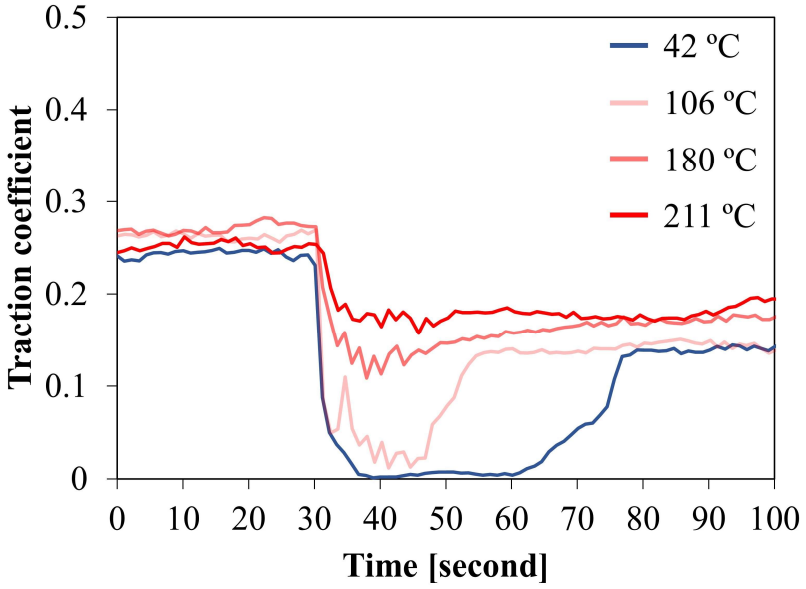

(a)

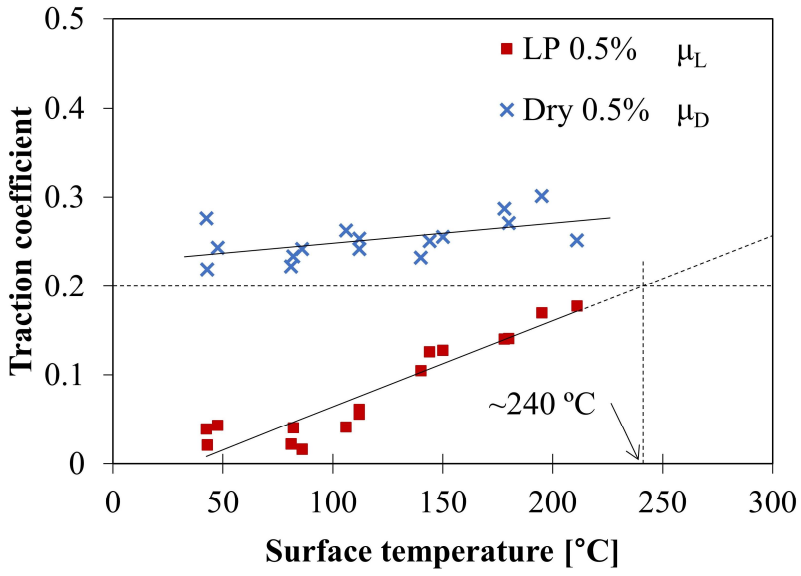

(b)

Figure 7.14 Traction behaviour of LP suspension with pre-heating process at 0.5 % slip (a) Comparison of traction data, (b) Relationship between temperature and traction coefficient

Figure 7.15 exhibits the traction behaviour of LP suspension at 1 % slip and various temperatures. In the same manner as the data at 0.5 % slip, μ_L became larger as the temperature increased. Due to this larger μ_L, the recovery region was hardly seen at 159 and 196 °C. These changes in μ_L and μ_D led to the larger traction coefficient at the higher temperature, which probably reaches 0.2 at around 240 °C. In contrast, μ_D decreased as the temperature increased, reflecting the negative effect of friction heat on the friction coefficient [135].

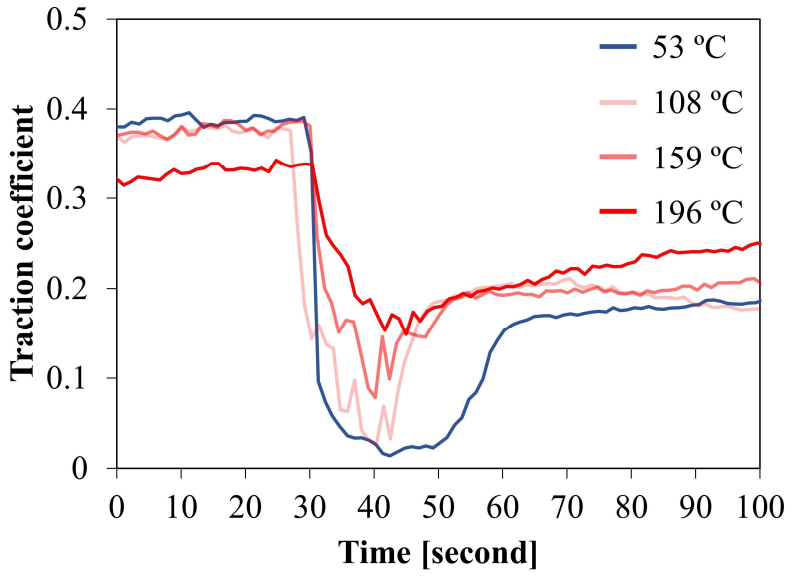

(a)

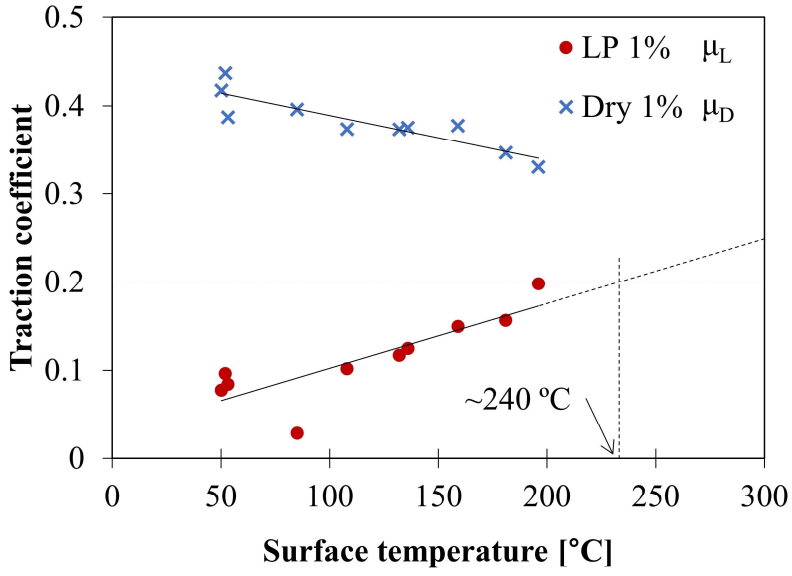

(b)

Figure 7.15 Traction behaviour of LP suspension with pre-heating process at 1 % slip (a) Comparison of traction data, (b) Relationship between temperature and traction coefficient

7.4 Discussion

The series of test with pre-heating process using LP suspension found that the surface temperature has an influence on the improvement of traction coefficients, showing the proportional relationship between the surface temperature and traction coefficient μ_L. The traction coefficient requirement, 0.2, would be achievable at approximately 240 °C, given that the linear relationship between the temperature and μ_L continues. This improvement at small slip values, 0.5 and 1 %, is very important for the actual train operation since it would be able to prevent the low adhesion, not relying on mechanical methods, such as sand particles and wheel slipping, which lead to damage of wheels and rails.

The pre-heating method used in this study must have involved in changes of the surface condition as well; an increase in the surface roughness is likely after the pre-heating process. This change could contribute to the traction improvement. However, the surface roughness was not assessed in this study since it has a limited effect on the adhesion level. The adhesion coefficient has been reported to saturate with the combined surface roughness 1-3 μm in wet conditions, and the surface temperature seems to have a greater effect on adhesion [137]. In the case of the SUROS machine, the surface roughness was reported to be 7 ± 3 μm for the wheel disc after 12,000 cycles (approximately 30 minutes) at different slip value up to 3 % [35]. This level of surface roughness seems to have less effect on the adhesion improvement according to the criteria in [137]. Furthermore, a surface roughness around 15 μm has been reported to lower the friction level of graphite [138], and the rougher surface does not dramatically increase the traction coefficient of grease for 15 seconds after the grease was applied [139]. Hence, it can be concluded that traction improvement seen in this study seems to be brought about by the high surface temperature rather than the change in the surface roughness.

Three potential reasons for this traction improvement were listed as follows: thinner water film due to lower viscosity of higher temperature water, decomposition of key organic acids and mechanical deterioration of leaves as shown in Figure 7.16. In this test, the sample suspension was dropped onto the upper rail disc running at 400 rpm. Until the applied sample suspension on the disc reaches the contact point, the water temperature should be raised to some extent, and the water viscosity could become lower. The high-temperature water has been reported to form a thinner water film due to this lower viscosity [140], [141]. However, this hypothesis is unlikely to be valid since the lubrication regime seems to be either boundary or mixed lubrication, taking into account the low testing speed (1 m/s) and small viscosity of water.

Additionally, the key organic acids of leaves, which are solved into the water, could be degraded by the heat energy. Moreover, the high temperature might change the

mechanical properties of the leaf; the heat can make the leaf powder more fragile. The brittle leaf powder could be unable to support the load, and the leaf powder is likely to fail to prevent the metal-metal contact between two discs, being expelled from the contact area.

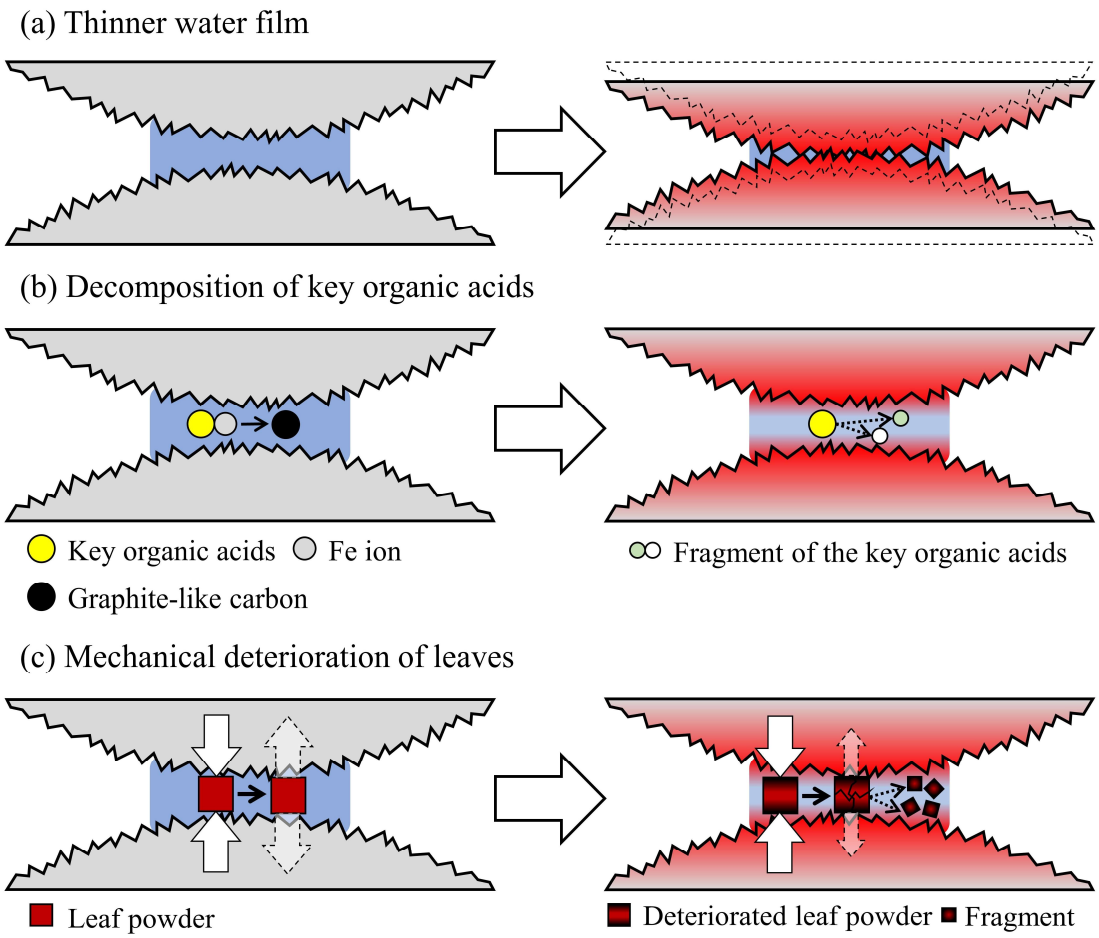

Figure 7.16 Three potential mechanisms of the traction improvement

One of the concerns of this heat application method is a high bonding strength of the leaf film. As suggested in 3.4, high temperature could enhance the chemical reaction and strengthen the bonding between leaf films and rails. Therefore, the effect of high temperature on the bonding should be conducted to assess the possibility of the heat application method.

To sum up, it was found that high temperature has a positive effect on traction improvement, showing that the heat application can be used as a mitigation method.

7.5 Conclusions

In this study, the temperature effect on the traction coefficient of leaf powder suspension was mainly investigated using a twin disc machine to simulate the rolling-sliding contact between the wheel and rail. The series of test elucidated that the leaf powder suspension had the low traction coefficient μ_L at 0.5 and 1 % slip during the sample application period, which is lower than the engine oil. The sliding distance SD_R was found to decrease at a higher slip, indicating that high surface temperature could affect the recovery. Influence of surface temperature was investigated by the traction test with high-temperature discs, which were pre-heated by operating the test for five to seven minutes at high slip ratio up to 20 %. It was found that μ_L proportionally increased as the surface temperature increased at 0.5 and 1 % slip, possibly meeting the traction requirement 0.2 at around 240 °C. This improvement in traction coefficients shows that the heat application can mitigate the low adhesion due to leaf contamination. Although the pre-heating method used in this study should have increased the surface roughness as well, the rougher surface seems to have less influence on the traction level. Hence, this traction improvement could have been brought by high surface temperature, which is possibly a mixed effect of the degradation of key organic acids discharged from leaves, thinner water film and mechanical deterioration of leaves.

One concern suggested in 6.4.2 is an effect of the high temperature on the bonding condition of leaf films. In other words, an increase in the bonding strength could occur when the surface is heated up according to the hypotheses presented in 3.4. Therefore, the temperature effect on the bonding should be investigated to examine the heat application method for prevention.

8 INVESTIGATION OF THE BONDING MECHANISM

8.1 Introduction

High temperature was found to mitigate the low adhesion conditions due to leaves; the traction requirement could be achieved at around 240 °C, showing that the heat application can be used as a new prevention and mitigation method. On the other hand, high temperature is expected to make a strong bond between leaf films and rails by enhancing the chemical reaction. If the leaf film adheres to the rail more tightly due to the heat application, this method is unacceptable since the adhered leaf film must contribute to a longer life expectancy of the leaf contamination problem.

Hence, the effect of high temperature on the bonding strength needs to be investigated. For this purpose, the bonding energy of the leaf film was quantitatively evaluated by a scratch test, examining the effect of temperature as well as the hypotheses for the bonding mechanism proposed in 3.4. Additionally, the low adhesion described in Chapter 7 is also discussed considering the result of chemical analysis.

8.2 Methodology

A black leaf layer was created on a disc specimen by using the SUROS machine. It was then analysed mechanically and chemically: Scratch Test, Laser Raman spectroscopy and Fourier transform infrared spectroscopy.

8.2.1 Leaf film creation

Leaf films were created by using a twin disc machine (SUROS). The basic procedure is similar to the friction test with pre-heating (7.2.4). The surface temperature was raised before the leaf film creation by the application of high slip up to 20 %, followed by a measurement of the surface temperature by a K type thermocouple. Then, 1 ml of 10 wt% LP suspension was applied onto the upper disc. Immediately after the application, the operation was stopped, and the disc was taken out. Figure 8.1 shows the procedure to create leaf layers on the disc. The more detailed procedure was as follows.

1. Two discs were cleaned with acetone in an ultrasonic bath and then mounted in the machine.

2. The discs were tested for five to seven minutes at one of these slip values: 7, 12 or 20 %.

3. The test was stopped, and the surface temperature of the rail disc was measured with a k-type thermocouple.

4. The machine was restarted and operated for one to two minutes at 1 % slip to stabilise the traction coefficient.

5. 1 ml of 10 wt% LP suspension was applied to the rail disc for approximately 30 to 40 seconds.

6. The operation was stopped as soon as the application finished, which usually takes under seven seconds.

For the information of the SUROS machine, see 7.2.2 and 7.2.3.

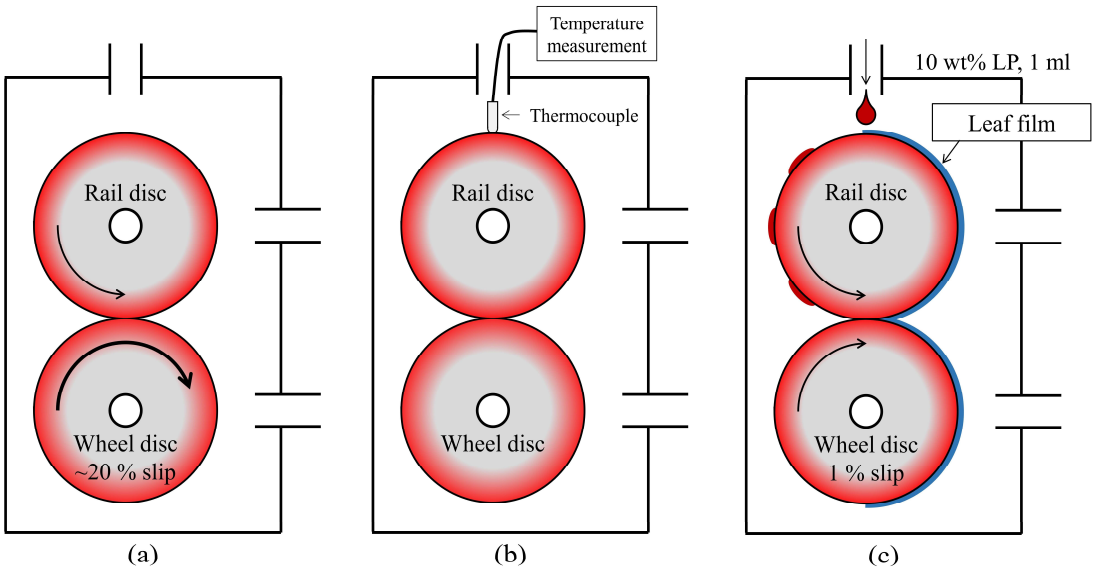

Figure 8.1 Leaf film creation on the disc

(a) Running in dry conditions at high slip, (b) Surface temperature measurement, (c) Leaf film creation

8.2.2 Scratch test

Scratch testing is a common technique used to mechanically estimate the bonding energy (adhesion energy) between substrates and films or coatings on them, e.g. resistant coatings [142]. Figure 8.2 illustrates the schematic figures of the conducted scratch tests. In this study, a simple scratch test was conducted at a constant load with a micro Rockwell stylus which has a 200 µm diameter diamond ball. Before

scratching, half of the leaf film on the disc was removed by sandpaper, exposing a bare steel surface as shown in Figure 8.2 (a). A Rockwell indenter was then pressed with 20 N, and it pulled across the surface at 0.05 mm/s, ploughing the disc surface and breaking the leaf film as shown in Figure 8.2 (b). After scratching, the width of the scratch traces was measured by an optical microscope (Figure 8.2 (c)). The bonding energy can be estimated by calculating the area while the leaf film was being destroyed by the indenter, as shown in Figure 8.2 (d). Finally, the bonding energy per unit area (Jm^{-2}) was calculated with the estimated scratch length in Figure 8.2 (d), following Equation 8.1 [143]–[145].

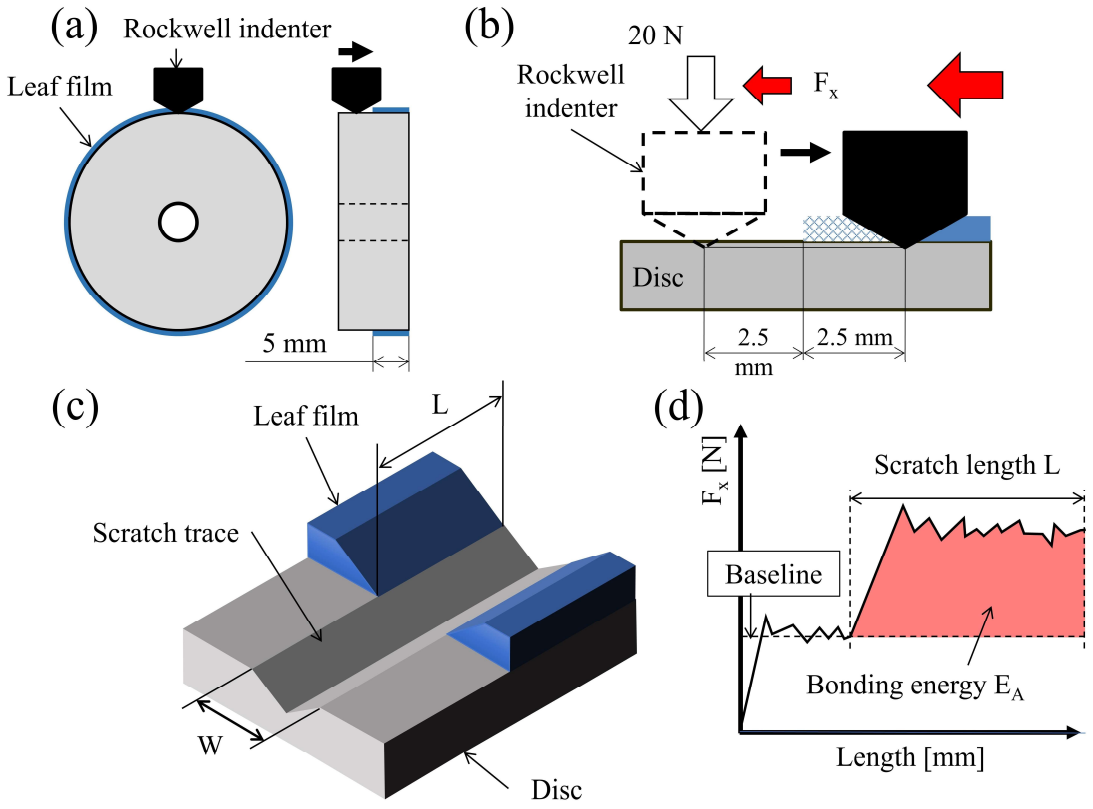

Figure 8.2 Schematic figures of scratch test

(a) Removal of leaf film, (b) Scratch test procedure, (c) Valuables, (d) Bonding energy calculation

$$\frac{E_A}{A} = \frac{E_A}{W \cdot L}$$

Equation 8.1

The main aim of the scratch tests was to estimate the approximate bonding energy of leaf films and compare the estimated bond strength of the films created at different temperature. Since the created leaf films were non-uniform and unsmooth, measurements of a critical load were not attempted, although that is more common in scratch tests [146].

8.2.3 Laser Raman Spectroscopy (RS)

A Renishaw inVia Raman Microscope was used for RS analysis with the black leaf film formed on the disc. The spectrum was acquired between 50 and 4000 cm^{-1} with the exposure time of 20 seconds and five-time accumulation, reducing the laser power to 10 % (approximately two mW). More detailed information was described in 5.2.4. The main aims of the RS analysis are to confirm the formation of graphite-like carbon in the leaf film and to study the effects of experimental conditions on the property of the leaf film.

8.2.4 Fourier Transform Infrared Spectroscopy (FT-IR)

A Bruker ALPHA Platinum-ATR was used, and the leaf films created at RT, 106, 140 and 227 °C were analysed. Other experimental conditions were the same as the description in 5.2.6. The objective of this FT-IR analysis is to study the effects of experimental conditions on the chemical bonds in the leaf film by comparing the spectrums.

8.3 Results

8.3.1 Visual inspection

Figure 8.3 depicts photographs of the created leaf layers at various temperatures: room temperature, 106 °C, 140 °C and 227 °C. The black material was formed on both the wheel and rail discs at room temperature. However, the black leaf film was created only on the wheel disc at 106, 140 and 227 °C, and the leaf film at 227 °C was patchy. This partially formed film at high temperature shows that thermal energy does not seem to enhance the chemical reaction and help the formation of leaf films. Note that the leaf film at room temperature was pretty powder-like, while the other black films seemed to be similar to the actual leaf films on a rail.

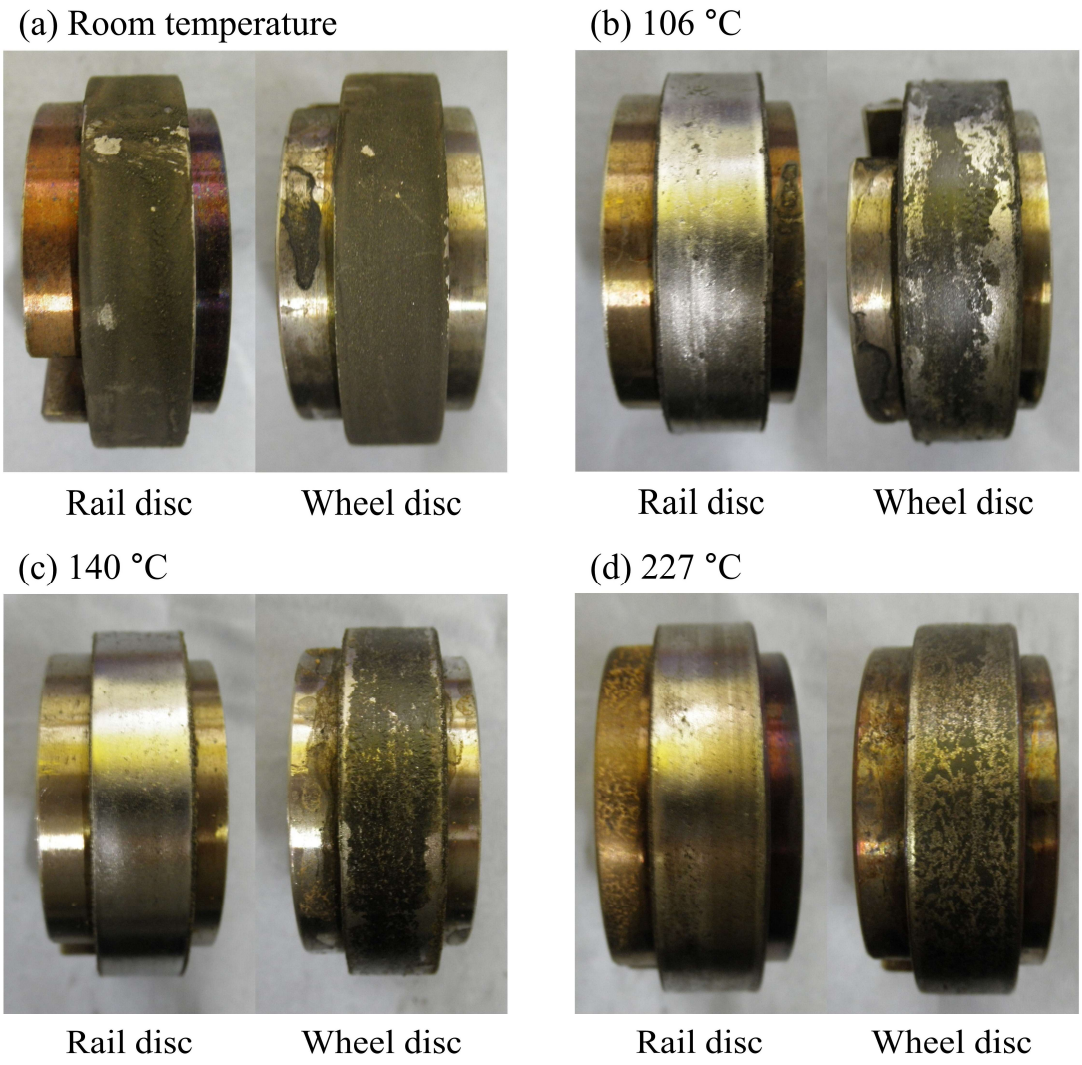

Figure 8.3 Created leaf films on SUROS discs at various temperature
Created at: (a) Room temperature, (b) 106 °C, (c) 140 °C, (d) 227 °C

8.3.2 Scratch tests

Figure 8.4 exhibits an example of the scratch test result conducted for the leaf film created at 106 °C. The mean value of the lateral force was calculated by averaging the lateral force in the exposed surface region, and the bonding energy was then estimated. It was found that the baseline showed a less constant level than expected, and this relatively large error, around 10 %, could be caused by the rougher surface due to the prior removal of leaf films by sandpaper.

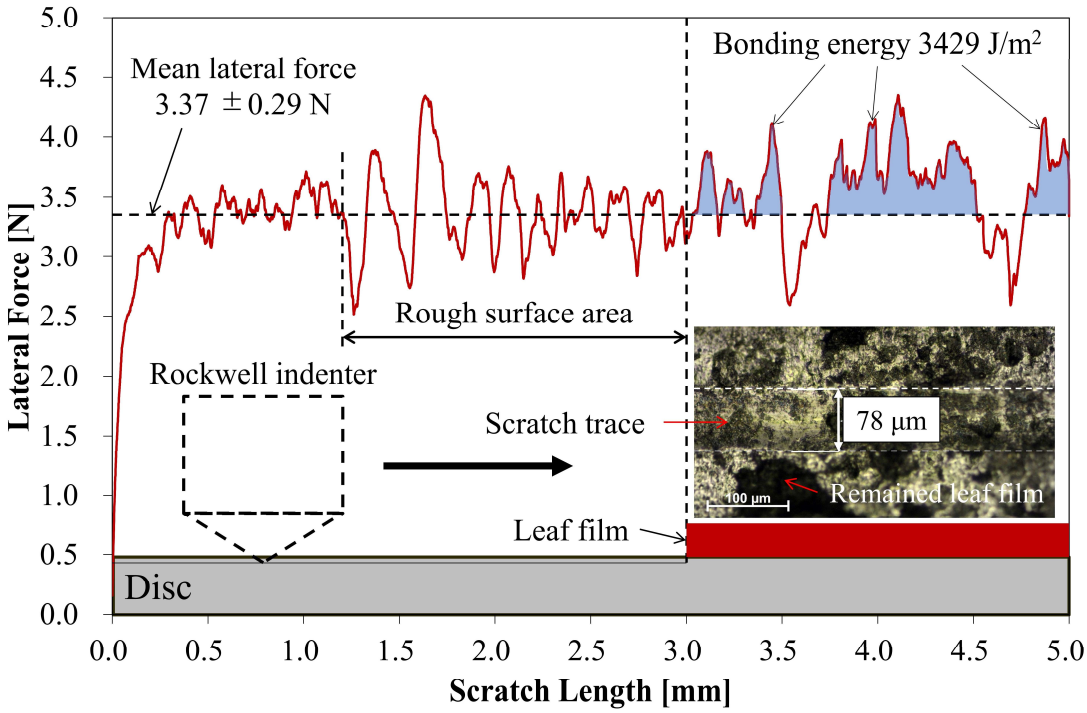

Figure 8.4 Example of scratch test result: leaf film created at 106 °C

Figure 8.5 shows the comparison of the bonding energy of the created leaf films at different temperatures. Note that the leaf film created at 227 °C could not be evaluated since there was not enough leaf film left. No clear difference in the bonding energy was found due to the large error, but the decreasing trend still can be seen between 106 and 140 °C. Since the leaf film became patchy at 227 °C, the high temperature is likely to weaken the bonding strength of leaf films as well as prevent the leaf film formation.

Furthermore, all the leaf films were easily removed by nail-scratching, showing that they did not tightly adhere to the rail substrate. This small energy indicates that the high temperature is unlikely to increase the bonding strength. Although there could be a better methodology to generate well-adhered leaf films, the application of heat energy was shown to be a potential prevention method without the significant negative impact on leaf film bonding.

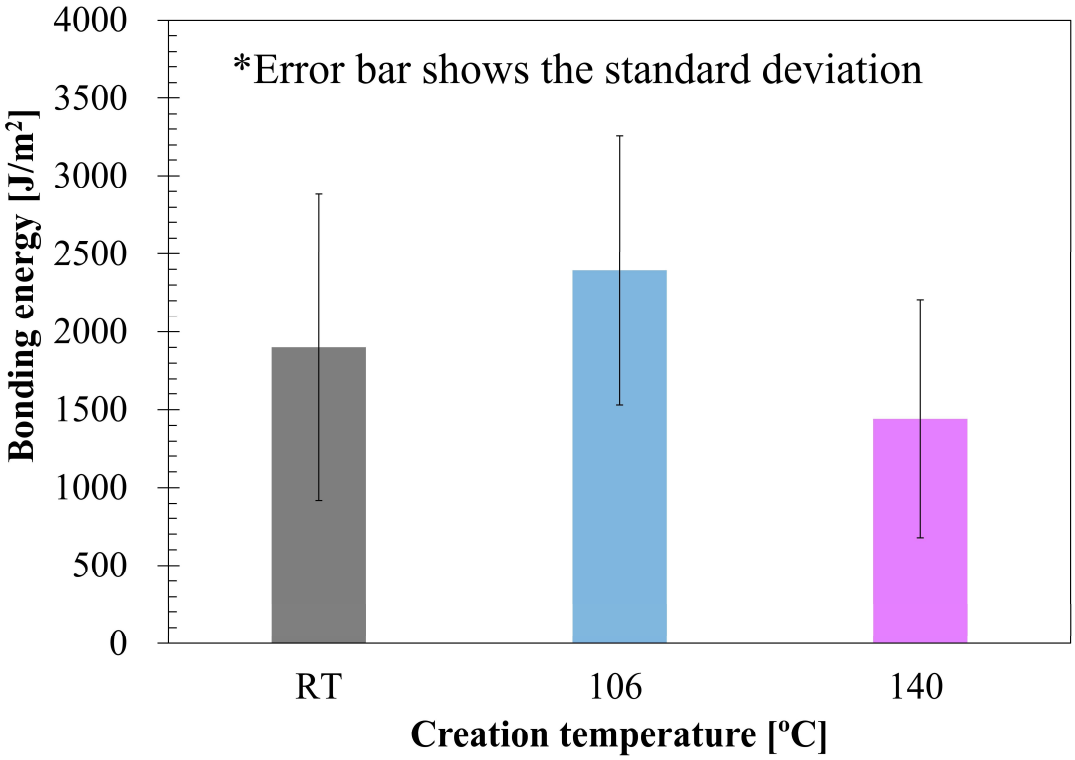

Figure 8.5 Comparison of bonding energy of leaf films generated at different temperatures

8.3.3 RS

Figure 8.6 shows the comparison between the acquired Raman spectra of the leaf films created at different temperatures, and Table 8.1 contains the detected Raman shifts and their assignments. The created leaf films were found to contain amorphous carbon, which shows peaks around 1330 cm^{-1} (D band: shoulder) and 1575 cm^{-1} (G band). The intensity ratio of the D band and G band (I_D/I_G) was calculated, and it was 0.57, 0.59 and 0.65 for the leaf films at RT, 106 and 140 °C, respectively. These low ratios show that the leaf films have partially-graphitised carbon on their surfaces [81], and it should be the main cause of low adhesion in friction tests in Chapter 7. Similar Raman spectra have been detected in black precipitate synthesised with leaf extracts and rail steel in 5.3.3. Hence, this black material on the leaf films seems to be the same as the artificial black precipitate.

It was also found that the peaks of iron oxides became sharper as the temperature increased. In particular, sharp peaks can be seen in the leaf film created at 227 °C. This result might indicate that high temperature prevents leaf powder from reacting with rail steel due to the quick evaporation and decomposition of organic acids. On the other hand, the black material was still formed at high temperature. Hence, further work needs to be done to clarify the relationship between temperature and chemical reaction.

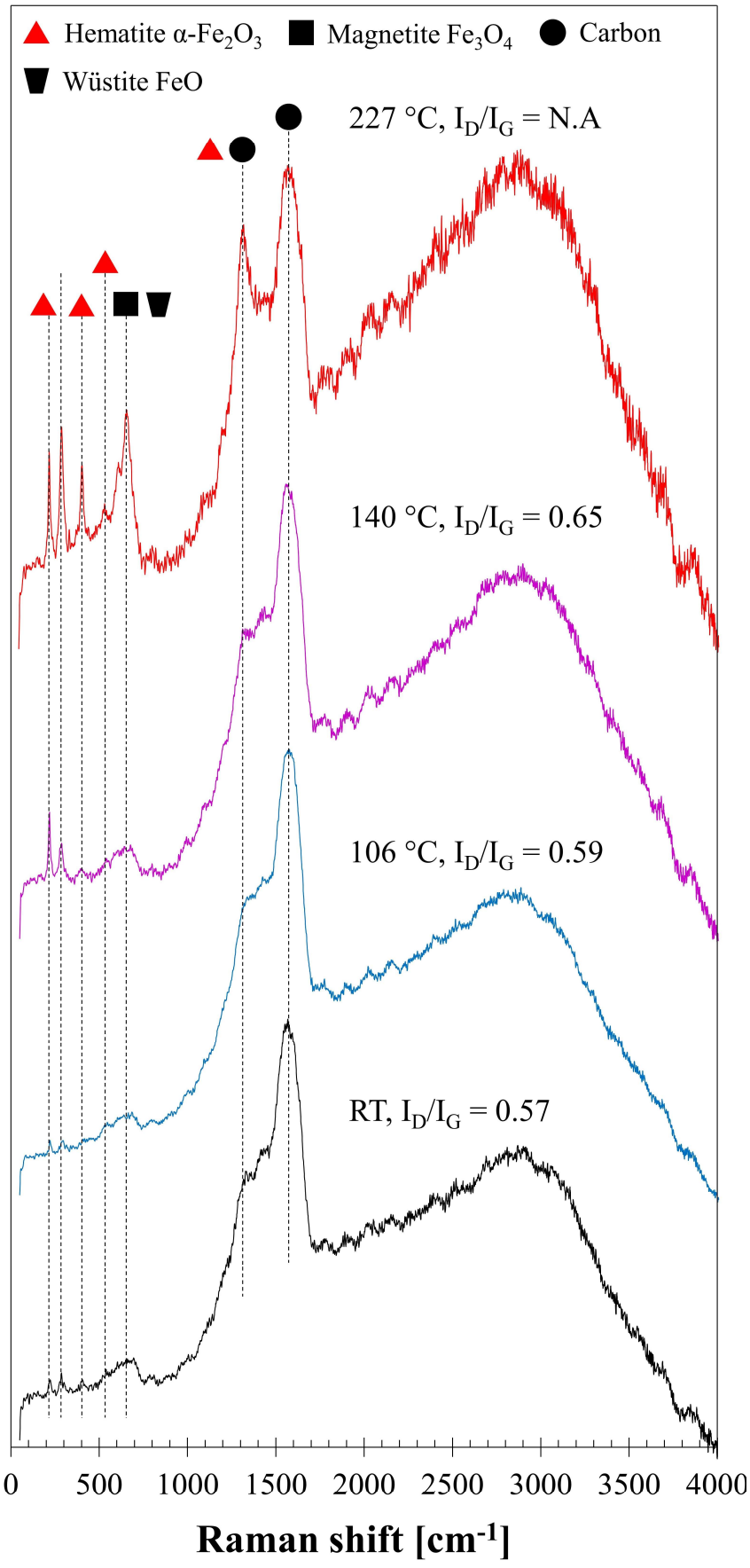

Figure 8.6 Raman spectra of the created leaf films at different temperatures

Table 8.1 Raman shifts and assignments of the created leaf films

RT [cm^{-1}]	106 °C [cm^{-1}]	140 °C [cm^{-1}]	227 °C [cm^{-1}]	Assignment	Reference	
222 m	220 m	218 m	222	α-Fe_2O_3	226.7	[77]
287 m	288 m	284 m	292	α-Fe_2O_3	292.5 299.3	[77]
-	(403)	(399)	407	α-Fe_2O_3	410.9	[38], [77]
-	-	-	606	α-Fe_2O_3	611.9	[77]
-	-	-	661	FeO Fe_3O_4	652 662.7	[77] [38]
1330	1330	1330	1316 s	Amorphous carbon α-Fe_2O_3	1355 1320	[38], [74], [77]
1571 s	1575 s	1572 s	1576 s	Amorphous carbon Sugar-derived carbon	1575 1580	[74] [83]

* m and s means medium and strong, respectively

8.3.4 FT-IR

Figure 8.7 illustrates the comparison of the acquired FT-IR spectra. As a reference, raw brown leaf powder was also analysed. Four samples showed the very similar absorption pattern to brown leaf powder, exhibiting that the created leaf films mainly consisted of bulk leaves. The double absorptions around 1400 and 1600 cm^{-1}, which are seen in the black precipitate as a characteristic feature (See 5.3.5), cannot be seen in the acquired spectra. This result suggests that the chemical reaction occurs only on the surface, forming a graphite-like carbon layer on top of the leaf film.

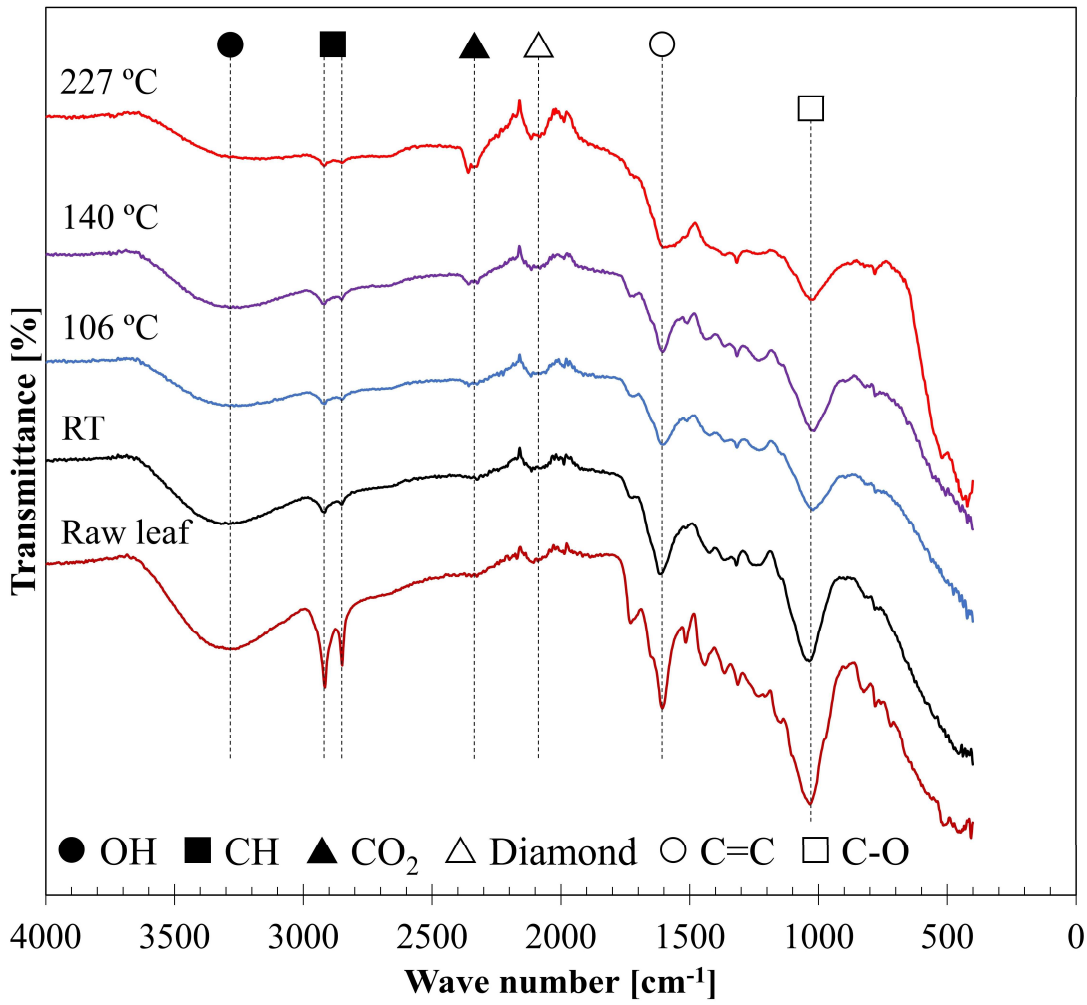

Figure 8.7 Comparison of FT-IR spectra

Table 8.2 shows the assignments of the absorption bands. All the acquired bands belonged to typical organic bonds, such as C-H and C-O, and no significant difference was seen in the peak positions. Therefore, the heat energy was found to have less effect on the chemical composition of leaf films.

Table 8.2 Assignment of the detected infrared bands

Assignment	Brown leaf powder [cm^{-1}]	RT [cm^{-1}]	106 °C [cm^{-1}]	140 °C [cm^{-1}]	227 °C [cm^{-1}]	Reference
OH stretch	3263	3290	3269	3244	-	[99]
CH stretch	2916 2849	2917 2851	2916 2851	2917 2851	2919 2849	[99]
C=C (Aromatic rings)	1606	1612	1605	1604	1600	[14], [99]
CO stretch	1032	1035	1021	1016	1022	[14], [99]

8.4 Discussion

8.4.1 Temperature effect

The scratch test revealed that the high surface temperature is likely to weaken the bonding of the leaf film rather than strengthening. In contrast, RS and FT-IR analysis showed that the heat did not significantly affect the chemistry of the created leaf films. It suggests that the key organic acids for the chemical reaction are not easily decomposed by high temperature. However, some difference in the spectra of RS and FT-IR was seen between the samples at 227 °C and the other temperature, and the leaf film became patchy at 227 °C (Figure 8.3). Hence, there could be some prevention effect of high temperature on the chemical reaction, but further work needs to be carried out for the proper assessment.

Overall, the heat application seems to be appropriate as a prevention method against the leaf contamination without significant side effects in terms of the bonding strength, although the prevention mechanism has not yet been clarified.

8.4.2 Bonding mechanism of leaf layers

Three hypotheses of the bonding mechanism were developed in 3.4. All of them were based on the idea that high temperature helps the formation of strong bonds by enhancing the chemical reaction. These hypotheses were found to be incorrect according to the result of the scratch test.

However, the scratch test was conducted for the laboratory-developed leaf films, not for leaf films on railway tracks. The actual leaf film was reported to stick to the rail surface [1], but the created leaf film in this study had small bonding energy; the leaf film could be easily removed by nail-scratching. Another laboratory-generated leaf film has been reported to be soft [2], supporting the finding in this study. Considering that the surface of the leaf film is covered with graphite-like carbon, the leaf film could be soft and easily shorn, rather than sticking to the rail.

Figure 8.8 depicts a schematic figure of the leaf film adhesion. Graphite has a low shear strength due to its layered-structure [105], and the graphite-like carbon layer on the leaf can be easily torn off by the shear stress. When some mechanical tool, such as a grinder and a scraper, attempts to remove the leaf film, only the upper layer is likely to be removed. This superficial removal might mislead to the understanding that the leaf film tightly adheres to the rail. Especially, the removal of the leaf film is likely to take a long time if the thickness is large. Further research should be necessary to find out the bonding mechanism using another or improved methodology, e.g. larger leaf powder instead of fine leaf powder.

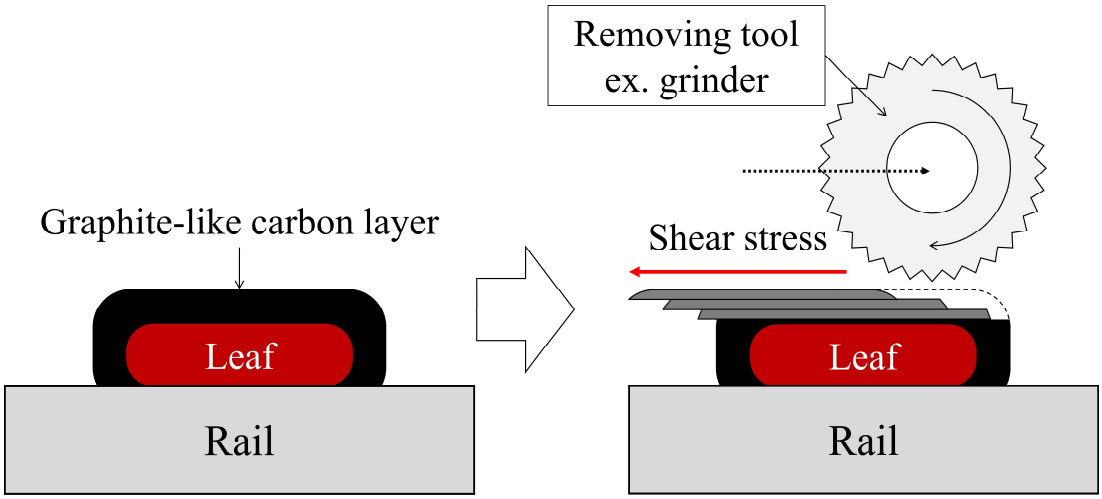

Figure 8.8 Mechanism of the leaf film bonding

To sum up, the proposed hypotheses are unlikely to be true, and the bonding mechanism has not yet been clarified.

8.4.3 Low adhesion mechanism in rolling-sliding contact

In the SUROS tests, the five wt% leaf powder suspension exhibited very low traction coefficients, becoming black immediately after the application. RS analysis of the created leaf film found that graphite-like carbon was formed on the created leaf film, which seems to be the same material as the artificial black precipitation powder tested and analysed in Chapter 4 and Chapter 5, respectively. Therefore, the graphite-like carbon is likely to be the primary cause of low adhesion in rolling-sliding conditions as well.

Another characteristic of the leaf film is that bulk leaves are likely under the surface carbon layer, supporting the hypothesis “Bulk leaf”. Although the superficial graphite-like carbon is mainly responsible for low adhesion phenomenon, the leaf should be a source of graphite-like carbon, continuously reacting with iron from the rail steel. Furthermore, lignin, which is a common organic component in leaves, has been studied as a functional additive of lubricants [147], [148]. Since the lignin was reported to improve anti-wear properties, the leaf powder itself could be the second factor of the long-term low adhesion.

To summarise all information acquired in this study, the low adhesion mechanism in the actual train operation was proposed as shown in Figure 8.9. Figure 8.9 (a) shows the first step of the mechanism; key organic acids are discharged into the water around the leaves by the passing-wheels, as suggested and examined in 5.4.3 and 6.4.1, respectively. A soft graphite-like carbon layer is then formed on top of the pieces of leaf thanks to the chemical reaction (Figure 8.9 (b)). When the following wheel rolls over the blackened leaves, the wheel is likely to slip due to the reduced

friction level. The slipping wheel helps pick up the soft graphite-like carbon layer, spreading the low adhesion according to the result in 8.3 (Figure 8.9 (c)). After passing wheels remove the superficial black layer, the chemical reaction might re-occur due to the freshly exposed leaf surface, re-forming the graphite-like carbon layer.

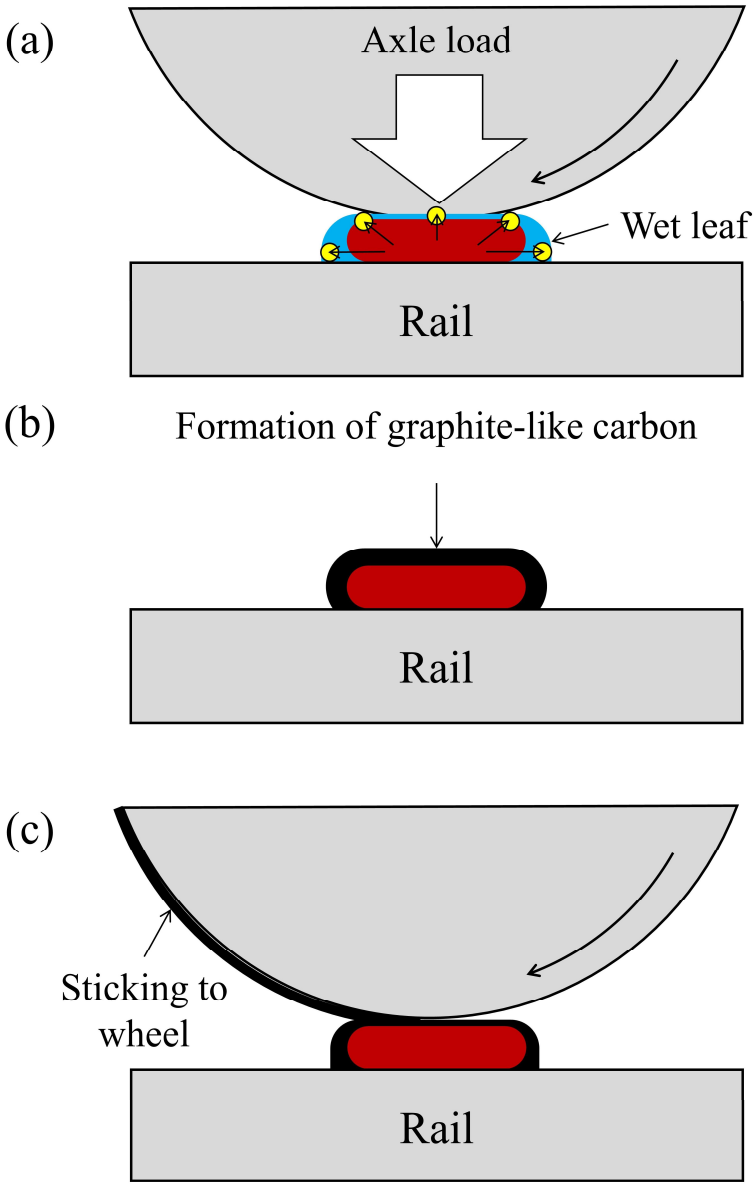

Figure 8.9 Mechanism of low adhesion in the train operation

(a) Crushed leaves, (b) Formation of graphite-like carbon, (c) Low adhesion and wheel-picking up

8.5 Conclusions

Leaf films were created using a twin disc machine, SUROS, at different temperatures. The visual inspection found that the leaf film at 227 °C was patchy compared to the other leaf films. The scratch test clarified that the bonding energy of the leaf film slightly decreased as the temperature increased; the heat application seems to weaken the bonding energy rather than strengthening. The RS analysis detected a graphite-like carbon layer on the surface of the leaf films, but bulk leaves were likely to be present underneath the surface layer according to the FT-IR analysis.

The heat application seems to be appropriate as a prevention method since no significant effect on the bonding energy has been confirmed. This fact shows that the hypotheses proposed in 3.4 are unlikely to be correct. The detected graphite-like carbon on the leaf film should be the main cause of low adhesion phenomenon due to leaf contamination, taking into account the results presented in Chapter 4 and Chapter 7.

9 FIELD INVESTIGATION AND PRACTICAL MEASURE

9.1 Introduction

A field test was conducted at the Quinton Rail Technology Centre in Long Marston, the UK, using a Class 117 DMU. Approximately 300 m straight track is available at this site, which is a part of 2.4 km loop. Using this straight track, a leaf layer was created on the rail; DMU passed five times on the sycamore-rich leaves laid on the track, which were fixed by adhesive tape and wetted by tap water before the DMU passes. This field test was carried out to assess mitigation methods for the low adhesion. However, a process of the leaf film creation has been observed, followed by a sample collection of the black leaf film for Raman spectroscopy analysis. Based on these results, a potential prevention and mitigation method is proposed. Further information regarding the field test can be found in [149].

9.2 Results

9.2.1 Observation in the field test

Figure 9.1 shows the observation during the process of the leaf film creation. The leaves laid down on the original application site (3 m) were gradually removed by passing wheels, and the black leaf film was formed outside the application site. The black leaf film was formed as far as 10 m, and it looked thicker than the leaf layer on the original application site, which was sometimes invisible [149]. This observation shows that the passing wheels must have picked up some softened leaves from the original site, and then they printed the leaf residue on the rail surface, spreading the leaf contamination.

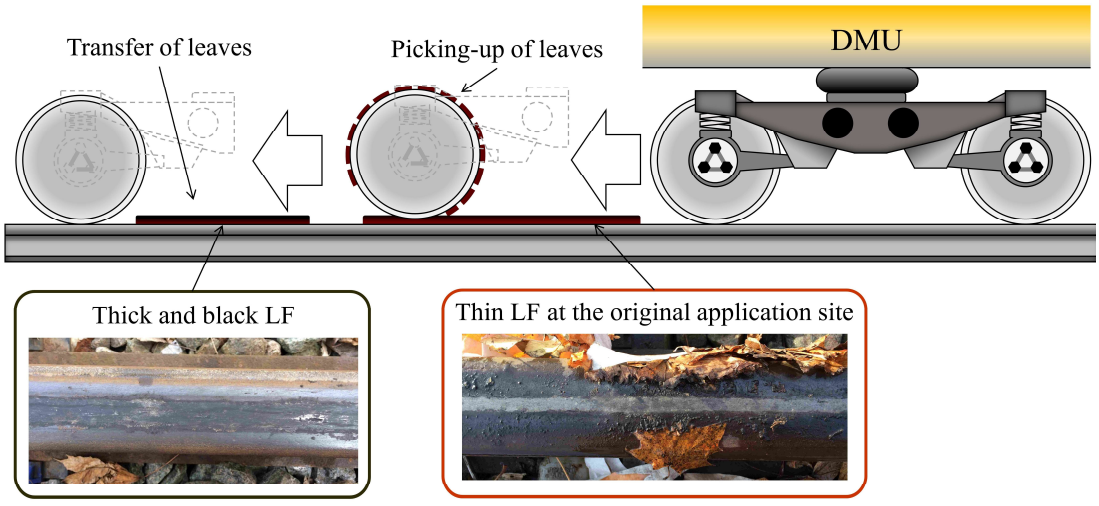

Figure 9.1 Behaviour of leaves on the rail track

9.2.2 RS analysis of black leaf films

Figure 9.2 illustrates the comparison of Raman spectra of the field samples, and Table 9.1 shows an assignment of the detected RS peaks in the field samples. The peak fittings are shown in Appendix C. The RS measurement was conducted in the same conditions described in 8.2.3. Both samples were found to have graphite-like carbon on their surface. Although some difference in the intensity of iron oxides can be seen, there was no apparent difference between these field samples and the leaf film on a SUROS disc. This RS result shows that the leaf film developed in a laboratory seems to be the same as the actual black leaf film. Therefore, the heat application method could be effective in the actual train operation as a prevention and mitigation method.

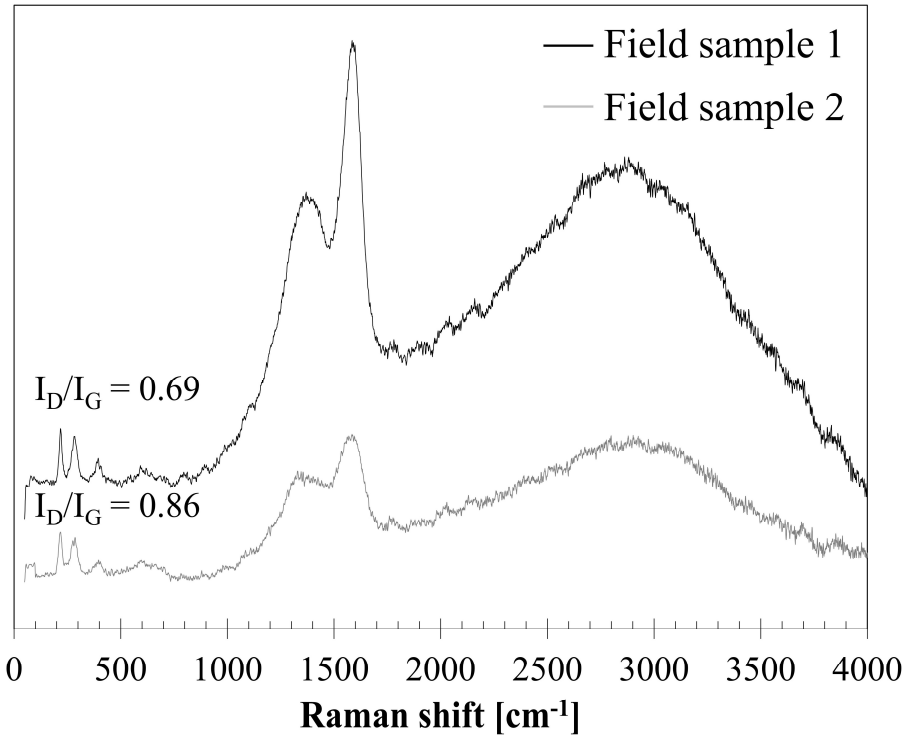

Figure 9.2 Comparison of Raman spectra

Table 9.1 Assignment of the detected peaks in RS analysis

Field sample 1 [cm^{-1}]	Field sample 2 [cm^{-1}]	Assignment	Reference	
218 m	217 m	α-Fe_2O_3	226.7	[77]
285 m	287 m	α-Fe_2O_3	292.5 299.3	[77]
1370	1361	Amorphous carbon α-Fe_2O_3	1355 1320	[38], [74], [77]
1587 s	1582 s	Amorphous carbon	1575 1580	[74] [83]

9.3 Practical measure

9.3.1 Drag-braking

The field test found that passing wheels can spread the leaf contamination. In other words, the leaf contamination could be minimised if the black leaf residue is removed from the wheel surface. Considering this observation, continuous tread braking during the autumn is proposed as a countermeasure in this study, which is very similar to drag braking for low adhesion due to snow [150].

Figure 9.3 illustrates the proposed method for prevention and mitigation. This method has two points to minimise the leaf contamination and improve adhesion levels: mechanical removal of leaf residue and heat application by braking temperature. Tread braking has been known to remove debris from a wheel surface and maintain surface roughness at a certain level. For instance, tread braking with a small braking force is used to remove snow on wheels in the winter, preventing the presence of snow between pads and wheels [150]. Similar mechanical removal could happen in the case of leaf residue, which is possibly effective to stop the contamination from being spread, as shown in Figure 9.3 (a).

Another advantage of this method is the heat application by tread braking as shown in Figure 9.3 (b); tread braking has been recognised to raise the surface temperature of the wheel [151]. This fact indicates that tread braking could apply enough thermal energy to mitigate the low adhesion in the same way described in Chapter 7, possibly preventing the chemical reaction between leaves and rail/wheel steels. If the surface temperature is controlled around 240 °C by adjusting a braking force/pressure, it can maintain enough adhesion levels even if the leaf contamination is present.

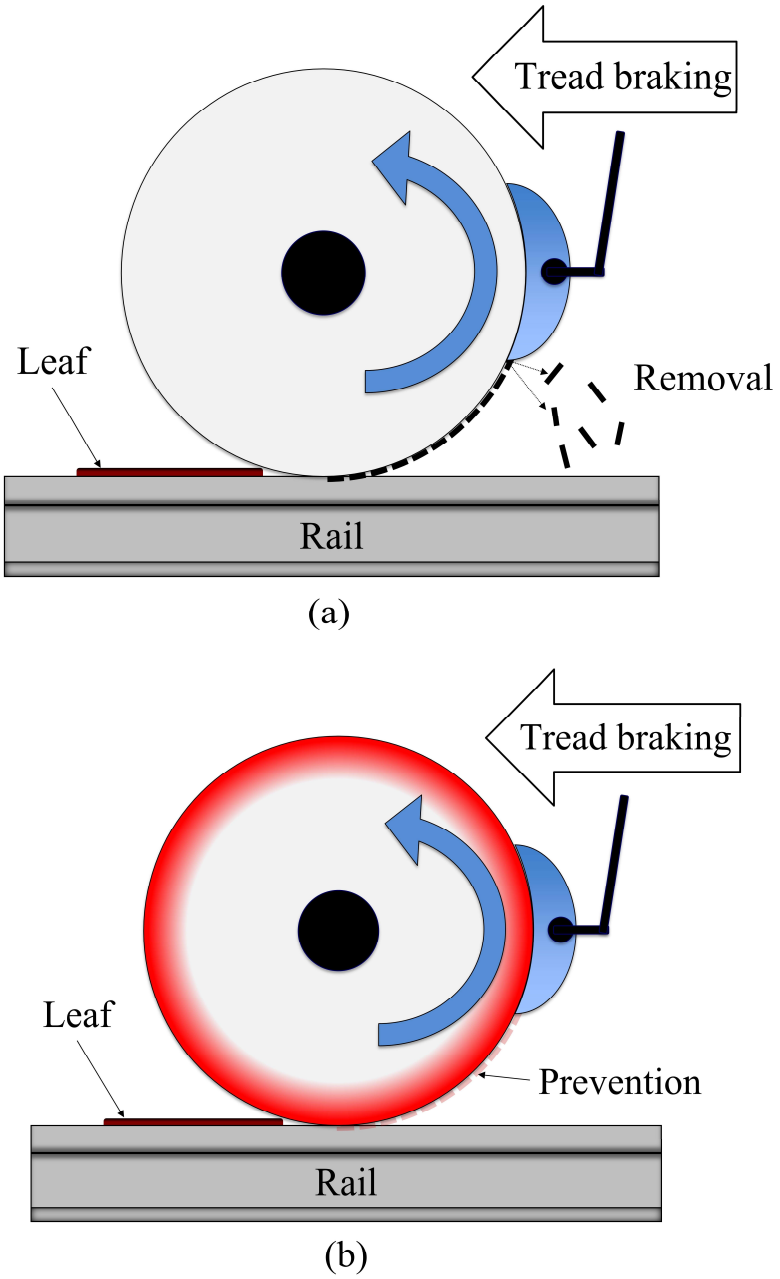

Figure 9.3 Proposed method for prevention and mitigation

(a) Prevention by mechanical removal, (b) Mitigation of the low adhesion

Negative aspects of this method are potential growth of thermal cracks on the wheel surface. When thermal cracks are present on the wheel surface, the wheel needs to be reprofiled at the maintenance centre, leading to an increase in maintenance costs. However, thermal cracks are generally grown above 400 °C, and no significant influence has been reported for thermal crack growth at around 240 °C [152]. Thereby, heat application by continuous tread braking could be a practical answer for leaf contamination, pushing all the risk to wheel-side and cutting the other costs. Of course, further laboratory-based tests and field tests are necessary to examine to what extent this method is effective.

9.3.2 Further research

To examine the possibility of this method, the following work should be done before applying this method to the field.

- **Determination of the wheel surface temperature for mitigation**

  In the SUROS test, both wheel and rail discs were heated up. However, high temperature should be given to only wheels by drag-braking in the train operation. Therefore, the mitigation effect should be assessed in the case of a hot wheel disc and cool rail disc. This research project could be carried out by a twin disc machine with braking equipment.

- **Assessment of braking performance when leaves/blackened leaves are present between wheels and braking blocks**

  Leaf residue on a wheel should remain at the edge of a brake block if this method is used. In that case, one of the concerns is a malfunction of braking equipment; the accumulated leaf residue can be transferred to the interface between the wheel tread and braking block, possibly lowering the friction level. Hence, braking performance should be examined with the artificially-contaminated braking blocks, which could be raw leaves, blackened leaves and black precipitation powder. This work should be conducted using a standard testing facility of braking.

- **Evaluation of the prevention effects on leaf film formation using a test track**

  Leaves can be spread on a railway track over a long distance by passing-wheels. However, no research has been conducted to understand how long a piece of leaf can be transferred from the original point. Accordingly, the degree of spreading should be studied, possibly using a test track. For example, the leaf film can be created following the methodology in [149], and then the rail surface is captured by a high-speed camera for a long distance, e.g. 200 m. Using an image processing technique, the degree of spreading can be quantitatively evaluated, and an effect of the drag-braking method should be assessed by comparing the results with/without the drag braking.

Overall, the drag-braking method can be attempted in the actual train operation once these three research questions are addressed for safety.

9.4 Conclusions

A field test found that the passing wheel picked up some leaves on the line and transferred them on another part of the line, helping spread the leaf contamination. RS analysis clarified that the black leaf film created in the field test contained amorphous carbon as well as iron oxides. These similarities to the leaf film and black material created in the laboratory indicate that the heat application method could be effective as a prevention and mitigation method, since they are likely to be created with the same chemical reaction process. Drag braking was proposed as a potential countermeasure; it can prevent leaves from being spread, and it also applies friction heat to the wheel to mitigate the low adhesion. Although some further research must be conducted to guarantee safety, this continuous tread braking is a new approach to the low adhesion problem due to leaves, and it could be an innovative method to be easily installed for train operating companies all over the world.

10 CONCLUSIONS

10.1 Project conclusions

The aims of this research project were the clarification of the low adhesion mechanism due to leaf contamination in the autumn and the elucidation of the bonding mechanism between leaf films and rails, which lead to the development of a practical countermeasure against leaf contamination. For these purposes, tribological tests using a ball-on-flat and twin disc method were carried out, as well as chemical and material analyses. Conclusions in each aim are shown below.

10.1.1 Low adhesion mechanism

The ball-on-flat test showed that the black precipitation powder, which was synthesised with water-soluble leaf organics and rail steels, surprisingly reduced a friction level in wet conditions, lower than a commercial engine oil and significantly lower than distilled water. The twin disc machine study also found that the suspension of black precipitation powder produced low adhesion in rolling-sliding conditions, as well as fine leaf powder suspension. Graphite-like carbon was present on the surface of the black precipitation, black leaf film generated on the disc specimen and the leaf film created in the field test. Hence, it was concluded that graphite-like carbon could be the primary cause of low adhesion.

Sycamore leaf powder was also identified to lower the friction by the tribological tests. Furthermore, the chemical and material analysis found that iron carboxylate and various ions in the black precipitation, including phosphate ion. They should also contribute to the low adhesion conditions, although the degree of contribution was not clarified.

To summarise, the low adhesion seems to be brought by four factors: graphite-like carbon, bulk leaf, iron carboxylate and various ions.

10.1.2 Bonding mechanism

The leaf film generated on disc specimen showed low bonding energy. Nail-scratching was enough to remove the leaf film, and the tight bond between the leaf film and rail was not reproduced in this study. Therefore, the bonding mechanism has not yet been elucidated.

However, it was confirmed that the bonding energy seemed to decrease as the surface temperature of the disc increased. In particular, the leaf film was not uniformly created over 200 °C, becoming patchy. Accordingly, it can be concluded that the high temperature did not affect the bonding strength between the leaf film and rail, rather making the bond stronger as suggested in the developed hypotheses.

Better understanding of the chemical reaction process between leaf organics and rail steels is necessary to clarify the bonding mechanism. The leaf extract analysis found that some organic acids were likely to involve in the reaction process, dissolving iron from the rail steels. However, the specific organic acids have not yet been identified. If they were discovered, the bonding mechanism should be more clearly explained.

To sum up, the bonding mechanism was not fully explained in this study due to the poor understanding of the chemical reaction, although surface temperature was found to have few effects on the bonding energy at least.

10.1.3 Potential countermeasure

The twin disc test with the pre-heating process found that high temperature was effective to mitigate low adhesion due to leaves. It also seemed to prevent the chemical reaction, forming a patchy leaf film. Furthermore, the field test showed that wheels picked up leaves on tracks and transferred them on another part of tracks. Taking into account the results shown above, a new direction of the potential countermeasure against leaf contamination was suggested: continuous drag braking.

Drag braking can prevent the spread of leaf contamination, stopping stuck leaves on a wheel surface at the edge of a brake block. Moreover, continuous braking can raise surface temperature of a wheel. This high temperature can mitigate low adhesion even if leaves are present in the contact between wheels and rails. Although there are some safety issues to be addressed, the drag braking method could be an innovative measure.

10.2 Publications and presentations

Publications:

- K. Ishizaka, S. R. Lewis, and R. Lewis, “The low adhesion problem due to leaf contamination in the wheel/rail contact: Bonding and low adhesion mechanisms,” *Wear*, vol. 378–379, pp. 183–197, 2017.
- K. Ishizaka, S. R. Lewis, D. Hammond, and R. Lewis, “Investigation of leaf chemistry and leaf layer: low adhesion mechanism,” *Proceedings of the 11th International Conference on Contact Mechanics and Wear of Rail/Wheel Systems, Delft, The Netherland, 2018.*
- K. Ishizaka, S. R. Lewis, D. Hammond, and R. Lewis, “Chemistry of black leaf films synthesised using rail steels and their influence on the low friction mechanism,” *RSC Adv.*, vol. 8, no. 57, pp. 32506–32521, 2018.
- K. Ishizaka, S. R. Lewis, and R. Lewis, “Influence of temperature on adhesion coefficient and bonding strength of leaf films: a twin disc study,” *Under review for Wear*, 2019.

Presentations:

- Presentation in the Mission of Tribology, hosted by the Institution of Mechanical Engineers (IMechE) in London, 2016, First prize.
- Presentation at the Future of Railway Event, hosted by IMechE and RSSB in Derby, 2017, Second place
- Presentation at TriboUK 2018 in Sheffield, 2018, First prize
- Presentation in the 11th International Conference on Contact Mechanics and Wear of Rail/Wheel Systems, Delft, The Netherland, 2018.

10.3 Further work

Further work regarding the leaf extract analysis and the use of drag braking could be conducted for the development of this study.

Leaf extract analysis:

- Identification of key organic acids which cause the chemical reaction with rail steels, possibly using a colourimetric method of Benedict's test, Ion Chromatography and Liquid Chromatography-Mass Spectrometry.
- Synthesis of a black material with artificial chemicals, followed by some chemical analysis such as FT-IR, RS and XPS.

Drag braking:

- Determination of the wheel surface temperature, which is the most appropriate and balanced temperature to mitigate low adhesion, using a twin disc machine with a braking facility.
- Assessment of braking performance when leaves/blackened leaves are present between wheels and braking blocks to ensure safety, using a standard brake test facility.
- Evaluation of the prevention effects on leaf film formation using a test track, capturing an image of the rail surface with a high speed camera.

REFERENCES

[1] C. R. Fulford, "Review of low adhesion research," *A report published by Railways Safety and Standards Board*, no. May, 2004.

[2] W. Poole, "Characteristics of Railhead Leaf Contamination," *A report published by Railways Safety and Standards Board*, 2007.

[3] U. Olofsson, Y. Zhu, S. Abbasi, R. Lewis, and S. R. Lewis, "Tribology of the wheel–rail contact – aspects of wear, particle emission and adhesion," *Vehicle System Dynamics*, vol. 51, no. 7, pp. 1091–1120, 2013.

[4] Rail Accident Investigation Branch, "Station overrun at Stonegate, East Sussex 8 November 2010," *A report published by Rail Accident Investigation Branch*, 2011.

[5] Rail Accident Investigation Branch, "Buffer stop collision at Chester station 20 November 2013," *A report published by Rail Accident Investigation Branch*, 2014.

[6] W. Voges and P. Spiess, "Optimising services with EMU ET42x in autumn 2004 and 2005," in *Proceedings of the 7th World Congress on Railway Research*, 2005, pp. 1–10.

[7] H. Chen, T. Furuya, S. Fukagai, S. Saga, K. Murakami, and T. Ban, "Influence of Leaves on the Adhesion between Wheel and Rail," *Railway Technical Research Institute Report*, vol. 31, no. 4, pp. 29–34, 2017.

[8] Y. Lyu, Y. Zhu, and U. Olofsson, "Wear between wheel and rail: A pin-on-disc study of environmental conditions and iron oxides," *Wear*, vol. 328–329, pp. 277–285, 2015.

[9] T. Pearce and D. Watkins, "Adhesion and leaves - A review of the problem and potential solutions," 1987.

[10] K. Ishizaka, S. R. Lewis, and R. Lewis, "The low adhesion problem due to leaf contamination in the wheel/rail contact: Bonding and low adhesion mechanisms," *Wear*, vol. 378–379, pp. 183–197, 2017.

[11] Z. Li, O. Arias-Cuevas, R. Lewis, and E. A. Gallardo-Hernández, "Rolling–Sliding Laboratory Tests of Friction Modifiers in Leaf Contaminated Wheel–Rail Contacts," *Tribology Letters*, vol. 33, no. 2, pp. 97–109, 2009.

[12] U. Olofsson and K. Sundvall, "Influence of leaf, humidity and applied lubrication on friction in the wheel-rail contact: pin-on-disc experiments," *Proceedings of the Institution of Mechanical Engineers, Part F: Journal of Rail and Rapid Transit*, vol. 218, no. 3, pp. 235–242, 2004.

[13] E.A. Gallardo-Hernandez and R. Lewis, "Twin disc assessment of wheel/rail adhesion," *Wear*, vol. 265, no. 9–10, pp. 1309–1316, 2008.

[14] P. M. Cann, "The 'leaves on the line' problem - A study of leaf residue film formation and lubricity under laboratory test conditions," *Tribology Letters*, vol. 24, no. 2, pp. 151–158, 2006.

[15] G. Vasić, F. Franklin, A. Kapoor, and V. Lučanin, "Laboratory simulation of low adhesion leaf film on rail steel," *International Journal of Surface Science*

and Engineering, vol. 2, pp. 84–97, 2008.

[16] O. Arias-Cuevas, Z. Li, R. Lewis, and E. A. Gallardo-Hernández, "Laboratory investigation of some sanding parameters to improve the adhesion in leaf-contaminated wheel–rail contacts," *Proceedings of the Institution of Mechanical Engineers, Part F: Journal of Rail and Rapid Transit*, vol. 224, no. 3, pp. 139–157, 2010.

[17] M. Omasta, M. Machatka, D. Smejkal, M. Hartl, and I. Křupka, "Influence of sanding parameters on adhesion recovery in contaminated wheel–rail contact," *Wear*, vol. 322–323, pp. 218–225, 2015.

[18] O. Arias-Cuevas and Z. Li, "Field investigations into the adhesion recovery in leaf-contaminated wheel-rail contacts with locomotive sanders," *Proceedings of the Institution of Mechanical Engineers, Part F: Journal of Rail and Rapid Transit*, vol. 225, no. 5, pp. 443–456, 2011.

[19] O. Arias-Cuevas and Z. Li, "Field investigations into the performance of magnetic track brakes of an electrical multiple unit against slippery tracks. Part 2: Braking force and side effects," *Proceedings of the Institution of Mechanical Engineers, Part F: Journal of Rail and Rapid Transit*, vol. 225, no. 6, pp. 613–636, 2011.

[20] P. Hyde, D. I. Fletcher, A. Kapoor, and S. Richardson, "Full scale testing to investigate the effect of rail head treatments of differing pH on railway rail leaf films," in *The World Congress on Railway Research*, 2008, pp. 18–22.

[21] D. Tamura, A. Numakura, and M. Takigawawa, "An effective measure for prevention against slippingsliding problems of the wheel due to leaf contamination on the railways," in *Proceedings of Japan Society of Civil Engineers*, 2007, pp. 4–226.

[22] S. R. Lewis, R. Lewis, J. Cotter, X. Lu, and D. T. Eadie, "A new method for the assessment of traction enhancers and the generation of organic layers in a twin-disc machine," *Wear*, vol. 366–367, pp. 258–267, 2016.

[23] Y. Zhu, U. Olofsson, and R. Nilsson, "A field test study of leaf contamination on railhead surfaces," *Proceedings of the Institution of Mechanical Engineers, Part F: Journal of Rail and Rapid Transit*, vol. 228, no. 1, pp. 71–84, 2014.

[24] U. Olofsson, "A multi-layer model of low adhesion between railway wheel and rail," *Proceedings of the Institution of Mechanical Engineers, Part F: Journal of Rail and Rapid Transit*, vol. 221, no. 3, pp. 385–389, 2007.

[25] S. R. Lewis, R. Lewis, and U. Olofsson, "An alternative method for the assessment of railhead traction," *Wear*, vol. 271, no. 1, pp. 62–70, 2011.

[26] H. Harrison, T. Mccanney, and J. Cotter, "Recent developments in coefficient of friction measurements at the rail/wheel interface," *Wear*, vol. 253, no. 1, pp. 114–123, 2002.

[27] B. T. White *et al.*, "A Study into the Effect of the Presence of Moisture at the Wheel / Rail Interface during Dew and Damp Conditions," in *10th International Conference on Contact Mechanics and Wear of rail/Wheel Systems*, 2015.

[28] P. Brimblecombe, "Temporal humidity variations in the heritage climate of

South East England," *Heritage Science*, vol. 3, pp. 1–11, 2013.

[29] K. Nagase, "A Study of Adhesion Between the Rails and Running Wheels on Main Lines: Results of Investigations by Slipping Adhesion Test Bogie," *Proceedings of the Institution of Mechanical Engineers. Part H, Journal of engineering in medicine*, vol. 210, no. 4. pp. 259–266, 1996.

[30] C. W. Jenks, "Improved methods for increasing wheel rail adhesion in the presence of natural contaminants," 1997.

[31] O. Arias-Cuevas, Z. Li, and R. Lewis, "A laboratory investigation on the influence of the particle size and slip during sanding on the adhesion and wear in the wheel-rail contact," *Wear*, vol. 271, no. 1–2, pp. 14–24, 2011.

[32] R. Lewis and R. S. Dwyer-Joyce, "Wear at the wheel/rail interface when sanding is used to increase adhesion," *Proceedings of the Institution of Mechanical Engineers Part F: Journal of Rail and Rapid Transit*, vol. 220, no. 1, pp. 29–41, 2006.

[33] R. Lewis and J. Masing, "Static wheel/rail contact isolation due to track contamination," *Proceedings of the Institution of Mechanical Engineers, Part F: Journal of Rail and Rapid Transit*, vol. 220, no. 1, pp. 43–53, 2006.

[34] R. Lewis, R. S. Dwyer-Joyce, and J. Lewis, "Disc machine study of contact isolation during railway track sanding," *Proceedings of the Institution of Mechanical Engineers, Part F: Journal of Rail and Rapid Transit*, vol. 217, no. 1, pp. 11–24, 2003.

[35] O. Arias-Cuevas, Z. Li, R. Lewis, and E. A. Gallardo-Hernández, "Rolling-sliding laboratory tests of friction modifiers in dry and wet wheel-rail contacts," *Wear*, vol. 268, no. 2–3, pp. 543–551, 2010.

[36] N. Somashekara, Z. . Saiyed, and C. . Ramchand, "Biochemistry of Railhead Leaf Film Contamination," 2006.

[37] Zhao Y.W, J. . Liu, and L. . Zheng, "The Oxide Film and Oxide Coating on Steels Under Boundary Lubrication," in *16th Leeds-Lyon Symposium on Tribology*, 1989, pp. 5–8.

[38] T. Nakahara, K. S. Baek, H. Chen, and M. Ishida, "Relationship between surface oxide layer and transient traction characteristics for two steel rollers under unlubricated and water lubricated conditions," *Wear*, vol. 271, no. 1–2, pp. 25–31, 2011.

[39] H. Chen, Y. Sone, K. Beak, T. Nakahara, and M. Ishida, "A fundamental study on effect of rust upon adhesion coefficient between wheel and rail," *Railway Technical Research Institute Report*, vol. 21, pp. 5–10, 2007.

[40] R. Lewis and U. Olofsson, *Wheel-rail Interface Handbook*. 2009.

[41] Y. Cao *et al.*, "Concurrent microstructural evolution of ferrite and austenite in a duplex stainless steel processed by high-pressure torsion," *Acta Materialia*, vol. 63, pp. 16–29, 2014.

[42] D. A. Rigney, "Transfer, mixing and associated chemical and mechanical processes during the sliding of ductile materials," *Wear*, vol. 245, no. 1–2, pp. 1–9, 2000.

[43] H. J. Baumann, G.; Knothe, K.; Fecht, “Surface modification, corrugation, and nanostructure formation of high speed railway tracks,” *Nanostructured Materials*, vol. 9, pp. 751–754, 1997.

[44] E. A. Gallardo-Hernandez, R. Lewis, and R. S. Dwyer-Joyce, “Temperature in a twin-disc wheel/rail contact simulation,” *Tribology International*, vol. 39, no. 12, pp. 1653–1663, 2006.

[45] J. Sundh and U. Olofsson, “Relating contact temperature and wear transitions in a wheel–rail contact,” *Wear*, vol. 271, no. 1–2, pp. 78–85, 2011.

[46] D. I. Fletcher, “Thermal contact stress and near surface rail cracks,” in *9th International Conference on Contact Mechanics and Wear of Rail/Wheel Systems*, 2012.

[47] T. Misawa, K. Hashimoto, and S. Shimodaira, “The mechanism of formation of iron oxide and oxyhydroxides in aqueous solutions at room temperature,” *Corrosion Science*, vol. 14, no. 2, pp. 131–149, 1974.

[48] J. Suzumura, Y. Sone, A. Ishizaki, D. Yamashita, Y. Nakajima, and M. Ishida, “In situ X-ray analytical study on the alteration process of iron oxide layers at the railhead surface while under railway traffic,” *Wear*, vol. 271, no. 1–2, pp. 47–53, 2011.

[49] H. Zhu, F. Cao, D. Zuo, L. Zhu, D. Jin, and K. Yao, “A new hydrothermal blackening technology for Fe3O4 coatings of carbon steel,” *Applied Surface Science*, vol. 254, no. 18, pp. 5905–5909, 2008.

[50] Y. Berthier, S. Descartes, M. Busquet, E. Niccolini, C. Desrayaud, and L. Baillet, “The role and effects of the third body in the wheel – rail interaction,” *Materials and Structures*, pp. 423–436, 2004.

[51] Y. Zhu Lyu, Y., Olofsson, U., “Mapping the friction between railway wheels and rails focusing on environmental conditions,” *Wear*, vol. 324–325, pp. 122–128, 2015.

[52] Y. Zhu, U. Olofsson, and H. Chen, “Friction Between Wheel and Rail: A Pin-On-Disc Study of Environmental Conditions and Iron Oxides,” *Tribology Letters*, vol. 52, no. 2, pp. 327–339, 2013.

[53] M. Azhar Uddin, H. Tsuda, S. Wu, and E. Sasaoka, “Catalytic decomposition of biomass tars with iron oxide catalysts,” *Fuel*, vol. 87, no. 4–5, pp. 451–459, 2008.

[54] A. Koriakin, H. Van Nguyen, D.-W. Kim, and C.-H. Lee, “Thermochemical Decomposition of Microcrystalline Cellulose Using Sub- and Supercritical Tetralin and Decalin with Fe3O4,” *Industrial & Engineering Chemistry Research*, vol. 54, no. 18, pp. 5184–5194, 2015.

[55] J. Crowe and T. Bradshaw, “Molecular shape and structure 2: the shape of large molecules,” in *Chemistry for the Biosciences: the essential concepts*, Oxford University Press, 2010, pp. 247–277.

[56] M. Sasaki, Z. Fang, Y. Fukushima, T. Adschiri, and K. Arai, “Dissolution and hydrolysis of cellulose in subcritical and supercritical water,” *Industrial & Engineering Chemistry Research*, vol. 39, no. 8, pp. 2883–2890, 2000.

[57] R. S. R. Parker and P. Taylor, *Adhesion & Adhesives*. 1966.

[58] T. L. K. Yong and Y. Matsumura, "Reaction kinetics of the lignin conversion in supercritical water," *Industrial and Engineering Chemistry Research*, vol. 51, pp. 11975–11988, 2012.

[59] R. J. a Gosselink *et al.*, "Lignin depolymerisation in supercritical carbon dioxide/acetone/water fluid for the production of aromatic chemicals," *Bioresource Technology*, vol. 106, pp. 173–177, 2012.

[60] Y. Nagamatsu and M. Funaoka, "Structural control of lignin-based polymers and the design of recyclable lignocellulosic composites," *Journal of the Adhesion Society of Japan*, vol. 37, no. 12, pp. 10–17, 2001.

[61] Z. Yuan, S. Cheng, M. Leitch, and C. C. Xu, "Hydrolytic degradation of alkaline lignin in hot-compressed water and ethanol," *Bioresource Technology*, vol. 101, no. 23, pp. 9308–9313, 2010.

[62] K. Okuda, X. Man, M. Umetsu, S. Takami, and T. Adschiri, "Efficient conversion of lignin into single chemical species by solvothermal reaction in water– p -cresol solvent," *Journal of Physics: Condensed Matter*, vol. 16, no. 14, pp. S1325–S1330, 2004.

[63] M. Osada, T. Sato, M. Watanabe, T. Adschiri, and K. Arai, "Low-temperature catalytic gasification of lignin and cellulose with a ruthenium catalyst in supercritical water," *Energy and Fuels*, vol. 18, no. 2, pp. 327–333, 2004.

[64] P. Dongre, M. Driscoll, T. Amidon, and B. Bujanovic, "Lignin-Furfural Based Adhesives," *Energies*, vol. 8, no. 8, pp. 7897–7914, 2015.

[65] N. E. El Mansouri, A. Pizzi, and J. Salvadó, "Lignin-based wood panel adhesives without formaldehyde," *Holz als Roh - und Werkstoff*, vol. 65, pp. 65–70, 2007.

[66] D. J. Cosgrove, "Assembly and enlargement of the primary cell wall in plants," *Annu Rev Cell Dev Biol*, vol. 13, pp. 171–201, 1997.

[67] A. Kawabata, S. Sawayama, and T. Kamata, "On the Mechanism of Association of Low-Methoxyl Pectin due to Calcium Ions," *Nippon Nogeikagaku Kaishi*, vol. 53, no. 2, pp. 61–67, 1979.

[68] N. Wellner, M. Kačuráková, A. Malovíková, R. H. Wilson, and P. S. Belton, "FT-IR study of pectate and pectinate gels formed by divalent cations," *Carbohydrate Research*, vol. 308, no. 1–2, pp. 123–131, 1998.

[69] M. Harmon and R. Lewis, "Review of top of rail friction modifier tribology," *Tribology - Materials, Surfaces and Interfaces*, vol. 10, no. 3, pp. 150–162, 2016.

[70] K. L. Mittal and A. Pizzi, *Adhesion promotion techniques*. 2002.

[71] J. Edgley, "Managing Low Adhesion," 2018.

[72] J. Williams, *Engineering Tribology*. New York: Cambridge University Press, 2004.

[73] L. . Harwood and Timothy D.W.C, *Introduction to Organic Spectroscopy*. Oxford: Oxford University Press, 1997.

[74] F. Tuinstra and J. L. Koenig, “Raman Spectrum of Graphite,” *The Journal of Chemical Physics*, vol. 53, no. 3, pp. 1126–1130, 1970.

[75] F. Guo, Y. Tian, Y. Liu, and Y. Wang, “Tribological behaviors of graphite sliding against cemented carbide in CaCl2 solution,” *Surface Topography: Metrology and Properties*, vol. 3, no. 4, p. 044003, 2015.

[76] M. Saravanan, M. Ganesan, and S. Ambalavanan, “An in situ generated carbon as integrated conductive additive for hierarchical negative plate of lead-acid battery,” *Journal of Power Sources*, vol. 251, pp. 20–29, 2014.

[77] D. L. A. de Faria, S. V. Silva, and M. T. de Oliveira, “Raman microspectroscopy of some iron oxides and oxyhydroxides,” *Journal of Raman Spectroscopy*, vol. 28, no. February, pp. 873–878, 1997.

[78] D. Lin-Vien, N. B. Colthup, W. G. Fateley, and J. G. Grasselli, *The handbook of infrared and Raman characteristic frequencies of organic molecules*. London: Academic Press, 1991.

[79] J. Ma, T. Xue, and X. Qin, “Sugar-derived carbon/graphene composite materials as electrodes for supercapacitors,” *Electrochimica Acta*, vol. 115, pp. 566–572, 2014.

[80] V. Sridhar and H. Park, “Sugar-derived disordered carbon nano-sheets as high-performance electrodes in sodium-ion batteries,” *New J Chem*, vol. 41, no. 11, pp. 4286–4290, 2017.

[81] A. C. Ferrari and J. Robertson, “Interpretation of Raman spectra of disordered and amorphous carbon,” *Phys Rev B*, vol. 61, no. 20, pp. 95–107, 2000.

[82] Y. Yuan, Y. Song, W. Jing, Y. Wang, X. Yang, and D. Liu, “Simultaneous determination of caffeine, gallic acid, theanine, (−)-epigallocatechin and (−)-epigallocatechin-3-gallate in green tea using quantitative 1H-NMR spectroscopy,” *Analytical Methods*, vol. 6, no. 3, pp. 907–914, 2014.

[83] M. Saravanan, M. Ganesan, and S. Ambalavanan, “An in situ generated carbon as integrated conductive additive for hierarchical negative plate of lead-acid battery,” *Journal of Power Sources*, vol. 251, pp. 20–29, 2014.

[84] Dick Wiebodt, “Understanding Raman Spectrometer Parameters,” *Spectroscopy*, no. Special Issues June, 2010.

[85] N. J. Everall, J. Lumsdon, and D. J. Christopher, “The Effect of Laser-Induced Heating Upon the Vibrational Raman-Spectra of Graphites and Carbon-Fibers,” *Carbon*, vol. 29, no. 2, pp. 133–137, 1991.

[86] “Thermo Scientific X-ray Photoelectron Spectroscopy XPS.” [Online]. Available: http://xpssimplified.com/.

[87] J. F. Moulder, W. F. Stickle, P. E. Sobol, and K. D. Bomben, *Handbook of X-ray Photoelectron Spectroscopy*. Minnesota: Perkin-Elmer Corporation, Physical Electronics Division, 1992.

[88] P. M. A. Sherwood, “Introduction to Studies of Phosphorus-Oxygen Compounds by XPS,” *Surface Science Spectra*, vol. 9, no. 1, pp. 62–66, 2002.

[89] D. Yang *et al.*, “Chemical analysis of graphene oxide films after heat and chemical treatments by X-ray photoelectron and Micro-Raman spectroscopy,”

Carbon, vol. 47, no. 1, pp. 145–152, 2009.

[90] D. Briggs, *Surface analysis of polymers by XPS and static SIMS*. New York: Cambridge University Press, 1998.

[91] M. Barathi, A. S. Krishna Kumar, C. U. Kumar, and N. Rajesh, "Graphene oxide-aluminium oxyhydroxide interaction and its application for the effective adsorption of fluoride," *RSC Advances*, vol. 4, no. 96, pp. 53711–53721, 2014.

[92] B. D. Ossonon and D. Bélanger, "Synthesis and characterization of sulfophenyl-functionalized reduced graphene oxide sheets," *RSC Adv*, vol. 7, no. 44, pp. 27224–27234, 2017.

[93] L. Madec, R. Petibon, J. Xia, J.-P. Sun, I. G. Hill, and J. R. Dahn, "Understanding the Role of Prop-1-ene-1,3-Sultone and Vinylene Carbonate in $LiNi_{1/3}Mn_{1/3}Co_{1/3}O_2$ /Graphite Pouch Cells: Electrochemical, GC-MS and XPS Analysis," *Journal of The Electrochemical Society*, vol. 162, no. 14, pp. A2635–A2645, 2015.

[94] T. Yamashita and P. Hayes, "Analysis of XPS spectra of Fe2+ and Fe3+ ions in oxide materials," *Applied Surface Science*, vol. 254, no. 8, pp. 2441–2449, 2008.

[95] A. P. Grosvenor, B. A. Kobe, M. C. Biesinger, and N. S. McIntyre, "Investigation of multiplet splitting of Fe 2p XPS spectra and bonding in iron compounds," *Surface and Interface Analysis*, vol. 36, no. 12, pp. 1564–1574, 2004.

[96] "NIST X-ray Photoelectron Spectroscopy Database." [Online]. Available: https://srdata.nist.gov/xps/.

[97] B. Demri and D. Muster, "XPS study of some calcium compounds," *Journal of Materials Processing Technology*, vol. 55, no. 3–4, pp. 311–314, 1995.

[98] D. R. Dreyer, S. Park, C. W. Bielawski, and R. S. Ruoff, "The chemistry of graphite oxide," *Chemical Society Reviews*, vol. 39, no. 1, pp. 228–240, 2010.

[99] D. H. Williams and Ian Fleming, *Spectroscopic Methods in Organic Chemistry*, Fourth. London: McGraw-Hill, 1989.

[100] V. Nikolic *et al.*, "The synthesis and characterization of iron(II): Gluconate," *Savremene tehnologije*, vol. 3, no. 2, pp. 16–24, 2014.

[101] V. Otero *et al.*, "Characterisation of metal carboxylates by Raman and infrared spectroscopy in works of art," *Journal of Raman Spectroscopy*, vol. 45, no. 11–12, pp. 1197–1206, 2014.

[102] M. C. D'Antonio *et al.*, "Spectroscopic investigations of iron(II) and iron(III) oxalates," *Journal of the Brazilian Chemical Society*, vol. 20, no. 3, pp. 445–450, 2009.

[103] E. G. Palacios, G. Juárez-López, and A. J. Monhemius, "Infrared spectroscopy of metal carboxylates II. Analysis of Fe(III), Ni and Zn carboxylate solutions," *Hydrometallurgy*, vol. 72, no. 1–2, pp. 139–148, 2004.

[104] V. P. Shinde and P. P. Patil, "Investigation on role of monomer(s) during electrochemical polymerization of aniline and its derivatives on low carbon steel by XPS," *Electrochimica Acta*, vol. 78, pp. 483–494, 2012.

[105] G. W. Stachowiak and A. W. Batchelor, *Engineering tribology*, Fourth. Oxford: Elsevier/Butterworth-Heinemann, 2014.

[106] S. S. Wang and S. C. Tung, "A Reaction Mechanism for Producing Low-Friction Iron Phosphate Coatings," *Tribology Transactions*, vol. 34, no. 1, pp. 45–50, 1991.

[107] M.-C. Corneci, F. Dekkiche, A.-M. Trunfio-Sfarghiu, M.-H. Meurisse, Y. Berthier, and J.-P. Rieu, "Tribological properties of fluid phase phospholipid bilayers," *Tribology International*, vol. 44, pp. 1959–1968, 2011.

[108] F. Gao, P. V. Kotvis, and W. T. Tysoe, "The friction, mobility and transfer of tribological films: Potassium chloride and ferrous chloride on iron," *Wear*, vol. 256, no. 11–12, pp. 1005–1017, 2004.

[109] P. J. John, S. V. Prasad, A. A. Voevodin, and J. S. Zabinski, "Calcium sulfate as a high temperature solid lubricant," *Wear*, vol. 219, no. 2, pp. 155–161, 1998.

[110] P. J. John and J. S. Zabinski, "Sulfate based coatings for use as high temperature lubricants," *Tribology Letters*, vol. 7, pp. 31–37, 1999.

[111] F. Zha, B. Wei, S. Chen, S. Dong, M. Zeng, and Z. Liu, "The Maillard reaction of a shrimp by-product protein hydrolysate: chemical changes and inhibiting effects of reactive oxygen species in human HepG2 cells," *Food Funct*, vol. 6, no. 6, pp. 1919–1927, 2015.

[112] U. Teruyuki, "The Maillard reaction in food," *Journal for the integrated study of dietary habits*, vol. 26, no. 1, pp. 11–19, 2015.

[113] N. Prefecture and A. Experiment, "Prediction of Japanese Green Tea Ranking by Gas Chromatography / Mass Spectrometry-Based Hydrophilic Metabolite Fingerprinting," *Journal of Agricultural and Food Chemistry*, vol. 55, pp. 231–236, 2007.

[114] G. Le Gall, I. J. Colquhoun, and M. Defernez, "Metabolite Profiling Using 1H NMR Spectroscopy for Quality Assessment of Green Tea, Camellia sinensis (L.)," *Journal of Agricultural and Food Chemistry*, vol. 52, no. 4, pp. 692–700, 2004.

[115] I. Birlouez-Aragon, V. Moreaux, M. Nicolas, and C. J. Ducauze, "Effect of iron and lactose supplementation of milk on the Maillard reaction and tryptophan content," *Food Additives and Contaminants*, vol. 14, no. 4, pp. 381–388, 1997.

[116] Y. Kato, K. Watanabe, and Y. Sato, "Effect of Some Metals on the Maillard Reaction of Ovalbumin," *Journal of Agricultural and Food Chemistry*, vol. 29, no. 3, pp. 540–543, 1981.

[117] D. T. Ramonaityte, M. Keršiene, A. Adams, K. A. Tehrani, and N. De Kimpe, "The interaction of metal ions with Maillard reaction products in a lactose-glycine model system," *Food Research International*, vol. 42, no. 3, pp. 331–336, 2009.

[118] A. S. P. Moreira, F. M. Nunes, M. R. Domingues, and M. A. Coimbra, "Coffee melanoidins: structures, mechanisms of formation and potential health impacts," *Food & Function*, vol. 3, no. 9, pp. 903–915, 2012.

[119] A. N. Wijewickreme and D. D. Kitts, “Modulation of metal-induced genotoxicity by Maillard reaction products isolated from coffee,” *Food and Chemical Toxicology*, vol. 36, no. 7, pp. 543–553, 1998.

[120] M. Saxena and S. Sarkar, “Involuntary graphene intake with food and medicine,” *RSC Advances*, vol. 4, no. 57, p. 30162, 2014.

[121] G. Piantanida, E. Menart, M. Bicchieri, and M. Strlič, “Classification of iron-based inks by means of micro-Raman spectroscopy and multivariate data analysis,” *Journal of Raman Spectroscopy*, vol. 44, no. 9, pp. 1299–1305, 2013.

[122] S. C. Boyatzis, G. Velivasaki, and E. Malea, “A study of the deterioration of aged parchment marked with laboratory iron gall inks using FTIR-ATR spectroscopy and micro hot table,” *Heritage Science*, vol. 4, no. 1, 2016.

[123] M. Bicchieri, M. Monti, G. Piantanida, and A. Sodo, “All that is iron-ink is not always iron-gall!,” *Journal of Raman Spectroscopy*, vol. 39, no. April, pp. 1074–1078, 2008.

[124] A. S. Lee, P. J. Mahon, and D. C. Creagh, “Raman analysis of iron gall inks on parchment,” *Vibrational Spectroscopy*, vol. 41, no. 2, pp. 170–175, 2006.

[125] G. K. Poon, “Analysis of catechins in tea extracts by liquid chromatography-electrospray ionization mass spectrometry,” *Journal of Chromatography, A*, vol. 794, no. 1/2, pp. 63–74, 1998.

[126] L. Mei, L. Liao, Z. Wang, and C. Xu, “Interactions between Phosphoric/Tannic Acid and Different Forms of FeOOH,” *Advances in Materials Science and Engineering*, vol. 2015, pp. 1–10, 2015.

[127] S. Nasrazadani, “The application of infrared spectroscopy to a study of phosphoric and tannic acids interactions with magnetite (Fe3O4), goethite (α-FeOOH) and lepidocrocit (γ-FeOOH),” *Corrosion Science*, vol. 39, no. l, pp. 1845–1859, 1997.

[128] B. Qian, B. Hou, and M. Zheng, “The inhibition effect of tannic acid on mild steel corrosion in seawater wet/dry cyclic conditions,” *Corrosion Science*, vol. 72, pp. 1–9, 2013.

[129] T. R. I. Cataldi, G. Margiotta, A. Del Fiore, and S. A. Bufo, “Ionic content in plant extracts determined by ion chromatography with conductivity detection,” *Phytochemical Analysis*, vol. 14, no. 3, pp. 176–183, 2003.

[130] P. J. Charley, B. Sarkar, C. F. Stitt, and P. Saltman, “Chelation of iron by sugars,” *Biochimica et biophysica acta*, vol. 69, pp. 313–321, 1963.

[131] C. P. Rao and K. Geetha, “Fe(III) complexes of D-glucose and D-fructose*,” *Biometals*, vol. 7, no. 1, pp. 25–29, 1994.

[132] A. Synytsya, “Fourier transform Raman and infrared spectroscopy of pectins,” *Carbohydrate Polymers*, vol. 54, no. 1, pp. 97–106, 2003.

[133] National Center for Biotechnology Information, “PubChem Database.” [Online]. Available: https://pubchem.ncbi.nlm.nih.gov/compound/Acetic-acid. [Accessed: 18-Sep-2019].

[134] National Center for Biotechnology Information, “PubChem Database.”

[Online]. Available: https://pubchem.ncbi.nlm.nih.gov/compound/Malic-acid. [Accessed: 18-Sep-2019].

[135] O. Polach, "Creep forces in simulations of traction vehicles running on adhesion limit," *Wear*, vol. 258, no. 7–8, pp. 992–1000, 2005.

[136] K. Ishizaka, S. R. Lewis, D. Hammond, and R. Lewis, "Chemistry of black leaf films synthesised using rail steels and their influence on the low friction mechanism," *RSC Advances*, vol. 8, no. 57, pp. 32506–32521, 2018.

[137] H. Chen and H. Tanimoto, "Experimental observation of temperature and surface roughness effects on wheel/rail adhesion in wet conditions," *International Journal of Rail Transportation*, vol. 6, no. 2, pp. 101–112, 2018.

[138] L. Xiaowei, Y. Suyuan, S. Xuanyu, and H. Shuyan, "The influence of roughness on tribological properties of nuclear grade graphite," *Journal of Nuclear Materials*, vol. 350, no. 1, pp. 74–82, 2006.

[139] S. R. Lewis, R. Lewis, G. Evans, and L. E. Buckley-Johnstone, "Assessment of railway curve lubricant performance using a twin-disc tester," *Wear*, vol. 314, no. 1–2, pp. 205–212, 2014.

[140] H. Chen, T. Ban, M. Ishida, and T. Nakahara, "Adhesion between rail/wheel under water lubricated contact," *Wear*, vol. 253, no. 1–2, pp. 75–81, 2002.

[141] H. Chen, T. Ban, M. Ishida, and T. Nakahara, "Experimental investigation of influential factors on adhesion between wheel and rail under wet conditions," *Wear*, vol. 265, no. 9–10, pp. 1504–1511, 2008.

[142] B. Ollivier and A. Matthews, "Adhesion of diamond-like carbon films on polymers: An assessment of the validity of the scratch test technique applied to flexible substrates," *Journal of Adhesion Science and Technology*, vol. 8, no. 6 pt 3, pp. 651–662, 1994.

[143] S. Das, D. Lahiri, D. Y. Lee, A. Agarwal, and W. Choi, "Measurements of the adhesion energy of graphene to metallic substrates," *Carbon*, vol. 59, pp. 121–129, 2013.

[144] A. K. Keshri, D. Lahiri, and A. Agarwal, "Carbon nanotubes improve the adhesion strength of a ceramic splat to the steel substrate," *Carbon*, vol. 49, no. 13, pp. 4340–4347, 2011.

[145] I. Lahiri, D. Lahiri, S. Jin, A. Agarwal, and W. Choi, "Carbon nanotubes: How strong is their bond with the substrate?," *ACS Nano*, vol. 5, no. 2, pp. 780–787, 2011.

[146] S. J. Bull, D. S. Rickerby, A. Matthews, A. Leyland, A. R. Pace, and J. Valli, "The use of scratch adhesion testing for the determination of interfacial adhesion: The importance of frictional drag," *Surface and Coatings Technology*, vol. 36, no. 1–2, pp. 503–517, 1988.

[147] L. Mu *et al.*, "Non-corrosive green lubricants: strengthened lignin-[choline][amino acid] ionic liquids interaction via reciprocal hydrogen bonding," *RSC Advances*, vol. 5, no. 81, pp. 66067–66072, 2015.

[148] L. Mu *et al.*, "Lignin from hardwood and softwood biomass as a lubricating additive to ethylene glycol," *Molecules*, vol. 23, no. 3, pp. 1–10, 2018.

[149] J. Lanigan *et al.*, “Towards a field test methodology for locomotive brake testing using a representative low adhesion simulation,” in *11th International Conference on Contact Mechanics and Wear of Rail/Wheel Systems*, 2018.

[150] U. Olofsson, J. Sundh, U. Bik, and R. Nilsson, “The influence of snow on the tread braking performance of a train: A pin-on-disc simulation performed in a climate chamber,” *Proceedings of the Institution of Mechanical Engineers, Part F: Journal of Rail and Rapid Transit*, vol. 230, no. 6, pp. 1521–1530, 2016.

[151] T. Vernersson, “Temperatures at railway tread braking. Part 1: modelling,” *Proceedings of the Institution of Mechanical Engineers, Part F: Journal of Rail and Rapid Transit*, vol. 221, pp. 167–182, 2007.

[152] K. Handa and F. Morimoto, “Influence of wheel/rail tangential traction force on thermal cracking of railway wheels,” *Wear*, vol. 289, pp. 112–118, 2012.

APPENDIX A

Table A1 Summary of paper grading

Paper	Grade	1st Category	2nd Category	Peer reviewed publication	Theory supported by testing	Scale test	Full scale test	Real world measurement	Conclusions evidence in paper	Conclusions operationally validated
1A	2	General adhesion	Academic research	No	No	No	No	No	Yes	Yes
2A	1	General adhesion	Academic research	No	No	No	No	No	Yes	No
2B	3	Prevention	Hydrophilic	No	No	No	Yes	Yes	Yes	No
6A	3	Mitigation	Other methods	No	No	No	No	Yes	Yes	Yes
11A	4	General adhesion	Laboratory testing	Yes	Yes	Yes	No	No	Yes	No
11B	4	Mitigation	Traction enhancer	Yes	Yes	Yes	No	No	Yes	No
12A	4	General adhesion	Laboratory testing	Yes	Yes	Yes	No	No	Yes	No
13A	4	General adhesion	Laboratory testing	Yes	Yes	Yes	No	No	Yes	No
13B	4	Mitigation	Sand	Yes	Yes	Yes	No	No	Yes	No
14A	4	General adhesion	Laboratory testing	Yes	Yes	Yes	No	No	Yes	No
14B	4	Principle research	Low adhesion mechanism	Yes	Yes	Yes	No	No	Yes	No
15A	4	General adhesion	Laboratory testing	Yes	Yes	Yes	No	No	Yes	No
16A	4	General adhesion	Laboratory testing	Yes	Yes	Yes	No	No	Yes	No
16B	4	Mitigation	Sand	Yes	Yes	Yes	No	No	Yes	No
17A	4	General adhesion	Laboratory testing	Yes	Yes	Yes	No	No	Yes	No
17B	4	Mitigation	Sand	Yes	Yes	Yes	No	No	Yes	No
18A	5	General adhesion	Field testing	Yes	Yes	No	Yes	Yes	Yes	No
18B	5	Mitigation	Sand	Yes	Yes	No	Yes	Yes	Yes	No
20A	4	Prevention	Hydrophilic	No	Yes	No	Yes	Yes	Yes	No
21A	2	Mitigation	Other methods	No	No	No	No	Yes	Yes	No
22A	4	Mitigation	Traction enhancer	Yes	Yes	Yes	No	No	Yes	No
23A	4	General adhesion	Field testing	Yes	Yes	No	No	Yes	Yes	No
23B	3	Principle research	Low adhesion mechanism	Yes	Yes	No	No	No	Yes	No
23C	3	Principle research	Bonding mechanism	Yes	Yes	No	No	No	Yes	No
24A	3	Principle research	Low adhesion mechanism	Yes	Yes	No	No	No	Yes	No
29A	5	General adhesion	Field testing	Yes	Yes	No	No	Yes	Yes	Yes
36A	1	Principle research	Bonding mechanism	No	No	No	No	No	Yes	No

APPENDIX B

Table A2 All metal ions detected in the ICP-MS analysis

Element	BLE before [µg/L]	BLE after [µg/L]	Distilled water [µg/L]
Fe	307.5	31040.1	1.9
Mn	1702.5	2262.0	0.0
Al	27.4	1253.8	0.7
B	552.6	588.6	34.9
Sr	239.2	230.2	0.3
Zn	54.9	62.9	1.6
Ba	72.5	56.4	0.1
Ni	33.7	36.5	0.0
Cr	75.9	35.2	0.0
Rb	26.8	25.5	0.0
Cu	20.3	9.1	0.7
Li	4.6	5.0	0.0
Co	0.2	1.6	0.0
Mo	1.7	1.4	0.0
Ga	1.5	1.4	0.0
Se	1.5	1.2	0.2
As	0.4	0.7	0.0
V	0.2	0.3	0.0
Pb	0.8	0.3	0.1
Ce	0.0	0.1	0.0
Bi	0.0	0.0	0.2

APPENDIX C

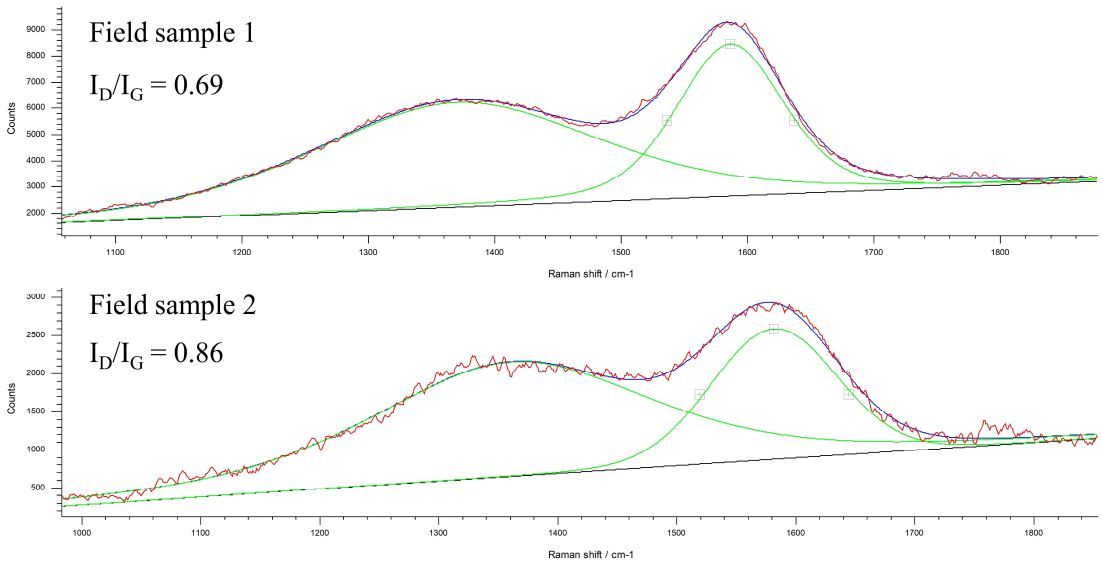

Figure A1 Peak fittings of Raman spectra of the leaf films in the field test